

CENTRAL RESEARCH LIBRARY
DOCUMENT COLLECTION

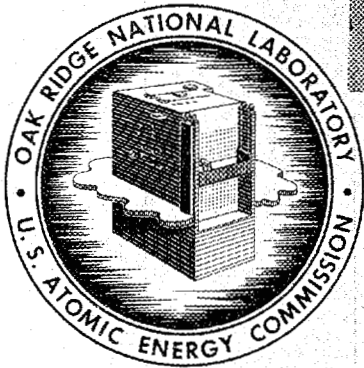


3 4456 0022351 3

ORNL-3778
UC-34 - Physics
TID-4500 (39th ed.)

PHYSICS DIVISION
ANNUAL PROGRESS REPORT
FOR PERIOD ENDING DECEMBER 31, 1964

CENTRAL RESEARCH LIBRARY
DOCUMENT COLLECTION
LIBRARY LOAN COPY
DO NOT TRANSFER TO ANOTHER PERSON
If you wish someone else to use the
document, send in name and address
and the library will arrange to loan it.



OAK RIDGE NATIONAL LABORATORY
operated by
UNION CARBIDE CORPORATION
for the
U.S. ATOMIC ENERGY COMMISSION

Printed in USA. Price \$6.00. Available from the Clearinghouse for Federal
Scientific and Technical Information, National Bureau of Standards,
U.S. Department of Commerce, Springfield, Virginia

LEGAL NOTICE

This report was prepared as an account of Government sponsored work. Neither the United States, nor the Commission, nor any person acting on behalf of the Commission:

- A. Makes any warranty or representation, expressed or implied, with respect to the accuracy, completeness, or usefulness of the information contained in this report, or that the use of any information, apparatus, method, or process disclosed in this report may not infringe privately owned rights; or
- B. Assumes any liabilities with respect to the use of, or for damages resulting from the use of any information, apparatus, method, or process disclosed in this report.

As used in the above, "person acting on behalf of the Commission" includes any employee or contractor of the Commission, or employee of such contractor, to the extent that such employee or contractor of the Commission, or employee of such contractor prepares, disseminates, or provides access to, any information pursuant to his employment or contract with the Commission, or his employment with such contractor.

col 2 over
~~_____~~

ERRATUM

ORNL-3778

PHYSICS DIVISION ANNUAL PROGRESS REPORT
FOR PERIOD ENDING DECEMBER 31, 1964

- p. 25, Fig. 1: Labeling of horizontal axis should read " α (fermis⁻¹)"
- p. 91, col. 1, line 6: " $f_{7/2}$ " should read " $f_{5/2}$ resonance."
- p. 98, col. 2, line 9: "factors are much less than the proton - " should read "factors are much more than the proton - "
- p. 99, Fig. 2
(and in caption) " $d_{3/2}$ " should read " $d_{5/2}$ "
- p. 149, last line
col. 1 and continuing
in col. 2: "and also offered for sale separately by the National Academy of Sciences - National Research Council (NAS-NRC) Printing and Publishing Office, 2101 Constitution Avenue, Washington, D. C. 20418, at a price of about \$3.00" should read "and may be printed later in revised form as an issue of the new journal, Nuclear Data Compilations."
- p. 156, col. 2, line 1: "reaction (1)" should read "reaction (2) -"
- p. 156, col. 2, line 3: "reaction (2)" should read "reaction (1) -"

Central
Research Library
Document Collection

NOV 27 1967
pdb

ORNL-3778

Contract No. W-7405-eng-26

PHYSICS DIVISION
ANNUAL PROGRESS REPORT
For Period Ending December 31, 1964

J. L. Fowler, Director
H. B. Willard, Associate Director

MAY 1965

OAK RIDGE NATIONAL LABORATORY
Oak Ridge, Tennessee
operated by
UNION CARBIDE CORPORATION
for the
U. S. ATOMIC ENERGY COMMISSION



3 4456 0022351 3

FOREWORD

This is the seventh Physics Division progress report made on an annual basis. As in previous years, the report contains the abstracts for papers which have been published or which have been prepared for publication. In such cases, reprints or preprints of the articles will be available. Preliminary results of work in progress are reported, as previously, in more detail. Since this work is of a preliminary nature, the authors should be contacted with regard to the inclusion of any of these results in other publications.

“Indexing words” or “key words” for experimental papers on nuclear structure have been supplied by the authors. These appear in boxes just under the abstract or the authors’ names. Comments on the usefulness of these terms to researchers and to those who collect data will be welcome.



TABLE OF CONTENTS AND SUMMARY

NEUTRON DIFFRACTION INVESTIGATION OF CHROMIUM WITH SMALL ADDITIONS OF MANGANESE AND VANADIUM	
Y. Hamaguchi, E. O. Wollan, and W. C. Koehler	1
Abstract of paper to be published in the <i>Physical Review</i> .	
MAGNETIC STRUCTURE OF RARE-EARTH-COBALT (RCO₂) INTERMETALLIC COMPOUNDS	
R. M. Moon, W. C. Koehler, and J. J. Farrell	1
Abstract of paper submitted to the <i>Journal of Applied Physics</i> .	
THE MAGNETIC PROPERTIES OF RARE-EARTH METALS AND ALLOYS	
W. C. Koehler	2
Abstract of paper to be published in the <i>Journal of Applied Physics</i> .	
MAGNETIC STRUCTURE vs ELECTRON NUMBER FOR SOME RARE-EARTH INTERMETALLIC COMPOUNDS	
J. W. Cable, W. C. Koehler, and H. R. Child	2
Abstract of paper submitted to the <i>Journal of Applied Physics</i> .	
THE MAGNETIC PROPERTIES OF HEAVY RARE EARTHS DILUTED BY YTTRIUM AND LUTETIUM	
H. R. Child, W. C. Koehler, E. O. Wollan, and J. W. Cable	3
Abstract of paper submitted to the <i>Physical Review</i> .	
ALIGNMENT OF RARE-EARTH MOMENTS IN DILUTE Pd-Fe ALLOYS	
J. W. Cable, E. O. Wollan, W. C. Koehler, and H. R. Child	3
Abstract of published paper: <i>J. Phys. Chem. Solids</i> 25, 1453 (1964).	
DISTRIBUTION OF MAGNETIC MOMENTS IN Pd-3d AND Ni-3d ALLOYS	
J. W. Cable, E. O. Wollan, and W. C. Koehler	3
Abstract of paper submitted to the <i>Physical Review</i> .	
ANTIFERROMAGNETISM OF PRASEODYMIUM	
J. W. Cable, R. M. Moon, W. C. Koehler, and E. O. Wollan	4
Abstract of published letter: <i>Phys. Rev. Letters</i> 12, 553 (1964).	
EFFECTIVE MAGNETIC FIELD AND ISOMER SHIFT FOR Au-Ni ALLOYS AS A FUNCTION OF COMPOSITION	
L. D. Roberts, F. E. Obenshain, J. O. Thomson, W. K. Robinson, and W. B. Newbolt	4
The hyperfine structure (hfs) coupling and isomer shift for Au dissolved in Ni has been investigated as a function of composition. Within experimental error, the hfs coupling is found to be proportional to the alloy magnetic moment, and the isomer shift is found to be proportional to the atomic fraction of Au.	
CORRELATION OF THE MÖSSBAUER ISOMER SHIFT AND THE RESIDUAL ELECTRICAL RESISTIVITY FOR ¹⁹⁷Au ALLOYS	
L. D. Roberts, R. L. Becker, F. E. Obenshain, and J. O. Thomson	6
Abstract of published paper: <i>Phys. Rev.</i> 137, A895 (1965).	

HYPERFINE STRUCTURE OF THE 14.4-kev GAMMA RAY OF ^{57}Fe IN HYDRATED FERRIC AMMONIUM SULFATE AS A FUNCTION OF THE MAGNETIZATION OF THE SALT	
F. E. Obenshain, L. D. Roberts, C. F. Coleman, D. W. Forester, and J. O. Thomson.....	7
Abstract of a paper submitted to <i>Physical Review Letters</i> .	
MÖSSBAUER MEASUREMENTS OF THE ^{57}Fe HYPERFINE STRUCTURE COUPLING IN FeRh ALLOYS NEAR 50 at. % RHODIUM	
D. W. Forester, F. E. Obenshain, H. H. Wegener, L. D. Roberts, and J. O. Thomson.....	7
Abstract of paper submitted to the <i>Physical Review</i> .	
"EXPLOSION" OF MULTICHARGED MOLECULAR IONS: CHEMICAL CONSEQUENCES OF INNER SHELL VACANCIES IN ATOMS	
T. A. Carlson and R. M. White	8
Abstract of paper to be published in the <i>Proceedings of the Symposium on Chemical Effects Associated with Nuclear Reactions and Radioactive Transformation, Vienna, Austria, December 7-11, 1964</i> .	
ELECTRON SHAKE-OFF RESULTING FROM K SHELL IONIZATION IN NEON MEASURED AS A FUNCTION OF PHOTOELECTRON VELOCITY	
T. A. Carlson and M. O. Krause	9
Abstract of paper to be submitted to the <i>Physical Review</i> .	
MULTIPLE IONIZATION IN ATOMS AND ITS RELATIONSHIP WITH ELECTRON CORRELATION	
T. A. Carlson and M. O. Krause	9
Measurements have been made of the relative abundance of ions resulting from photo-ionization in the outer shells of He, Ne, and Ar and from the <i>L-MM</i> Auger process in Ar. It has been suggested that most of the excess ionization observed is related to the phenomenon of electron correlation.	
EXPERIMENTAL EVIDENCE FOR DOUBLE ELECTRON EMISSION IN AN AUGER PROCESS	
T. A. Carlson and M. O. Krause	13
Abstract of paper submitted to <i>Physical Review Letters</i> .	
ATOMIC READJUSTMENT TO VACANCIES IN THE K AND L SHELLS OF ARGON	
T. A. Carlson and M. O. Krause	13
Abstract of paper to be published in the <i>Physical Review</i> .	
DETERMINATION OF THE L ENERGY LEVELS IN KRYPTON BY THE PHOTOELECTRON METHOD	
M. O. Krause	13
Abstract of paper to be submitted to the <i>Physical Review</i> .	
INFRARED SPECTRAL STUDY OF SECOND-ORDER TRANSITIONS IN CF_4	
R. G. Steinhardt, H. W. Morgan, and P. A. Staats	14
The infrared spectra of liquid and solid CF_4 have been observed, and discontinuous changes in band width and intensity have been found at the first- and second-order transition temperatures. The combination band ($\nu_2 + \nu_4$) shows virtually no discontinuity at these points, and the calculations are being made on the CF_4 molecular lattice in an attempt to explain this behavior.	
INFRARED ABSORPTION SPECTRA OF LIQUID BORON TRIFLUORIDE	
R. G. Steinhardt, M. W. Jordan, and G. E. S. Fetsch.....	15
Abstract of paper submitted to the <i>Journal of Chemical Physics</i> .	

LOW-TEMPERATURE LIQUID INFRARED ABSORPTION CELL	
H. W. Morgan, P. A. Staats, and R. G. Steinhardt	15
A low-temperature liquid infrared cell has been constructed for use in the range 300–77°K. Silver chloride or cesium bromide windows are employed with a special flange to maintain pressure while the temperature changes. Spectra have been recorded from a number of low-temperature liquids.	
SIMPLIFIED CONSTRUCTION OF A HELIUM-NEON VISIBLE LASER	
K. L. Vander Sluis, G. K. Werner, P. M. Griffin, H. W. Morgan, O. B. Rudolph, and P. A. Staats.....	16
Abstract of paper accepted by the <i>American Journal of Physics</i> for publication in March 1965.	
EFFECT OF PLASMA POTENTIAL ON MINIMUM-B STABILITY	
T. K. Fowler	17
Abstract of paper submitted to the <i>Physics of Fluids</i> .	
BOUNDS ON PLASMA FLUCTUATIONS AND ANOMALOUS DIFFUSION	
T. K. Fowler	17
Abstract of paper submitted to the <i>Physics of Fluids</i> .	
AMBIPOLAR SCATTERING LOSSES FROM MAGNETIC MIRRORS	
T. K. Fowler and M. Rankin	18
Abstract of published paper: <i>J. Nucl. Energy: Pt. C</i> 6, 513 (1964).	
IMAGE FORMATION IN A HIGH-RESOLUTION ELECTRON MICROSCOPE	
T. A. Welton.....	19
A detailed numerical study of the image plane intensity distribution in an electron microscope has been performed for various configurations of atoms in the object plane, for a variety of beam energies, for different defocus distances, and for primary and secondary spherical aberration. An apparently feasible high-resolution instrument will reliably image medium and heavy atoms.	
RELATIVISTIC QUANTUM MECHANICS WITH A FUNDAMENTAL LENGTH	
T. A. Welton.....	22
A formalism has been constructed for the systematic introduction of a fundamental length into relativistic quantum mechanics by use of noncommuting coordinate operators.	
HARTREE-FOCK CALCULATIONS OF FINITE NUCLEI	
K. T. R. Davies and M. Baranger	22
A different way of setting up parameters for Green's velocity-dependent potential is discussed. It is suggested that this potential may be used as an "effective interaction" in nuclear Hartree-Fock calculations. A new method for calculating oscillator brackets has been developed and should be very useful in computations which involve only relative <i>s</i> , <i>p</i> , and <i>d</i> waves.	
CALCULATION OF THE PROPERTIES OF THE GROUND STATE OF ¹⁶O IN THE BRUECKNER APPROXIMATION	
R. L. Becker and A. D. MacKellar	24
A reaction-matrix calculation for closed-shell nuclei is described. The Bethe-Goldstone equation is solved directly for nuclear pairs initially in harmonic oscillator states. The tensor force is treated accurately by solving coupled equations. Some results are presented for ¹⁶ O.	

A COMPUTER PROGRAM FOR LARGE-SHELL-MODEL CALCULATIONS	
E. C. Halbert, J. B. McGroory, S. S. M. Wong, and J. B. French.....	25
An IBM 7090 program has been written to carry out large-shell-model calculations.	
DISTORTED-WAVE CALCULATIONS AND SPECTROSCOPIC FACTORS	
G. R. Satchler	26
Abstract of invited paper presented at Symposium on Nuclear Spectroscopy with Direct Reactions, Chicago, March 9-11, 1964. Proceedings of conference published in <i>Nuclear Spectroscopy with Direct Reactions. II. Proceedings</i> , ANL-6878, p. 23.	
"FINITE-RANGE" EFFECTS IN THE DISTORTED-WAVE THEORY OF STRIPPING REACTIONS	
R. M. Drisko and G. R. Satchler.....	26
Abstract of published paper: <i>Phys. Letters</i> 9 , 342 (1964).	
OPTICAL-MODEL ANALYSIS OF "QUASI-ELASTIC" (p,n) REACTIONS	
G. R. Satchler, R. M. Drisko, and R. H. Bassel.....	26
Abstract of published paper: <i>Phys. Rev.</i> 136 , B637 (1964).	
THE SHELL MODEL AND INELASTIC SCATTERING BY NUCLEI	
R. H. Bassel, R. M. Drisko, R. M. Haybron, M. B. Johnson, L. W. Owen, and G. R. Satchler.....	27
Inelastic scattering from nuclei is being studied using an effective two-body interaction and shell-model wave functions.	
FORM FACTORS FOR NUCLEAR STRIPPING REACTIONS	
W. T. Pinkston and G. R. Satchler.....	27
Abstract of paper to be submitted for publication in <i>Nuclear Physics</i> .	
SLATER INTEGRALS AND FORM FACTORS FOR INELASTIC SCATTERING USING REALISTIC SINGLE-PARTICLE WAVE FUNCTIONS: THE CODE ATHENA	
M. B. Johnson and L. W. Owen.....	28
Abstract of ORNL-TM-964.	
PRIOR-FORM DWBA STRIPPING PROGRAM	
F. P. Gibson	28
A computer program is being written which calculates the <i>d-p</i> stripping differential cross section, using the prior form of the distorted-wave Born approximation matrix element.	
RADIAL INTEGRALS USING REALISTIC SINGLE-PARTICLE WAVE FUNCTIONS AND THE CODE OVERLAP	
L. W. Owen.....	29
Abstract of ORNL-TM-958.	
ANALYSIS OF THE SCATTERING OF 28-Mev ALPHA PARTICLES	
G. R. Satchler	29
Abstract of paper submitted to <i>Nuclear Physics</i> .	

- THE REACTIONS $^{48}\text{Ti}(n,d)^{47}\text{Sc}$, $^{16}\text{O}(n,d)^{15}\text{N}$, $^{10}\text{B}(n,d)^9\text{Be}$, AND $^6\text{Li}(n,d)^5\text{He}$ AT 14.4 Mev**
 V. Valkovic, G. Paic, I. Slaus, P. Tomas, M. Cerineo, and G. R. Satchler..... 29
 Abstract of paper to be submitted to the *Physical Review*.
 NUCLEAR REACTIONS. $^{48}\text{Ti}(n,d)$, $^{16}\text{O}(n,d)$, $^{10}\text{B}(n,d)$, $^6\text{Li}(n,d)$, $E = 14.4$ Mev; measured $\sigma(E_d, \theta)$. ^{47}Sc , ^{15}N , ^9Be , ^5He deduced levels, π , l , spectroscopic factors.
- EXCITATION OF LOW-LYING LEVELS IN ^{40}Ca BY (p,p') SCATTERING AT $E_p = 55$ Mev**
 K. Yagi, H. Ejiri, M. Furukawa, Y. Ishizaki, M. Koike, K. Matsuda, Y. Nakajima, I. Nonaka, Y. Saji,
 E. Tanaka, and G. R. Satchler..... 30
 Abstract of published paper: *Phys. Letters* **10**, 186 (1964).
 NUCLEAR REACTIONS. $^{40}\text{Ca}(p,p')$, $E = 55$ Mev; measured $\sigma(E_p, \theta)$. ^{40}Ca deduced levels, J , π , $B(\lambda)$.
- PROTON EXCITATION OF VIBRATIONAL STATES OF ^{126}Te**
 G. C. Pramila, R. Middleton, T. Tamura, and G. R. Satchler..... 30
 Abstract of published paper: *Nucl. Phys.* **61**, 448 (1965).
 NUCLEAR REACTIONS. $^{126}\text{Te}(p,p')$, $E = 12$ Mev; measured $\sigma(E_p, \theta)$. ^{126}Te deduced levels, J , π , $B(\lambda)$.
- ELASTIC SCATTERING OF DEUTERONS BY ^{40}Ca**
 R. H. Bassel, R. M. Drisko, and G. R. Satchler..... 31
 Abstract of published paper: *Phys. Rev.* **136**, B960 (1964).
 NUCLEAR REACTIONS. $^{40}\text{Ca}(d,d)$, $E = 7, 8, 9, 10, 11, 12$ Mev; measured $\sigma(\theta)$.
- $^{40}\text{Ca}(d,p)^{41}\text{Ca}$, A TEST OF THE VALIDITY OF THE DISTORTED-WAVE BORN APPROXIMATION**
 L. L. Lee, Jr., J. P. Schiffer, B. Zeidman, G. R. Satchler, R. M. Drisko, and R. H. Bassel..... 31
 Abstract of published paper: *Phys. Rev.* **136**, B971 (1964).
 NUCLEAR REACTIONS. $^{40}\text{Ca}(d,p)$, $E = 7, 8, 9, 10, 11, 12$ Mev; measured $\sigma(E_p, \theta)$. ^{41}Ca deduced levels, l , π , spectroscopic factors.
- LEVELS IN ^{43}Ca AND ^{46}Ca STUDIED BY THE $^{43}\text{Ca}(d,d')$, $^{46}\text{Ca}(d,d')$, AND $^{46}\text{Ca}(p,p')$ REACTIONS**
 T. A. Belote, J. H. Bjerregaard, Ole Hansen, and G. R. Satchler..... 32
 Abstract of paper submitted to the *Physical Review*.
 NUCLEAR REACTIONS. $^{43}\text{Ca}(d,d')$, $E = 8.522$ Mev; $^{46}\text{Ca}(d,d')$, $E = 10$ Mev; $^{46}\text{Ca}(p,p')$, $E = 7$ Mev; measured $\sigma(E', \theta)$. ^{43}Ca , ^{46}Ca deduced levels, π , l .
- LOW-LYING LEVELS IN ^{42}Ca EXCITED BY THE $^{43}\text{Ca}(d,t)$ REACTION**
 J. H. Bjerregaard, H. R. Blieden, O. Hansen, G. Sidenius, and G. R. Satchler..... 32
 Abstract of published paper: *Phys. Rev.* **136**, B1348 (1964).
 NUCLEAR REACTIONS. $^{43}\text{Ca}(d,t)$, $E = 8.5$ Mev; measured $\sigma(E_t, \theta)$. ^{42}Ca deduced levels, l , π , spectroscopic factors.
- ELASTIC SCATTERING OF ^3He AND THE $(^3\text{He},d)$ REACTION**
 R. H. Bassel, G. R. Satchler, and R. M. Drisko..... 33
 Abstract of paper presented at the International Conference on Nuclear Physics, Paris, July 2-8, 1964. Proceedings of the conference will be published in *Proceedings of the International Conference on Nuclear Physics*.
- SHELL-MODEL SELECTION RULES AND EXCITATION OF 4^+ STATES IN THE $\text{Ti}(\alpha, \alpha')$ REACTION**
 G. R. Satchler, J. L. Yntema, and H. W. Broek..... 33
 Abstract of published paper: *Phys. Letters* **12**, 55 (1964).
 NUCLEAR REACTIONS. $^{46,48,50}\text{Ti}(\alpha, \alpha')$, $E = 43$ Mev, measured $\sigma(\theta)$. $^{46,48,50}\text{Ti}$ deduced levels, J , π .

WIDE-ANGLE SCATTERING OF 43-Mev ALPHA PARTICLES BY ^{58}Ni	
H. W. Broek, J. L. Yntema, B. Buck, and G. R. Satchler	33
Abstract of paper submitted to <i>Nuclear Physics</i> .	
NUCLEAR REACTIONS. $^{58}\text{Ni}(\alpha, \alpha')$, $E = 43$ Mev, measured $\sigma(E_{\alpha'}, \theta)$. ^{58}Ni deduced levels, $J, \pi, B(\lambda)$.	
OPTICAL-MODEL ANALYSIS OF 182-Mev PROTON SCATTERING	
G. R. Satchler and R. M. Haybron.....	34
Abstract of published paper: <i>Phys. Letters</i> 11, 313 (1964).	
SYMPLECTIC SYMMETRY IN $f_{7/2}$ SHELL NUCLEI	
J. N. Ginocchio	34
Abstract of published paper: <i>Nucl. Phys.</i> 63, 449 (1965).	
ANALYSES OF THE SCATTERING OF NUCLEAR PARTICLES BY COLLECTIVE NUCLEI IN TERMS OF THE COUPLED-CHANNEL CALCULATION	
Taro Tamura.....	34
Abstract of paper submitted to the <i>Physical Review</i> .	
ADIABATIC AND NONADIABATIC COUPLED-CHANNEL CALCULATIONS OF THE SCATTERING OF PROTONS BY DEFORMED NUCLEI	
Taro Tamura.....	35
Abstract of published paper: <i>Phys. Letters</i> 12, 121 (1964).	
EXCITATION OF THE UNNATURAL-PARITY 3^+ STATE IN ^{24}Mg IN THE INELASTIC SCATTERING OF ALPHA PARTICLES	
Taro Tamura.....	35
Abstract of paper submitted to <i>Nuclear Physics</i> .	
POSSIBLE ADMIXTURE OF ONE-PHONON 2^+-STATE AMPLITUDE TO THE SECOND EXCITED STATE OF ^{64}Zn	
Taro Tamura.....	37
Scattering of 17.5-Mev protons by ^{64}Zn was analyzed in terms of the coupled-channel calculation.	
INELASTIC SCATTERING OF PROTONS BY ^{114}Cd AND POSSIBLE QUADRUPOLE-OCTUPOLE TWO-PHONON STATES	
M. Sakai and T. Tamura	37
Abstract of published paper: <i>Phys. Letters</i> 10, 323 (1964).	
NUCLEAR REACTIONS. $^{114}\text{Cd}(p, p')$, enriched target, $E_p = 12.16$ Mev; measured $\sigma(\theta)$, p' spectrum. ^{114}Cd deduced levels, J, π .	
COUPLED-CHANNEL ANALYSIS OF THE SCATTERING OF PROTONS BY ^{165}Ho AND ^{156}Gd	
Taro Tamura.....	38
Abstract of published paper: <i>Phys. Letters</i> 9, 334 (1964).	
TOTAL NEUTRON CROSS SECTIONS AT 1.44 eV	
L. A. Rayburn and E. O. Wollan.....	38
Abstract of paper to be published in <i>Nuclear Physics</i> .	

LEVEL SPACINGS AND s-WAVE NEUTRON STRENGTH FUNCTIONS OF THE ISOTOPES OF HAFNIUM

T. Fuketa and J. A. Harvey 38

Neutron transmission measurements from 0.2 to ~ 240 eV have been made on enriched samples of the six isotopes of hafnium. About one hundred resonances were analyzed to obtain the average level spacing and s-wave strength function for each isotope.

NUCLEAR REACTIONS. ^{174}Hf , ^{176}Hf , ^{177}Hf , ^{178}Hf , ^{179}Hf , ^{180}Hf ; measured σ_{nT} . Deduced resonance parameters, E_0 , Γ_n , Γ_γ ; level densities and $\bar{\Gamma}_n^0/D$ for isotopes. Enriched targets.

HIGH-RESOLUTION MEASUREMENTS OF THERMAL NEUTRON CAPTURE GAMMA RAYS

G. G. Slaughter and J. A. Harvey 44

A lithium-drifted germanium crystal was used to make high-resolution measurements of the gamma rays following thermal neutron capture in samples of Bi, Nb, Y, and enriched samples of ^{238}U and the Sn isotopes. Gamma-ray energies (measured to ± 10 keV) and relative intensities are correlated with level energies and spins measured by the (d,p) reaction.

NUCLEAR REACTIONS. Bi(n,γ), thermal; $^{238}\text{U}(n,\gamma)$, thermal; Nb(n,γ), thermal; $^{117,118,120}\text{Sn}(n,\gamma)$, thermal; Y(n,γ), thermal; measured E_γ , I_γ . ^{210}Bi , ^{239}U , ^{94}Nb , $^{118,119,121}\text{Sn}$, ^{90}Y deduced levels, J , π . ^{238}U , $^{117,118,120}\text{Sn}$ enriched target.

CAPTURE CROSS-SECTION MEASUREMENTS ON ^{182}W , ^{183}W , ^{184}W , AND ^{186}W AT THE RPI LINAC

R. C. Block, J. E. Russell, and R. W. Hockenbury 53

Capture cross-section measurements were made upon samples of ^{182}W , ^{183}W , ^{184}W , and ^{186}W with the 1.25-m-diam liquid-scintillator detector at the Rensselaer Polytechnic Institute's linear accelerator. In the energy region up to 4000 eV, 66 resonances were detected in ^{182}W , 47 in ^{184}W , and 45 in ^{186}W ; 116 resonances were observed in ^{183}W up to 3000 eV. The data have been reduced to capture cross sections as a function of energy from ~ 35 eV to 10 keV.

NUCLEAR REACTIONS. ^{182}W , ^{183}W , ^{184}W , $^{186}\text{W}(n,\gamma)$. Measured $\sigma_{n\gamma}(E_n)$ from ~ 35 eV to 10 keV, average level spacings. Enriched targets.

GAMMA-RAY SPECTRA FROM NEUTRONS CAPTURED IN ^{56}Fe AT THE 1148-eV RESONANCE

R. C. Block 64

The large NaI crystal at the ORNL fast chopper was used to measure the gamma-ray spectrum from neutrons captured in the 1148-eV resonance in ^{56}Fe . Five distinct gamma rays were observed at energies of 7.64, 7.48 ± 0.08 , 6.36 ± 0.04 , 4.9 ± 0.1 , and 4.4 ± 0.1 MeV with relative strengths of approximately 10, 2, 4, 1, and 1 respectively. Comparative measurements were carried out for thermal neutron capture in iron, and it was observed that the intensity of photons per capture was the same in resonance and thermal capture for the 7.64-MeV gamma ray.

NUCLEAR REACTIONS. $^{56}\text{Fe}(n,\gamma)$ at 1148-eV resonance; measured E_γ , I_γ . Deduced partial radiation widths and J of resonance. Natural target.

STUDY OF THE EVEN-EVEN COMPOUND NUCLEI AT THE FIRST s-WAVE STRENGTH FUNCTION RESONANCE

W. M. Good, Daniel Paya, and Rolf Wagner 69

The even-odd target nuclei in the region of the first s-wave resonance have been studied for manifestation of the 28-neutron shell closure. Results indicate the strength functions predicted by optical model, but non-uniformly distributed below 60 keV.

NUCLEAR REACTIONS. ^{43}Ca , ^{47}Ti , ^{49}Ti , ^{53}Cr , ^{57}Fe , ^{63}Cu , ^{65}Cu , measured $\sigma_n(E)$, $E \leq 60$ keV. ^{44}Ca , ^{48}Ti , ^{50}Ti , ^{54}Cr , ^{58}Fe , ^{64}Cu , ^{66}Cu , deduced levels, I_γ , level density, resonances, resonance parameters, $\bar{\Gamma}_n^0/D$. Enriched targets.

A STUDY OF THE GAMMA-RAY SPECTRA EMITTED IN THE RESONANCE CAPTURE OF NEUTRONS BY ^{19}F

J. R. Bird, J. A. Biggerstaff, J. H. Gibbons, and W. M. Good 76

Abstract of paper submitted for publication in the *Physical Review*.NUCLEAR REACTIONS. $^{19}\text{F}(p,\gamma)$, measured $\sigma(E, E_\gamma)$, $E \leq 80$ kev. ^{20}F , deduced relative intensities, γ -reduced widths. Natural target.**A STUDY OF THE RESONANCE STRUCTURE OF THE EVEN ZIRCONIUM ISOTOPES AT BELOW 60-kev NEUTRON ENERGY**

J. A. Biggerstaff, W. M. Good, and H. J. Kim 76

The neutron resonance structure of the even isotopes of zirconium has been studied up to 60 kev. Below about 20 kev, the average strength is $(1.2 \pm 0.8) \times 10^{-4}$. From 20 kev to 60 kev, the strength is $(2.5 \pm 0.6) \times 10^{-4}$.NUCLEAR REACTIONS. ^{90}Zr , ^{92}Zr , ^{94}Zr , ^{96}Zr , measured $\sigma_T(E)$, $E \leq 60$ kev. ^{91}Zr , ^{93}Zr , ^{95}Zr , ^{97}Zr , deduced levels, level density, resonances, resonance parameters Γ_n^0/D . Enriched targets.**NEUTRON CAPTURE DATA AT STELLAR TEMPERATURES**

R. L. Macklin and J. H. Gibbons 81

Abstract of published paper: *Rev. Mod. Phys.* **37**, 166 (1965).**RESONANCE NEUTRON CAPTURE AND TRANSMISSION IN SULFUR, IRON, AND LEAD**

R. L. Macklin, P. J. Pasma, and J. H. Gibbons 82

Abstract of published paper: *Phys. Rev.* **136**, B695 (1964).NUCLEAR REACTIONS. Targets ^{32}S , ^{56}Fe , $^{206,7,8}\text{Pb}$, (n,γ and total), $E = 10$ -80 kev. Measured σ_{nT} , σ_{nA} . Deduced resonances, resonance parameters, Γ , Γ_γ , J , π , level densities (for $l = 0, 1$ separately), effective nuclear radii. Enriched and natural targets.**THE INTERACTION OF 350-kev POLARIZED NEUTRONS WITH ORIENTED ^{165}Ho NUCLEI**

R. Wagner, P. D. Miller, T. Tamura, and H. Marshak 82

Abstract of paper to be submitted to the *Physical Review*. A preliminary account has been published: *Phys. Letters* **10**, 216 (1964).NUCLEAR REACTIONS. $^{165}\text{Ho}(n)$, $E_n = 350$ kev; measured $\sigma_T(\theta, n$ polarization).**METHOD FOR OBTAINING BURSTS OF POLARIZED NEUTRONS OF ENERGY 10-700 kev**

J. W. T. Dabbs and J. A. Harvey 83

Polarization by the use of the right-left asymmetry in scattering from He, together with moderation by graphite, appears to be possible at the proposed linac.

DIFFERENTIAL SCATTERING OF NEUTRONS FROM ^{16}O

C. H. Johnson and J. L. Fowler 85

A phase-shift analysis of differential scattering of neutrons from ^{16}O at a number of energies between 2 and 4 Mev gives the following resonant parameters for resonances in ^{17}O : $(3.40, \frac{3}{2}^+, 0.5)$ $(3.75, \frac{3}{2}^-, 0.2)$ $(3.77, \frac{5}{2}^-, 0.1)$ $(3.82, \frac{3}{2}^+, 0.05)$, where the resonant energy in Mev is followed by the J -value, parity, and reduced widths in units of $3\hbar^2/2ma^2$.NUCLEAR REACTIONS. $^{16}\text{O}(n,n)$, $E_n = 2.25$ -4.00 Mev; measured $\sigma(\theta)$. ^{17}O , deduced resonance parameters, phase shifts.**RESONANCE PARAMETERS FOR NEUTRON SCATTERING FROM ^{208}Pb**

J. L. Fowler 89

Results are presented of a partial-wave phase-shift analysis of neutron scattering from ^{208}Pb . Reduced widths of resonances are discussed in terms of intermediate states.NUCLEAR REACTIONS. $^{208}\text{Pb}(n)$, enriched target, $E_n = 0.7$ -1.9 Mev; measured $\sigma(E, \theta)$. ^{209}Pb , deduced resonance parameters, phase shifts.

EXCITATION OF COLLECTIVE STATES BY THE INELASTIC SCATTERING OF 14-Mev NEUTRONS

P. H. Stelson, R. L. Robinson, H. J. Kim, J. Rapaport, and G. R. Satchler 93

Abstract of paper submitted for publication in *Nuclear Physics*.NUCLEAR REACTIONS. (n,n) , (n,n') ; Bi, Pb, Sb, Sn, Cd, Zn, Ni, Cr, S, P, Si, Al, Mg; $E_n = 14$ Mev, absolute $\sigma(\theta)$, β_2 , β_3 .**ELASTIC SCATTERING OF 17- TO 21-Mev NEUTRONS FROM ^{12}C**

M. V. Harlow, Jr., R. L. Robinson, and B. B. Kinsey 93

Abstract of paper submitted for publication in *Nuclear Physics*.NUCLEAR REACTIONS. $^{12}\text{C}(n,n)$, $E_n = 17-21$ Mev; measured $\sigma_T(E)$, $\sigma(E,\theta)$. ^{13}C , deduced level.**TOTAL NEUTRON CROSS SECTIONS OF HYDROGEN AND CARBON IN THE 20-30 Mev REGION**

M. L. West II, C. M. Jones, and H. B. Willard 94

The total cross sections of ^1H and ^{12}C for neutrons have been measured from 19.58 to 30.46 Mev.NUCLEAR REACTIONS. $^1\text{H}(n,n)$, $^{12}\text{C}(n,n)$, polyethylene and graphite samples, $E_n = 19.58-30.46$ Mev, measured $\sigma_t(E)$.**A STUDY OF FLUCTUATING LOW-ENERGY (p,n) REACTION CROSS SECTION**

H. J. Kim 95

Abstract of published paper: *Phys. Letters* **14**, 51 (1956)NUCLEAR REACTIONS. $^{53}\text{Cr}(p,n)^{53}\text{Mn}$, $2.3 < E < 3.1$ Mev, measured $\sigma(E_n)$.**CROSS SECTIONS FOR (p,n) REACTIONS IN FIVE ISOTOPES OF TIN**

R. L. Kernell and C. H. Johnson 95

Cross sections for (p,n) reactions have been measured from 2.5 to 5.5 Mev for five isotopes of tin. At 5 Mev, the cross sections range from 16.2 mb for ^{117}Sn to 21.5 mb for ^{124}Sn . A value of $Q = -3465 \pm 7$ kev was determined for the reaction $^{120}\text{Sn}(p,n)^{120}\text{Sb}$.NUCLEAR REACTIONS. $^{117}\text{Sn}(p,n)$, $^{119}\text{Sn}(p,n)$, $^{120}\text{Sn}(p,n)$, $^{122}\text{Sn}(p,n)$, $^{124}\text{Sn}(p,n)$, $E = 2.5-5.5$ Mev; measured $\sigma(E)$, Q . Enriched targets.**ISOBARIC ANALOG STATES IN ^{90}Zr , ^{116}Sb , ^{118}Sb , ^{120}Sb**

C. H. Johnson and R. L. Kernell 97

The main purpose of this work was to measure with good resolution the (p,n) cross sections near isobaric analog resonances for targets of ^{89}Y , ^{115}Sn , ^{117}Sn , and ^{119}Sn . The energies for the well known 2^- and 3^- resonances in $^{89}\text{Y}(p,n)$ are found to be 4804 ± 6 kev and 5007 ± 6 kev, and the total widths Γ for both are about 25 kev. Resonances are observed at 4330 ± 15 kev for $^{115}\text{Sn}(p,n)$, 4491 ± 6 kev for $^{117}\text{Sn}(p,n)$, and 4642 ± 6 kev for $^{119}\text{Sn}(p,n)$. The positions of these resonances indicate that they are 0^+ analogs to the ground states of even tin isotopes. The natural widths, Γ , for the two heavier targets are each 30 kev, and the width for the ^{115}Sn target is about 30 kev. In addition, a threshold was found at 4751 ± 7 kev for $^{89}\text{Y}(p,n)$ which corresponds to a level at 1084 ± 8 kev in ^{90}Zr . The fact that this threshold is observed indicates that $\frac{3}{2}^-$ is the correct one of the two possible assignments, $\frac{1}{2}^-$ or $\frac{3}{2}^-$.

NUCLEAR REACTIONS. $^{89}\text{Y}(p,n)$, $^{115}\text{Sn}(p,n)$, $^{117}\text{Sn}(p,n)$, $^{119}\text{Sn}(p,n)$, $E = 3.6$ to 5.1 Mev; measured $\sigma(E)$, Q . ^{90}Zr , ^{116}Sb , ^{118}Sb , ^{120}Sb , deduced levels, J , Γ . Enriched targets.**ELASTIC AND INELASTIC SCATTERING OF 12- AND 13-Mev PROTONS FROM ^{106}Pd AND ^{108}Pd**

R. L. Robinson, J. L. C. Ford, Jr., P. H. Stelson, and G. R. Satchler 101

The differential cross sections for elastic scattering and inelastic scattering of 12- and 13-Mev protons to the quadrupole, two phonon, and octupole states of ^{106}Pd and ^{108}Pd have been measured. Comparisons are made with the predictions of the distorted-wave theory for direct nuclear interactions.NUCLEAR REACTIONS. $^{106,108}\text{Pd}(p,p')$, enriched targets, $E_p = 12, 13$ Mev; measured $\sigma(\theta)$. $^{106,108}\text{Pd}$, deduced levels, β_2 , β_3 .

SEQUENTIAL EMISSION IN THE REACTION ${}^7\text{Li}(d,n)2\alpha$

C. M. Jones, J. K. Bair, C. H. Johnson, H. B. Willard, and M. Reeves III 104

Abstract of paper presented at Topical Conference on Correlations of Particles Emitted in Nuclear Reactions, Gatlinburg, Tenn., October 15–17, 1964. (Proceedings of conference will be published in *Reviews of Modern Physics*.)

NUCLEAR REACTIONS. ${}^7\text{Li}(d,2\alpha)$; measured $\sigma(E; E_{\alpha_1}, E_{\alpha_2}, \theta_{\alpha_1}, \theta_{\alpha_2}, \phi_{\alpha_1}, \phi_{\alpha_2})$. Deduced reaction mechanism. Enriched target.

Q VALUES OF THREE-BODY NUCLEAR REACTIONS

Mark Reeves III 104

Abstract of ORNL-TM-938.

 ${}^{15}\text{N}({}^3\text{He},p){}^{17}\text{O}$ AND ${}^{15}\text{N}({}^3\text{He},d){}^{16}\text{O}$ REACTIONS AND INTERMEDIATE RESONANCES

K. K. Seth, G. Walter, P. D. Miller, J. A. Biggerstaff, and G. R. Satchler 104

The ${}^{15}\text{N}({}^3\text{He},p){}^{17}\text{O}$ and ${}^{15}\text{N}({}^3\text{He},d){}^{16}\text{O}$ reactions have been investigated. An angular distribution was measured at $E_{{}^3\text{He}} = 6.41$ Mev. The results were interpreted in terms of states in ${}^{16}\text{O}$ and ${}^{17}\text{O}$ consisting of one or two particles, respectively, being captured into $2s-1d$ shells. The $p_{1/2}^{-1}$ core of the ${}^{15}\text{N}$ target was preserved.

NUCLEAR REACTIONS. ${}^{15}\text{N}({}^3\text{He},d){}^{16}\text{O}$, ${}^{15}\text{N}({}^3\text{He},p){}^{17}\text{O}$ reactions. Angular distribution at $E_{{}^3\text{He}} = 6.41$ Mev. Deduced character of states in residual nuclei.

TOTAL CROSS SECTION FOR ${}^9\text{Be}(\alpha,n)$

J. H. Gibbons and R. L. Macklin 110

Abstract of paper accepted by the *Physical Review*.

NUCLEAR REACTIONS. ${}^9\text{Be}(\alpha,n)$, $E = 1.7-10.5$ Mev; measured $\sigma(E)$. Nucleus ${}^{13}\text{C}$ deduced levels, Γ . Other than ${}^{12}\text{C}$, ${}^{12}\text{C}^*$ final states dominant near $E_{\alpha} = 10$ Mev. Natural target.

TOTAL NEUTRON YIELD FROM THE REACTION ${}^{14}\text{C}(\alpha,n){}^{17}\text{O}$

J. K. Bair, J. L. C. Ford, Jr., and C. M. Jones 111

Abstract of a paper to be submitted to the *Physical Review*.

NUCLEAR REACTIONS. ${}^{14}\text{C}(\alpha,n)$; measured $\sigma(E)$. ${}^{18}\text{O}$ deduced levels, Γ .

COULOMB EXCITATION OF VIBRATIONAL TRIPLET STATES AND OCTUPOLE STATES IN THE EVEN CADMIUM NUCLEI

F. K. McGowan, R. L. Robinson, P. H. Stelson, and J. L. C. Ford, Jr. 111

Abstract of paper submitted to *Nuclear Physics*.

NUCLEAR REACTIONS. ${}^{110,112,114,116}\text{Cd}({}^{16}\text{O}, {}^{16}\text{O}'\gamma)$, ${}^{110,112,114,116}\text{Cd}(\alpha, \alpha'\gamma)$, enriched targets, $E_{{}^{16}\text{O}} = 42-49$ Mev, $E_{\alpha} = 9-10.9$ Mev; measured γ , $\gamma\gamma$ spectra. ${}^{110,112,114,116}\text{Cd}$, deduced levels, J , π , $B(E2)$, $B(E3)$.

LOW-LYING LEVELS IN ${}^{75}\text{As}$

R. L. Robinson, F. K. McGowan, J. L. C. Ford, Jr., and P. H. Stelson 112

Seven levels in ${}^{75}\text{As}$ below 900 keV have been Coulomb excited with alpha particles and oxygen ions. Level properties for these are reported.

NUCLEAR REACTIONS. ${}^{75}\text{As}(\alpha, \alpha'\gamma)$, $E_{\alpha} = 3.5-8.1$ Mev, ${}^{75}\text{As}({}^{16}\text{O}, {}^{16}\text{O}'\gamma)$, $E_{{}^{16}\text{O}} = 36-38$ Mev; measured E_{γ} , I_{γ} , $\gamma\gamma$ spectra, $\gamma^{16}\text{O}$ spectra, $\gamma(\theta)$. ${}^{75}\text{As}$, deduced levels, J , π , $B(E2)$, $B(M1)$, δ , $\tau_{1/2}$.

GAMMA-RAY SPECTROSCOPY WITH A LITHIUM-DRIFTED GERMANIUM DETECTOR

R. L. Robinson, P. H. Stelson, F. K. McGowan, J. L. C. Ford, Jr., and W. T. Milner 116

The energies of gamma rays from about 50 nuclides have been measured to within a few tenths of a keV. Previously unresolved gamma-ray doublets in the decay of ${}^{102}\text{Rh}$ and ${}^{106}\text{Rh}$ and in the Coulomb excitation of ${}^{77}\text{Se}$ are reported.

DECAY OF $^{79}\text{Kr} \rightarrow ^{79}\text{Br}$

R. L. Robinson 119

Singles and coincidence gamma-ray spectra of the decay of ^{79}Kr are investigated. An energy-level diagram of ^{79}Br based on these results is proposed.

RADIOACTIVITY. ^{79}Kr [from $^{79}\text{Br}(p,n)$], measured E_γ , I_γ , $\gamma\gamma$ spectra. ^{79}Br deduced levels, $\log ft$, J , π . Natural target.

INTERNAL BREMSSTRAHLUNG FROM ^6He

J. K. Bienlein and Frances Pleasonton 122

Abstract of paper submitted to *Nuclear Physics*.

RADIOACTIVITY. ^6He measured shape of internal bremsstrahlung spectrum.

INTERNAL BREMSSTRAHLUNG ACCOMPANYING THE BETA DECAY OF ^{42}K

J. K. Bienlein and Frances Pleasonton 123

Abstract of paper to be published in the *Proceedings of the International Conference on Nuclear Physics, Paris, 1964*, sponsored by IUPAP, UNESCO, and Societe Francaise.

RADIOACTIVITY. ^{42}K . Measured total yield of internal bremsstrahlung in the beta decay of $^{42}\text{K} \rightarrow ^{42}\text{Ca}$.

SOME HEAVY-ION STOPPING POWERS

C. D. Moak and M. D. Brown 123

Multicomponent beams of Br and I ions from the Tandem Van de Graaff Accelerator have been used to measure the stopping powers of several elements in the energy range of 10 to 100 Mev.

RESPONSE OF GERMANIUM AND SILICON DETECTORS TO ENERGETIC BROMINE AND IODINE IONS

W. W. Walker, C. D. Moak, and J. W. T. Dabbs 125

Pulse-height response of germanium and silicon surface barrier detectors to ^{79}Br and ^{127}I ions has been determined; detector resolutions and pulse-height defects have been shown to be similar for the two types of detector, and it has been shown that resolution and pulse-height defect are only partially related, if at all.

FISSION OF ORIENTED NUCLEI

J. W. T. Dabbs and G. W. Parker 127

An improvement in counting rate by a factor of ~ 9 has been achieved.

FISSION FRAGMENT ENERGY CORRELATION EXPERIMENTS

H. W. Schmitt, J. H. Neifer, and F. J. Walter 129

Experimental results based on new absolute energy calibrations are given for ^{252}Cf spontaneous fission and ^{235}U thermal-neutron-induced fission.

NUCLEAR FISSION. ^{252}Cf and ^{235}U , measured correlated fragment energies, deduced mass and energy distributions, mass-energy correlations.

CORRELATED FRAGMENT ENERGY MEASUREMENTS AND MASS-vs-ANGLE CORRELATIONS IN **$^{226}\text{Ra} + p$ FISSION**

H. W. Schmitt, J. W. T. Dabbs, and P. D. Miller 140

Mass distributions and mass-energy correlations have been studied for $E_p = 11.0, 12.0,$ and 13.5 Mev. For $E_p = 13.5$ Mev, a small variation in the mass distribution as a function of angle was found.

NUCLEAR FISSION. ^{226}Ra , proton-induced, measured fragment energies, deduced mass and energy distributions, mass-energy and mass-angle correlations.

AVERAGE NUMBER AND ENERGY OF GAMMA RAYS EMITTED AS A FUNCTION OF FRAGMENT MASS IN ^{235}U THERMAL-NEUTRON-INDUCED FISSION

H. Maier-Leibnitz, H. W. Schmitt, and P. Armbruster 146

Abstract of paper to be published in the *Proceedings of the IAEA Symposium on the Physics and Chemistry of Fission*, Salzburg, Austria, March 1965.

NUCLEAR FISSION. ^{235}U , measured correlated prompt γ and fragment energies, deduced $\langle E_\gamma \rangle$ as function of fragment mass.

PRECISION MEASUREMENTS OF CORRELATED ENERGIES AND VELOCITIES OF ^{252}Cf FISSION FRAGMENTS

H. W. Schmitt, W. E. Kiker, and C. W. Williams 147

Abstract of published paper: *Phys. Rev.* **137**, B837 (1965).

NUCLEAR FISSION. ^{252}Cf , measured correlated fragment energies and velocities, deduced mass and energy distributions, mass-energy correlations, and $\nu(M)$; absolute energy calibration for semiconductor detectors.

ABSOLUTE ENERGY CALIBRATION OF SOLID-STATE DETECTORS FOR FISSION FRAGMENTS AND HEAVY IONS

H. W. Schmitt, W. M. Gibson, J. H. Neiler, F. J. Walter, and T. D. Thomas 147

Abstract of paper to be published in the *Proceedings of the IAEA Symposium on the Physics and Chemistry of Fission*, Salzburg, Austria, March 1965.

NUCLEAR FISSION. Absolute energy calibration and pulse-height response of semiconductor detectors for fission fragments and heavy ions.

CORRELATED ENERGY AND TIME-OF-FLIGHT MEASUREMENTS OF FISSION FRAGMENTS WITH SEMICONDUCTOR DETECTORS: SYSTEM DESIGN AND PERFORMANCE

C. W. Williams, W. E. Kiker, and H. W. Schmitt 148

Abstract of published paper: *Rev. Sci. Instr.* **35**, 116 (1964).

NUCLEAR FISSION. Instrumentation for correlated energy and velocity measurements.

NUCLEAR DATA PROJECT

K. Way, A. Artna, W. B. Ewbank, N. B. Gove, M. J. Martin, H. Ogata, A. K. Sen Gupta, E. C. Campbell, G. H. Fuller, and C. S. Han 149

Analyses of 104 nuclei have been completed. Special compilations of rotational band parameters, gamma transition half-lives, recent references, magnetic moments, nuclear masses, and the grounds for spin-parity arguments have been made.

COMPILATION OF CHARGED-PARTICLE NUCLEAR CROSS SECTIONS

F. K. McGowan, H. J. Kim, and W. T. Milner 150

Progress on the compilation of cross-section data in tabular form is outlined.

WAVE FUNCTIONS FOR MUON CAPTURE IN HYDROGEN μ -MOLECULAR IONS

R. L. Becker and M. R. Patterson 150

Binding energies, muon-proton overlap, and mean internuclear separation are given in the adiabatic approximation for the ground and first excited states of the $p\mu p$ and $d\mu d$ molecules.

SEARCH FOR HYPERFRAGMENTS IN THE $\Sigma^- + \text{He}$ REACTION

H. O. Cohn and W. M. Bugg 152

We have examined 400 Σ^- -hyperon interactions in helium for possible hyperfragment formation. The Σ^- hyperons were produced by slow K^- mesons in the Northwestern University helium bubble chamber. Energetically, the only permissible hyperfragments are hydrogen and neutron hyperfragments. Five hydrogen hyperfragments were identified. A search for neutron hyperfragments yielded a negative result.

EXCHANGE MECHANISM FOR ω PRODUCTION IN π^+ -n INTERACTIONS

H. O. Cohn, W. M. Bugg, and G. T. Condo 153

The exchange mechanism for ω production in π^+ + n interactions is studied through an analysis of angular correlations from π^+ + d \rightarrow p + p + π^+ + π^- + π^0 interactions. Values for the spin matrix elements ρ_{00} and $\rho_{1,-1}$ are obtained and compared to the one- ρ exchange model.

NEUTRAL DECAY AND ISOTOPIC SPIN OF THE ρ^0

N. Gelfand, G. Lutjens, M. Nussbaum, J. Steinberger, H. O. Cohn, W. M. Bugg, and G. T. Condo 156

Abstract of published paper: *Phys. Rev. Letters* **12**, 567 (1964).

ANALYSIS OF Σ^- ABSORPTION IN HELIUM

K. H. Bhatt, H. O. Cohn, and W. M. Bugg 156

Abstract of paper submitted to *Nuovo Cimento*.

REACTION $\Sigma^- + {}^4\text{He} \rightarrow \Lambda^0 + n + {}^3\text{H}$

H. O. Cohn, K. H. Bhatt, and W. M. Bugg 156

Abstract of published paper: *Phys. Rev. Letters* **13**, 668 (1964).

PUBLICATIONS 157**PAPERS PRESENTED AT SCIENTIFIC AND TECHNICAL MEETINGS** 162**FOREIGN TRAVEL** 166**ANNOUNCEMENTS** 167**ADVISORY COMMITTEE** 169**AMERICAN PHYSICAL SOCIETY** 169**NUCLEAR CROSS SECTIONS ADVISORY GROUP** 170**MISCELLANEOUS ACTIVITIES OF DIVISIONAL PERSONNEL** 170**ACTIVITIES RELATED TO EDUCATIONAL INSTITUTIONS** 172**ORNL PHYSICS SEMINARS** 182



NEUTRON DIFFRACTION INVESTIGATION OF CHROMIUM WITH SMALL ADDITIONS OF MANGANESE AND VANADIUM¹

Y. Hamaguchi² E. O. Wollan W. C. Koehler

The magnetic properties of chromium alloys with small amounts of manganese (0.5%, 0.74%, 2.1%) and vanadium (1.0%, 1.9%) have been investigated by neutron diffraction, and these results and others involving higher manganese concentrations are compared with theoretical calculations by Tachiki and Nagamiya. The addition of vanadium (1.0%) tends first to destroy the long-range modulation

of the moment configuration and then rapidly to eliminate the magnetic moment of the system. The addition of manganese progressively modifies the temperature-dependent properties of the modulated moment structure of pure chromium and the temperature of the spin flip transition. Over a small composition range both the simple antiferromagnetic and the modulated moment structures appear to be stable. Above 2.1% manganese, only the simple antiferromagnetic structure is observed. The changes in the magnetic properties of the alloys have a qualitative relation to the theoretical calculations.

¹Abstract of paper to be published in the *Physical Review*.

²Guest scientist from Japan Atomic Energy Research Institute.

MAGNETIC STRUCTURE OF RARE-EARTH-COBALT (RCO₂) INTERMETALLIC COMPOUNDS¹

R. M. Moon W. C. Koehler J. J. Farrell²

Saturation magnetization and neutron diffraction measurements have been performed on cubic Laves phase compounds, RCo₂, in which R is Nd, Tb, Ho, and Er. Neutron powder patterns obtained at room temperature and at 15°K allowed the determination of the magnetic structures. The low-temperature patterns are of the ferromagnetic or ferrimagnetic type, with large magnetic intensities superimposed on the nuclear peaks. For the compounds of Tb, Ho, and Er, the rare-earth atoms show nearly the full moment expected for the free trivalent ion, and the cobalt moment is about

1 Bohr magneton. The rare-earth moments are coupled parallel to each other, but antiparallel to all the cobalt moments. For NdCo₂, the observed Nd moment of 2.6 ± 0.2 Bohr magnetons is smaller than the free-ion value of 3.27 Bohr magnetons, and it is coupled parallel to the cobalt moment of 0.8 ± 0.2 Bohr magneton. In the Nd ion, the spin is opposite to the moment ($J = L - S$), while for the heavier rare earths the spin is parallel to the total moment ($J = L + S$). Thus, in all cases there is antiparallel coupling between the spins of the rare-earth and cobalt atoms. The values for the total moment per molecule based on the neutron diffraction results are in satisfactory agreement with the magnetization measurements.

¹Abstract of paper submitted to the *Journal of Applied Physics*.

²University of Pittsburgh, Pittsburgh, Pa.

MAGNETIC PROPERTIES OF RARE-EARTH METALS AND ALLOYS¹

W. C. Koehler

A review of neutron diffraction studies of the magnetic properties of rare-earth metals and alloys is presented. For each of the pure metals Tb, Dy, Ho, Er, and Tm there is observed a transition at a temperature T_N to an oscillatory antiferromagnetic configuration (helical or linear oscillator type). At lower temperatures, further transitions to ferromagnetic, ferromagnetic spiral, or antiphase domain-type configurations are observed. For Gd, only the ferromagnetic configuration is found. The magnetic moments in the ordered configurations at low temperatures approach the values expected from the corresponding free tripositive ions. In the first half of the series, only Nd has been studied by single-crystal methods, but Ce, Pr,

and Eu have now been investigated with polycrystalline samples. The data for Ce are complicated by the existence of several allotropic forms, but a complex antiferromagnetic structure appears to be associated with the hexagonal form at low temperatures. For Nd and Pr, oscillatory antiferromagnetic configurations are observed at very low temperatures in which, as in Ce, the moments have magnitudes considerably smaller than the free-ion values. This result suggests a strong influence due to the crystalline field. A helical spin structure in bcc Eu has been reported in which the moment of Eu is somewhat smaller than that of Eu^{2+} . A number of alloy systems, R-Y, R-R', and R-La, where R and R' are among the group Tb-Tm, have been investigated, and results are discussed. These results and those for the pure metals are discussed relative to the theory of the magnetism of the rare-earth metals.

¹Abstract of paper to be published in the *Journal of Applied Physics*.

MAGNETIC STRUCTURE vs ELECTRON NUMBER FOR SOME RARE-EARTH INTERMETALLIC COMPOUNDS¹

J. W. Cable

W. C. Koehler

H. R. Child

Neutron diffraction measurements were made on a series of rare-earth compounds in the Tb(Pd,Ag) and Tb(Ag,In) systems. Most of these compounds exhibit the CsCl type of crystal structure and, for these, magnetic structure determinations were made in order to relate the type of magnetic struc-

ture to the number of valence electrons. Two types of antiferromagnetic structures were observed: the $(\pi\pi 0)$ type consisting of an antiparallel array of ferromagnetic (110) planes of moments, and the (00π) type with ferromagnetic (001) planes of moments alternating in direction. On the basis of 0, 1, 3, and 3 valence electrons for Pd, Ag, In, and Tb respectively, the $(\pi\pi 0)$ structure is found in the region of 3.5 to 4 valence electrons per unit cell and the (00π) structure in the region of 5 valence electrons per unit cell.

¹Abstract of paper submitted to the *Journal of Applied Physics*.

MAGNETIC PROPERTIES OF HEAVY RARE EARTHS DILUTED BY YTTRIUM AND LUTETIUM¹

H. R. Child

W. C. Koehler

E. O. Wollan

J. W. Cable

A neutron diffraction study of the heavy rare earths Tb, Dy, Ho, Er, and Tm diluted with yttrium and of Tb with lutetium is reported. The modulated antiferromagnetic structures of the rare-earth metals are found to exist in the alloys, but the ferromagnetic phases of Tb and Dy are destroyed with small admixtures of Y. The Néel temperatures of the alloys and the pure metals are found to be a universal function of the average of the square

of the spin projection on J , given for these heavy rare-earth alloys by $\xi = c(g - 1)^2 J(J + 1)$, where c is the atomic concentration of rare earth. The value of the interlayer angle ω at T_N , which is related to the wavelength of the modulation of the magnetic structure, is also found to be a universal function of ξ , and the temperature variation of ω decreases with decreasing ξ , so that ω approaches a temperature-independent value of about 50° per layer for small ξ , regardless of the magnetic ion in the alloy.

¹Abstract of paper submitted to the *Physical Review*.

ALIGNMENT OF RARE-EARTH MOMENTS IN DILUTE Pd-Fe ALLOYS¹

J. W. Cable

E. O. Wollan

W. C. Koehler

H. R. Child

Magnetization measurements were made on the ternary alloy system $\text{Pd}_{0.96}\text{Fe}_{0.03}\text{R.E.}_{0.01}$, for which R.E. = La, Ce, Pr, Nd, Gd, Tb, Dy, Ho, Er, Tm, and Yb, in order to determine the relative alignment of the rare-earth moments in the ferromagnetic Pd-Fe matrix. Those rare earths to the left of Gd were aligned parallel and those to the right of Gd antiparallel to the Pd and Fe moments.

This is consistent with an antiferromagnetic interaction between the rare-earth spin and the d band of the host matrix, since, for the former, $J = L - S$ and, for the latter, $J = L + S$. Neutron magnetic-disorder scattering measurements were also made on the Dy alloy, and these showed only partial alignment of the available Dy moments. This suggests that the interaction between the rare earths and the Pd-Fe matrix depends on the local environment of the rare-earth atoms.

¹Abstract of published paper: *J. Phys. Chem. Solids* 25, 1453 (1964).

DISTRIBUTION OF MAGNETIC MOMENTS IN Pd-3d AND Ni-3d ALLOYS¹

J. W. Cable

E. O. Wollan

W. C. Koehler

Neutron scattering and magnetization measurements were made on a series of face-centered cubic Pd-3d and Ni-3d alloys to determine the distribution of magnetic moments in these ferromagnetic binary alloys. The specific alloys studied were: Ni_3Co , NiCo , Pd_3Co , PdCo , Pd_3Fe

(ordered and disordered), PdFe , $\text{Pd}_{0.93}\text{Fe}_{0.07}$, and $\text{Pd}_{0.97}\text{Fe}_{0.03}$. Magnetic moments of about 3.0, 1.8, and 0.6 Bohr magnetons per atom were found for Fe, Co, and Ni respectively, and these were essentially independent of concentration. The average Pd moment varies with concentration and approaches a maximum of about 0.4 Bohr magneton per atom in the concentrated alloys.

¹Abstract of paper submitted to the *Physical Review*.

ANTIFERROMAGNETISM OF PRASEODYMIUM¹

J. W. Cable R. M. Moon W. C. Koehler E. O. Wollan

In contrast with previous analyses of magnetic susceptibility and specific heat data which suggested the absence of magnetic order in metallic

praseodymium, this neutron diffraction study showed the development of long-range antiferromagnetic order below 25°K for this material. It is tentatively suggested that this magnetic order is of the neodymium type.

¹Abstract of published letter: *Phys. Rev. Letters* 12, 553 (1964).

EFFECTIVE MAGNETIC FIELD AND ISOMER SHIFT FOR Au-Ni ALLOYS AS A FUNCTION OF COMPOSITION

L. D. Roberts F. E. Obenshain J. O. Thomson¹
W. K. Robinson² W. B. Newbolt³

In earlier work^{4,5} we reported on the Mössbauer hyperfine structure (hfs) spectra for ¹⁹⁷Au in Au-Ni solid-solution alloys. We are now reporting further measurements at much higher resolution for the Ni-rich alloys and for pure Au metal. All measurements were made at 4.2°K, using a ¹⁹⁷Pt source which decays through the 77.3-keV state of ¹⁹⁷Au.

The six-line hfs spectra for alloys of 1, 3, 7, 10, and 20 at. % Au in Ni all consist of two unresolved triplets, each triplet barely resolved from the other. The center of gravity of the spectrum is displaced by the isomer shift V_I . These data have been fitted with theoretical absorption curves,⁴ taking absorber thickness into account and using the following Hamiltonians for the ground and excited states:

$$H_{\text{ground}} = -\frac{2}{3} \mu H' I_z,$$

$$H_{\text{excited}} = V_I - 2\mu^* H' I_z^*,$$

with $\mu = 0.1439$ nuclear magneton as the ground-state magnetic moment. A typical fit for 1% Au in Ni is shown in Fig. 1. Here H' is the effective magnetic field, and I_z and I_z^* are the z components of the spin of the ground and excited nuclear states respectively. We have taken a value for the excited-state magnetic moment $\mu^* = 0.39$ nuclear magneton from our previous measurements.⁴ In fitting the theoretical absorption curves to the data (Figs. 1, 3, and 4), we have used the natural line width for the 77.3-keV state of ¹⁹⁷Au as determined from new measurements on pure Au. This line width, Fig. 2, corresponds to a lifetime of $(1.8 \pm 0.1) \times 10^{-9}$ sec, in agreement with our previous value and with electronic measurements. We have also fitted the Au-Ni data by using a line width approximately 5% greater than that measured above (at the upper limit of the experimental error of the line width) and obtained somewhat better fits to the data, but the latter curves are not presented here. The fact that the best fit was obtained with six lines of very nearly the line

¹Consultant, University of Tennessee, Knoxville.

²Research participant from St. Lawrence University, Canton, N.Y.

³Research participant from Washington and Lee University, Lexington, Va.

⁴L. D. Roberts and J. O. Thomson, *Phys. Rev.* 129, 664 (1963).

⁵L. D. Roberts *et al.*, to be published in the *Physical Review*.

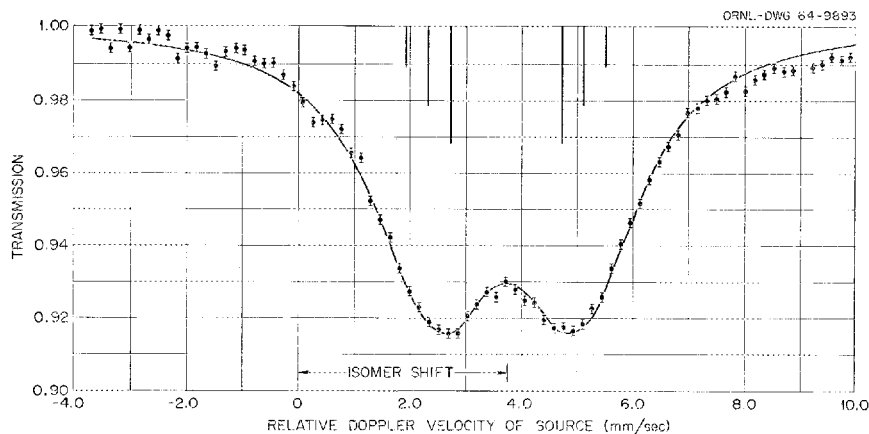


Fig. 1. Hyperfine Structure of the 77.3-keV State of 1 at. % ^{197}Au Dissolved in Ni. The solid curve gives the theoretical absorption function for the six-line spectrum. The lines were at the positions shown and had intensities 1:2:3:3:2:1. The natural line width (see Fig. 2) was assumed, but absorber thickness was suitably taken into account.

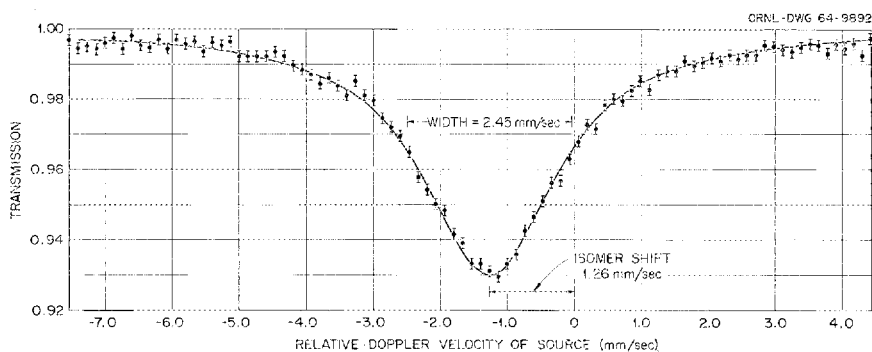


Fig. 2. Single-Line Absorption Spectrum of the 77.3-keV State of ^{197}Au . The line width at half height corresponds to a lifetime of $(1.8 \pm 0.1) \times 10^{-9}$ sec.

width found for pure gold indicates that inhomogeneous broadening effects are small.

The hfs coupling determined by the above curve-fitting process is found to be proportional within the experimental error of a few percent to $[1 - (c/0.60)]$, where c is the atomic fraction of Au (Fig. 3). From this fact and from our previous magnetization measurements on Au-Ni alloys,⁴ it is observed that, within our error, the hfs coupling is proportional to the average magnetic moment per atom of the alloy. Thus the proportionality found previously⁴ between the hfs coupling and the magnetic moment of the host metal

in the case of $\frac{1}{2}\%$ Au in Fe, 1% Au in Co, and 1% Au in Ni extends to the more concentrated Au-Ni alloy system. The hyperfine field found for 1% Au in Ni, assuming $\mu^* = 0.39$, is 340 ± 10 kilogauss.

The observed isomer shift as a function of c for the Au-Ni alloys, within the experimental error of about 0.1 mm/sec, follows a straight line passing through the observed isomer shift for pure Au of -1.26 ± 0.06 mm/sec (Figs. 2 and 4). In particular, there appears to be no flattening of the slope of dV_I/dc below $c = 0.03$, where the Au atoms are becoming relatively widely separated and where they might be expected to act more

independently. Also, the experimental results give no reason to invoke a change of slope near 60% Au, where the magnetic properties of the alloy change markedly. These observations are in agreement with our earlier measurements.⁴

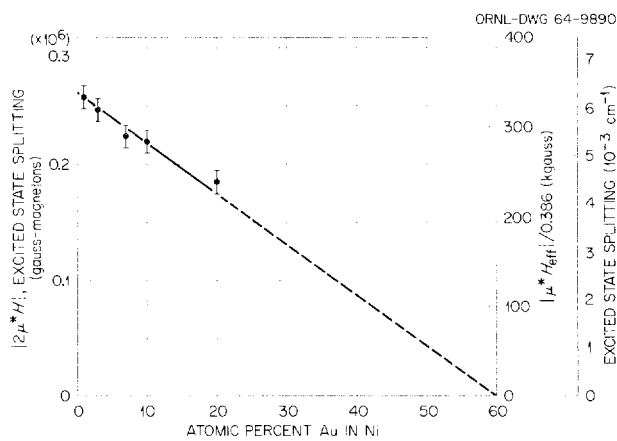


Fig. 3. Hyperfine-Structure Coupling as a Function of Composition for ^{197}Au Dissolved in Ni.

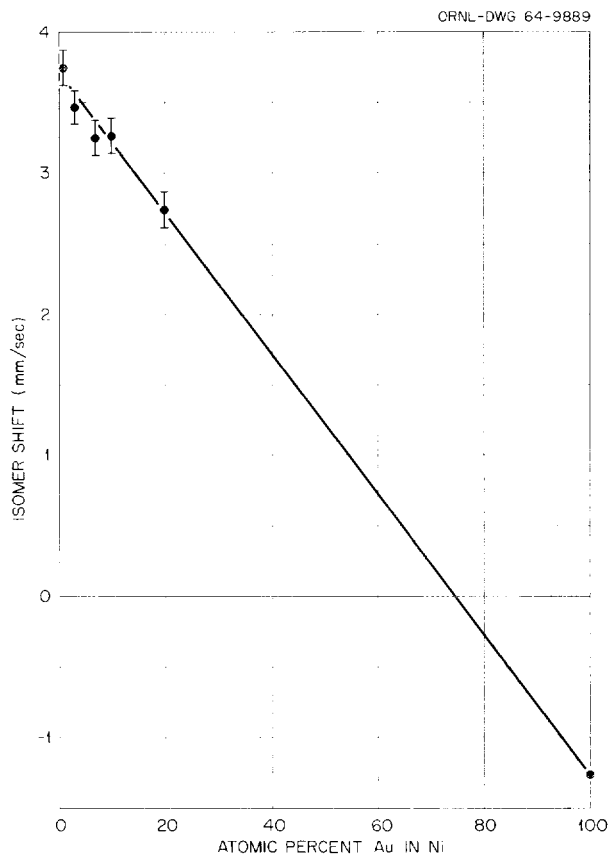


Fig. 4. Isomer Shift as a Function of Composition for ^{197}Au Dissolved in Ni with Au in Pt as the Gamma-Ray Source.

CORRELATION OF THE MÖSSBAUER ISOMER SHIFT AND THE RESIDUAL ELECTRICAL RESISTIVITY FOR ^{197}Au ALLOYS¹

L. D. Roberts

R. L. Becker

F. E. Obenshain

J. O. Thomson²

The Mössbauer isomer shift, which is simply related to the charge density at the Mössbauer nucleus, has been measured for pure ^{197}Au and for ^{197}Au as an impurity in Cu, Ag, Ni, Pd, and

Pt. Since the isomer shift associated with an impurity and the residual electrical resistance due to it are properties of a common conduction-band wave function, one may expect a correlation of the residual resistance with the isomer shift through a suitable model. We have thus made residual resistance as well as isomer-shift measurements at 4.2°K for the above dilute gold alloys. These measurements have been correlated through

¹Abstract of published paper: *Phys. Rev.* **137**, A895 (1965).

²Consultant from the University of Tennessee, Knoxville.

a theoretical model, using (1) the residual electrical resistivity and the Friedel sum rule to specify the asymptotic wave function at the Fermi level, and (2) a pseudopotential which will produce this asymptotic wave function and which is used to continue the *s* partial wave inward to the gold nucleus at the origin. The correlation of our

experimental results, using the theoretical model, is good if we assume that a gold impurity presents an attractive potential to the *s* partial wave of the host *s*-band conduction electrons, and if we assume the *s*-band fillings to have the values 1, 1, 0.58, and 0.37 for Cu, Ag, Pd, and Pt.

HYPERFINE STRUCTURE OF THE 14.4-keV GAMMA RAY OF ^{57}Fe IN HYDRATED FERRIC AMMONIUM SULFATE AS A FUNCTION OF THE MAGNETIZATION OF THE SALT¹

F. E. Obenshain L. D. Roberts C. F. Coleman²
D. W. Forester³ J. O. Thomson⁴

The hyperfine structure (hfs) spectra of the 14.4-keV gamma ray of the nucleus ^{57}Fe in the paramagnetic salt, hydrated ferric ammonium sulfate, have been measured through the use of

the Mössbauer effect. These measurements were performed at an absolute temperature *T* in the liquid-helium region in zero applied magnetic field, and also in the presence of applied magnetic fields *H* large enough to produce a substantial polarization of the unpaired electron spins of the Fe^{3+} ions. The behavior of the Mössbauer line widths and the shapes and spacings of the hfs spectra observed here differ markedly from the hfs spectra found for either magnetically dense or exceedingly dilute magnetic materials.

¹Abstract of a paper submitted to *Physical Review Letters*.

²AERE, Harwell, England.

³University of Nebraska, Lincoln.

⁴University of Tennessee, Knoxville.

MÖSSBAUER MEASUREMENTS OF THE ^{57}Fe HYPERFINE STRUCTURE COUPLING IN FeRh ALLOYS NEAR 50 at. % RHODIUM¹

D. W. Forester² F. E. Obenshain H. H. Wegener³
L. D. Roberts J. O. Thomson⁴

Mössbauer measurements of the hyperfine structure (hfs) splitting of the nucleus ^{57}Fe in FeRh alloys have been made for three alloys with compositions near 50, 52, and 53 at. % Rh. It was

found by magnetization measurements that the 50% sample is ferromagnetic above 100°K. The temperature dependence of the hfs of this sample was measured from 100 to 714°K. The Curie temperature was found to be $710 \pm 4^\circ\text{K}$. These measurements are described by a Brillouin function with $S = \frac{3}{2}$ and $H_{\text{eff}}(0) = 285$ kilogauss at 0°K. The 52% sample displayed a Curie temperature of $654 \pm 5^\circ\text{K}$. It was antiferromagnetic below 330°K and ferromagnetic above this temperature.

¹Abstract of paper submitted to the *Physical Review*.

²University of Nebraska, Lincoln.

³University of Erlangen, Erlangen, Germany.

⁴University of Tennessee, Knoxville.

The hfs was measured from 4.2 to 670°K. In the ferromagnetic region a Brillouin function with $S = \frac{3}{2}$ and $H_{\text{eff}}^F(0) = 295$ kilogauss was used to fit the data. The experimentally observed hfs in the antiferromagnetic region fell below this Brillouin function and could again be described by a Brillouin function with $H_{\text{eff}}^{A.F.}(0) = 275$ kilooersteds and $S = \frac{3}{2}$. An effective Néel temperature $T_N = 615$ was obtained from this fit. As indicated above, $B(S = \frac{3}{2})$ gives a good description of the hfs for the 50% alloy. If it is assumed that this function may be used to extrapolate the high-temperature ferromagnetic behavior to 0°K for the 52% alloy, then it may be suggested that the intrinsic effective field per iron atom [i.e., $H_{\text{eff}}(0)$] is slightly lower in the antiferromagnetic than in the ferromagnetic phase. This 52% sample was obtained from J. Kouvel and is a sample on which magnetization measurements have been made.

Comparison of the temperature dependence of the hfs splitting and these magnetization measurements was made. The ferromagnetic to antiferromagnetic transition temperatures determined by both methods agree very closely. At higher temperatures, near the Curie temperature where critical fluctuations may be important, the two curves do not agree. The hfs splitting measurements decrease to zero more rapidly, giving a lower value for the Curie temperature than that obtained from the magnetization measurements.

The theory of fluctuation effects for the Mössbauer effect has not been worked out, and without this theory it is difficult to determine the curve of the hfs splitting as a function of temperature near the Curie temperature. However, the Curie temperature may be determined very well by observing the complete collapse of the hfs spectrum into a single line.

"EXPLOSION" OF MULTICHARGED MOLECULAR IONS: CHEMICAL CONSEQUENCES OF INNER SHELL VACANCIES IN ATOMS¹

T. A. Carlson

R. M. White²

Molecules containing atoms which undergo internal conversion or electron capture are subject to extensive decomposition. This decomposition results from the large number of electrons that an atom loses as it adjusts to a vacancy in one of its inner shells. Electrons are pulled from the rest of the molecule to the region of high positive charge, and the whole molecule literally "explodes" from Coulombic repulsion.

In this paper a short review is first made of the past work on the molecular consequences to inner shell vacancies, with particular emphasis on gases examined with a charge spectrometer. This previous work, however, has been limited to qualitative observations. A description is then given

of a new charge spectrometer, which utilizes x rays to initiate inner shell vacancies. With this spectrometer it is possible to measure the relative abundances of all the fragment ions formed in the decomposition of the parent molecule without the errors that arose earlier from a dependence of collection efficiency on recoil energy. Furthermore, it has been possible to measure the recoil spectrum for each of the ions.

As an example, some recently acquired data are given on the decomposition of CH_3I following vacancies formed primarily in the L shell of iodine by x rays. The decomposition is violent, with the molecule decomposing almost entirely into H^+ , C^{n+} , and I^{n+} . The relative abundance of molecular ions is very small. The sums of the carbon, iodine, and hydrogen ions are in the approximate ratios of 1:1:3, suggesting that the quantity of neutral species is also small. The most abundant carbon ion is C^{2+} , which possesses an average

¹Abstract of paper to be published in the *Proceedings of the Symposium on Chemical Effects Associated with Nuclear Reactions and Radioactive Transformation, Vienna, Austria, December 7-11, 1964.*

²Summer participant, Baker University, Baldwin, Kan.

recoil energy of about 40 ev. The most abundant iodine species is I^{5+} , which contrasts with an average charge of eight from an analysis of Xe ions produced with x rays of the same energy.

These and other data on the recoil and charge spectra from CH_3I are compared with calculations, using a model of a multiple-ion Coulomb "explosion."

ELECTRON SHAKE-OFF RESULTING FROM *K*-SHELL IONIZATION IN NEON MEASURED AS A FUNCTION OF PHOTOELECTRON VELOCITY¹

T. A. Carlson

M. O. Krause

The relative abundances of the differently charged ions that result from photo-ionization in the *K* shell of neon were measured with a specially designed mass spectrometer. Results were obtained as a function of the x-ray energy from 17.5 to 0.93 keV with the aid of characteristic lines from a variety of targets. The charge spectrum at 1.5 keV is as follows: Ne^+ , 8.1 ± 0.7 ; Ne^{2+} , 100 ± 0.7 ; Ne^{3+} , 29.6 ± 0.4 ; Ne^{4+} , 4.3 ± 0.2 ; Ne^{5+} , 0.4 ± 0.1 . At higher energies the spectrum, with the exception of charge 1, remained essentially the same. At lower energies, however, the relative abundances for ions of charges greater than 2 began to drop at about 300 ev above the *K* edge

of neon, where the velocity of the photoelectron is 1.0×10^9 cm/sec. From this data and from previous data taken with x rays just above the *K* edge, the extent of electron shake-off arising from photo-ionization has been assessed. Specifically, it was found that when the photoelectron leaves the *K* shell of neon with a velocity high enough to give validity to the sudden approximation, there is about an 18% probability for electron shake-off, which agrees well with calculations. In addition, the amount of electron shake-off has been experimentally obtained under conditions where the sudden approximation no longer holds. Finally, it has been possible to set upper limits for the probability of double *K* and *KL* photoelectron emission, which cannot arise from electron shake-off. They are 1 and 5% respectively.

¹Abstract of paper to be submitted to the *Physical Review*.

MULTIPLE IONIZATION IN ATOMS AND ITS RELATIONSHIP WITH ELECTRON CORRELATION

T. A. Carlson

M. O. Krause

This report gives the results of an investigation on photo-ionization in the outer shells of He, Ne, and Ar. These results have shown that the process often occurs with the ejection of more than one electron. Likewise, double electron emission has

been found with Auger processes, namely, the *K-LL* transition in Ne (ref. 1) and the *L-MM* transition in Ar.

¹T. A. Carlson and M. O. Krause, submitted to *Physical Review Letters*.

Earlier measurements^{2,3} on the extent of ionization resulting from atomic readjustment to inner shell vacancies showed more than had been predicted by calculations, based on models depicting photo-ionization and subsequent Auger processes as events that involve the emission of only one electron. In the present studies this "excess ionization" has been examined more carefully by avoidance of the complexities of readjustment to vacancies in the inner shells. That is, a vacancy produced in the outermost shell of the rare gases cannot give rise to subsequent Auger processes, and ionization may be attributed solely to photo-electron emission. In the case of Auger processes, we have avoided complexity by producing a vacancy in the penultimate shell with x rays having only enough energy to cause photo-ionization, but not enough to give rise to any additional electron excitation and/or removal, so that "excess ionization" must arise only from the single Auger process allowed.

The investigation of multiple ionization was based on measurements of the relative abundances of the differently charged ions formed as the result of x irradiation. The studies were carried out with

a specially designed mass spectrometer at gas pressures low enough to preclude ion-molecule reactions. The equipment and experimental procedures have been described elsewhere.³

Results

In Table 1 are listed the charge spectra for He, Ne, and Ar ions, formed as the result of x irradiation. In each case only photo-ionization in the outer shell is energetically possible. We discover, therefore, that multiple electron ejection in photo-ionization is a rather common event for the outer shells. It will be also noted from Table 1 that the extent of multiple ionization is fairly constant over a fairly wide range of x-ray energies. Previous to these studies, the only other experimental determination of double photo-ionization was obtained from absorption data of Ar in which electron ejection from the *M* shell accompanied *K* photo-ionization in about 1 to 3% of the cases.^{4,5} This value was obtained under conditions where contributions from electron shake-off were supposedly negligible.

²M. O. Krause *et al.*, *Phys. Rev.* **133**, A385 (1964).

³T. A. Carlson and M. O. Krause, to be published in the *Physical Review*.

⁴H. W. Schnopper, *Phys. Rev.* **131**, 1558 (1963).

⁵C. Bonnelle and F. Wuilleumier, *Compt. Rend.* **256**, 5106 (1963).

Table 1. Multiple Ionization as the Result of Photoelectron Emission in the Outer Shells of Rare Gases

X rays are produced by bombarding a W target with electrons of energy E_{max}

Charge of Ion	Relative Abundance								
	He			Ne			Ar		
	A	B	C	D	B	C	E	F	G
1	100	100	100	100	100	100	100	100	100
2	4.0 ± 1.4	3.8 ± 0.4	3.4 ± 0.4	11 ± 4	13.7 ± 0.5	11.8 ± 0.6	11 ± 3	17 ± 2	14 ± 2
3				2 ± 2	0.8 ± 0.1	0.4 ± 0.1		0.9 ± 0.6	

A: $E_{max} = 3.4$ kev; filter = 450 $\mu\text{g}/\text{cm}^2$ of Ni.

B: $E_{max} = 800$ ev; filter = 230 $\mu\text{g}/\text{cm}^2$ of polystyrene.

C: $E_{max} = 300$ ev; filter = 65 $\mu\text{g}/\text{cm}^2$ of polystyrene.

D: $E_{max} = 850$ ev; filter = 450 $\mu\text{g}/\text{cm}^2$ of Cu + 110 $\mu\text{g}/\text{cm}^2$ of polystyrene.

E: $E_{max} = 236$ ev; filter = 230 $\mu\text{g}/\text{cm}^2$ of polystyrene.

F: $E_{max} = 236$ ev; filter = 65 $\mu\text{g}/\text{cm}^2$ of polystyrene.

G: $E_{max} = 220$ ev; filter = 65 $\mu\text{g}/\text{cm}^2$ of polystyrene.

Table 2. Study of Multiple Ionization Following the $L_{II,III}$ - MM Auger Transition

Ion	Relative Abundance at E_{\max} (ev) ^a of:			
	400	315	276	265
Ar ⁺	13.0 ± 0.7	25 ± 1	64 ± 5	73 ± 5
Ar ²⁺	100	100	100	100
Ar ³⁺	11.8 ± 0.7	11.2 ± 1.1	10.4 ± 1.4	9.5 ± 1.0

^aMaximum energy of bremsstrahlung as produced from W target and passed through filter of 230 $\mu\text{g}/\text{cm}^2$ of polystyrene.

In Table 2 are listed results on Ar in which vacancies were principally formed in the $L_{II,III}$ shell. The x-ray source was the bremsstrahlung from a tungsten target as passed through a 230- $\mu\text{g}/\text{cm}^2$ polystyrene filter. Of particular interest are the results in the last column, for in this run the maximum energy (E_{\max}) possible for an x ray was 265 ev. Under this condition, $L_{II,III}$ vacancies are created by x rays with energy insufficient to create further ionization. (The $L_{II,III}$ binding energies are 244 and 246 ev, and the minimum energy necessary to remove an extra electron is about 29 ev higher.⁶) In such an event one should expect to find only Ar²⁺, since photo-ionization can remove only one electron, while the $L_{II,III}$ - MM Auger process (which occurs with nearly 100% probability) will eject a second. Ions of higher charge are evidence for multiple ionization resulting from the Auger process. Vacancies can also be produced in the M shell, but they give rise primarily to Ar⁺, and the small contribution of the more highly charged ions can be evaluated from the charge spectra of Ar in Table 1. Since the polystyrene filter strongly transmits x rays just below the carbon edge (284 ev), most of the L vacancies formed in the other runs given in Table 2 occur with x rays of energies below 284

⁶The ionization potential for Ar⁺ with a 2p hole has been obtained (1) from a Hartree-Fock solution for Ar⁺ with the proper configuration (29 ev) and (2) by interpolating between the ionization potential for K II and Ar I with the help of Slater's rules for screening constants (29 ev).

ev, thus essentially eliminating the chance for producing vacancies in the L_I shell, whose binding energy is 287 ev. X rays of energies between 284 and 273 ev can also give rise to multiple photo-ionization, and the differences between the data taken at higher E_{\max} and the results in the last column are due to contributions from double photo-ionization.

Electron Shake-Off

Part of the multiple ionization observed both in photo-ionization and in Auger processes comes from electron shake-off as the result of a sudden change in effective charge. This contribution can be calculated by use of the sudden approximation from the following equation:

$$P_{nl} = 1 - \left| \int \psi_f^* \psi_i d\tau \right|^2, \quad (1)$$

where P_{nl} is the probability for an electron to vacate its shell as given by the principal and angular quantum numbers, n and l , and ψ_i and ψ_f are single electron wave functions for the initial and final states. Solutions to the wave functions were obtained from Hartree-Fock calculations for the appropriate configurations.⁷ Since not all electrons, upon vacating their shell, go into the continuum, these calculations represent an upper limit to shake-off, although most vacancies do result in ionization.⁸ In the case of helium, wave functions for all the bound states of He⁺, including the excited states, are well known; so we may calculate all transitions that will not lead to ionization and, upon subtracting these values from unity, obtain a more exact probability for ionization. The results of the electron shake-off calculations are given in column 3 of Table 3. It can be seen that, in every case, electron shake-off is unable to account for the bulk of the observed "excess ionization." We have assigned this role to the phenomena of electron correlation.

⁷These solutions were computed on the 1604-A from a code devised by Charlotte Froese.

⁸Though this is not the case in He, it does seem to be true for the other rare gases [cf. A. E. S. Green, *Phys. Rev.* **107**, 1646 (1957); T. A. Carlson, *Phys. Rev.* **130**, 2361 (1963)].

Table 3. Summary of Studies Showing Possible Contributions to Multiple Ionization from Electron Correlation

Study	Percent of Excess Ionization		
	Experiment	Electron Shake-Off ^a	Electron Correlation ^b
Photo-ionization in <i>K</i> shell of He	3.7	1.0	2.7
Photo-ionization in <i>L</i> shell of Ne	12.7	4.6	8.1
Photo-ionization in <i>M</i> shell of Ar	13.5	3.8	9.7
Photo-ionization in <i>K</i> shell of Ne			<1 ^c
<i>K-LL</i> Auger process in Ne	7.5	0.5	7.0
<i>L-MM</i> Auger process in Ar	9.2	0.7	8.5

^aExcept for He these calculated values represent an upper limit.

^bExperiment -- electron shake-off. This unexplained remainder is interpreted as arising from the effects of electron correlation.

^cThis value was arrived at from an interpretation of data taken with x-ray energies in excess of double *K* ionization.

Electron Correlation

A description of photo-ionization or an Auger process usually avoids the many-body aspect of the atom. To designate the initial and final states as many-electron-wave functions in the form of antisymmetrized sums of products of orthogonalized single-electron states means that a perturbing energy in the form of a one-particle operator (photo-ionization) can eject only one electron. Similarly, a perturbing energy in the form of a two-electron operator (Coulomb interaction) may involve only two electrons, of which one is in the continuum in the case of an Auger process. With real functions, we expect departures from these rules of the magnitude determined by the electron correlation present in the actual states.

Recent experimental results on multiple excitation by far-ultraviolet radiation have prompted Fano and Cooper⁹ to initiate theoretical investigations into the problem of electron correlation. It is hoped that the present work on multiple ionization will help form a wider experimental base for the many-body problem of the atom. In the absence of a fully-worked-out theory with which to compare our results, some generalizations might

be made regarding the "excess ionization," which we have interpreted as being related to electron correlation (cf. column 4, Table 3).

1. The extent of ionization in the outer octet (i.e., for Ne and Ar) seems to be independent of *Z*, although let it be noted that the effective charge in both these cases does not change appreciably.

2. Additional electron ejection is independent of the nature of the process initiating the ionization, but depends on the particular shell of the particular atom in which the primary electron is removed. That is, an Auger event produces about the same amount of "excess ionization" as does photoelectron emission, when one compares the same shell of the same atom from which the primary electron is emitted, although the comparison is complicated by the fact that in an Auger process a second electron drops into the inner shell vacancy.

3. Examination of the extent of ionization in the *K* shells of He and Ne shows a decrease in "excess ionization" with *Z*. Oversimplifying the picture, one might expect that an increase in effective charge causes a corresponding increase in the central potential, but does not substantially alter the interaction between the electrons of a given shell, thereby lessening the effects of electron correlation.

⁹U. Fano and J. W. Cooper, to be published.

EXPERIMENTAL EVIDENCE FOR DOUBLE ELECTRON EMISSION IN AN AUGER PROCESS¹

T. A. Carlson

M. O. Krause

Measurements were made on the relative abundances of neon ions resulting from photo-ionization with x rays of energies just above the *K* edge. At these energies no multiple ionization can arise directly from the photoelectron emission but must

be attributed to the subsequent *K-LL* Auger process. From the relative abundance of Ne^{3+} to Ne^{2+} , it was determined that $(7.5 \pm 1.0)\%$ double electron ejection occurs in the *K-LL* Auger process of neon. Calculation of contributions from electron shake-off accounted for only 0.5%, and therefore it is suggested that the "excess ionization" comes from the phenomena of electron correlation.

¹Abstract of paper submitted to *Physical Review Letters*.

ATOMIC READJUSTMENT TO VACANCIES IN THE *K* AND *L* SHELLS OF ARGON¹

T. A. Carlson

M. O. Krause

The relative abundances have been measured for the argon ions formed as the result of atomic readjustment to vacancies in the *K* and *L* shells of argon. Initial vacancies were produced by x rays, and the ions were analyzed with a magnetic spectrometer such as that used by Snell and Pleasanton in their work on radioactive rare gases. A new source volume for extracting the ions was used and is described. Measurements were made of charge spectra resulting from x rays of the ap-

proximate energies, 17.5, 4.5, 1.5, and 1.0 kev. The spectra obtained with x-ray energies above the *K* edge of argon bore a close resemblance to that obtained from $^{37}\text{Ar} \xrightarrow{\text{E.C.}} ^{37}\text{Cl}$. For comparison with the experimental results, each of the charge spectra was computed from knowledge of radiative and Auger transition rates. In addition, calculations were made of the electron shake-off that arises from sudden changes in the effective charge. In general, the agreement between the calculated and the experimental values is good, although there is some evidence that there may be other sources of additional ionization.

¹Abstract of paper to be published in the *Physical Review*.

DETERMINATION OF THE *L* ENERGY LEVELS IN KRYPTON BY THE PHOTOELECTRON METHOD¹

M. O. Krause

Energies of the photoelectrons $\text{Kr } L_{I,II,III}(\text{Mo } L_{\alpha})$, $\text{Kr } L_I(\text{Mo } L_{\beta})$, $\text{Kr } L_I(\text{Ti } K_{\alpha})$, and $\text{Kr } L_I(\text{Cr } K_{\alpha})$

were measured with a 90° electrostatic analyzer having spherical sector plates. Krypton was irradiated in the gaseous phase. The binding energies of the krypton *L* electrons were determined with an accuracy of about 1 ev as follows: $L_I = 1922$ ev, $L_{II} = 1727$ ev, $L_{III} = 1675$ ev.

¹Abstract of paper to be submitted to the *Physical Review*.

INFRARED SPECTRAL STUDY OF SECOND-ORDER TRANSITIONS IN CF_4

R. G. Steinhardt¹

H. W. Morgan

P. A. Staats

The infrared spectra of CF_4 in the liquid and in the solid state have been recorded at many different temperatures, using a low-temperature liquid cell.² Three absorption bands were studied, the ν_4 fundamental and the combination bands ($\nu_4 + \nu_1$) and ($\nu_4 + \nu_2$). All other absorptions were either too weak, too intense (the fundamental ν_3), or so badly overlapped by other bands that the contours could not be accurately determined.

The ν_4 and ($\nu_4 + \nu_1$) absorptions exhibit large discontinuous changes in band width at the second-order transition temperature (76°K), and smaller discontinuous changes upon passing through the melting point. The second-order transition discontinuity occurs over an experimental temperature

range of less than $\frac{1}{2}^\circ\text{K}$. This is the first reported observation of such a transition in infrared spectra. The change in the fundamental ν_4 is shown in Fig. 1. The combination band ($\nu_2 + \nu_4$) shows virtually no change at either the first-order (melting point) or second-order transition temperatures, as shown in Fig. 2. It appears from the half-widths and integrated absorbance that the absorption by this band is not influenced by the onset of restricted rotational motion in the lattice.

In an attempt to explain this spectral behavior, the theory of Guthrie and McCullough³ was reexamined, and calculations were made for CF_4 molecules in various orientations in the lattice. It was indicated that the second-order transition is a transition from molecules librating about a single equilibrium orientation (probably one T_d orientation) to molecules able to reorient between all the T_d and C_{3v} orientations. Such a transition

¹Hollins College, Hollins College, Va.

²R. G. Steinhardt, M. W. Jordan, and G. E. S. Fetsch, following paper in this report.

³G. B. Guthrie and J. P. McCullough, *J. Phys. Chem. Solids* **18**, 53 (1961).

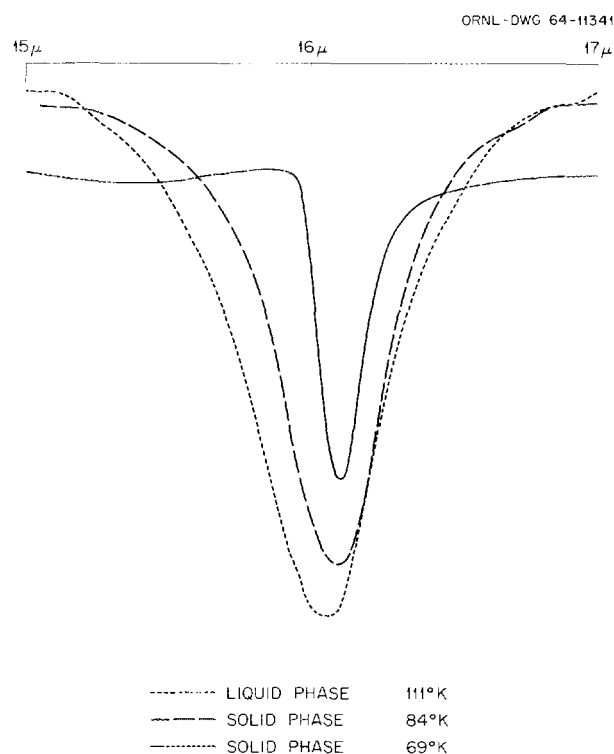


Fig. 1. The ν_4 Band of Carbon Tetrafluoride at 625 cm^{-1} .

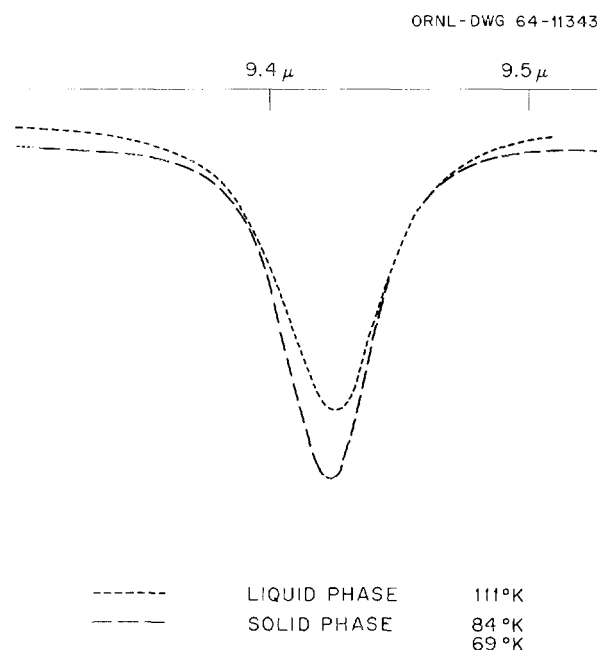


Fig. 2. The ($\nu_2 + \nu_4$) Band of Carbon Tetrafluoride at 1066 cm^{-1} .

gives an entropy change in agreement with that of Eucken and Schroder.⁴ The model also is consistent with the nuclear magnetic resonance data of Aston, Stottlemeyer, and Murray.⁵

⁴A. Eucken and E. Schroder, *Z. Physik. Chem.* B41, 307 (1938).

⁵J. G. Aston, Q. R. Stottlemeyer, and G. R. Murray, *J. Am. Chem. Soc.* 82, 1281 (1960).

There is as yet no explanation for the observed difference in behavior of the ($\nu_4 + \nu_2$) band. Calculations are continuing, based on our model of the CF_4 orientations, and more precise infrared measurements, analyzed by computer, are expected to provide better data on the absorptions already studied and to provide band width and intensity data on additional bands.

INFRARED ABSORPTION SPECTRA OF LIQUID BORON TRIFLUORIDE¹

R. G. Steinhardt²

M. W. Jordan²

G. E. S. Fetsch²

The absorption spectrum of liquid BF_3 at 163°K has been experimentally studied from 400 to 3000 cm^{-1} . Virtually all of the absorption peaks have been positively identified and compared with previous infrared studies of BF_3 in the solid and

gaseous states, as well as with a previous Raman study of the liquid. There is no evidence of an appreciable concentration of dimer in the liquid. However, the magnitude of the frequency shift of the symmetrical bending mode in comparing the gas with the liquid suggests that there may be appreciable association in the liquid as well as in the solid. Previous reports of anomalies in the viscosity and entropy of vaporization of BF_3 have been shown to be in error.

¹Abstract of paper submitted to the *Journal of Chemical Physics*. Work performed at ORNL under ORINS contract S807.

²Hollins College, Hollins College, Va.

LOW-TEMPERATURE LIQUID INFRARED ABSORPTION CELL

H. W. Morgan

P. A. Staats

R. G. Steinhardt¹

The physical characteristics of infrared transparent materials have made difficult the design and construction of liquid or gas absorption cells which remain vacuum tight when cycled over a large temperature range. A rather complex liquid cell for low temperatures was described by Holden *et al.*,² while simpler cells have been used by

McMahon *et al.*³ and Ewing.⁴ Each of these cells has had some disadvantage in complexity, in sample volume, or in versatility.

A low-temperature liquid cell has been constructed by modification of the conventional sealed infrared cell. It has been repeatedly cycled through the range 300–77°K; by the use of various liquids

¹Hollins College, Hollins College, Va.

²R. B. Holden, W. J. Taylor, and H. L. Johnston, *J. Opt. Soc. Am.* 40, 757 (1950).

³H. O. McMahon, R. M. Hainer, and G. W. King, *J. Opt. Soc. Am.* 39, 786 (1949).

⁴G. E. Ewing, *J. Chem. Phys.* 37, 2250 (1962).

at their boiling or freezing points, the cell has been maintained at fixed intermediate temperatures for extended periods. The liquid cell is formed by a gold-foil spacer pressed between two circular windows. The windows must have some plasticity to make a vacuum-tight seal. Cesium bromide is normally used, though silver chloride works satisfactorily and is less subject to chemical attack. The cell is sealed by pressure applied through a specially designed ring, as shown in Fig. 1. Pressure is applied through eight bolts distributed around the perimeter. These bolts are tightened until the ring shows a slight deformation. Two small pieces of gold foil placed near the center of the sample area minimize changes in cell thickness as the window deforms slightly under pressure. The sample area has a maximum aperture of 1 in., which may be reduced by the design of the spacer. Access to the sample volume is provided by two $\frac{1}{32}$ -in.-ID stainless steel tubes connected to valves outside the vacuum jacket. A vacuum-tight seal of the access lines to the cell is made by an indium gasket.

The cell is cooled by conduction, the housing being a part of the base of a thin-walled stainless steel Dewar. The Dewar mounts in a vacuum jacket with two infrared transmitting windows. To minimize radiation loss and to prevent corrosion, all parts of the cell other than windows and stainless steel are gold plated.

For use with condensable gases, one access line is coupled to the gas supply and the second to a vacuum line. After evacuation of the cell and vacuum jacket, the Dewar is cooled to the temperature at which the gas will liquefy, and the sample is admitted into the cell. When the

liquid level has passed the top of the sample area, the access line is sealed and the spectrum taken. The sample can usually be removed by applying vacuum to the access tubing, and the cell immediately checked if necessary for window bands. In using liquids, the sample is placed in the cell by suction or pressure, at room temperature, and the Dewar is then cooled.

The cell operates reliably and is simple to assemble and disassemble for cleaning or modification. Spectra have been recorded of liquid methane, ethane, and other hydrocarbons, as well as liquid BF_3 and solutions of BF_3 in liquid Xe.

ORNL-DWG 63-4331R3

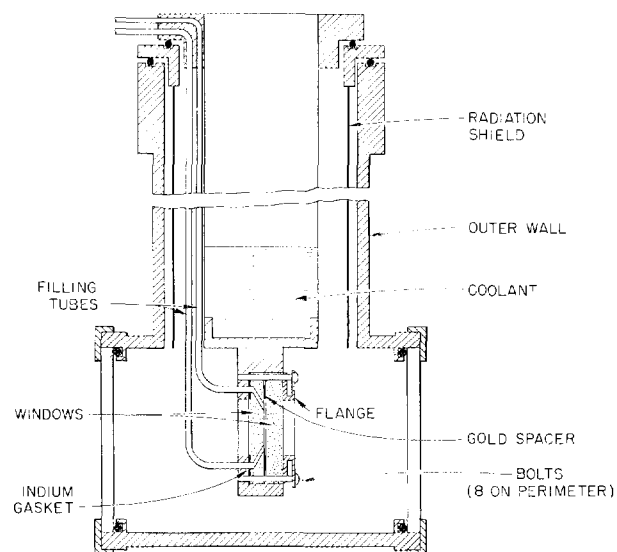


Fig. 1. Low-Temperature Infrared Cell.

SIMPLIFIED CONSTRUCTION OF A HELIUM-NEON VISIBLE LASER¹

K. L. Vander Sluis
H. W. Morgan

G. K. Werner
O. B. Rudolph

P. M. Griffin
P. A. Staats

Detailed instructions are given for the construction of a simple, inexpensive dc-powered helium-neon laser with 6328 Å output. The design is for

¹Abstract of paper accepted by the *American Journal of Physics* for publication in March 1965.

a 60-cm confocal resonator with a few milliwatts of coherent power output and rich mode structure. Variations to the basic design are suggested. Basic demonstrations that can be performed with the laser are described.

EFFECT OF PLASMA POTENTIAL ON MINIMUM- B STABILITY¹

T. K. Fowler

The early proofs that magnetic wells (minimum- B) inhibit interchange instabilities applied only to charge-neutral plasmas at low pressure. Recently, Hastie and Taylor² have shown that stability persists to high plasma pressure. We have now found that stability persists also despite the sizable plasma potential expected to develop because of the difference in ion and electron loss rates with mirror confinement. The potential ϕ has two destabilizing influences: interchange moves a net charge outward from the charge center and thereby reduces the potential energy, and it moves a net charge toward weaker fields and thereby reduces $E \times B$ drift energy. However, since we find that $\nabla\phi$ and ∇B are parallel, in a magnetic well these

energy decreases are always compensated by an increase in magnetic potential, μB . We estimate $e\phi \sim T_e$ and $|\nabla \ln \phi|^{-1} \sim R$, the plasma radius. Then the changes in electric potential energy and drift energy are smaller than the change in magnetic potential by factors $(\lambda_{De}/R)^2(B/\Delta B)$ and $(a_i/R)^2(B/\Delta B)$ respectively, where λ_{De} is the Debye length, a_i the ion gyroradius, and ΔB the magnetic well depth. Thus previous stability criteria, neglecting the electric energies, remain valid, and stability is assured if the plasma pressure is maximum at the magnetic minimum.³ Equilibria having this property can be exhibited. Recent experiments by Gibbons and Lazar in which flutes in arcs are suppressed by very shallow magnetic wells give qualitative support to our results.

¹Abstract of paper submitted to the *Physics of Fluids*.

²R. J. Hastie and J. B. Taylor, *Phys. Letters* 9, 241 (1964); *Phys. Rev. Letters* 13, 123 (1964).

³J. B. Taylor, *Phys. Fluids* 7, 767 (1964); H. P. Furth, *Phys. Rev. Letters* 11, 308 (1963).

BOUNDS ON PLASMA FLUCTUATIONS AND ANOMALOUS DIFFUSION¹

T. K. Fowler

Upper limits on the intensity and growth rate of plasma fluctuations are calculated from purely thermodynamic considerations. From these limits an upper bound on diffusion across a magnetic field by microinstabilities is estimated. Experimental results do not violate the bound. At low β the dominant contribution to the bound is thermal energy which feeds fluctuations through a mechanism akin to expansion cooling of a gas, possible only in finite plasmas. A rapid decrease in anomalous diffusion in discharge afterglows when the radius R exceeds a critical value, $R_0 \sim 10-20$ ion gyroradii, can be explained if the instability radial wavelength, a parameter in the theory, is

restricted to $\lesssim R_0$. Then the bound on the stochastic diffusion coefficient decreases like R^{-3} if $R > R_0$. With this restriction on wavelength, the bound used as a scaling law predicts adequately long thermonuclear confinement (~ 0.1 sec) in a torus of 100-cm minor radius if the torus is stabilized against frequencies below the ion cyclotron frequency, now perhaps feasible. Otherwise, low-frequency resonant diffusion may limit containment. This result holds at least up to β of a few percent.

Bounds on velocity diffusion are obtained, also. Both spatial and velocity diffusion are slow if electrons are cold compared with ions, which may account for observations in plasmas created by energetic ion injection.

¹Abstract of paper submitted to the *Physics of Fluids*.

AMBIPOLAR SCATTERING LOSSES FROM MAGNETIC MIRRORS¹

T. K. Fowler

M. Rankin²

A previous investigation³ of ambipolar scattering losses of plasmas confined by magnetic mirrors has been extended. The aim is to cover specifically the new class of experiments initiated by Ioffe,⁴ which are designed to test the minimum- B stabilization principle.⁵ Characteristically, the mirror ratio in these experiments is small, and often $T_e/T_i \sim 0.1$, so that a sizable plasma potential presumably develops. For one charge species, the plasma potential effectively weakens the mirror still more, thereby enhancing losses. It is, of course, essential in these experiments to distinguish between the instabilities one seeks to cure and more ordinary plasma losses. The temperature is often not high, ~ 1 keV, whence scattering is a quite competitive loss, and even small enhancement factors may be significant.

Generally, the electrons escape through mirrors more readily than ions, so that the potential is positive. If electron and ion currents, I_+ and I_- , are equal, in principle the ambipolar potential can sufficiently weaken the effective mirror seen by the ions to equate the ion loss rate to that of the electrons, an enhancement of $(m_i/m_e)^{1/2} = 43$ (H^+ ions). However, in practice the enhancement is less unless microinstabilities play a role. The reason is that the potential ϕ reduces the scattering time but not the ion velocity diffusion time. Only ions with energy very near ϕ are lost rapidly. Unless the ion distribution is a δ function at ϕ ,

the average loss time is the velocity diffusion time τ_v in order to reach this lossy region,

$$\tau_v \sim (T_i - \phi)/m_i D_v, \quad (1)$$

where D_v is the velocity diffusion constant. For diffusion by collisions, τ_v is of the order of the scattering time; hence little enhancement. In that case the potential acts to equate $I_+ = I_-$, not by ejecting ions but by trapping electrons. On the other hand, if D_v were enhanced by microinstabilities, the ion losses would be greater. Lacking information about instability enhancements, we restrict ourselves to the classical case.

The scattering time is determined by solving the ion and electron steady-state Fokker-Planck equations discussed by Fowler and Rankin.³ However, the simple scattering formula there has been replaced by that recommended by Bing and Roberts,⁶ which is more accurate for small mirror ratios, R . As we are interested in the possibility that scattering dominates, charge-exchange losses are omitted.

Only the product $n\tau$ is determined by the calculation, where n is the ion density and τ is the ion lifetime. The result is

$$n\tau = 2 \times 10^9 E_0^{3/2}, \quad (2)$$

where E_0 is the ion injection energy in keV. The actual lifetime and density depend on I_+ through the relation

$$I_+ \tau = nV, \quad (3)$$

where V is the plasma volume.

¹Abstract of published paper: *J. Nucl. Energy: Pt. C* **6**, 513 (1964).

²Thermonuclear Division.

³T. K. Fowler and M. Rankin, *J. Nucl. Energy: Pt. C* **4**, 311 (1962).

⁴Yu. D. Gott, M. S. Ioffe, and V. G. Telkovsky, *Nucl. Fusion, Suppl.*, Vol. III, 1045 (1962).

⁵J. B. Taylor, *Phys. Fluids* **6**, 1529 (1963).

⁶G. F. Bing and J. E. Roberts, *Phys. Fluids* **4**, 1039 (1961).

IMAGE FORMATION IN A HIGH-RESOLUTION ELECTRON MICROSCOPE

T. A. Welton

A series of calculations have been performed to explore the feasibility of molecular structure determination by use of a suitably designed electron microscope. It has first been shown that the spherical aberration of the conventional microscope objective, which presently limits resolution to 5 or 6 Å, can be compensated by inserting in the path of the beam a conducting film (graphite, 50–100 Å thick). This film is to be maintained at an apparently feasible negative potential with respect to symmetrically placed, pierced, grounded electrodes on either side of the film. If the illuminating beam is suitably monoenergetic ($\delta V/V \approx 10^{-6}$), if coherence is maintained over the illuminated area (100×100 Å, roughly), if a vacuum of 10^{-7} torr can be maintained, and if suitable mechanical stability and electronic registration can be provided, a high-resolution instrument of very superior performance can be produced. All these features are presently being considered, and the conclusion is strong that feasibility seems extremely likely. In anticipation of the probable existence of such an instrument, a careful study of image formation in electron microscopes has been undertaken.

We are particularly concerned with the question of atomic visibility, with a view to the possible use of such an instrument as a supplement to the growing repertoire of techniques for determining the necessary details of the exceedingly complex molecules of biological interest. We have accordingly developed a set of CDC 1604-A programs for calculating electron intensity distributions in the image plane under various assumptions as to defocus, primary and secondary spherical aberration, chromatic aberration, atomic number of the object atoms, and their spacing and location in the object plane, as well as other parameters of interest.

We have assumed, for convenience, that a given atom has a charge distribution which is given by the universal Fermi-Thomas function, and have verified that no large errors from this source are to be anticipated. We have further ignored the typical off-axis aberrations (e.g., coma) as being unimportant in the actual instrument, as well as astigmatism (which is, in practice, correctable to

the attainable resolution). The result is a particularly convenient computation scheme in which the image plane amplitudes due to atoms of various atomic numbers are first calculated as a function of radial distance from the image center and stored on magnetic tape. Another program then adds these amplitudes, with prescribed lateral displacements, to take care of all the atoms in the object plane. This resultant amplitude is then squared and stored on tape. This tape is then processed by a routine which produces a tape for the plotter, which scans repeatedly across the paper, with the pen rising and falling to deposit ink in accordance with the stored intensity information. The result is a reasonably true rendition of the contrast to be expected in an actual instrument. The elementary intensities due to single atoms can also be printed out, and detailed tables have been prepared for a wide range of conditions.

The conclusions to date are as follows:

1. A conventional instrument (100-keV, 10^{-2} -radian aperture, 5-Å resolution), when properly defocused for optimum phase contrast, can yield only about 5% contrast (intensity increment at image center/background intensity) for a carbon atom. For a heavy atom such as gold or osmium, this increases to about 20%, which is marginally feasible for observation.
2. A high-resolution instrument (100-keV, 4×10^{-2} -radian aperture, 1-Å resolution, with improvements listed earlier) will yield about 25% contrast for carbon, 200% for bromine, and correspondingly higher figures for heavier atoms.
3. Radiation damage restrictions place a stringent limitation on the atomic location information which can be extracted from a single molecule. For a typical biological molecule, a total dose of 10^2 electrons/Å² will cause very serious rebonding and consequent structural distortions. It will accordingly be necessary to piece together records of runs on many different molecules of the same substance (similarly oriented, if possible) in order to obtain convincing structures.
4. For selected problems in molecular biology, such a high-resolution electron microscope

offers a valuable supplement to existing methods (e.g., x-ray diffraction for suitable crystalline substances). Simple viewing of the molecule of interest will not be possible, but information can be obtained from which a useful picture can be constructed.

The study of the DNA sequence problem is a particularly attractive possibility for the high-resolution microscope, because of the known possibility of loading halogen-substituted nucleotides into DNA by genetic and biochemical tricks.

Figure 1 shows a useful summary of much of the data obtained. The numbers are for the case of no aberrations, perfect focus, finite objective aperture, and ideal phase contrast. Comparison with the other results obtained shows that these ideal numbers can be applied to useful, nonideal situations. Nearly ideal phase contrast can be obtained by a small amount of defocus, which does not appreciably impair resolution. In addition, the aberrations produce only a small effect if the aperture

is kept below the actual optimum aperture for a given aberrational situation. We write

$$\frac{I(\infty) - I(r)}{I(\infty)} \approx C(1 - C/4) \approx C, \quad (1)$$

where

$$\begin{aligned} I(\infty) &= \text{background intensity,} \\ I(r) &= \text{intensity at distance } r \text{ from image center,} \\ C &= \text{contrast (for } C/4 \ll 1, \text{ at any rate).} \end{aligned}$$

If phase contrast is obtained by defocus, the sign of C should be reversed. The contrast can be written as a universal function by introducing a new function F , and use of a scaled radial variable

$$\begin{aligned} C(r, Z, V, \alpha) &= Z(10^5/V)^{1/2} \\ &\times F\left(Z^{1/3}r, Z^{-1/3}\alpha(V/10^5)^{1/2}\right), \quad (2) \end{aligned}$$

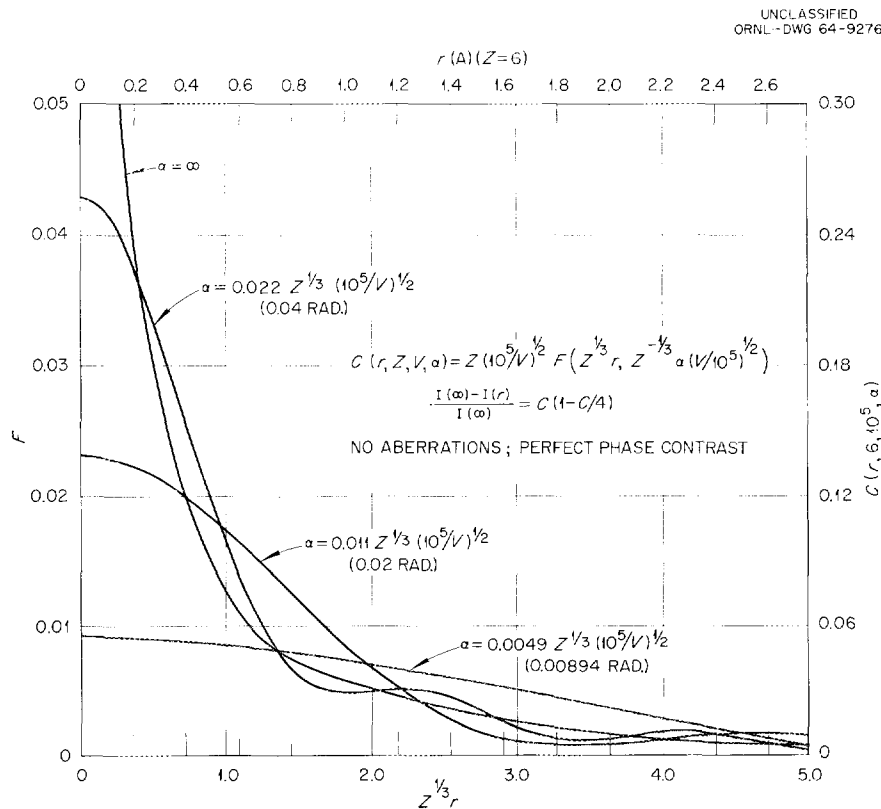


Fig. 1. Atomic Image Contrast as a Function of Atomic Number, Objective Aperture, Beam Voltage, and Radial Distance from Image Center.

where

- Z = atomic number,
- V = beam energy in volts,
- α = objective aperture in radians,
- r = distance in angstroms from image center
(assuming unit magnification).

On the left we give the scale of F , the "universal" contrast function, while a scale for the actual contrast in the case of carbon is given on the right. At the bottom is the scale for the "universal" radial variable, while at the top is the corresponding scale in angstroms for carbon. We have taken $V = 10^5$ v for the carbon numbers. The curve labeled ($\alpha = \infty$) gives the theoretical case of perfect resolution and just follows the curve for the Fermi-Thomas potential, integrated through the atom along the beam direction and projected on to the object plane. The curve marked ($\alpha = 0.04$ radian) gives the high-resolution result for carbon, or results at somewhat differing conditions for other atoms. The curve marked (0.02 radian) is an intermediate-resolution instrument (~ 2.5 Å), viewing carbon. The lowest curve, marked (0.00894 radian), is essentially a conventional instrument viewing carbon. Remembering the $Z^{1/3}$ conversion factors, we see that the intermediate-resolution curve will also describe the situation for $\alpha = 0.04$ radian and $Z = 48$, $V = 10^5$; or for $Z = 6$, $V = 0.25 \times 10^5$, for example.

Figure 2 shows a sample image plane intensity plot for the conventional instrument when eight bromine atoms are placed 3.4 Å apart in the form of a hollow square. Contrast has been achieved by defocus, but neither the contrast nor the resolution is adequate for useful measurement. Figure 3, on the other hand, shows the same atomic configuration at high resolution. Note the high visibility of the bromine atoms, which are spaced roughly as they might be in bromine-substituted DNA. Complicated three-dimensional structures present much more severe problems, and an attempt is being made to investigate the limitations on the determination of such structures imposed by considerations of statistical errors in electron intensity distributions and other practical problems.

ORNL-DWG 64-9461

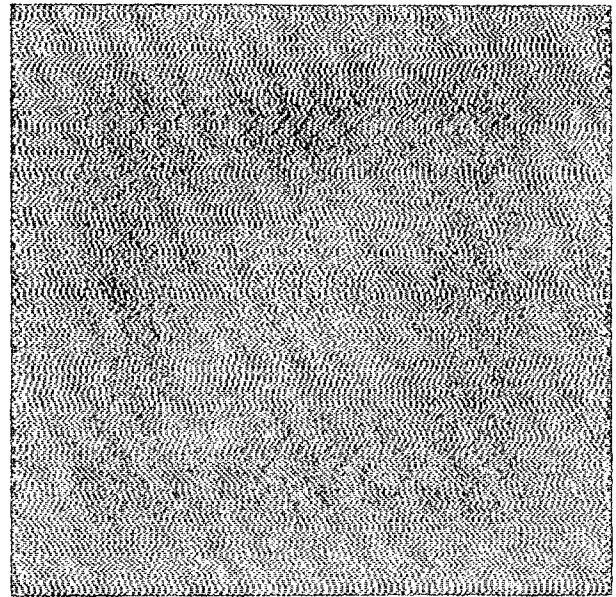


Fig. 2. Image Plane Intensity Distribution for Conventional Microscope with Eight Bromine Atoms in Object Plane.

ORNL-DWG 64-9463

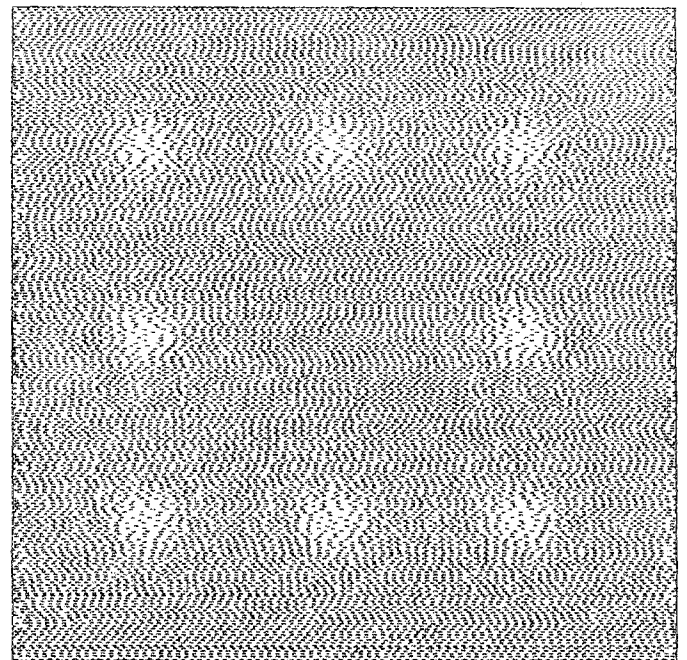


Fig. 3. Image Plane Intensity Distribution for High Resolution Microscope with Eight Bromine Atoms in Object Plane.

RELATIVISTIC QUANTUM MECHANICS WITH A FUNDAMENTAL LENGTH

T. A. Welton

A formalism has been constructed for the systematic introduction of a fundamental length into relativistic quantum mechanics by use of noncommuting coordinate operators. The theory is in principle not Lorentz invariant, although this can become experimentally manifest only under conditions which are extremely difficult to achieve, the recently observed apparent failure of *CP* invariance in the decay of the neutral *K* meson being possibly such a manifestation. A systematic investigation has been performed of the value of the new length

constant (*a*) required by a number of experimental results. A value for *a* of as much as 0.3 fermi would be allowed by all experimental results, while a value less than about 0.2 fermi would be uncomfortably small for some purposes. A form factor $\exp(-k^2 a^2/2)$ is predicted for the electron-electron scattering. As an interesting by-product, a formulation of weak interaction theory is given with the length *a* obviating in a natural way the theoretical need for the presently unobserved intermediate boson. (A paper is being written for publication.)

HARTREE-FOCK CALCULATIONS OF FINITE NUCLEI

K. T. R. Davies

M. Baranger¹

There has been much interest in recent years in calculating finite nuclei by various kinds of Hartree-Fock methods,² starting from a "realistic" two-body interaction. From such calculations, one can obtain, throughout the periodic table, many interesting nuclear properties, for example, ground-state energies of nuclei, single-particle levels, nuclear deformations, energy gaps, and other quantities which follow from these.

In our research we have been concentrating on two related phases of the Hartree-Fock program: (1) the determination of a two-body force or "effective interaction," and (2) methods for evaluating the most general types of two-body matrix elements one is likely to encounter in a Hartree-Fock calculation. The second phase of the work is most important, since we want to have available computer programs which can be used to treat any two-body force, not just the particular interaction that we propose. These two phases of the research will now be discussed in more detail.

¹Carnegie Institute of Technology, Pittsburgh, Pa.

²Hartree-Bogoliubov theory may be necessary in some cases. This is the generalization of Hartree-Fock theory in order to include pairing effects. See, for example, M. Baranger in *1962 Cargese Lectures in Theoretical Physics* (ed. by M. Levy), p. V-65, Benjamin, New York, 1963.

Determination of the Two-Body Force

We require that the interactions have the following properties:

1. First and foremost, the matrix elements of the force between single-particle wave functions must be reasonably easy to calculate. Eventually we want to be able to treat deformed nuclei, so it would also be desirable to have an effective interaction which separates easily into *x*, *y*, and *z* relative coordinates. For this reason, Gaussian or combinations of Gaussian potentials seem particularly suitable.
2. The two-body force should yield the right energy and density of nuclear matter. This will correctly take into account the volume term in the Weizsäcker semiempirical mass formula.
3. In order to obtain good convergence with our Hartree-Fock approximation, we shall require that the second-order Goldstone terms in nuclear matter be fairly small. This can be done by avoiding potentials which have hard cores or other singularities and by making the ranges of the potential sufficiently long.
4. Some attempt should be made to fit the two-body data with the force. The effective ranges and scattering lengths for the singlet, even

and triplet, even potentials should be fitted, and the s -wave phase shifts should be approximately correct. In particular, the 1S_0 phase shift should change sign between 200 and 300 Mev, and the 3S_1 phase shift should become negative somewhat above 300 Mev. An attempt should be made to roughly fit the p -wave phase shifts, and after tensor forces have been included in the potential, the deuteron quadrupole moment and the percentage of d state should also be fitted. Trying to fit the other phase shifts, although desirable, would undoubtedly make the force too complicated; we will, therefore, concentrate only on the two-body data mentioned above.

We have been using local, Gaussian potentials, with velocity-dependent repulsive parts. This interaction is of the same form as the potential used by Green,³ although we parametrize the force in a different way. In particular, the ranges of the repulsive parts are not nearly as short as those occurring in Green's potential. So far, we have concentrated on a very simple potential, namely, a central force which has only singlet, even and triplet, even terms. For this simple force, programs have been written for calculating the two-body data, the energy and density of nuclear matter, and the second-order Goldstone terms in nuclear matter. Fits to the relevant data are now being made. In the future we plan to treat the odd potentials and also the tensor and spin-orbit parts of the force.

Evaluation of Two-Body Matrix Elements

In order to calculate the most general types of two-body matrix elements, it is necessary to make use of the transformation or oscillator brackets.^{4,5} These brackets connect the wave functions for two particles in a harmonic oscillator potential with the center-of-mass and relative wave functions. Brody and Moshinsky have tabulated a large number of these brackets,⁵ which will be denoted as follows:

$$\langle n_1 l_1, n_2 l_2; \lambda | n l, N L; \lambda \rangle.$$

The total angular momentum of the system is λ ; $n_1 l_1$ and $n_2 l_2$ pertain to particles 1 and 2; $n l$ refers to the relative coordinates; $N L$ to the center-of-mass coordinates.

There exists a new method for calculating the oscillator brackets. This method is particularly suitable for use in Hartree-Fock calculations and differs considerably from the approach of Brody and Moshinsky. In the Hartree-Fock program we do not know whether each single-particle wave function (SPWF) will turn out to be accurately represented by a harmonic oscillator wave function (HOWF). It is then desirable to use the HOWF's as a basis for expansion of the SPWF's, and one of the questions we wish to investigate is how many HOWF's are required in order to give a good representation of an SPWF. Therefore, we want to consider HOWF's with large values of n_1 and n_2 ; Brody and Moshinsky only calculated the brackets for values of n_1 and n_2 up to 3.

On the other hand, it is not necessary to tabulate the brackets for large values of the relative angular momentum, l . It has been shown by Kuo and Baranger that only $l = 0$ and 1, and to a small extent $l = 2$, make appreciable contributions to nuclear matrix elements.⁶ Therefore we will be most concerned with calculating the brackets for $l = 0, 1$, and 2.

Our approach is thus seen to be quite different from that of Brody and Moshinsky. They derived an explicit expression for $n_1 = n_2 = 0$, any l , and then used a recursion formula to go to higher n_1 and n_2 . To use this formula to calculate the brackets for large values of n_1 and n_2 is much too complicated for our purposes. The method that we are using is based on deriving an explicit expression for $l = 0$, any n_1 and n_2 , and then calculating brackets for $l = 1$ and $l = 2$ in terms of those with $l = 0$.

Actually, there are many simple nuclear calculations that one can do with a force which acts only in relative s states, so that only the $l = 0$ brackets are needed. Therefore, this new technique should be of practical use, not only in Hartree-Fock calculations, but for many other types of nuclear computations as well. Programs for calculating the brackets by this method are now being written.

³A. M. Green, *Nucl. Phys.* **33**, 218 (1962).

⁴M. Moshinsky, *Nucl. Phys.* **13**, 104 (1959).

⁵T. A. Brody and M. Moshinsky, *Tables of Transformation Brackets*, University of Mexico, Physics Dept., 1960.

⁶T. S. Kuo (thesis), University of Pittsburgh, Pittsburgh, Pa.

CALCULATION OF THE PROPERTIES OF THE GROUND STATE OF ^{16}O IN THE BRUECKNER APPROXIMATION

R. L. Becker

A. D. MacKellar¹

The use of perturbation theory in terms of a reaction matrix t instead of the nucleon-nucleon potential v permits calculations of nuclear properties in which realistic strong nuclear interactions are used. Extensive tests of Brueckner's approximation, the analog of the Hartree-Fock approximation with t replacing v , have been made for infinite nuclear matter. While it may be necessary to include some higher terms in order to obtain excellent agreement with the volume term in the Weizsacker binding energy formula, it seems that Brueckner's approximation is a good first approximation. Similar calculations for finite nuclei are much more difficult because of the lack of translation invariance.

Brueckner, Gammel, and co-workers² have attempted to use their infinite matter reaction matrix elements in calculations for finite nuclei, but have consistently obtained too little binding. Their "local density" approximation, which neglects terms involving the derivatives of the nucleon density, has recently been tested in model calculations by Kohler.³ He finds that the local density approximation tends to seriously underestimate the binding energy. We assume therefore that the low binding energies obtained by Brueckner *et al.* arise from the local density approximation and not, for example, from the inadequacy of the assumed nucleon-nucleon interaction or the importance of three-body clusters.

Eden and Emery⁴ have outlined an approach to the Brueckner approximation for closed-shell nuclei which avoids the local density approximation by calculating reaction matrix elements directly between shell model states. The method

relies on the ease of expanding products of single-particle harmonic oscillator wave functions in terms of similar wave functions in center-of-mass and relative coordinates. Their detailed calculations involved many approximations and relatively crude numerical procedures, but gave promising results for ^{16}O .

To date we have performed calculations for ^{16}O in which the details of the Eden-Emery calculation have been improved upon in several ways. Also greater numerical accuracy is attained, parameters are being explored more extensively, and more recent nucleon-nucleon potentials are being used. A generalization of the method to permit departure of the single-particle potential from the local harmonic oscillator form, which requires a considerable increase in complexity, is being developed.

At this time we should like to stress the importance of an accurate treatment of the tensor force. Figure 1 contains plots of calculations of the binding energy of ^{16}O as a function of the range parameter, α , of the single-particle potential. For all three curves the same Gammel-Thaler nucleon-nucleon potential was used. The curve labeled EES is that of Eden, Emery, and Sampanthar.⁵ Curve 1 differs from curve EES only in that coupled Bethe-Goldstone equations were solved for $u_{1s}(r)$ and $w_{1s}(r)$, the s and d radial wave functions arising from the relative $1s$ oscillator function, whereas EES had used an approximation which neglected the influence of w_{1s} on u_{1s} . The value of α , namely α_0 , for which the Brueckner-Hartree-Fock self-consistency condition

$$\langle n|V|n \rangle = \sum_{m \text{ (occupied)}} \left[\langle nm|t|nm \rangle - \langle nm|t|mn \rangle \right]$$

is most nearly satisfied is quite different for the two curves. Moreover, the predicted binding energies at the respective α_0 's differ by about 25

¹Oak Ridge Graduate Fellow from Texas A & M University.

²K. A. Brueckner, J. L. Gammel, and H. Weitzner, *Phys. Rev.* **110**, 431 (1958); K. A. Brueckner, A. M. Lockett, and M. Rotenberg, *Phys. Rev.* **121**, 255 (1961); K. S. Masterson and A. M. Lockett, *Phys. Rev.* **129**, 776 (1963).

³H. S. Kohler, "Theory of Finite Nuclei," to be published in the *Physical Review*; "On the Properties of Finite Nuclei," preprint.

⁴R. J. Eden and V. J. Emery, *Proc. Roy. Soc. (London)* **A248**, 266 (1958).

⁵R. J. Eden, V. J. Emery, and S. Sampanthar, *Proc. Roy. Soc. (London)* **A253**, 177, 186 (1959).

Mev. When the predicted binding energies are compared at the same value of α , the difference is even greater, ~ 55 Mev for $\alpha = 0.5$ and ~ 105 Mev for $\alpha = 0.6$.

A very simple kind of velocity dependence of the single-particle potential is contained in the Eden-Emery method through a spatially constant term which differs from state to state. The constants can be varied to most nearly satisfy the self-consistency condition at a given value of α . Curve 2 of Fig. 1 differs from curve 1 in taking into account the dependence of these constants on the state of the center-of-mass motion of the pair. This improvement has little effect on the nuclear radius but results in greater binding energy. Similar calculations are being made, using the more recent Hamada-Johnston nucleon-nucleon potential.

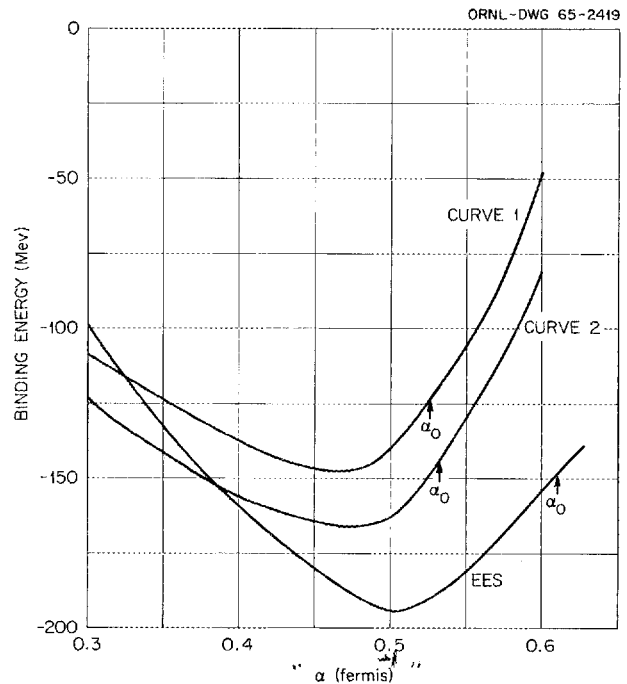


Fig. 1. Calculated Ground State Binding Energy of ^{16}O vs α , the Harmonic Oscillator Range Parameter. Curves are labeled as described in the text.

A COMPUTER PROGRAM FOR LARGE-SHELL-MODEL CALCULATIONS

E. C. Halbert¹ J. B. McGrory S. S. M. Wong² J. B. French²

An IBM 7090 program has been written to carry out large-shell-model calculations in which particles are allowed to occupy several different j shells. The technique of the calculation is based on a second-quantized formalism developed by J. B. French.³ Particles in a given j shell are coupled to form single-shell states quantized

in J , T , seniority, and reduced isotopic spin. Multishell states quantized in J and T are formed by appropriate coupling of single-shell states. The residual interaction is introduced into the calculation in the form of appropriately antisymmetrized two-body matrix elements, which make up part of the program input data for each calculation. Methods for the elimination of spurious states are incorporated in the program for those cases in which the nuclear radial wave functions are approximated by those of the harmonic oscillator.

¹Electronuclear Division.

²University of Rochester, Rochester, N.Y.

³Unpublished notes.

DISTORTED-WAVE CALCULATIONS AND SPECTROSCOPIC FACTORS¹

G. R. Satchler

The accuracy of spectroscopic factors obtained from distorted-wave analysis of stripping reactions is reviewed, and some of the remaining theoretical problems are discussed.

¹Abstract of invited paper presented at Symposium on Nuclear Spectroscopy with Direct Reactions, Chicago, March 9-11, 1964. Proceedings of conference published in *Nuclear Spectroscopy with Direct Reactions. II. Proceedings*, ANL-6878, p. 23.

"FINITE-RANGE" EFFECTS IN THE DISTORTED-WAVE THEORY OF STRIPPING REACTIONS¹

R. M. Drisko²

G. R. Satchler

The effects of removing the zero-range approximation in the distorted-wave theory are shown by exact calculation for a number of typical stripping reactions.

¹Abstract of published paper: *Phys. Letters* **9**, 342 (1964).

²Work performed while on leave of absence from the University of Pittsburgh, Pittsburgh, Pa.

OPTICAL-MODEL ANALYSIS OF "QUASI-ELASTIC" (p,n) REACTIONS¹

G. R. Satchler

R. M. Drisko²

R. H. Bassel³

Measured differential cross sections for (p,n) transitions between isobaric analog states are compared with the predictions of an optical model which includes an isobaric spin-dependent potential proportional to $t \cdot T_0$, where t and T_0 are the isobaric spins of projectile and target respectively. The magnitudes of the measured cross sections indicate a strength for this potential which is

close to the symmetry potential found from analysis of elastic proton scattering. The shapes of the angular distributions give strong evidence for the radial shape of this potential to be peaked at the nuclear surface. The calculations are made in the distorted-wave Born approximation, using optical-potential parameters determined by fits to elastic scattering. Numerical studies are made of the sensitivity of the predictions to various parameter changes to determine the significance of the fits obtained to experiment. Finally, some discussion is given of the "quasi-inelastic" transitions to excited isobaric states, in terms of the collective-model description of inelastic scattering.

¹Abstract of published paper: *Phys. Rev.* **136**, B637 (1964).

²Work performed while on leave of absence from the University of Pittsburgh, Pittsburgh, Pa.

³Electronuclear Division.

THE SHELL MODEL AND INELASTIC SCATTERING BY NUCLEI

R. H. Bassel¹ R. M. Drisko² R. M. Haybron³
 M. B. Johnson⁴ L. W. Owen⁵ G. R. Satchler

In recent years the inelastic scattering of various projectiles from nuclei has been successfully interpreted in terms of the collective model. This assumes that the optical-model potential is non-spherical. However, in order to study the consequences of recent nuclear structure calculations, using shell-model wave functions, a more detailed, microscopic description of the interaction between projectile and target is needed. The present studies assume that this arises from a two-body force between the projectile and each target nucleon. Such an interaction has the characteristics of a one-body operator in the space of the target nucleons, and all the apparatus of the algebra of tensor operators is available to study its properties, such as selection rules imposed by particular assumptions about the shell-model configurations.

At high energies the impulse approximation may be used; the effective two-body force becomes the scattering amplitude between the projectile and a free nucleon and may be taken from experiment. Calculations of the scattering of 150- to 200-Mev protons from light nuclei indicate that this can be a very useful tool; the present need is for more extensive and more accurate experimental data, rather than further theoretical sophistication. Study of the available data seems to confirm the general validity of the hole-particle wave functions recently proposed.

At lower energies, the effective two-body force has to be treated phenomenologically; it is hoped that study of nuclei whose wave functions are reasonably well understood will determine the parameters of the force. Some progress has been made in this direction for proton scattering from ⁴⁰Ca, ⁵¹V, and ⁹⁰Zr. The scattering of alpha particles and deuterons is also being analyzed with this model. An attempt is being made to use, for the alpha interaction, the optical potential which fits nucleon-helium scattering. This includes a spin-orbit term which could give rise to nonnormal parity transitions in inelastic alpha scattering.

¹Electronuclear Division.

²University of Pittsburgh, Pittsburgh, Pa.

³On loan from Michigan State University, East Lansing.

⁴Participant in Student Cooperative Program from Virginia Polytechnic Institute.

⁵Graduate student, University of Tennessee, Knoxville.

FORM FACTORS FOR NUCLEAR STRIPPING REACTIONS¹

W. T. Pinkston^{2,3} G. R. Satchler

The wave function, or form factor, to be used for the captured particle in a stripping reaction is discussed. It is shown that the structure of the nucleus must be taken into account, and leads to a set of coupled equations for this form factor.

Approximate solutions to these equations are studied, and their relations to various phenomenological prescriptions for the form factor are discussed. It is stressed that if an effective one-body potential well is used to generate the wave function, it is probably not sufficient to merely vary its depth; but changes in shape (particularly in radius) must be considered. The procedure of using an effective binding energy different from the separation energy is shown, in principle, to be wrong.

¹Abstract of paper to be submitted for publication in *Nuclear Physics*.

²Work performed while on leave at the Bartol Research Foundation of the Franklin Institute, Swarthmore, Pa.

³Present address: Department of Physics, Vanderbilt University, Nashville, Tenn.

**SLATER INTEGRALS AND FORM FACTORS FOR INELASTIC SCATTERING
USING REALISTIC SINGLE-PARTICLE WAVE FUNCTIONS:
THE CODE ATHENA¹**

M. B. Johnson²L. W. Owen³

A FORTRAN code has been written for the IBM 7090 which computes Slater integrals and form

factors suitable for inelastic scattering calculations, using single-particle wave functions which are eigenstates of motion in a Woods-Saxon potential well. Two-body forces of Gauss, Yukawa, double-Yukawa ("soft core"), and Coulomb radial dependence may be used. Nonlocal effects on the single-particle wave functions may be included in the local energy approximation.

¹Abstract of ORNL-TM-964.

²Participant in Student Cooperative Program, from Virginia Polytechnic Institute.

³Graduate student, University of Tennessee, Knoxville.

PRIOR-FORM DWBA STRIPPING PROGRAM

F. P. Gibson¹

A computer program is being written which calculates the d - p stripping differential cross section, using the prior form of the distorted-wave Born approximation matrix element. This element in the infinite mass approximation is written as follows (using center-of-mass and relative coordinates):

$$T = \left\langle F_p^{(-)} \left(\vec{R} + \frac{\vec{r}}{2} \right) G_n \left(\vec{R} - \frac{\vec{r}}{2} \right) \left| V_{pI} \left(\left| \vec{R} + \frac{\vec{r}}{2} \right| \right) + V_{nI} \left(\left| \vec{R} - \frac{\vec{r}}{2} \right| \right) - U_{dR}(R) \right| \phi_d(r) F_d^+(\vec{R}) \right\rangle,$$

where the meaning of the symbols is obvious. The potentials and ϕ , the internal deuteron wave function, are assumed to be spherically symmetric. We also assume the deuteron scattering potential to be

$$U_{dR}(R) = V_{pI}(R) + V_{nI}(R).$$

Then, using translation operators, we write T as

$$T = \left\langle F_p^{(-)}(\vec{R}) G_n(\vec{R}) \left| \theta_+ V_{pI}(R) + \theta_- V_{nI}(R) \right| \phi_d(r) F_d^+(\vec{R}) \right\rangle,$$

where

$$\theta_{\pm} = \exp \left[\frac{\vec{r}}{2} \cdot (\nabla_p - \nabla_n \pm \nabla_{\pm}) \right] - \exp \left[\frac{\vec{r}}{2} \cdot (\nabla_p - \nabla_n) \right].$$

The ∇_+ acts on V_{nI} , ∇_- acts on V_{pI} , ∇_p acts on F_p , and ∇_n acts on G_n . Each Taylor operator is integrated over solid angle and expanded; for example,

$$\begin{aligned} \int d\omega_r \exp \left[\frac{\vec{r}}{2} \cdot (\nabla_p - \nabla_n) \right] &= 4\pi \frac{\sinh(r/2) |\nabla_p - \nabla_n|}{(r/2) |\nabla_p - \nabla_n|} \\ &= 4\pi \sum_n \frac{[r^2 (\nabla_p - \nabla_n)^2]^n}{2^{2n} (2n+1)!}. \end{aligned}$$

The resultant terms are simplified with the aid of Green's theorem and the Schrodinger equation.

¹ORINS Postgraduate Fellow.

RADIAL INTEGRALS USING REALISTIC SINGLE-PARTICLE WAVE FUNCTIONS AND THE CODE OVERLAP¹

L. W. Owen²

A FORTRAN code has been written to compute radial integrals of a variety of radial operators, using single-particle wave functions which are

eigenstates of motion in a Woods-Saxon potential well. The radial operators currently available are r^n , $0 \leq n \leq 5$, and $(d/dx)(e^x + 1)^{-1}$, where $x = (r - R_0)/a_0$. Other functional forms may be added easily.

¹Abstract of ORNL-TM-958.

²Graduate student, University of Tennessee, Knoxville.

ANALYSIS OF THE SCATTERING OF 28-Mev ALPHA PARTICLES¹

G. R. Satchler

The elastic and the inelastic scattering of 28-Mev alpha particles from the nuclei Ne, Mg, Al, Si, Ti, Ni, Co, Ag, Cd, and Sn have been analyzed, using a nonspherical optical-model potential and the distorted-wave approximation. A four-parameter Woods-Saxon potential was used. Good fits are

obtained for the medium-weight and the heavy nuclei, qualitative fits for the lighter nuclei. The deformabilities extracted are in good agreement with those found by other methods. Coulomb excitation is found to be important for the heavy nuclei. Some account is taken of quadrupole contributions to the elastic scattering from aluminum.

¹Abstract of paper submitted to *Nuclear Physics*.

THE REACTIONS $^{48}\text{Ti}(n,d)^{47}\text{Sc}$, $^{16}\text{O}(n,d)^{15}\text{N}$, $^{10}\text{B}(n,d)^9\text{Be}$, AND $^6\text{Li}(n,d)^5\text{He}$ AT 14.4 Mev¹

V. Valkovic² G. Paic² I. Slaus^{2,3} P. Tomas²
M. Cerineo² G. R. Satchler

NUCLEAR REACTIONS. $^{48}\text{Ti}(n,d)$, $^{16}\text{O}(n,d)$, $^{10}\text{B}(n,d)$, $^6\text{Li}(n,d)$, $E = 14.4$ Mev; measured $\sigma(E_d, \theta)$. ^{47}Sc , ^{15}N , ^9Be , ^5He deduced levels, π , l , spectroscopic factors.

The reactions $^{48}\text{Ti}(n,d)^{47}\text{Sc}$, $^{16}\text{O}(n,d)^{15}\text{N}$, $^{10}\text{B}(n,d)^9\text{Be}$, and $^6\text{Li}(n,d)^5\text{He}$ have been studied

at 14.4 Mev. The absolute differential cross sections have been analyzed, using the distorted-wave method and assuming simple proton pickup. The effects of finite range, nonlocality, and radial cutoff have been investigated. Good fits obtained for the reactions $^{16}\text{O}(n,d)^{15}\text{N}$ (ground state), $^{10}\text{B}(n,d)^9\text{Be}$ (ground state), and $^{10}\text{B}(n,d)^9\text{Be}$

¹Abstract of paper to be submitted to the *Physical Review*.

²Institute "Ruder Boskovic," Zagreb, Yugoslavia.

³Present address: University of California at Los Angeles.

(2.43 Mev) yield spectroscopic factors in close agreement with shell model predictions. The shape of the angular distribution of the reaction $^{48}\text{Ti}(n,d)^{47}\text{Sc}$ is well explained, but a discrepancy in absolute magnitude of about a factor of 4 is

not yet understood. The agreement between theory and experiment for the reaction $^6\text{Li}(n,d)^5\text{He}$ (ground state) is not satisfactory, and this may indicate the importance of other processes such as knock-on.

EXCITATION OF LOW-LYING LEVELS IN ^{40}Ca BY (p,p') SCATTERING AT $E_p = 55$ Mev¹

K. Yagi² H. Ejiri² M. Furukawa^{2,3} Y. Ishizaki²
 M. Koike² K. Matsuda² Y. Nakajima^{2,4} I. Nonaka²
 Y. Saji² E. Tanaka^{2,5} G. R. Satchler

NUCLEAR REACTIONS. $^{40}\text{Ca}(p,p')$, $E = 55$ Mev; measured $\sigma(E_p, \theta)$. ^{40}Ca deduced levels, $J, \pi, B(\lambda)$.

The measured differential cross section for excitation of states at 0, 3.7, 4.5, and 6.9 Mev in ^{40}Ca are analyzed, using the distorted-wave method and the simple collective model.

¹Abstract of published paper: *Phys. Letters* 10, 186 (1964).

²Institute for Nuclear Study, University of Tokyo, Tokyo, Japan.

³Now at Department of Nuclear Engineering, University of Tokyo, Tokyo, Japan.

⁴Department of Nuclear Engineering, University of Hiroshima.

⁵Department of Physics, Tohoku University.

PROTON EXCITATION OF VIBRATIONAL STATES OF ^{126}Te ¹

G. C. Pramila^{2,3} R. Middleton^{4,5} T. Tamura⁶
 G. R. Satchler

NUCLEAR REACTIONS. $^{126}\text{Te}(p,p')$, $E = 12$ Mev; measured $\sigma(E_p, \theta)$. ^{126}Te deduced levels, $J, \pi, B(\lambda)$.

The differential cross sections for the elastic and inelastic scattering of 12-Mev protons by ^{126}Te have been measured. The results are interpreted in terms of the collective model, using both the distorted-wave and coupled-channel methods.

¹Abstract of published paper: *Nucl. Phys.* 61, 448 (1965).

²Nuclear Physics Laboratory, Oxford, England.

³On leave from Tata Institute of Fundamental Research, Bombay, India, and supported by the Commonwealth Scholarship Commission.

The quadrupole and octupole vibrational states are identified at 0.67 and 2.395 Mev respectively. Levels at 1.36 and 1.42 Mev are interpreted as due to two quadrupole phonons. Scattering to some of the group of states just above 2 Mev is in agreement with the predictions for the excitation of three quadrupole phonons.

⁴AWRE, Aldermaston, Berkshire, England.

⁵Present address: University of Pennsylvania, Philadelphia.

⁶On leave from Tokyo University of Education.

ELASTIC SCATTERING OF DEUTERONS BY ^{40}Ca ¹R. H. Bassel² R. M. Drisko³ G. R. Satchler

NUCLEAR REACTIONS. $^{40}\text{Ca}(d,d)$, $E = 7, 8, 9, 10, 11, 12$ Mev; measured $\sigma(\theta)$.

The elastic scattering from ^{40}Ca of deuterons with energies of 7, 8, 9, 10, 11, and 12 Mev has been measured and subjected to optical-model

analysis, as a preliminary to a distorted-wave study of the $^{40}\text{Ca}(d,p)$ reaction. Considerable ambiguities in the optical-model parameters are found, and the results are discussed in detail. Inclusion of a polarization potential and of spin-orbit coupling is found to have little effect. An attempt is made to find a set of parameters that gives a good overall fit at all the energies.

¹Abstract of published paper: *Phys. Rev.* **136**, B960 (1964).

²Electronuclear Division.

³Department of Physics, University of Pittsburgh, Pittsburgh, Pa.

 $^{40}\text{Ca}(d,p)^{41}\text{Ca}$, A TEST OF THE VALIDITY OF THE DISTORTED-WAVE BORN APPROXIMATION¹L. L. Lee, Jr.² J. P. Schiffer² B. Zeidman² G. R. Satchler
R. M. Drisko³ R. H. Bassel⁴

NUCLEAR REACTIONS. $^{40}\text{Ca}(d,p)$, $E = 7, 8, 9, 10, 11, 12$ Mev; measured $\sigma(E_p, \theta)$. ^{41}Ca deduced levels, I, π , spectroscopic factors.

The reaction $^{40}\text{Ca}(d,p)^{41}\text{Ca}$ has been studied at deuteron energies of 7.0, 8.0, 9.0, 10.0, 11.0, and 12.0 Mev. Absolute differential cross sections for the four most prominent proton groups were meas-

ured and are compared with predictions based on the distorted-wave Born approximation. Particular emphasis is placed on the ability of this approach to extract precise spectroscopic factors, which for this reaction are expected to be known a priori. Effects of variation of optical parameters and of inclusion of spin-orbit and finite-range effects are discussed in detail. It can be concluded that, if one uses optical potentials which fit elastic-scattering data, spectroscopic factors can be extracted with an accuracy of 20% or better.

¹Abstract of published paper: *Phys. Rev.* **136**, B971 (1964).

²Argonne National Laboratory, Argonne, Ill.

³University of Pittsburgh, Pittsburgh, Pa.

⁴Electronuclear Division.

LEVELS IN ^{43}Ca AND ^{46}Ca STUDIED BY THE $^{43}\text{Ca}(d,d')$, $^{46}\text{Ca}(d,d')$,
AND $^{46}\text{Ca}(p,p')$ REACTIONS¹

T. A. Belote² J. H. Bjerregaard³ Ole Hansen^{2,3} G. R. Satchler

NUCLEAR REACTIONS. $^{43}\text{Ca}(d,d')$, $E = 8.522$ Mev; $^{46}\text{Ca}(d,d')$, $E = 10$ Mev; $^{46}\text{Ca}(p,p')$,
 $E = 7$ Mev; measured $\sigma(E',\theta)$. ^{43}Ca , ^{46}Ca deduced levels, π , l .

The $^{43}\text{Ca}(d,d')$ and $^{46}\text{Ca}(d,d')$ reactions were studied at bombarding energies of 8.522 and 10.005 Mev respectively. The deuterons were recorded on photographic emulsions in a multiple-gap heavy-particle spectrograph with an energy resolution of 15 kev. The measured angular distributions were analyzed, using the distorted-wave theory, and probable values of the angular momentum change involved in the excitations were determined. The

absolute cross sections are compared with the predictions obtained by using shell-model wave functions as well as collective vibrational wave functions. A simple model for the deuteron-nucleus interaction is introduced. In addition to the (d,d') experiments, the $^{46}\text{Ca}(p,p')$ reaction was studied at 3.8- and 7.00-Mev bombarding energies. The energies (in Mev) of the states observed in ^{46}Ca and their assigned spins and parities are 1.347 (2^+), 2.423, 2.575, 3.023 ($2, 3^+$), 3.614 (3^{--}), 3.645, 3.780, and 4.434 (3^-). In $^{43}\text{Ca}(d,d')$ we observe levels at 0.369 ($5/2^-$), 0.595 ($3/2^-$), 1.675 ($1^1/2 ? , -$), 1.932 ($?^-$), 2.051 ($3/2^-$), 2.070 ($1^5/2 ? , -$), 2.098 ($9/2 ? , -$), and 2.252 ($?^-$) Mev.

¹Abstract of paper submitted to the *Physical Review*.

²Laboratory for Nuclear Science, Massachusetts Institute of Technology, Cambridge.

³Institute for Theoretical Physics, University of Copenhagen, Copenhagen, Denmark.

LOW-LYING LEVELS IN ^{42}Ca EXCITED BY THE $^{43}\text{Ca}(d,t)$ REACTION¹

J. H. Bjerregaard² H. R. Blieden^{2,3} Ole Hansen²
G. Sidenius² G. R. Satchler

NUCLEAR REACTIONS. $^{43}\text{Ca}(d,t)$, $E = 8.5$ Mev; measured $\sigma(E_t,\theta)$. ^{42}Ca deduced levels, l , π , spectroscopic factors.

Angular distributions of triton groups corresponding to (d,t) transitions to five states in ^{42}Ca have been observed at a bombarding energy of 8.522 Mev. The tritons were recorded in a multigap broad-range spectrograph. The elastic scattering of deuterons from ^{43}Ca was also measured and fitted with an optical-model potential, which was

then used in a distorted-wave analysis of the (d,t) cross sections. The results are in good agreement with the predictions for an $(f_{7/2})^3$ configuration for ^{43}Ca and $(f_{7/2})^2$ for ^{42}Ca , except that the 2^+ parentage is split approximately equally between the 1.53- and 2.44-Mev states of ^{42}Ca . The data do not allow $l = 1$ pickup with more than a few percent of the single-particle strength. Transitions to the second 0^+ state at 1.84 Mev are not observed. The results are discussed in terms of the seniority coupling scheme and in terms of the shell model with residual interactions.

¹Abstract of published paper: *Phys. Rev.* **136**, B1348 (1964).

²University of Copenhagen, Copenhagen, Denmark.

³Present address: CERN, Geneva 23, Switzerland.

ELASTIC SCATTERING OF ${}^3\text{He}$ AND THE $({}^3\text{He}, d)$ REACTION¹

R. H. Bassel² G. R. Satchler R. M. Drisko³

The ${}^{40}\text{Ca}({}^3\text{He}, d){}^{41}\text{Sc}$ reaction is analyzed in zero-range distorted-wave approximation. Optical parameters for the ${}^3\text{He}$ channel are found by fitting

¹Abstract of paper presented at the International Conference on Nuclear Physics, Paris, July 2-8, 1964. Proceedings of the conference will be published in *Proceedings of the International Conference on Nuclear Physics*.

²Electronuclear Division.

to experimental elastic-scattering data. Reasonable agreement between theory and experiment is found. The absolute normalization from the $({}^3\text{He}, d)$ analysis is in fair agreement with that found from the ${}^{40}\text{Ca}(d, {}^3\text{He}){}^{39}\text{K}$ reaction.

³Permanent address: University of Pittsburgh, Pittsburgh, Pa.

SHELL-MODEL SELECTION RULES AND EXCITATION OF 4^+ STATES IN THE $\text{Ti}(\alpha, \alpha')$ REACTION¹

G. R. Satchler J. L. Yntema² H. W. Broek²

NUCLEAR REACTIONS. ${}^{46,48,50}\text{Ti}(\alpha, \alpha')$, $E = 43$ Mev, measured $\sigma(\theta)$. ${}^{46,48,50}\text{Ti}$ deduced levels, J, π .

Analysis of the double excitation of 4^+ states in the titanium isotopes shows the influence of

the shell-model selection rule, which prevents direct excitation in ${}^{48}\text{Ti}$.

¹Abstract of published paper: *Phys. Letters* 12, 55 (1964).

²Argonne National Laboratory, Argonne, Ill.

WIDE-ANGLE SCATTERING OF 43-Mev ALPHA PARTICLES BY ${}^{58}\text{Ni}$ ¹

H. W. Broek² J. L. Yntema² B. Buck³ G. R. Satchler

NUCLEAR REACTIONS. ${}^{58}\text{Ni}(\alpha, \alpha')$, $E = 43$ Mev, measured $\sigma(E_{\alpha'}, \theta)$. ${}^{58}\text{Ni}$ deduced levels, $J, \pi, B(\lambda)$.

Elastic and inelastic scattering of 43-Mev alpha particles by ${}^{58}\text{Ni}$ has been observed over the angular range from 15 to 142° c.m. Angular dis-

tributions were derived for elastic scattering and for inelastic scattering to the 2^+ first excited level at 1.45 Mev, the two-phonon group at 2.47 Mev, and the strong 3^- level at 4.45 Mev. The angular distributions show strong oscillations (with a period of 10°) at angles less than about 70°, but the oscillations become less pronounced

¹Abstract of paper submitted to *Nuclear Physics*.

²Argonne National Laboratory, Argonne, Ill.

³Nuclear Physics Laboratory, Oxford University.

for angles greater than 70° . The oscillation period tends to increase with increasing angle to a value of about 15° at the largest angles observed. Optical-model analysis of the elastic scattering has been made, and the inelastic scattering to the 2^+ and 3^- levels has been calculated, using the distorted-wave method. A coupled-channel analysis of the elastic scattering and of the in-

elastic scattering to the 2^+ and 4^+ levels was also undertaken. Good agreement with experiment is found in all cases. It was necessary to use an optical potential in which the absorptive potential has a somewhat different shape than the real potential. There is also some indication that better results are obtained by using a complex coupling in the distorted-wave calculations.

OPTICAL-MODEL ANALYSIS OF 182-Mev PROTON SCATTERING¹

G. R. Satchler

R. M. Haybron²

In order to obtain optical potentials for use in calculations of nuclear reactions with high-energy

protons, the data on the elastic scattering of 182-Mev protons were reanalyzed. Good fits were obtained, yielding a χ^2 that was one or two orders of magnitude smaller than those for previously quoted "best fits."

¹Abstract of published paper: *Phys. Letters* 11, 313 (1964).

²On loan from Michigan State University, East Lansing.

SYMPLECTIC SYMMETRY IN $f_{7/2}$ SHELL NUCLEI¹

J. N. Ginocchio²

The status of the conservation of symplectic symmetry in the nuclear $f_{7/2}$ shell is investigated (1) by comparing the two-body interaction with the most general symplectic-conserving interaction using an a priori criterion developed for the purpose, (2) by examining symplectic admixtures in the cal-

culated nuclear wave functions, and (3) by studying the calculated symplectic energy bands. The interaction is determined from the best available data of the ^{42}Sc spectrum. It is concluded that, except in special cases, symplectic symmetry is not approximately conserved, and predictions based on a simple symplectic model are therefore invalid. Some comments are made concerning an alternative approach for studying the structure of the j^n configuration.

¹Abstract of published paper: *Nucl. Phys.* 63, 449 (1965).

²Now at the Department of Physics, Rutgers University, New Brunswick, N.J.

ANALYSES OF THE SCATTERING OF NUCLEAR PARTICLES BY COLLECTIVE NUCLEI IN TERMS OF THE COUPLED-CHANNEL CALCULATION¹

Taro Tamura

A detailed formalism for a coupled-channel calculation of the scattering of various nuclear par-

ticles by collective nuclei is presented. The formalism is sufficiently general that projectiles of any spin and targets of any kind of collectivity can be treated, and excitations of many states can

¹Abstract of paper submitted to *Physical Review*.

be included. The results of numerical calculations, made by using a computer program based on the above formalism, are given for several typical cases, so that the behavior of various cross sections as functions of parameters and the scheme of coupling taken in each calculation can be seen. Comparison of the theoretical results with various experimental data is made, and

it is seen that very good agreement was obtained in most of the cases. It is concluded that the coupled-channel calculation is a very powerful tool for explaining scattering data and in turn for clarifying the structure of nuclei. Interesting possibilities, both theoretical and experimental, are suggested for future studies.

ADIABATIC AND NONADIABATIC COUPLED-CHANNEL CALCULATIONS OF THE SCATTERING OF PROTONS BY DEFORMED NUCLEI¹

Taro Tamura

Adiabatic and nonadiabatic coupled-channel calculations were compared with each other in relation to the analyses of the scattering data² of 17.5-Mev protons by ¹⁶⁵Ho and ¹⁵⁶Gd. It was

found that the adiabatic calculation is more accurate and needs much shorter machine time, in the present case, than does the nonadiabatic calculation.³ Very good agreement with experiment was achieved by using parameters that seem more reasonable than those used in the previous non-adiabatic calculation.³

¹Abstract of published paper: *Phys. Letters* **12**, 121 (1964).

²A. Lieber and C. A. Whitten, *Phys. Rev.* **132**, 2582 (1963).

³T. Tamura, *Phys. Letters* **9**, 334 (1964).

EXCITATION OF THE UNNATURAL-PARITY 3⁺ STATE IN ²⁴Mg IN THE INELASTIC SCATTERING OF ALPHA PARTICLES¹

Taro Tamura

As an example of the excitation of unnatural-parity states² in even nuclei by the inelastic scattering of alpha particles, an analysis is made of data³ of ²⁴Mg(α, α')²⁴Mg* processes for $E_\alpha = 28.5$ Mev. The theoretical cross sections are obtained through the coupled-channel calculation, in which 0⁺, 2⁺, 4⁺, 6⁺, 2⁺, and 3⁺ states are coupled together, where the first four states are assumed as members of the $K = 0$ ground band,

while the last two are assumed as members of the $K = 2$ γ -vibrational band. Reasonably good agreement with experiment was obtained, allowing one to conclude that the multiple-excitation processes can account for the excitation of the unnatural-parity states. Comparison of our final result with experiment is made in Fig. 1.

¹Abstract of paper submitted to *Nuclear Physics*.

²W. W. Eidson and J. G. Cramer, Jr., *Phys. Rev. Letters* **9**, 497 (1962).

³J. Kokame *et al.*, *Phys. Letters* **8**, 742 (1964).

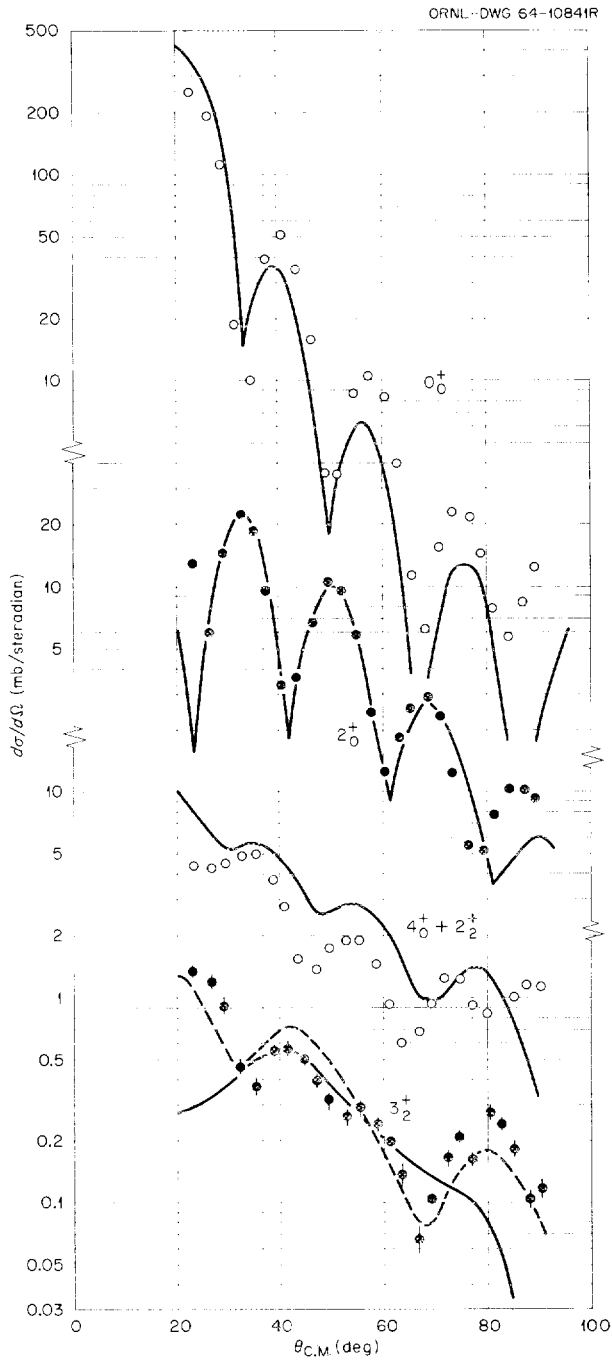


Fig. 1. Scattering Cross Sections of 28.5-Mev Alpha Particles by ^{24}Mg . The solid lines are the results of the calculation explained in the text. The dotted line for the 3^+ state is twice the theoretical result obtained with a weaker excitation assumed of the γ -vibrational states. This curve is shown in order to show that good agreement of shape can be obtained if the experimental 3^+ cross section were somewhat overestimated, a possibility which cannot be ruled out (J. Kokame, private communication).

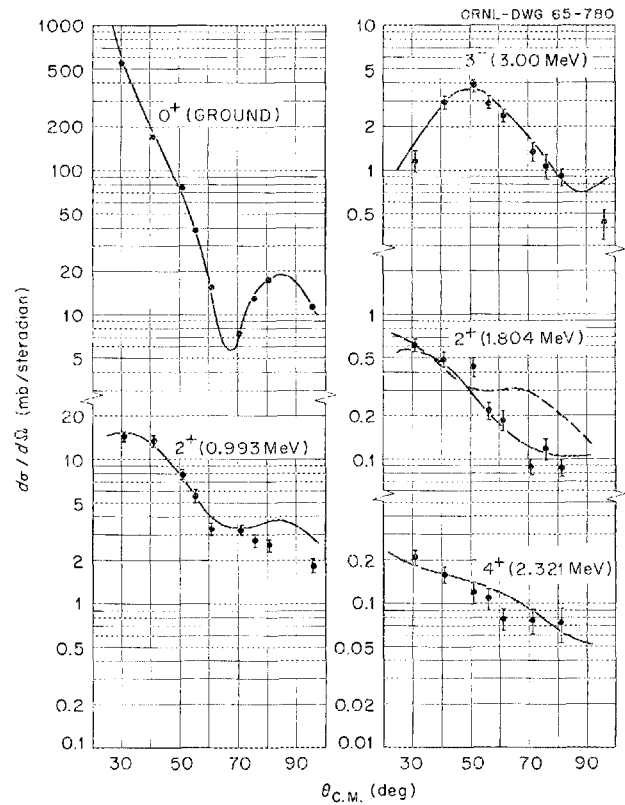
POSSIBLE ADMIXTURE OF ONE-PHONON 2^+ -STATE AMPLITUDE TO THE SECOND EXCITED STATE OF ^{64}Zn

Taro Tamura

Data of the scattering¹ of 17.5-Mev protons by ^{64}Zn were analyzed in terms of the coupled-channel calculation, and the result is shown in Fig. 1. The solid line for the second 2^+ state was obtained by considering a small admixture of one-phonon amplitude to the dominant two-phonon amplitude, while the dotted line was obtained without assuming the admixture. The much better agreement with experiment of the former than of the latter indicates that the former model is more reasonable than the latter.

¹N. R. Roberson, private communication.

Fig. 1. Scattering of 17.5-Mev Protons by ^{64}Zn .



INELASTIC SCATTERING OF PROTONS BY ^{114}Cd AND POSSIBLE QUADRUPOLE-OCTUPOLE TWO-PHONON STATES¹

M. Sakai²

T. Tamura

NUCLEAR REACTIONS, $^{114}\text{Cd}(p, p')$, enriched target, $E_p = 12.16$ Mev; measured $\sigma(\theta)$, p' spectrum. ^{114}Cd deduced levels, J, π .

Scattering cross sections of 12.16-Mev protons by ^{114}Cd were observed and fitted by the coupled-

¹Abstract of published paper: *Phys. Letters* 10, 323 (1964).

²Institute for Nuclear Study, Tokyo University, Tokyo, Japan.

channel calculation. The observed inelastic cross-section data to 12 excited states were all fitted very well by our calculation. Possible spin assignments were made to states that could be interpreted as the quadrupole-octupole two-phonon states.

COUPLED-CHANNEL ANALYSIS OF THE SCATTERING OF PROTONS BY ^{165}Ho AND ^{156}Gd ¹

Taro Tamura

Coupled-channel calculations were made for the scattering of 17.5-Mev protons by ^{165}Ho and ^{156}Gd . For the former a $7/2^- - 9/2^- - 11/2^-$ coupling was considered, while for the latter the

considered coupling was $0^+ - 2^+ - 4^+ - 6^+$. The agreement with experiments² was quite good in both cases.

¹Abstract of published paper: *Phys. Letters* 9, 334 (1964).

²A. Lieber and C. A. Whitten, *Phys. Rev.* 132, 2582 (1963).

TOTAL NEUTRON CROSS SECTIONS AT 1.44 eV¹L. A. Rayburn²

E. O. Wollan

Neutron transmission cross sections of several elements, separated isotopes, and compounds have been measured at the indium resonance energy, 1.44 eV.

¹Abstract of paper to be published in *Nuclear Physics*.

²Permanent address: University of Georgia. The work reported in this paper was carried out while Dr. Rayburn was a member of the ORNL staff (1950-52). For various reasons a complete report of the work was delayed for these many years.

LEVEL SPACINGS AND *s*-WAVE NEUTRON STRENGTH FUNCTIONS OF THE ISOTOPES OF HAFNIUMT. Fuketa¹

J. A. Harvey

NUCLEAR REACTIONS. ^{174}Hf , ^{176}Hf , ^{177}Hf , ^{178}Hf , ^{179}Hf , ^{180}Hf ; measured σ_{nT} .
Deduced resonance parameters, E_0 , Γ_n , Γ_γ ; level densities and Γ_n^0/D for isotopes.
Enriched targets.

Neutron transmission measurements have been made on enriched samples of the six isotopes of hafnium from ^{174}Hf to ^{180}Hf by use of the fast-chopper time-of-flight spectrometer at the ORR. The measurements were made from 0.2 to ~240 eV with an energy resolution from 1 to 2% below

50 eV and 60 nsec/m above 50 eV with the 45-m flight path. Higher-resolution measurements (0.3% energy resolution) with the 180-m flight path at the ORR were not made, since high-resolution capture and total cross-section measurements at higher energies were planned at the RPI linear accelerator.

¹Visiting scientist from the Japan Atomic Energy Research Institute, Tokai, Japan.

The enriched hafnium samples were all used in the powdered oxide form. Samples of the five

abundant isotopes were pressed into cylinders $2\frac{1}{4}$ in. in diameter and vacuum sealed in thin aluminum containers by E. Olszewski of the Target Preparation Group of the Isotopes Division. These samples were fabricated for capture measurements at the RPI linac and were suitable for transmission measurements with the ORNL fast-chopper spectrometer. Since only 0.660 g of ^{174}Hf was available, it was loaded into a standard chopper sample holder with inside dimensions $0.062 \times 0.60 \times 1.06$ in. The isotopic enrichments and specifications of the various samples are listed in Table 1.

The transmission data have been analyzed, using the area and shape analysis programs,² and parameters have been obtained for about 100 resonances. Listed in Table 2 are the parameters of the resonances from the area analysis program based on a value of 60×10^{-3} eV for Γ_γ for all the isotopes. The parameters are, in general, averages of several values, since there was considerable energy overlap of individual runs, and strong resonances in a particular isotope could easily be measured in a sample enriched in another isotope. The errors are based on the statistical accuracy of the transmission measure-

ment, the estimated error due to sample thickness, the error in isotopic abundance of the sample, and the agreement between the several values. Only the two lowest energy resonances were analyzed with the shape analysis program. The results for several of the runs are listed in Table 3. The errors on Γ_n are mostly due to the errors in sample thicknesses and isotopic abundances of the samples. These two resonances are in the ^{177}Hf isotope, but the ^{177}Hf sample was much too thick for its transmission to be analyzed by the shape analysis program in this energy region. The quoted errors on the individual values of Γ include the effect of an estimated error of 5% in the Doppler width, of 20% in the resolution, and a small error in the base line. The averaged values of Γ and Γ_γ include the effects of these systematic errors. The values of Γ_γ for these two resonances are in excellent agreement with previously reported values,³ but the values of Γ_n are somewhat smaller. The parameters of the resonances listed in Table 2 are in reasonable agreement with the results from older measurements,⁴ but the present data are of higher accuracy and extend to higher energies.

²S. E. Atta and J. A. Harvey, *Numerical Analysis of Neutron Resonances*, ORNL-3205 (1961) and Addendum (1963).

³H. H. Landon, *Phys. Rev.* 100, 1414 (1955).

⁴J. A. Harvey *et al.*, *Phys. Rev.* 99, 10 (1955).

Table 1. Isotopic Enrichments and Specifications of the Enriched Samples of the Hafnium Isotopes

Sample	Enrichment (%)						Grams of Oxide	Transmission Thickness (atoms/barn)
	^{174}Hf	^{176}Hf	^{177}Hf	^{178}Hf	^{179}Hf	^{180}Hf		
^{174}Hf	12.1	13.3	22.7	23.0	9.1	19.9	0.7785	0.00528
^{176}Hf	<0.1	68.7	14.9	8.7	2.7	5.0	11.388	0.00128
^{177}Hf	<0.05	1.15	84.5	9.2	2.2	2.9	17.7	0.00198
^{178}Hf (thin)							17.7	0.00198
^{178}Hf (thick)	<0.05	0.52	4.4	89.1	2.9	3.1	64.8	0.00723
^{179}Hf	<0.05	0.46	2.96	8.0	74.6	14.0	17.7	0.00197
^{180}Hf (thin)							17.7	0.00196
^{180}Hf (thick)	<0.05	0.23	1.00	2.2	2.7	93.9	64.8	0.00716

Table 2. Resonance Parameters of Hafnium Isotopes

	E_0 (ev)	Γ_n (mv)		E_0 (ev)	Γ_n (mv)	
^{174}Hf	4.25 ± 0.03	0.017 ± 0.004	^{177}Hf	46.3 ± 0.1	$+ 1.5$	
	13.38 ± 0.08	4.8 ± 0.9		7.3	$- 0.8$	
	29.94 ± 0.15	32 ± 7		48.9 ± 0.1	35 ± 10	
	70.5 ± 0.3	12 ± 5		49.6 ± 0.2	7 ± 3	
	77.9 ± 0.3	65 ± 6		54.8 ± 0.1	19.5 ± 1.0	
	107.1 ± 0.6	122 ± 25		56.5 ± 0.2	14.5 ± 1.5	
	124.6 ± 0.7	50 ± 20		57.2 ± 0.3	3.0 ± 1.0	
	147.6 ± 1.0	$+ 50$		120	59.4 ± 0.2	3.5 ± 1.0
		$- 30$			62.3 ± 0.3	~ 4
	153.5 ± 1.0	85 ± 20		63.6 ± 0.2	78 ± 4	
	211 ± 2	180 ± 60		66.8 ± 0.2	43 ± 4	
	^{176}Hf	48.3 ± 0.1		125 ± 15	71.6 ± 0.3	18 ± 2
53.2 ± 0.2		2.0 ± 0.5	76.1 ± 0.2	18 ± 1		
67.1 ± 0.2		20 ± 7	84.9 ± 0.3	40 ± 7		
123.8 ± 0.6		48 ± 10	88.6 ± 0.4	3.8 ± 0.7		
177.0 ± 1.5		50 ± 15	93.2 ± 0.4	5 ± 1		
201 ± 1.5		37 ± 12	97.3 ± 0.4	20 ± 4		
^{177}Hf	1.099 ± 0.002	1.92 ± 0.04	103.3 ± 0.4	55 ± 10		
	2.385 ± 0.005	8.95 ± 0.15	111.5 ± 0.6	4.5 ± 1.5		
	5.89 ± 0.02	5.1 ± 0.3	115.2 ± 0.6	3.6 ± 1.5		
	6.57 ± 0.02	$+ 2.0$	123.1 ± 0.6	14 ± 5		
		9.5	132.1 ± 1.0	55 ± 10		
	$- 0.8$	136.9 ± 1.0	12 ± 5			
	8.87 ± 0.02	6.7 ± 0.6		$+ 10$		
	10.94 ± 0.03	0.44 ± 0.04	140.1 ± 1.5	12		
	13.65 ± 0.05	0.60 ± 0.15		$- 5$		
	13.94 ± 0.03	$+ 0.3$	142.8 ± 1.0	35 ± 9		
		$- 0.4$	146.7 ± 1.5	12 ± 7		
	22.04 ± 0.05	3.3 ± 0.5	149.2 ± 1.5	$+ 7$		
	23.47 ± 0.10	1.5 ± 0.5		10		
	25.68 ± 0.15	0.41 ± 0.14	163.4 ± 1.5	$- 5$		
	26.95 ± 0.10	2.6 ± 0.6	170.9 ± 1.5	45 ± 14		
	32.7 ± 0.2	1.3 ± 0.3		24 ± 8		
	36.25 ± 0.20	5.0 ± 2.5	176.5 ± 1.5	$+ 20$		
	36.9 ± 0.3	$+ 3$		160		
7			$- 40$			
$- 2$						
42.9 ± 0.2	4.7 ± 0.7	^{178}Hf	7.78 ± 0.02	51 ± 3		
45.2 ± 0.1	3.8 ± 0.2		104.4 ± 0.5	9 ± 2		
			164.4 ± 1.0	14 ± 3		

Table 2. (continued)

	E_0 (ev)	Γ_n (mv)		E_0 (ev)	Γ_n (mv)
^{179}Hf		+ 0.4	^{179}Hf	92.4 ± 0.4	50 ± 15
	5.68 ± 0.03	4.2		101.3 ± 0.4	130 ± 25
		- 0.3		103.8 ± 0.5	10 ± 3
	17.62 ± 0.04	2.15 ± 0.30		107.7 ± 0.6	13 ± 3
	19.05 ± 0.10	0.12 ± 0.04		117.0 ± 0.6	39 ± 7
		+ 0.7		122.1 ± 0.6	29 ± 7
	23.55 ± 0.10	8.3		129.6 ± 0.7	12 ± 4
		- 1.3		137.3 ± 1.0	50 ± 15
	26.44 ± 0.15	1.0 ± 0.3		144.4 ± 1.0	30 ± 8
	27.23 ± 0.15	0.43 ± 0.14		147.1 ± 1.5	9 ± 5
	31.02 ± 0.10	7.5 ± 0.7		156.0 ± 1.0	50 ± 15
	36.30 ± 0.20	30 ± 3		166.4 ± 1.5	20 ± 12
	40.0 ± 0.2	25 ± 3		173.5 ± 1.5	160 ⁺²⁰ - 40
	42.1 ± 0.2	13 ± 2		178.8	~28
	50.9 ± 0.2	2.2 ± 0.5		185.9	~20
	54.8 ± 0.1	5.3 ± 1.0		187.4	~20
	69.0 ± 0.2	10.0 ± 1.0			
73.8 ± 0.3	7 ± 3				
76.6 ± 0.3	3.0 ± 0.9				
83.1 ± 0.3	6 ± 2	^{180}Hf	72.5 ± 0.3	55 ± 3	
85.2 ± 0.4	8 ± 3		171.9 ± 1.0	119 ± 20	

NOTE: g , the statistical weight factor, is assumed to be $\frac{1}{2}$ for ^{177}Hf and ^{179}Hf .

Table 3. Parameters of 1.098- and 2.384-ev Resonances in ^{177}Hf from Shape Analysis

Sample	Energy (ev)	Γ_n (mv)	Γ (mv)	Γ_γ (mv)
^{176}Hf	1.099 ± 0.002	1.93 ± 0.04	76 ± 5	
^{178}Hf (thin)	1.094 ± 0.002	1.92 ± 0.04	68 ± 2	
^{178}Hf (thick)	1.099 ± 0.002	1.83 ± 0.06	73 ± 3	
^{179}Hf	1.098 ± 0.002	1.94 ± 0.04	68.3 ± 1.5	
^{180}Hf (thin)	1.098 ± 0.002	1.99 ± 0.10	67 ± 2	
^{180}Hf (thick)	1.099 ± 0.002	1.91 ± 0.10	69 ± 2	
Average values	1.099 ± 0.001	1.92 ± 0.03	68.3 ± 1.0	66.4 ± 1.0
^{176}Hf	2.384 ± 0.003	8.5 ± 0.3	75 ± 4	
^{178}Hf (thin)	2.383 ± 0.003	8.9 ± 0.2	70 ± 3	
^{179}Hf	2.386 ± 0.003	8.9 ± 0.2	70.0 ± 1.6	
^{180}Hf (thin)	2.382 ± 0.003	9.2 ± 0.5	71 ± 2	
^{180}Hf (thick)	2.384 ± 0.003	8.8 ± 0.5	70 ± 3	
Average values	2.384 ± 0.002	8.9 ± 0.2	70.2 ± 1.5	61.3 ± 1.5

The number of resonances is plotted vs neutron energy for the odd-*A* and the even-*A* target nuclides in Figs. 1 and 2 respectively. The average level spacing, *D*, for each isotope per spin state is given by the slope of the straight line, which includes a correction for the "missed" resonances.⁵ This correction for "missed" resonances was 11% for ¹⁷⁷Hf in the

⁵T. Fuketa and J. A. Harvey, *Nuclear Instruments and Methods*, in press.

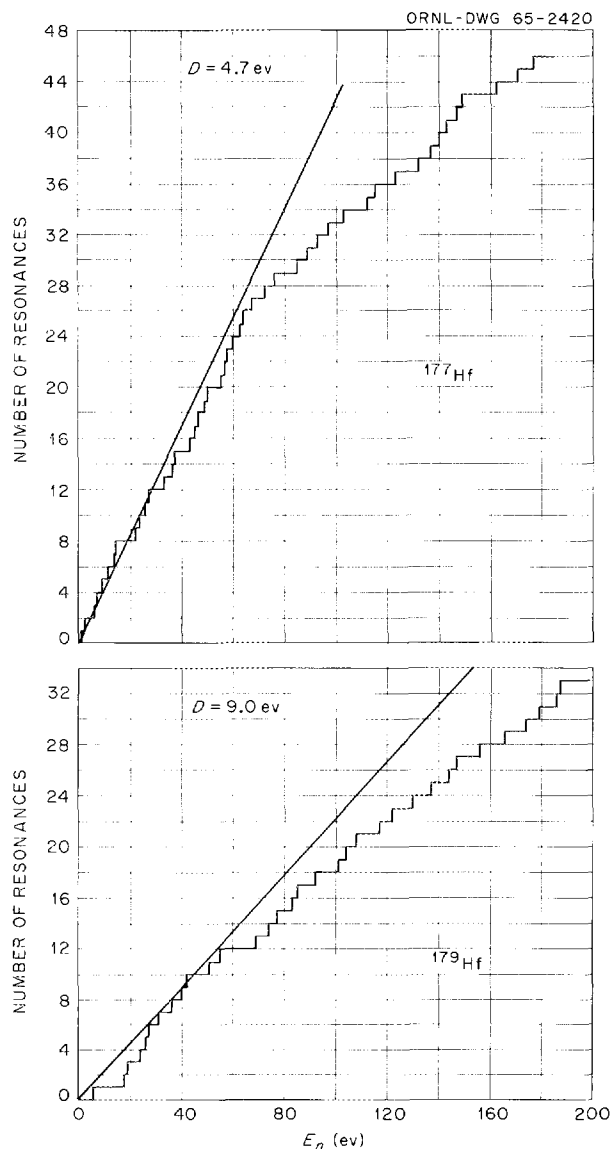


Fig. 1. Plot of the Number of Resonances vs Neutron Energy for the Odd-*A* Target Nuclides.

energy range from 0 to 70 eV, 14% for ¹⁷⁹Hf from 0 to 100 eV, 22% for ¹⁷⁴Hf from 0 to 140 eV, 18% for ¹⁷⁶Hf from 0 to 200 eV, 12% for ¹⁷⁸Hf and ¹⁸⁰Hf from 0 to 240 eV. A summary is given in Table 4 of average level spacings with probable

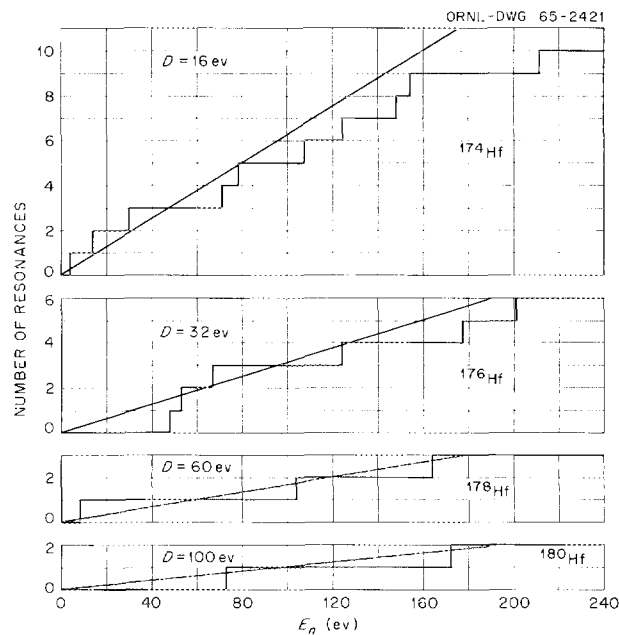


Fig. 2. Plot of the Number of Resonances vs Neutron Energy for the Even-*A* Target Nuclides.

Table 4. Average Level Spacings per Spin State *D* and *s*-Wave Strength Function S_0 for the Hafnium Isotopes^a

Target Nuclide	Average Level Spacing per Spin State <i>D</i> (eV)	<i>s</i> -Wave Strength Function, $S_0 = 10^4 \times \bar{\Gamma}_n^0 / D$
¹⁷⁷ Hf	4.7 ± 0.6	2.8 ± 0.4
¹⁷⁹ Hf	9.0 ± 1.3	2.1 ± 0.4
¹⁷⁴ Hf	16 ± 3	2.8 ± 1.0
¹⁷⁶ Hf	32 ± 7	1.4 ± 0.6
¹⁷⁸ Hf	60 ± 20	1.1 ± 0.7
¹⁸⁰ Hf	100 ± 40	0.7 ± 0.5

^aThe level spacings for the two spin states in ¹⁷⁷Hf and ¹⁷⁹Hf are assumed equal.

errors calculated from the equations; fractional error is $0.67/\sqrt{2n}$ for the even- A isotopes and $0.67/\sqrt{n}$ for the odd- A isotopes, where n is the number of resonances used to determine D . The gradual decrease in the level spacing with increasing mass is expected, due to the decrease in neutron binding energy. The small average level

spacings for the odd- A target nuclides are also expected, due to the neutron binding energy differences between odd- A and even- A nuclides.

In Figs. 3 and 4 the sums of the reduced neutron widths Γ_n^0 are plotted vs neutron energy for the odd- A and even- A target nuclides respectively. The s -wave strength function $S_0 = 10^4 \times \Gamma_n^0/D$ for each isotope is obtained from the slope of the straight line, which includes a small correction for "missed" resonances. The data over the entire energy range can be used, since the corrections for "missed" levels were less than a few percent. A summary is given in Table 4 of the s -wave strength functions with probable errors computed from the formula $0.67 \times \sqrt{2.5/n}$. Although the uncertainties in the values for the even- A target nuclides are large because of the small number of observed resonances, there are

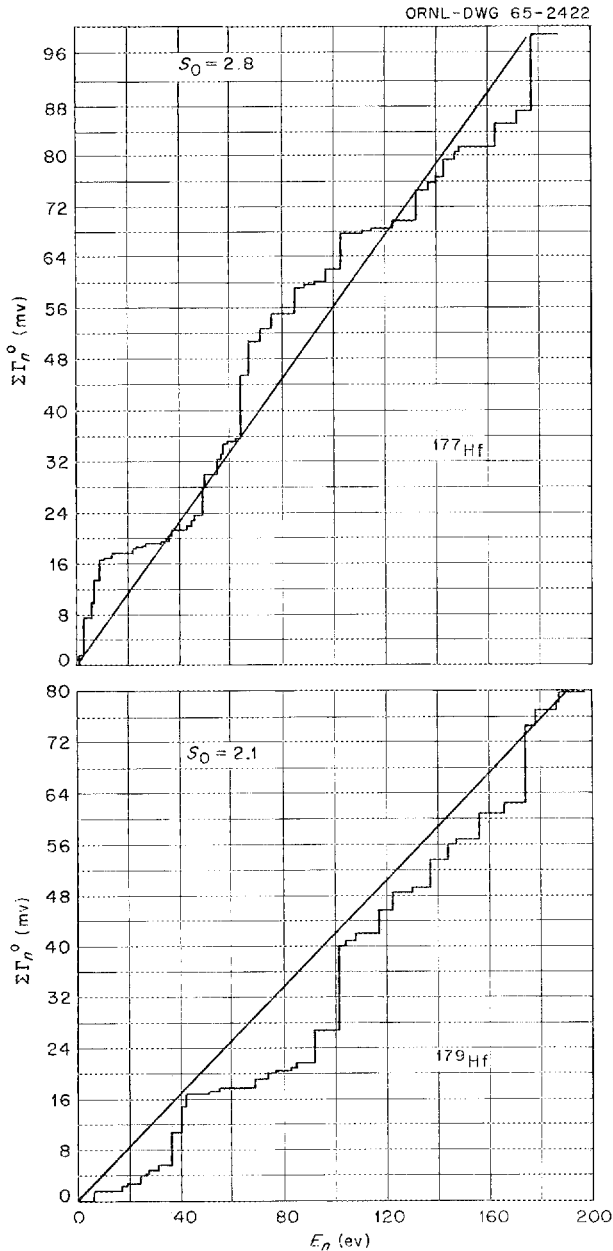


Fig. 3. Plot of the Sum of Γ_n^0 vs Neutron Energy for the Odd- A Target Nuclides.

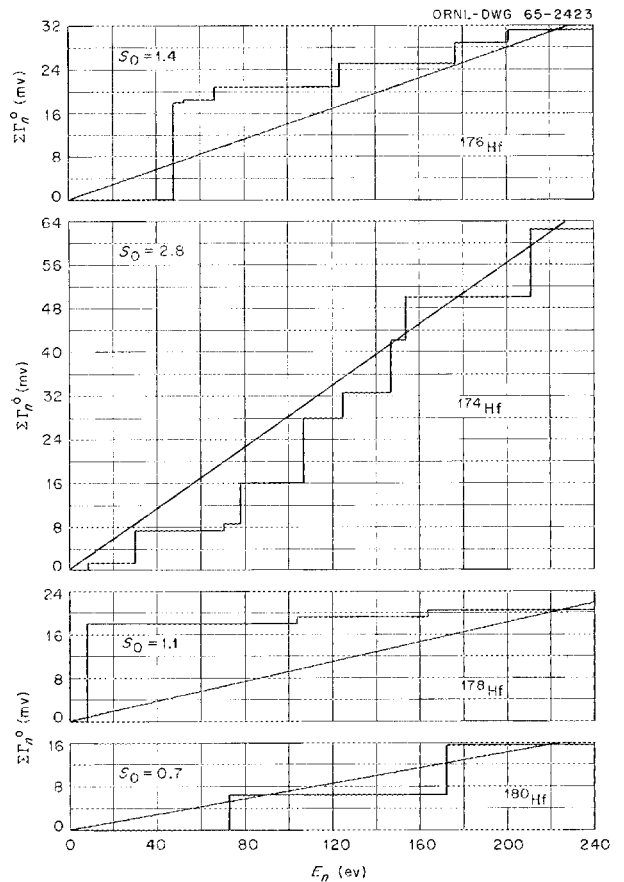


Fig. 4. Plot of the Sum of Γ_n^0 vs Neutron Energy for the Even- A Target Nuclides.

indications of a decrease of the s -wave strength function with increasing mass number. This apparent decrease is not in agreement with calculations from the complex, spheroidal nuclear potential with deformation appropriate to this atomic-weight region. For both ^{177}Hf and ^{179}Hf , as can be readily seen in Fig. 3, there is an apparent local variation of the s -wave strength

function⁶ with neutron energy which might be interpreted in terms of the recent "doorway-state" model of nuclear reactions. However, a rigorous statistical treatment must be made to be sure that the fluctuations are significant.

⁶T. Fuketa, *Bull. Am. Phys. Soc.* **9**, 20 (1964).

HIGH-RESOLUTION MEASUREMENTS OF THERMAL NEUTRON CAPTURE GAMMA RAYS

G. G. Slaughter

J. A. Harvey

NUCLEAR REACTIONS. $\text{Bi}(n, \gamma)$, thermal; $^{238}\text{U}(n, \gamma)$, thermal; $\text{Nb}(n, \gamma)$, thermal; $^{117,118,120}\text{Sn}(n, \gamma)$, thermal; $\text{Y}(n, \gamma)$, thermal; measured E_γ, I_γ . ^{210}Bi , ^{239}U , ^{94}Nb , $^{118,119,121}\text{Sn}$, ^{90}Y deduced levels, J, π . ^{238}U , $^{117,118,120}\text{Sn}$ enriched target.

A neutron beam doubly reflected from Inconel mirrors is used at the ORR fast-chopper facility as a source of thermal neutrons for neutron capture gamma-ray measurements. Neutrons, ranging in energy from the peak of the thermal spectrum down, are reflected through a total angle of 4.2 milliradians to pass directly down the fast-chopper flight path. Fast neutrons and gamma rays are removed by a collimator between the two mirrors. For a factor of 2.5 loss in thermal neutrons in the beam, the fast neutrons and gamma rays are reduced by three to four orders of magnitude. The resultant highly pure thermal neutron beam makes it possible to take the neutron capture gamma-ray spectrum of nuclides having relatively small thermal absorption cross sections without undue background from fast neutrons and gamma rays. After reflection and collimation, the beam contains about 7×10^7 neutrons/sec in an area of 6×12 cm at the 11-m flight-path station. Neutron capture gamma rays from a sample placed in the beam at the 11-m station are detected by a lithium-drifted germanium crystal 2.6 cm^2 in area by 7 mm thick with a solid angle of about 1 part in 2×10^{-4} .

The useful interaction in the gamma-ray energy range above 2000 keV is pair production with subsequent escape of both annihilation quanta. For the crystal use, this double-escape peak exhibits a resolution of about 11 keV at a gamma-ray energy of 4000 keV, and is eight to ten times the amplitude of the Compton edge resulting from the single gamma ray. In general, there is a complex spectrum with many gamma rays. As a result, the double-escape peaks of gamma rays of low intensity may be obscured by the Compton edges of other gamma rays. The crystal detects 4000-keV gamma rays with an intrinsic efficiency for the double-escape peak of about 0.3%. For runs of several days duration subject to an appreciable amount of electronic drift, the energies of the lines may be measured to ± 10 keV absolute and ± 5 keV relative to other lines. For runs of shorter duration having careful intercalibrations with lines of known energies, the errors can be much smaller than the values quoted above. For the crystal used, the double-escape-peak efficiency rises sharply from zero at the threshold (1022 keV gamma-ray energy) to a maximum at ~ 3000 keV, and falls slowly above 6000

keV. In the energy range from 600 to 1600 keV deposited in the crystal, there is some ambiguity as to whether a peak is the full energy peak of a gamma ray or the double-escape peak of a gamma ray having 1022 keV more energy.

The crystal used in this experiment was furnished by R. J. Fox, Instrumentation and Controls Division. It is encapsulated in an evacuated thin-wall aluminum can, in which the closure is effected by cold welding. This technique results in a crystal which maintains its characteristics for a long period of time, perhaps indefinitely, if the crystal is kept cold. Since a considerable amount of time is invested in each crystal to determine its response function, longevity is an important consideration.

Spectra were taken of the gamma rays following thermal neutron capture in samples of Bi, ^{238}U , Nb, Sn isotopes, and Y.

Bismuth

Neutron capture by ^{209}Bi forms a compound nucleus which can be considered as a neutron and a proton outside a doubly-closed-shell ^{208}Pb core. In this case of unlike nucleons outside a stable core, it appears necessary to invoke tensor forces or appreciable configuration mixing to explain the inverted level sequence (1^- , ground state, 0^- first excited state) and the anomalously small magnetic moment. Experimental and theoretical evidence indicates that the ^{210}Bi nucleus has an almost pure $h_{9/2}$ proton $g_{9/2}$ neutron configuration. In this case it is expected that there will be a ground-state multiplet of ten levels having intensities in the (d,p) reaction proportional to $(2J + 1)$.

Figure 1 is a level diagram inferred from the results of (d,p) experiments upon ^{209}Bi . The references are cited in the figure. The spins and parities of the levels are those known from other information or inferred from the relative intensities in the (d,p) work. The ticks on the energy scale represent the locations of all the levels found in the (d,p) experiment, and the excitation energies of some of the levels are given under the line representing the level. The solid vertical lines connecting the $(4^-, 5^-)$

s-wave neutron capturing state at 4593 keV excitation with various levels represent primary gamma-ray transitions which have been observed with the Ge(Li) detector. The dotted vertical lines represent gamma rays which, because of low intensity or concurrence with background lines, may not actually arise from the $\text{Bi}(n,\gamma)$ reaction. The numbers in parentheses on the vertical lines are the energies (in keV) of the gamma rays as measured with the Ge(Li) crystal; the numbers preceding these are the differences (in keV) between the neutron binding energy and the levels found by the (d,p) experiment.

Relative-intensity measurements were possible for the four dominating lines in the spectrum and are given in the figure. The relative intensities of the three strongest lines agree well with the relative intensities found for these lines by Motz.¹ These four lines are $M1$ transitions or higher multipolarity if the (d,p) spin assignments are correct. The large relative intensities of these lines tend to corroborate the (d,p) spin assignments. The level at 433 keV is probably a doublet, according to the (d,p) work. The corresponding gamma transition is seen as single in the present experiment, but the transition from the capturing state to the 7^- state ($E2$ or higher multipolarity) probably would be of too low intensity to be seen. The primary transition to a 2^- state at 320 keV excitation would be an $E2$ or higher multipolarity. Since the single-particle estimate of an $E2$ transition rate is only a factor of 20 slower than for an $M1$ transition rate in this energy range, it is not too surprising that this $E2$ is observed. The presence of this transition and the strength of the transition to the 6^- level at 547 keV indicate that thermal neutron capture in bismuth probably proceeds through both the 4^- and 5^- capturing states. Figure 2 shows the double-escape peaks in the Ge(Li) crystal for the four strongest gamma rays. Table 1 lists the stronger gamma rays, showing their correlation with the (d,p) results. The gamma-ray lines at 3632, 3396, and 3356 keV may represent either primary transitions to levels not excited in the (d,p) reaction or transitions other than primary.

¹Von L. Jarczyk *et al.*, *Z. Angew. Math. Phys.* 13, 117 (1962).

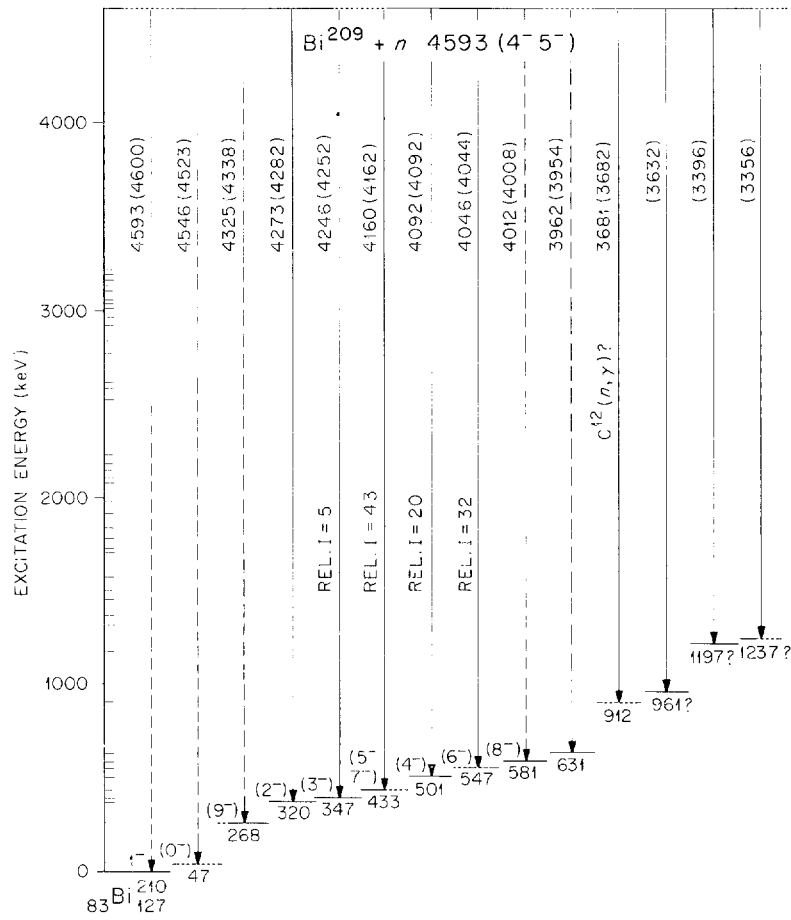


Fig. 1. ^{210}Bi Level Scheme. From Erskine, Buechner, and Enge, *Phys. Rev.* 128, 720 (1962) and Mukherjee, *Phys. Rev.* 131, 2162 (1963).

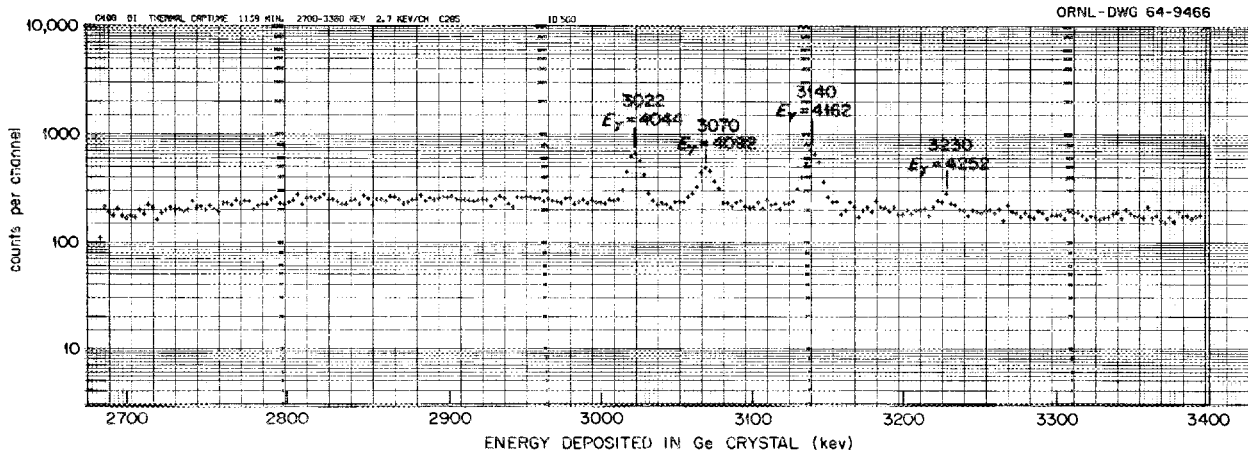


Fig. 2. Double Escape Peaks of Four Strongest Lines in the $\text{Bi}(n,\gamma)$ Reaction.

Table 1. Correlation of Neutron Capture Gamma Rays with Levels Excited by the (d,p) Reaction in ^{209}Bi ^a

Relative Intensity	E_γ (keV)	$BE-E_\gamma$ (keV)	$E_x(d,p)$ (keV)	Remarks
	4282	311	320	
5	4252	341	347	
43	4162	431	433	
20	4092	501	501	
32	4044	549	547	
	3682	911	912	$^{12}\text{C}, ^{14}\text{N}(n,\gamma)?$
	3632	961		
	3396	1197		
	3356	1237		

^aWeak lines not listed.

Uranium-238

Many previously unreported gamma-ray lines were observed in the $^{238}\text{U}(n,\gamma)$ reaction. The most significant feature of the spectrum is the resolution of a group of lines around 4060 keV. Previous measurements by other experimenters with an NaI detector showed a single line at 4.06 MeV which exhibited a remarkable lack of intensity variation from resonance to resonance. This implied that ν , the number of degrees of freedom available to a specific gamma ray for decay, was of the order of 5 to 90. The resolution of this line into at least four other lines at 3981, 3987, 4059, and 4094 keV within the resolution width of an NaI crystal indicates that the contributions of these lines are responsible for the lack of variation of the single line as seen by the NaI crystal. Other unreported lines of significant intensity were found at 4585, 4622, and 4675 keV.

Niobium

It has been suggested^{2,3} that the strongly bound ^{90}Zr nucleus may serve as a core for some

additional nucleons. The compound nucleus ^{94}Nb formed by neutron capture by ^{93}Nb could then be considered as one proton and three neutrons outside a ^{90}Zr core. Calculations^{2,3} were made on this basis and compared with the results of (d,p) and (n,γ) experiments on ^{93}Nb . A comparison of these experimental results and the present experimental results is given in Table 2.

Many gamma rays were found which correspond to primary transitions from the capturing state (4^+ , 5^+ for s-wave neutrons) to levels excited in the (d,p) reaction, and other gamma rays were found which correspond to transitions from these levels to the ground state (6^+). Inasmuch as Table 2 considers only the above type of correlation, it is perhaps surprising that so many (53) are found. In 12 of the cases, both components of a two-component cascade were seen. Of perhaps more interest are the cases in which correlation with the (d,p) results does not exist. A strong gamma-ray transition of 6830 ± 10 keV energy presumably represents a transition from the capturing state to an excited state at 399 keV which is not found in the (d,p) results. This level may correspond to an excited proton configuration and thus not be populated² in the (d,p) reaction. This explanation may be in order for some other gamma lines, particularly for a fairly intense group which corresponds to transitions from the capturing state to levels having excitation energies from 1800 to 2200 keV.

A comparison of the present results with the bent-crystal results for the $^{93}\text{Nb}(n,\gamma)$ reaction shows that all of the lines seen by the bent-crystal spectrometer with relative intensities $>10\%$ were also observed by the Ge(Li) spectrometer. The lines from the bent-crystal spectrometer which were not observed in the present experiment are not listed in Table 2.

It is of interest to comment upon the spins and parities suggested³ for the low-lying levels in ^{94}Nb based on estimates of relative intensities from the present experiment and crude arguments concerning the relative probabilities for transitions of various multipole orders. The 7229-keV primary transition from the capturing state to the (6^+) ground state is weak, which implies that thermal neutron capture proceeds predominantly through the 4^+ rather than the 5^+ capturing state. The very strong 7188-keV primary transition to the (3^+) level at 41 keV excitation corroborates this spin assignment if the capturing state is 4^+ . The

²R. K. Sheline *et al.*, to be published in *Nuclear Physics*.

³U. Gruber *et al.*, to be published in *Nuclear Physics*.

Table 2. Correlation of Levels Excited by the (d,p) Reaction in ^{93}Nb with Capture Gamma Rays^a

Relative Intensity	E_γ (kev)	$BE-E_\gamma$ (kev)	E_x (d,p) (kev)	Relative Intensity (d,p)	Bent Crystal		Suggested ^b Spin and Parity of Level
					E_γ (kev)	Relative Intensity (kev)	
(Compare $(BE-E_\gamma)$ and E_x)							
	7229	0	0	1			6 ⁺
2.7	{	7186	43	41	0.49		3 ⁺
		7167	62	59	0.69		4 ⁺
				78	0.85		7 ⁺
0.2	7115 ^c	114	113	1.0			5 ⁺
1.0	6917 ^c	312	314				5 ⁺
	6884	345	335				2 ⁺
4.3	{	6830	399				(3 ⁻ ?)
		6802	427				
0.3	6599	630	637				6 ⁺
	6517	712					
	6482	747					
0.5	6439	790	794				
	6411 ^c	818	820				
0.6	6335	894					
0.4	6297	932		960			
				1004			
				1062			
1.3	6067	1162	1168				
	5987	1242	1233				
1.7	{	5964	1265				
		5954 ^c	1275	1278			
4.6	{	5898	1331	1324			
		5887	1342				
1.4	5772	1457	1402				
	5732	1497	1496				
	5708	1521					
	5650 ^c	1579	1572				
	1.0	5612 ^c	1617	1625			
	1.3	5595	1634				
	5577 ^c	1652	1654				

Table 2. (continued)

Relative Intensity	E_γ (keV)	$BE - E_\gamma$ (keV)	E_x (d,p) (keV)	Relative Intensity (d,p)	Bent Crystal		Suggested ^b Spin and Parity of Level
					E_γ (keV)	Relative Intensity (keV)	
	5539	1690	1696				
5.6	{	5517	1712				
		5501	1728	1724			
		5454	1775	1784			
	5404	1825	1808				
4.3	{	5370 ^c	1859	1863			
		5351	1878				
1		5309	1920				
		5284	1945				
2.2	{	5254	1975				
		5248	1981				
4.7	{	5209	2020				
		5196	2033				
		5182	2047	2051			
	5132	2097					
	5108	2121					
	5102	2127					
	5090	2139	2142				
2.7		5072	2157				
1.2		5034	2195	2190			
		4980	2249				
		4912 ^c	2317	2305			
2.1		4849	2380	2372			
		4826	2403				
		4789	2440	2441			
3.9		4754	2475	2474			
		4737	2492				Ta(n, γ)?
		4672	2557	2542			?
			2574				
	4604	2625	2623				
	4592 ^c	2637	2651				?
	4560 ^c	2669	2675				
	4501	2728					N(n, γ)?
	4467	2762	2763				

Table 2. (continued)

Relative Intensity	E_γ (kev)	$BE - E_\gamma$ (kev)	E_x (d,p) (kev)	Relative Intensity (d,p)	Bent Crystal		Suggested ^b Spin and Parity of Level
					E_γ (kev)	Relative Intensity (kev)	
			1784				
			1724				
			1696				
	1649		1654				
	1635		1625				
	1586		1572				
			1496				
			1402				
			1324				
	1287		1278				
			1233				
			1168				
			1062				
			1004				
	955		960		949	14	
	840?		820	?	836	18	
			794				
			637				6 ⁺
	552						
	333		335		337	23	2 ⁺
	305		314		309	29	5 ⁺
	291				293 ^d	29	
	252				~254 ^d	124 (2 lines)	
	111		113	1.0	113	35	5 ⁺
	98				99	100	
			78	0.85			7 ⁺
			59	0.69			4 ⁺
	54				55 ^d	1.9	
			41	0.49			3 ⁺
			0	1.0			6 ⁺

^aWeak, uncorrelated gamma rays not listed.

^bSee ref. 3.

^cOther member of two-component cascade observed.

^dNonprimary transition terminating on excited state.

strong 7170-keV primary transition to the (4^+) 59-keV excited state is in agreement with this assignment, but gives no information concerning the capturing state. The missing 7151-keV primary transition to the (7^+) 78-keV excited state is very weak evidence for a 4^+ capturing state. The strengths of the 7116-keV primary transition to the (5^+) state at 113 keV and the 6915-keV primary transition to the (5^+) state at 314 keV are in agreement with the spin assignments, and allow either spin for the capturing state. The observation of the weak 6830-keV primary transition to the (2^+) 335-keV state indicates that the capturing state probably has a spin and parity of 4^+ if the 2^+ assignment for this level is correct. In summary, the relative intensities found in this measurement corroborate the assigned spins if a 4^+ capturing state is assumed.

Tin-117, -118, and -120

Gamma-ray spectra from thermal neutron capture in several of the isotopes of tin were measured

with the Ge(Li) spectrometer to supplement earlier gamma-ray spectra measurements with a large NaI spectrometer. A strong gamma ray with an energy of 9.31 MeV (the ground-state transition) was observed from thermal neutron capture in a 35-g sample enriched to 89% in ^{117}Sn ($\frac{1}{2}^+$). Since the ground state has zero spin, this capturing state must be 1^+ , and the gamma ray is a strong M1 transition. Many other gamma-ray lines were observed, including a strong line at 7.63 MeV going to an excited state at 1.68 MeV, a weak line at 8.09 MeV going to an excited state at 1.22 MeV, and a strong line at 1.23 MeV. More than 15 gamma rays were observed from thermal capture in a 160-g sample enriched to 97% in ^{118}Sn . More than 20 gamma rays were observed in a 200-g sample enriched to 98% in ^{120}Sn . Two high-energy gamma rays with energies of 6164 and 6104 keV correspond to transitions to the ground state and probably to an excited state at 60 keV. The data from these three isotopes will be compared with the results from (d,p) measurements to obtain energy-level diagrams. Measurements of

Table 3. Correlations of Neutron Capture Gamma Rays with Levels^{5,6} Excited by the (d,p) Reaction in $^{89}\text{Y}^a$

E_γ (keV)	$BE - E_\gamma^b$ (keV)	E_x^c (keV)	Suggested ^c Spin and Parity of Levels	E_γ (keV)	$BE - E_\gamma^b$ (keV)	E_x^c (keV)	Suggested ^c Spin and Parity of Levels
<u>6084</u> ^d	774 ^e		2^+	3422	3436 ^e	3430; 3410	
<u>5647</u> ^d	1211	1214	0^-	3372	3486	3480	
5482	1376	1374	1^-	3294	3564	3584?	
5037	1821	1819		3156	3702	3680; 3158	
4657	2201	2245?; 4630?		3095	3763	3750	
4614	2244	2245		2830 ^d	4028	4068; 2853	
<u>4377</u>	2481 ^e	2479	2^-	<u>2742</u>	4116	4126; 2754	?; 1^+
<u>4347</u>	2511	2504; 4330?		2499	4359	4330?	
<u>4106</u> ^d	2752 ^e	2754	1^+	2469	4389	2479	2^-
4007	2851 ^e	2853		<u>775</u> ^d	6083		
3867	2991	3002; 3861	4^- ; ?	<u>573</u> ^d	6285		
3602	3256	3230		<u>199</u> ^d	6659	202	3^-

^aWeak, uncorrelated lines not listed. Stronger lines underlined.

^bCompare $(BE - E_\gamma)$ or E_γ with E_x .

^cSee ref. 6.

^dAlso reported in ref. 4. Other lines from this paper not listed.

^eOther component of two-component cascade possibly seen.

the gamma-ray spectra from thermal neutron capture will also be made for the other isotopes of tin.

Yttrium

The present measurements have yielded information in addition to that previously available concerning the correlation of capture gamma rays⁴ and the levels in ⁹⁰Y found through the (d,p)

⁴G. A. Bartholomew *et al.*, *Nucl. Phys.* 10, 590 (1959).

reaction.^{5,6} Table 3 lists the gamma-ray energies showing the correlations with the (d,p) results, similar to the previous tables. All of the stronger gamma lines and some of the weaker lines showed a correlation with the (d,p) results. Again it is surprising that so many of the gamma rays are either primary transitions or terminate at the ground state. In five of the cases the second component of a two-component cascade was probably seen. Analysis is continuing on these preliminary results.

⁵E. W. Hamburger and A. I. Hamburger, to be published.

⁶Charles Watson, C. F. Moore, and R. K. Shelton, *Nucl. Phys.* 54, 519 (1964).

CAPTURE CROSS-SECTION MEASUREMENTS ON ¹⁸²W, ¹⁸³W, ¹⁸⁴W, AND ¹⁸⁶W AT THE RPI LINAC

R. C. Block

J. E. Russell¹

R. W. Hockenbury¹

NUCLEAR REACTIONS. ¹⁸²W, ¹⁸³W, ¹⁸⁴W, ¹⁸⁶W (n,γ). Measured $\sigma_{n\gamma}(E_n)$ from ~35 eV to 10 keV, average level spacings. Enriched targets.

Experimental Method

Radiative capture measurements have been carried out on samples enriched in ¹⁸²W, ¹⁸³W, ¹⁸⁴W, and ¹⁸⁶W with the ORNL 1.25-m-diam liquid-scintillator capture detector installed at the RPI linear accelerator laboratory. The experimental method is very similar to that given in the 1963 annual report² and will only be briefly reviewed here. The RPI linac was used to produce intense bursts of neutrons through the bombardment of a tungsten target by short bunches (~0.1 μsec wide) of 60-MeV electrons (see Fig. 1). The resulting

¹Rensselaer Polytechnic Institute.

²R. C. Block, J. E. Russell, and R. W. Hockenbury, *Phys. Div. Ann. Progr. Rept. Jan. 31, 1963*, ORNL-3425, p. 64.

photoneutrons were moderated in a 1-in.-thick polyethylene moderator, and these moderated neutrons provided the pulsed source of resonance-energy neutrons which were allowed to pass through an evacuated flight path to the detectors located in the 25-m flight station (see Fig. 2). The linac was operated at repetition frequencies up to 480 pulses/sec. A 0.6-g/cm² boron 1/v filter was placed between the neutron moderator and the detectors to reduce the background of low-energy "overlap" neutrons (i.e., neutrons produced in earlier pulses).

In contrast to the earlier reported measurements, counts from the large liquid-scintillator capture detector and counts from the ¹⁰B-NaI neutron detector were collected simultaneously in time-of-flight analyzers so that information on the capture and the total cross section of a sample

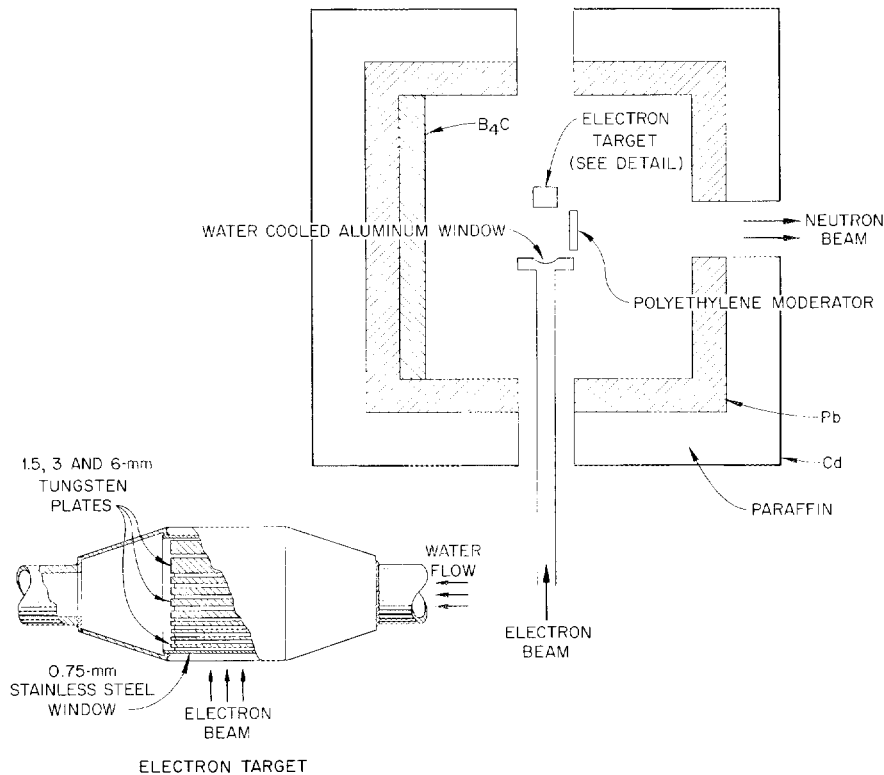


Fig. 1. Neutron Production Target at RPI. Two inches of water-cooled tungsten plates are used to produce photoneutrons from the electron beam, and the polyethylene moderator (5 in. diam. by 1 in. thick) is used to moderate the photoneutrons into the resonance energy range.

was obtained in the same experiment. The ORNL Fast Chopper Group's 4096-channel two-parameter analyzer was used to record either the capture-detector counts as a function of time of flight (with channel widths as narrow as $0.08 \mu\text{sec}$) or to record the pulse-height spectra from the capture detector as a function of time of flight. Two conventional Technical Measurements Corporation (TMC) 1024-channel time analyzers and one conventional TMC 256-channel time analyzer were used in conjunction with the 4096-channel analyzer to record the capture detector and neutron detector counts from 10 keV to ~ 4 eV.

The measurements were made over a neutron energy range from about 4 eV to 10 keV, and with a $0.1\text{-}\mu\text{sec}$ -wide electron burst; the time resolution for the capture measurements was approximately 5 nsec/m at the higher neutron energies. The neutron flux was determined by (1) measuring the

counting rate from the $^{10}\text{B-NaI}$ neutron detector with a very thin gold monitor sample placed in the beam inside the large scintillator, (2) correcting the neutron counting rate for detector efficiency (as a function of neutron energy), and (3) normalizing the efficiency-corrected neutron counting rate to the capture-detector counting rate observed in the region of either the 4.9- or 60.6-eV gold resonances. The efficiency of the large scintillator was determined in the manner reported by Gibbons *et al.*³ by measuring the "spectrum fraction" for neutron capture in the sample under investigation. (The spectrum fraction is defined as that fraction of capture counts which falls within the single-channel window setting on the output of the capture-detector amplifier.) The window was set to count only pulses corresponding to gamma rays between

³J. H. Gibbons *et al.*, *Phys. Rev.* **122**, 182 (1961).

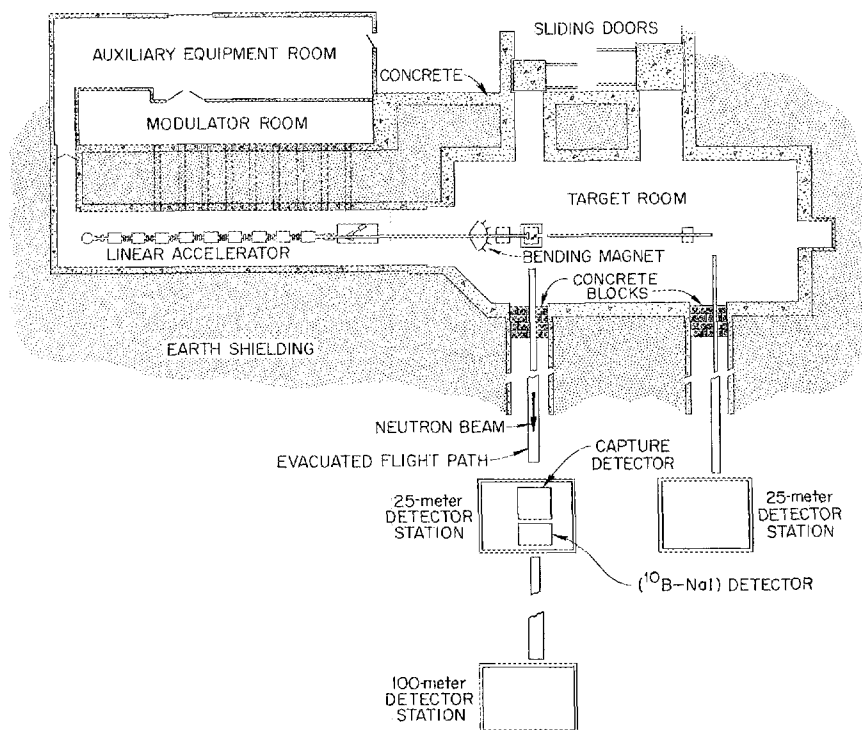


Fig. 2. Floor Plan of Experimental Arrangement at RPI.

3 and 13 Mev. For the heavy nuclei, where, in general, neutron capture is followed by a complicated cascade of gamma rays, the large scintillator detector efficiency is taken as equal to the spectrum fraction. This was the procedure used in reducing the capture counting data for the tungsten isotopes to capture cross sections. The counting data obtained with the $^{10}\text{B-NaI}$ detector have not yet been converted to transmissions and will not be presented here.

Results

^{182}W , ^{183}W , ^{184}W , and ^{186}W Capture Cross Sections. — Measurements were made on samples of separated tungsten isotopes; the properties of these samples are listed in Table 1, columns 1 through 6. These samples were prepared by the

Isotopes Division in the form of WO_3 compressed into 2.25-in.-diam disks.

The capture counting data were reduced to the number of captures per neutron by application of the following equation:

$$F_{xi} = \frac{C_{xi} - (TDB)_i - (B)}{\eta_x \phi_i}, \quad (1)$$

where F_{xi} is the number of captures per neutron incident upon sample x over the time-of-flight interval corresponding to channel i , C_{xi} is the number of capture counts (corrected for deadtime losses) recorded in channel i , $(TDB)_i$ is the time-dependent background per channel in the detector at time channel i , (B) is the constant background per channel observed during the measurement, η_x is the detection efficiency for capture in sample x (taken as equal to the spectrum fraction), and ϕ_i is the total number of neutrons incident on

Table 1. Properties of the Tungsten Separated Isotope Samples

Sample	N_w^a (atoms/barn)	Atomic Percent of Isotope				Scale Factors to Be Used with Capture Cross-Section Curves			
		^{182}W	^{183}W	^{184}W	^{186}W	^{182}W	^{183}W	^{184}W	^{186}W
$^{182}\text{WO}_3$	3.79×10^{-3}	94.4	2.53	2.32	0.8	1.08	40.5	44.1	128
$^{183}\text{WO}_3$	1.99×10^{-3}	6.4	82.5	9.6	1.5	13.5	1.05	9.01	57.7
$^{184}\text{WO}_3$	2.52×10^{-3}	1.91	1.87	94.3	1.91	53.2	54.4	1.08	53.2
$^{186}\text{WO}_3$	10.1×10^{-3}	0.38	0.31	2.05	97.23	297	364	55.0	1.16

^aBased on the total number of tungsten atoms per barn, not just the number of atoms per barn of the enriched isotope.

sample x over the time-of-flight interval corresponding to channel i .

The time-dependent background was measured by comparing the counting rate in the capture detector with a 0.5-in.-thick high-purity carbon sample placed inside the detector to the counting rate with no sample placed inside the detector. The constant background was determined from the counting rate in the capture detector at long times of flight when the boron overlap filter had essentially removed all the resonance-energy neutrons from the beam and all time-dependent background effects had died away. As discussed previously, the number of neutrons per channel, ϕ_i , was determined from the $^{10}\text{B-NaI}$ neutron-detector counting rate and the capture-detector counting rate from a thin gold monitor sample left inside the capture detector throughout the measurements. The spectrum fractions for the tungsten isotopes were obtained by measuring the capture-detector pulse-height distributions for isolated tungsten resonances below ~ 200 ev. When two or more resonances were measured in the same isotope, the spectrum fraction was observed to be essentially constant from resonance to resonance. (This constancy of spectrum fraction is consistent with the interpretation that the gamma-ray cascades following capture in tungsten are so complex that the efficiency of the large detector is essentially

constant from resonance to resonance.) The spectrum fractions for the tungsten isotopes were measured to be 0.59, 0.70, 0.60, and 0.54, respectively, for ^{182}W , ^{183}W , ^{184}W , and ^{186}W . These spectrum fractions were obtained with the capture-detector single-channel analyzer window set to accept pulses corresponding to gamma rays between 3 and 13 Mev.

When the capture sample is sufficiently thin so that the effects of exponential attenuation of the neutron beam and the effects of multiple scattering of neutrons in the sample can both be neglected, the capture cross section is equal to

$$\sigma'_{xi}(n, \gamma) = \frac{F_{xi}}{N_x}, \quad (2)$$

where $\sigma'_{xi}(n, \gamma)$ is the "thin-sample" capture cross section⁴ (in barns) at the time of flight corresponding to channel i , N_x is the thickness of sample x (in atoms/barn), and F_{xi} is the number of captures per neutron, as defined in Eq. (1). The capture data obtained for the samples enriched in ^{182}W , ^{183}W , ^{184}W , and ^{186}W were reduced to the form of "thin-sample" capture cross sections and are plotted in Figs. 3-6. Since each sample contained

⁴This "thin-sample" capture cross section includes the effect of Doppler and resolution broadening.

significant amounts of minor isotopes, and hence capture from more than one isotope was present in each sample, it was convenient to use the same value of η_x in Eq. (1) for all the data. The value of η_x of 0.61 was used in generating all these curves. (This η_x was equal to the spectrum fraction for capture in the gold resonances and is close to the spectrum fraction for the tungsten isotopes.) The total number of tungsten atoms per barn, listed in column 2 of Table 1, was used in applying Eq. (2). In order to determine $\sigma'_{xi}(n,\gamma)$ for each isotope present in each sample, the ordinates in Figs. 3-6 must be multiplied by an appropriate

scale factor which includes the isotopic enrichment and deviation of the isotope's spectrum fraction from 0.61. These scale factors have been determined and are listed in columns 6-9 in Table 1. For example, to obtain the value of $\sigma'_{xi}(n,\gamma)$ for the ^{183}W isotope present in the $^{184}\text{WO}_3$ sample, the ^{184}W cross sections in Figs. 3-6 should be multiplied by the scale factor of 54.4 in column 8 of Table 1.

It is apparent in the capture cross-section curves of the tungsten isotopes that at low energies the resonances are quite well resolved from each other, but in the kev energy region the effect of

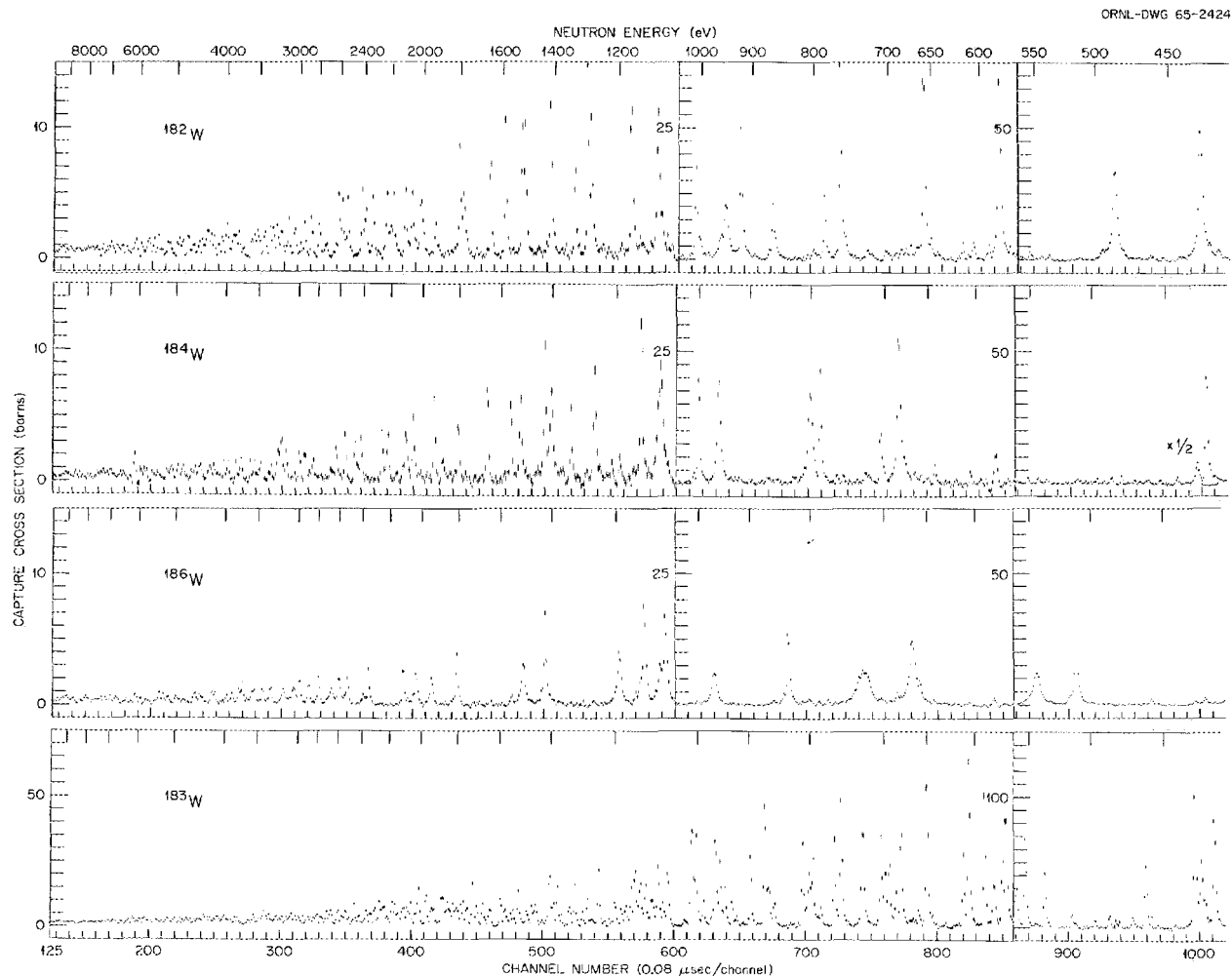


Fig. 3. Capture Cross Sections of the Isotopically Enriched Samples of Tungsten. (These cross sections must be corrected for isotopic enrichment and for the change in the capture detection efficiency for each isotope.)

finite resolution is showing up in the merging of the resonances. These data have been analyzed for the energies of the observed resonances through the use of a computer code which locates the center of each resonance by least-squares fitting a second-order polynomial to each peak in the capture cross section. Corrections have been made for small resonances due to the gold monitor inside the capture detector during the experiment, and isotopic assignments were made by comparing the capture data from all four enriched samples. These results are listed in Tables 2--5, and the integral level-spacing distributions for the tungsten

isotopes are plotted in Fig. 7. (The low-energy resonances have also been included in plotting Fig. 7.) In this figure a straight line has been drawn through the low-energy portion of the ^{183}W integral level-spacing distribution, and it is apparent that above ~ 1000 ev the data significantly depart from this line. This departure is interpreted as a loss of observed resonances due to the effect of increasingly poorer energy resolution with increasing energy. However, below ~ 1000 ev it appears that most of the resonances in ^{183}W have been observed, and thus the line with slope of 15 ev per resonance is a reasonable interpretation

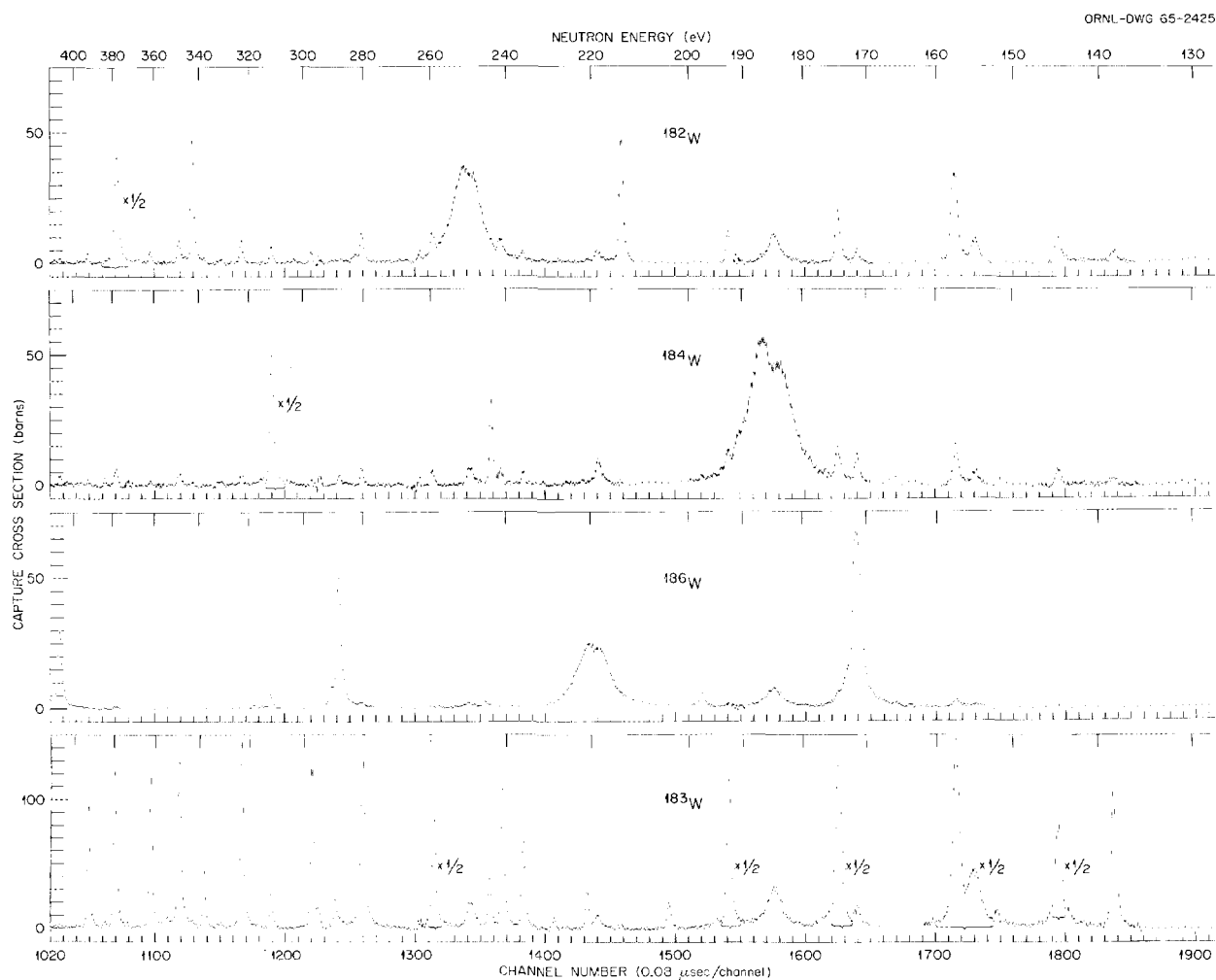


Fig. 4. Capture Cross Sections of the Isotopically Enriched Samples of Tungsten. (These cross sections must be corrected for isotopic enrichment and for the change in the capture detection efficiency for each isotope.)

of the level spacing. If it is assumed that most of the levels up to 1000 ev are *s*-wave levels, and hence lead to compound states in ^{184}W of total angular momentum $J = 0$ or $J = 1$, and if the $(2J + 1)$ level-spacing law is valid here, then the average level spacing for resonances in ^{183}W is equal to 60 ± 12 and 20 ± 2 ev for levels of $J = 0$ and $J = 1$ respectively. (The errors are based on the number of levels observed in an energy interval. The fractional error in determining the average level spacing from the observation of N levels of the same spin and parity is approximately equal to $\sqrt{1/2 N}$. Assuming the $(2J + 1)$ law to apply,

approximately 16 $J = 0$ and 48 $J = 1$ resonances comprise the 64 resonances observed up to 1000 ev; the errors are based on these 16 and 48 levels.)

For the even-even isotopes of tungsten, however, the plots in Fig. 7 are more difficult to interpret. For example, the ^{182}W integral plot can be fitted with a straight line of slope 38 ev per resonance in the region up to 800 ev, but above 800 ev the data can be fitted with a slope of 69 ev per resonance. The effect of finite energy resolution predicts a gradual loss of observed resonances with increasing energy and does not explain the

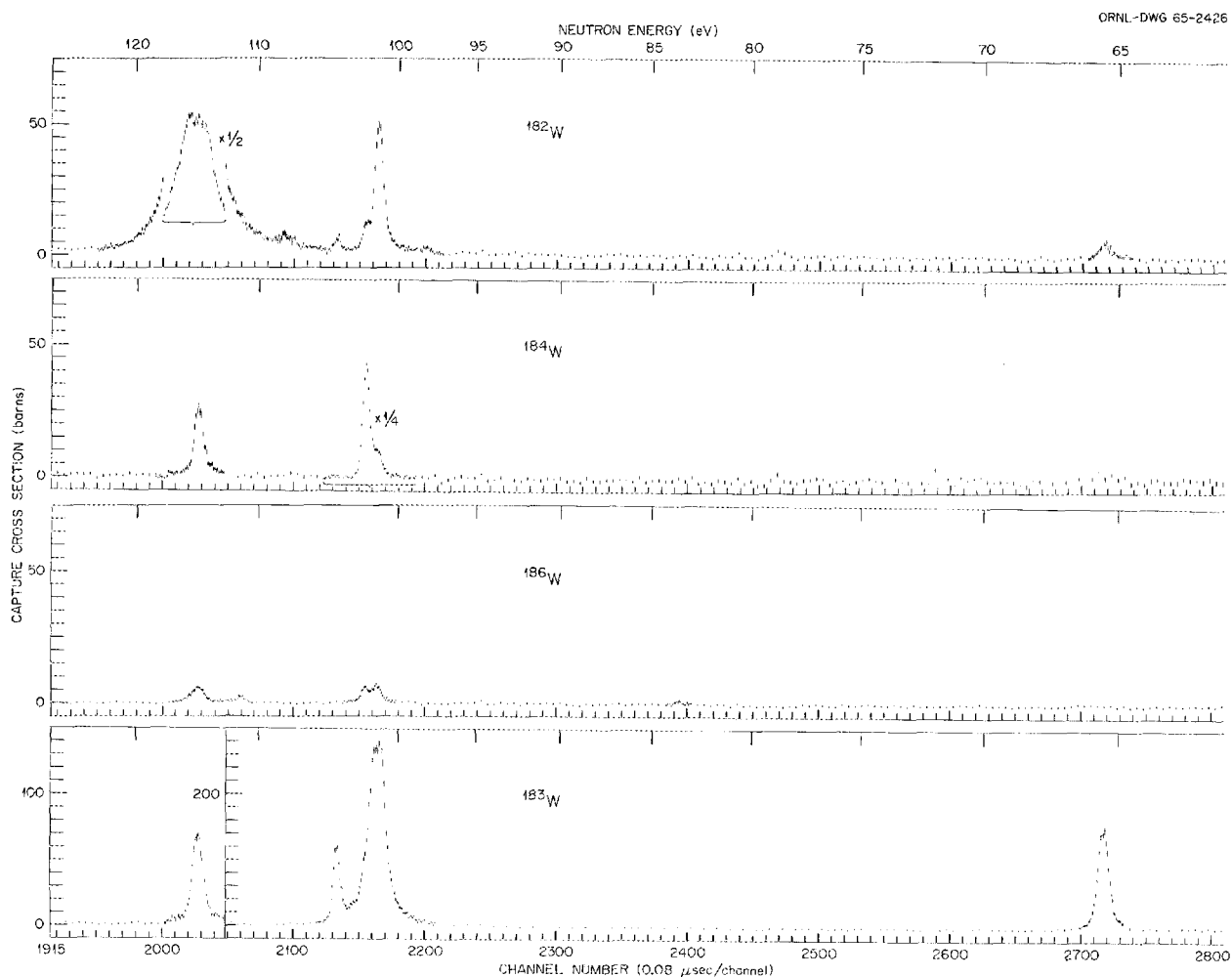


Fig. 5. Capture Cross Sections of the Isotopically Enriched Samples of Tungsten. (These cross sections must be corrected for isotopic enrichment and for the change in the capture detection efficiency for each isotope.)

sudden change of slope observed in this experiment. Thus the ^{182}W data could be interpreted to have either an average level spacing of 38 ± 6 ev for the 20 resonances observed up to 800 ev, or an average level spacing of 69 ± 7 ev for the 46 resonances observed between 800 and 4000 ev, where the errors are derived from the number of observed levels in each interval. In like manner the integral level-spacing distributions for ^{186}W , and to a somewhat lesser extent ^{184}W , also exhibit unusual-looking changes of slope in Fig. 7. However, a more detailed analysis must be carried out upon the statistical significance of selecting specific regions of energy to analyze these data

before physical interpretations of local level-density fluctuations can be made regarding these abrupt changes of slope.

In order to compare the average level spacings of the tungsten isotopes over the full energy interval up to 4000 ev, the total number of observed resonances in each isotope was divided into the energy interval. This resulted in average level spacings of 61, 86, and 89 ev, respectively, for ^{182}W , ^{184}W , and ^{186}W . (The fractional error in such a measurement is usually taken as equal to about $1/\sqrt{2N}$, where N is the total number of observed levels, and this would lead to errors of ± 5 , ± 9 , and ± 9 ev, respectively, for the average

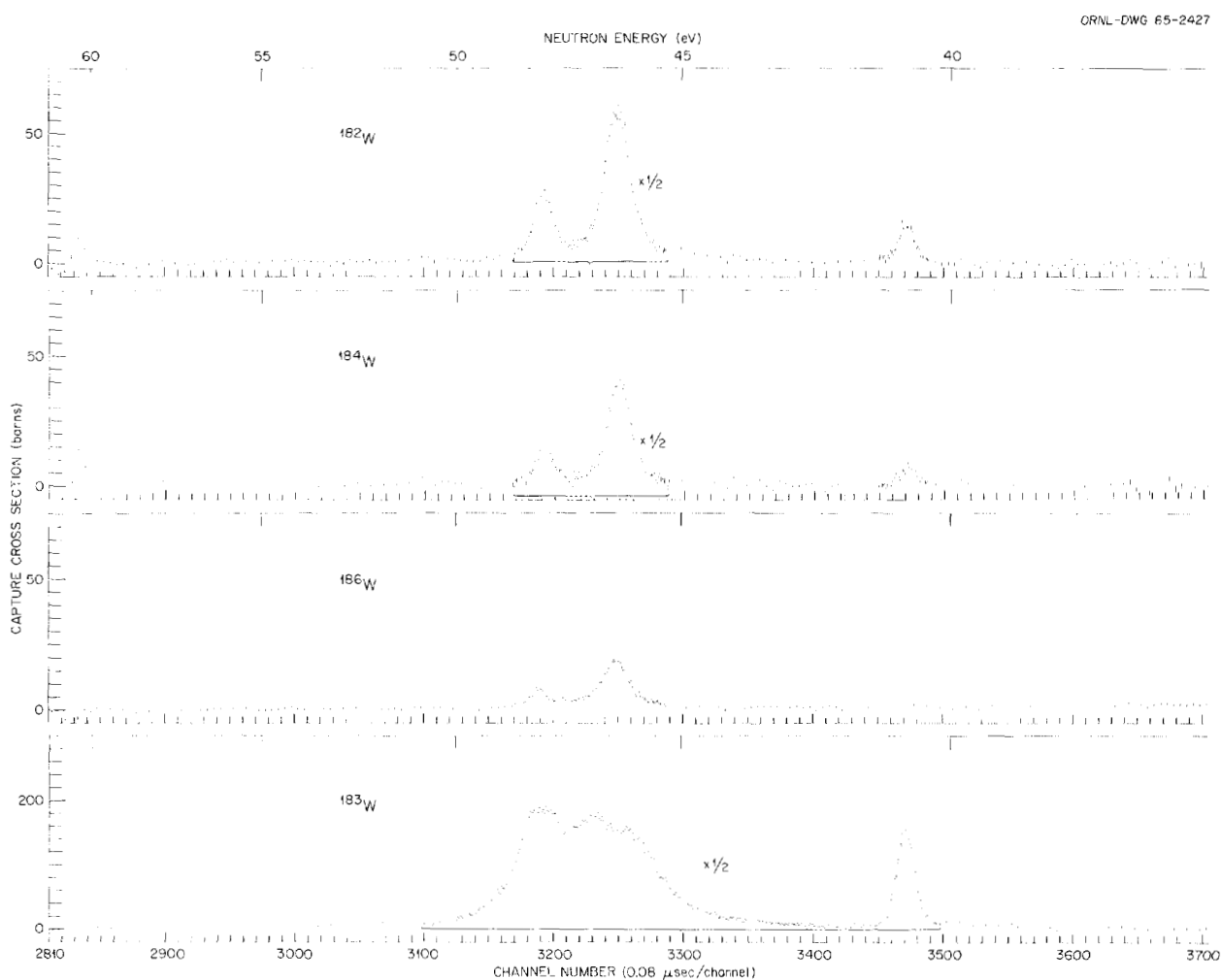


Fig. 6. Capture Cross Sections of the Isotopically Enriched Samples of Tungsten. (These cross sections must be corrected for isotopic enrichment and for the change in the capture detection efficiency for each isotope.)

level spacing in ^{182}W , ^{184}W , and ^{186}W . However, the presence of abrupt changes in slope of the integral level-spacing distributions tends to indicate that these errors may not be applicable here.)

In the energy region from ~ 1 to 10 keV, the tungsten capture cross sections begin to "smooth" out due to the averaging over many resonances by the experimental resolution (see Fig. 3). Hence it is more pertinent in this region to average the data over wide energy intervals and then to interpret these average data. Accordingly, the capture data for each sample have been averaged, corrected for the presence of isotopes of low enrichment, and corrected for the spectrum fraction of each isotope (assuming that this spectrum fraction is the same in the keV energy region as was measured in isolated resonances below 200 eV). These results are listed in Table 6 in columns 3-6. Columns 1 and 2 are the energy intervals over which the average was taken, and column 7 is the average capture cross section expected for a natural sample of tungsten based on the natural isotopic abundances and the isotopic capture cross sections in

columns 3-6. No corrections have been made for resonance self-protection or for the effects of multiple scattering in the samples. It is estimated that the capture cross sections in Table 6 are accurate to about 15%.

Table 3. Energies of Resonances in ^{183}W
from About 35 to 2800 eV

Energy (eV)	Energy (eV)	Energy (eV)	Energy (eV)
40.7	426.9	986.8	1718
46.2	430.6	1003	1744
47.9	461.3	1012	1763
65.5	470.0	1066	1774
101.3	514.4	1076	1814
104.1	536.2	1088	1842
138.3	552.8	1103	1873
144.6	560.1	1118	1921
154.9	569.8	1131	1961
157.3	573.0	1144	2006
174.3	589.9	1155	2054
192.6	605.2	1169	2076
203.8	610.6	1182	2099
220.8	649.2	1199	2130
228.3	678.2	1245	2155
235.8	692.5	1318	2172
240.9	697.7	1335	2236
244.2	703.2	1375	2295
259.4	726.0	1402	2326
280.4	755.0	1453	2360
289.2	764.1	1467	2454
297.1	795.0	1487	2527
322.8	810.7	1519	2588
338.0	855.8	1539	2658
348.5	872.0	1550	
353.9	897.5	1572	
361.4	931.4	1592	
378.8	944.5	1637	
392.1	954.6	1669	
419.1	964.3	1698	

Table 2. Energies of Resonances in ^{182}W
from About 35 to 4000 eV

Energy (eV)	Energy (eV)	Energy (eV)	Energy (eV)
98.0	672.5	1653	2806
114.7	762.3	1781	2886
130.5	784.7	1801	2956
213.5	866.0	1930	3000
249.6	922.1	2016	3061
282.4	951.3	2069	3135
303.2	1011	2112	3221
342.7	1099	2190	3275
377.6	1166	2236	3325
410.1	1281	2340	3359
430.1	1292	2394	3434
447.0	1332	2423	3536
486.2	1414	2541	3575
580.2	1509	2588	3615
615.9	1519	2620	3872
657.6	1588	2739	4005

Table 4. Energies of Resonances in ^{184}W
from About 35 to 4000 ev

Energy (ev)	Energy (ev)	Energy (ev)
102.1	1339	2631
184.7	1405	2850
243.5	1429	2937
311.3	1519	2997
424.4	1559	3148
594.8	1661	3204
683.5	1799	3236
705.4	1880	3328
786.8	1928	3468
801.7	2053	3557
960.5	2100	3613
1002	2219	3751
1088	2262	3831
1136	2421	3962
1215	2466	4025
1265	2552	

Table 5. Energies of Resonances in ^{186}W
from About 35 to 4000 ev

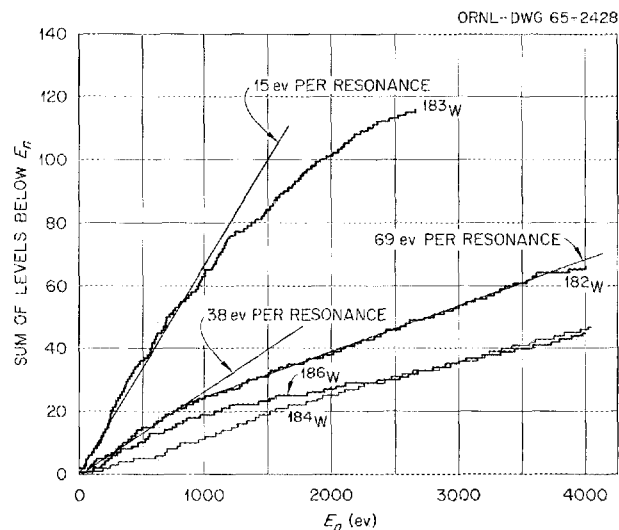
Energy (ev)	Energy (ev)	Energy (ev)
111.3	834.8	2606
171.5	857.6	2671
197.6	967.7	2793
218.4	1075	2893
245.1	1127	2993
287.8	1192	3055
317.9	1424	3179
407.3	1506	3332
457.9	1551	3442
511.8	1802	3589
531.9	1942	3732
543.4	2035	3786
666.0	2116	3895
732.0	2360	3985
774.2	2529	

Table 6. Average Capture Cross Sections

Energy Interval over Which Data Are Averaged (kev)		$\sigma'(n, \gamma)$ (barns)				
E_{lower}	E_{upper}	^{182}W	^{184}W	^{186}W	^{183}W	$\bar{W}^{(a)}$
11.0	8.9	0.581	0.373	0.431	1.25	0.570
8.9	7.3	0.697	0.424	0.427	1.30	0.622
7.3	6.1	0.778	0.522	0.407	1.62	0.714
6.1	5.18	0.812	0.495	0.418	1.88	0.755
5.18	3.87	1.10	0.700	0.485	2.40	0.988
3.87	3.00	1.28	0.862	0.776	2.66	1.21
3.00	2.15	1.53	0.938	0.663	3.65	1.40
2.15	1.49	1.87	1.213	0.603	4.99	1.75
1.49	1.01	1.87	1.69	1.10	5.49	2.11

$$^{(a)}\sigma = 0.264\sigma_{^{182}\text{W}} + 0.144\sigma_{^{183}\text{W}} + 0.306\sigma_{^{184}\text{W}} + 0.284\sigma_{^{186}\text{W}}$$

Fig. 7. Integral Level-Spacing Distribution for the Tungsten Isotopes.



In Fig. 8a the logarithms of the average capture cross sections listed in Table 6 are plotted as a function of the logarithm of the neutron energy. Typically, the s -wave component of the average capture cross section is expected to vary as $1/\sqrt{E}$ for neutron energies below ~ 1 kev and to vary as $1/E$ for neutron energies above ~ 10 kev, and the data in Fig. 8 all seem to be consistent with an energy dependence in between these two extremes. Actually, the data of Fig. 8 for each isotope (except, perhaps, ^{186}W) could be fitted to a straight line in the energy region from ~ 3 to 10 kev, with the region from 3 to 1 kev progressively falling below this line. This "falling away" effect is consistent with the net effect of resonance self-protection and multiple scattering. At the lower neutron energies the samples become very black at the resonance energies, and this effect more than compensates for the increase in the capture counting rate due to multiple scattering in the samples. Therefore at the lower neutron energies this treatment of the data tends to underestimate the value of the capture cross section.

In the energy range near ~ 10 kev, the average capture cross section becomes proportional to the ratio of the radiation width to the average level spacing. Since the radiation widths of resonances in the even-even tungsten isotopes are comparable to each other, the average capture cross sections should vary from isotope to isotope as the reciprocal of the average level spacing. The average level

spacings of ^{182}W , ^{184}W , and ^{186}W are 61, 86, and 89 ev respectively (up to 4 kev), and thus the average capture cross sections should be in the ratio of approximately 1.5:1:1. It is seen in Fig. 8a that the magnitudes of the experimental average capture cross sections near 10 kev do vary in about this ratio. The radiation width for the ^{183}W resonances is slightly larger than the radiation widths for the even-even tungsten isotopes, and in addition the average level spacing per spin state is much smaller for the ^{183}W resonances than for the resonances in the even-even isotopes. Therefore the ^{183}W average capture cross section should be substantially larger than the average capture cross section of any even-even isotope, and in Fig. 8a it is seen that the magnitude of the ^{183}W cross section is at least twice that of any even-even isotope.

In Fig. 8b are plotted the average tungsten capture cross sections listed in column 7 of Table 2. As indicated in Table 2, this natural-tungsten average capture cross section is simulated by weighting the measured isotopic cross sections by the isotopic abundances found in nature. The 30-kev capture cross section measured for tungsten by Gibbons *et al.*³ is also plotted in Fig. 8b, and it is seen that a straight-line fit to the data from 1 to 10 kev extrapolates through the 30-kev point. Thus, to within the estimated accuracy of this experiment of $\sim 15\%$, these measurements agree with the result of Gibbons *et al.*³

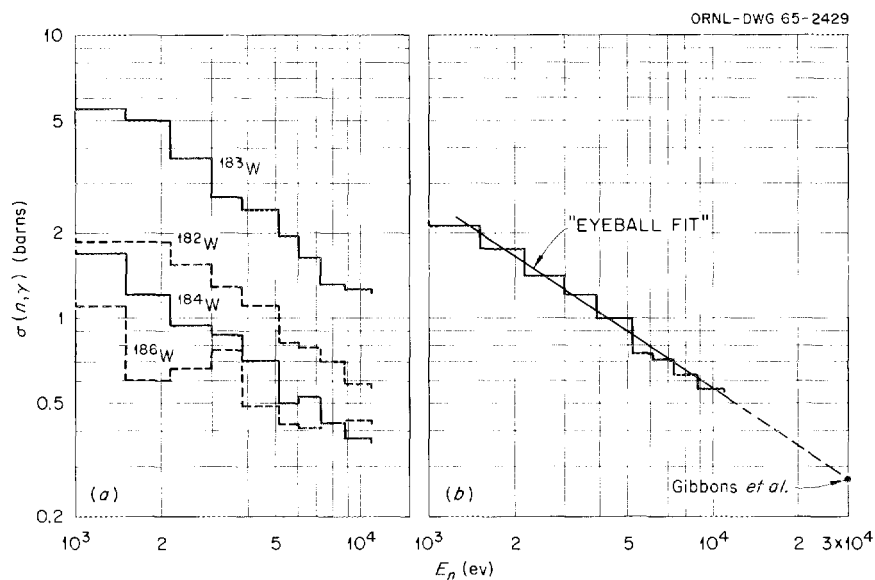


Fig. 8. (a) Average Capture Cross Sections of the Tungsten Isotopes from 1 keV to 10 keV. (b) The Average Capture Cross Section of Natural Tungsten, Based on the Average Capture Cross Sections of Fig. 8. The point at 30 keV is from Gibbons *et al.*⁴

GAMMA-RAY SPECTRA FROM NEUTRONS CAPTURED IN ^{56}Fe AT THE 1148-eV RESONANCE

R. C. Block

NUCLEAR REACTIONS. $^{56}\text{Fe}(n, \gamma)$ at 1148-eV resonance; measured E_γ , I_γ . Deduced partial radiation widths and J of resonance. Natural target.

In 1960 a new low-energy resonance was reported by Isakov *et al.*¹ to occur in the capture cross section of iron at a neutron energy of 1180 ± 80 eV. Neutron capture measurements by Block *et al.*² and Moxon *et al.*³ confirmed the existence of this

¹A. J. Isakov, Yu P. Papov, and E. L. Shapiro, *J. Expt. Theoret. Phys. (USSR)* **38**, 989-92 (1960) [*Soviet Phys. JETP (English Transl.)* **11**, 712 (1960)].

²R. C. Block, J. E. Russell, and R. W. Hockenbury, *Conference on Low Energy Nuclear Physics*, p. 1, Harwell, United Kingdom, September 1962 [AERE-R4131 (1962)].

³M. C. Moxon and E. R. Rae, *Conference on Low Energy Nuclear Physics*, p. 1, Harwell, United Kingdom [AERE-R4131 (1962)].

resonance, and through the use of separated isotopes, Block *et al.*² assigned this resonance to ^{56}Fe target nuclei. Subsequent measurements by Moore *et al.*⁴ have confirmed the isotopic assignment, and the resonance has been assigned to s-wave neutrons on the basis of the similarity of the gamma-ray spectrum from the capture of resonance-energy neutrons to the spectrum from the capture of thermal-energy neutrons. Recent high-resolution transmission measurements at

⁴J. A. Moore, H. Palevsky, and R. E. Chrien, *Phys. Rev.* **132**, 801 (1963).

Harwell⁵ have shown that this resonance cannot be produced by *s*-wave neutrons, and this resonance has been assigned to *p*-wave neutrons at a resonance energy of 1148 ± 3 eV.

For thermal neutron capture in ^{56}Fe , only *s*-wave interactions can effectively take place, so that the capturing state in ^{57}Fe has a spin and parity of $\frac{1}{2}^+$. The low-lying states of ^{57}Fe are of negative parity and low spin, so that the high-energy gamma ray observed in thermal neutron capture can be attributed to *E1* transitions (i.e., $\Delta I = 1$ plus a change of parity). However, for the *p*-wave resonance at 1148 eV the capturing state is either $\frac{1}{2}^-$ or $\frac{3}{2}^-$, and the high-energy gamma transitions cannot be *E1*, but are most probably *M1* transitions ($\Delta I = 1$, no change in parity). It thus appeared interesting to measure the capture-gamma-ray spectra with a gamma-ray resolution superior to that used by Moore *et al.*, so that the similarity of spectra could be studied in more detail.

The 9-in.-diam \times 12-in. NaI crystal detector installed at the 25-m flight station of the ORNL fast-chopper facility⁶ was used to make the measurements (see Fig. 1). For the resonance-energy measurements the rotor was spun at 6520 rpm to achieve a neutron energy resolution of 10% at 1148 eV; the thermal-energy measurements were carried out with a rotor speed of 220 rpm. The NaI detector pulse-height data were collected in a Technical Measurements Corporation (TMC) 4096-channel two-parameter analyzer simultaneously as functions of time of flight and pulse height. For the resonance capture the analyzer was divided into 16 channels of time of flight by 256 channels of pulse height; Fig. 2 shows the analyzer display. Each time-of-flight channel is $1.28 \mu\text{sec}$ wide, and the intensified pattern of dots represents the intense high-energy gamma-ray lines appearing in the 1148-eV resonance capture. The resonance-capture spectrum was determined by subtracting the spectra from "off-resonance" time channels from the spectra of "on-resonance" time channels. The thermal-capture spectrum was determined by

alternating a cadmium sheet in and out of the neutron beam and subtracting the two pulse-height spectra for these two conditions.

The thermal and resonance capture pulse-height spectra are plotted in Fig. 3. Both spectra have been normalized to unity for the high-energy gamma-ray lines, and the error bars are standard deviations derived from the counting statistics. The thermal-capture spectrum was obtained overnight, and the 7.64-MeV line had more than 10,000 counts in the peak. The resonance-capture spectrum was measured for a period of eight days, and about 1500 counts were collected in the high-energy peak. For the thermal-capture spectrum, the background counting rate was only $\frac{1}{2}\%$ of spectrum counting rate at 7.64 MeV, and from 1 to 7 MeV the background did not exceed 8%. In the resonance measurements the background was 13% at the 7.64-MeV peak, and from 2 to 7 MeV the background varied from 20 to 60%. The scintillator detector was periodically checked with a gamma-ray source, and the overall gain shift of the equipment did not exceed 2% during the experiment.

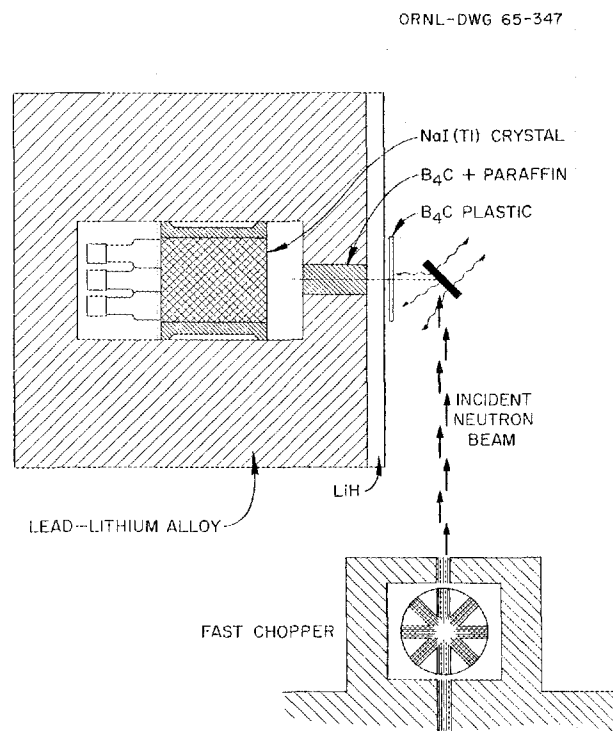


Fig. 1. NaI Crystal Detector at the ORNL Fast Chopper Facility.

⁵R. C. Block, "High Resolution Neutron Transmission Measurements of the 1148-eV Resonance in ^{56}Fe ," to be published in *Physics Letters*.

⁶G. G. Slaughter *et al.*, *Phys. Div. Ann. Progr. Rept. Jan. 31, 1963*, ORNL-3425, p. 60; J. A. Harvey *et al.*, *Phys. Div. Ann. Progr. Rept. Jan 31, 1964*, ORNL-3582, p. 62.

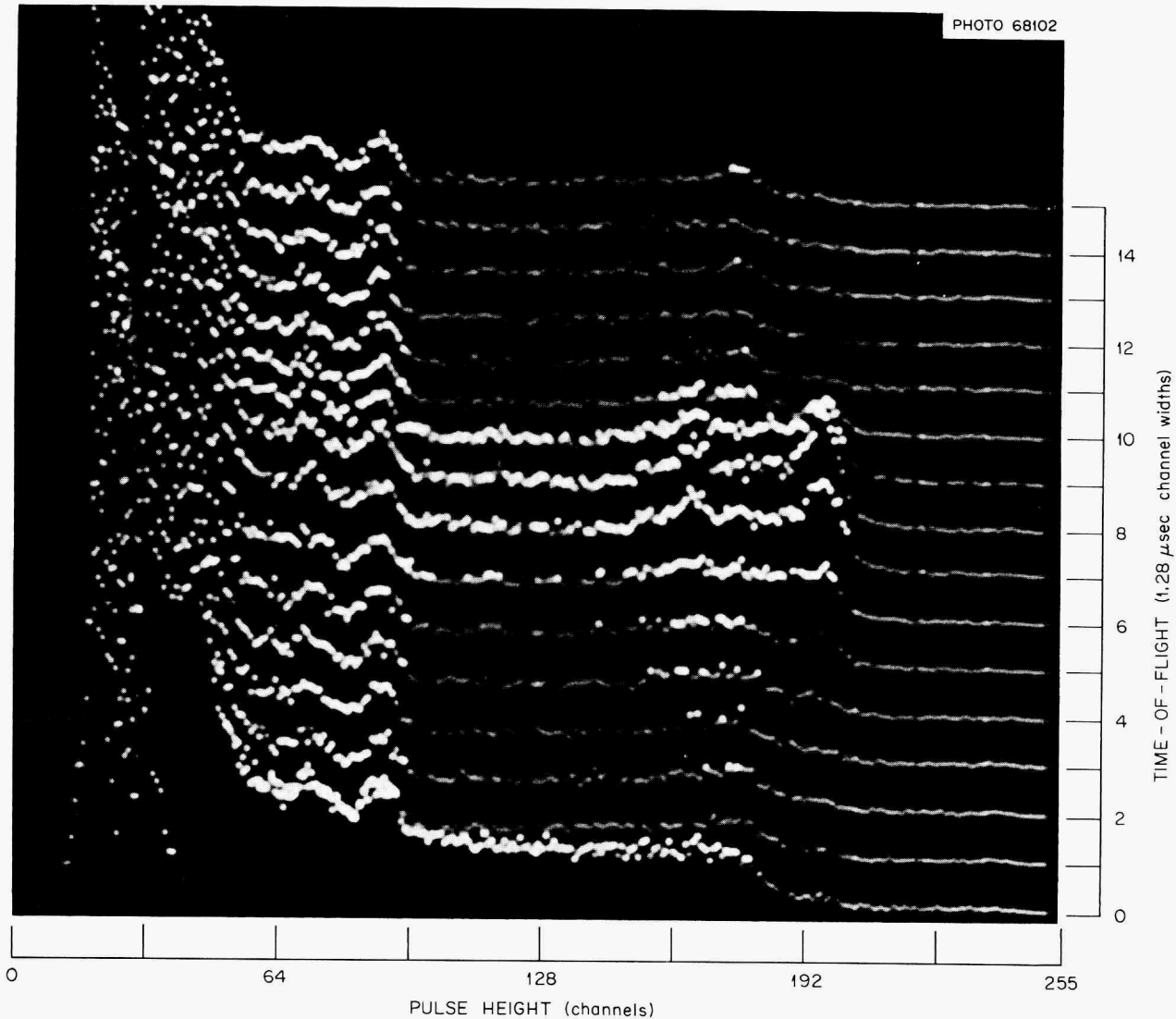


Fig. 2. Oscilloscope Display of the TMC 4096-Channel Two-Dimensional Analyzer. The data represent neutron capture in iron near 1148 eV; the analyzer is divided into 256 channels of pulse height by 16 channels of time of flight.

Considering that the resonance and thermal spectra are produced respectively by p -wave and s -wave capture, the two spectra in Fig. 3 are surprisingly similar in that both spectra are dominated by a strong 7.64-MeV gamma ray going to either the ^{57}Fe ground state or first excited state at 0.014 MeV. However, the strong 5.95-MeV line in the thermal spectrum does not show up in the resonance capture, but a strong line is observed in resonance capture at 6.36 MeV which does not show up in the thermal capture. In addition, there are two weak gamma rays with energies slightly

smaller than the binding energy of the neutron at 7.48 and 7.38 MeV, respectively, for resonance and thermal capture.

The relative intensities of the three highest-energy gamma-ray lines were obtained by graphically "stripping" off a line shape determined by thermal neutron capture in ^{207}Pb . These single lines are plotted below the respective spectra in Fig. 3. The intensities of the prominent lower-energy gamma rays were determined by comparing their peak heights with the peak height of the highest-energy line. All of these relative intensities

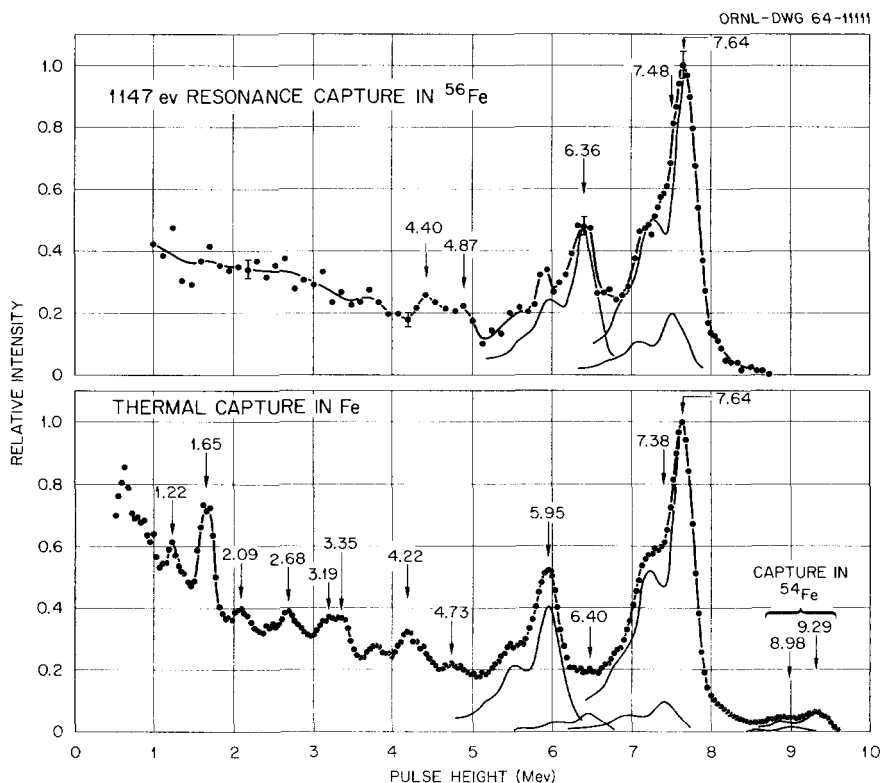


Fig. 3. Gamma-Ray Pulse-Height Spectra from Thermal and 1148-ev Resonance-Energy Neutron Capture in ^{56}Fe .

were then corrected for the relative efficiency of the NaI detector to different-energy gamma rays. (This relative efficiency was measured by observing well-known cascades of gamma rays in the thermal capture of neutrons upon C, Be, Ca, and S.) These relative intensities for gamma rays above 4 Mev are listed in Table 1 along with comparative results from Groshev *et al.*⁷ and Moore *et al.*⁴; for convenience these intensities have been normalized to 100 for the 7.64-Mev gamma ray. A comparison of the gamma-ray energies and relative intensities for thermal capture between this experiment (columns 5 and 6) and the results of Groshev *et al.* (columns 7 and 8) show that within the accuracy of this experiment the results are in agreement. (For comparison the intensities of multiple lines observed by Groshev, as indicated by bracketed energies in column 7, have been summed in column 8.) However, a comparison of the gamma-ray energies and relative intensities for the 1148-ev resonance capture from this experiment (columns

1 and 2) with those of Moore *et al.* (columns 3 and 4) is not in agreement. It must be pointed out that Moore *et al.* used 3-in.-diam \times 3-in. NaI crystals for their experiment, and these small crystals suffer from a very poor line shape for high-energy gamma rays. Thus the results of Moore *et al.* depended very sensitively on the accuracy of their line shapes, and a glance at the observed capture spectra in Fig. 2 of their paper indicates the great difficulty they had in stripping off the highest-energy gamma rays to determine the intensities of the lower-energy gamma rays.

In Fig. 3 the area under the resonance-capture spectrum is approximately equal to the area under the thermal-capture spectrum. Since both spectra have been normalized to unit intensity for the 7.64-Mev gamma ray, the fraction of 7.64-Mev gamma rays per neutron capture is approximately the same for both thermal and resonance capture. Thus it is possible to normalize the relative intensities in the resonance-capture spectrum to the absolute intensities determined in thermal-capture measurements. Groshev *et al.*⁷ have

⁷L. V. Groshev *et al.*, *Nucl. Phys.* **58**, 465 (1964).

Table 1. Relative Intensities of Gamma Rays in Thermal and Resonance Capture

1148-ev Resonance Capture in ^{56}Fe				Thermal Capture in Fe			
This Experiment		Moore <i>et al.</i> ⁴		This Experiment		Groshev <i>et al.</i> ⁷	
E_γ (Mev)	Relative Intensity	E_γ (Mev)	Relative Intensity	E_γ (Mev)	Relative Intensity	E_γ (Mev)	Relative Intensity
7.64 ± 0.08	100	7.639	100	9.29 ± 0.04^a	8 ± 1	9.298^a	7.7^a
				8.98 ± 0.009^a	2.0 ± 0.7	$\begin{bmatrix} 8.882 \\ 8.368 \end{bmatrix}^a$	1.9^a
7.48 ± 0.08	21 ± 6	7.273	25	7.64 ± 0.08	100	$\begin{bmatrix} 7.643 \\ 7.629 \end{bmatrix}$	100
(6.9)	<8)	6.932	35	7.38 ± 0.08	10 ± 5	7.277	13
6.36 ± 0.08	41 ± 6	6.440	21	6.40 ± 0.12	5 ± 3	$\begin{bmatrix} 6.504 \\ 6.379 \\ 6.269 \end{bmatrix}$	2.1
(6.0)	<8)	$\begin{bmatrix} 6.009 \\ 5.911 \end{bmatrix}$	49	5.95 ± 0.08	35 ± 7	$\begin{bmatrix} 6.018 \\ 5.920 \end{bmatrix}$	42
4.9 ± 0.1	~ 7			4.22 ± 0.08	13 ± 5	4.217	8
4.4 ± 0.1	~ 7						

^aCapture in ^{54}Fe .

Table 2. Partial Radiation Widths of the 1148-ev Resonance

E_γ (Mev)	Intensity (%)	Partial Radiation Width (ev)	k_{M1}^a
7.64	43	0.25	34×10^{-3}
7.48	9	0.05	8×10^{-3}
6.36	18	0.10	25×10^{-3}
4.9	~ 3	~ 0.02	$\sim 9 \times 10^{-3}$
4.4	~ 3	~ 0.02	$\sim 9 \times 10^{-3}$

^aIn units of 10^{-6} Mev^{-3} .

measured the sum of the intensities of thermal-capture gamma rays going to the ground state and the 0.014-Mev excited state of ^{57}Fe to be 43%, and the resonance-capture 7.64-Mev gamma-ray intensity has been set equal to this number. These normalized intensities are listed in column 2 of Table 2. The total radiation width of the 1148-ev resonance has been determined in ref. 5 to be 0.58 ev, and thus the partial radiation widths can be obtained by multiplying the intensities in column 2 by 0.58 ev. These widths are listed in column 3 of Table 2. According to Bartholomew,⁸ the reduced width for the M1 transition, k_{M1} , is equal to $\Gamma'_\gamma(M1)_{\text{obs}}/\epsilon^3 D$, where $\Gamma'_\gamma(M1)_{\text{obs}}$ is the partial radiation width in ev, ϵ is the gamma-ray

⁸G. A. Bartholomew, *Ann. Rev. Nucl. Sci.* 11, 259 (1961).

energy in Mev, and D is the average level spacing in Mev in the vicinity of the capturing state of levels of the same spin and parity. The average s -wave level spacing for resonances in ^{56}Fe is observed to be about 25 kev,⁹ and assuming the $(2J + 1)$ level-spacing law to be valid, the average p -wave level spacing will be the order of one to one-half of the average s -wave spacing. Thus, assuming a p -wave spacing of ~ 16 kev, the k_{M1} for the resonance-capture transitions have been calculated and listed in column 4 of Table 2.

In the review paper by Bartholomew,⁸ he finds that for $A > 20$ the measured values of k_{M1} from thermal capture do not exceed 40×10^{-3} and that the average value of k_{M1} is $\sim 4 \times 10^{-3}$. The magnitudes of the k_{M1} in Table 2 fall within the range of the thermal-capture k_{M1} 's, and thus the assignment of the 1148-ev resonance to p -wave capture plus predominant $M1$ deexcitation does not lead to any anomalously large values of reduced radiation widths. On the other hand, the assignment

of any of the transitions in Table 2 as $E2$ transitions leads to very large $E2$ strengths, not at all consistent with the observations of Bartholomew for the $E2$ transitions measured for thermal capture.

Referring again to the resonance-capture spectrum in Fig. 3, the observation of the gamma ray at 7.48 ± 0.08 Mev favors a $3/2^-$ spin assignment to the 1148-ev resonance. Since the compound state in ^{57}Fe is formed essentially at an energy of 7.64 Mev, the (7.48 ± 0.08) -Mev gamma ray is interpreted as the transition to a (0.16 ± 0.08) -Mev state in ^{57}Fe . The low-lying states of ^{57}Fe nearest 0.16 Mev are the $3/2^-$ state at 0.014 Mev, the $5/2^-$ state at 0.136 Mev, and the $3/2^-$ state at 0.366 Mev.¹⁰ If the (7.48 ± 0.08) -Mev gamma ray is interpreted as a transition to the 0.136-Mev state, then of the two possible choices of a $1/2^-$ or $3/2^-$ p -wave capturing state, only the $3/2^-$ capturing state can lead to an $M1$ transition to the $5/2^-$ state. Better spectrum data, however, will be required before a more confident spin assignment can be made to this level.

⁹Neutron Cross Sections, BNL-325, 2d ed., suppl. 1 (1960).

¹⁰Nuclear Data Sheets, NRC 61-2-13.

STUDY OF THE EVEN-EVEN COMPOUND NUCLEI AT THE FIRST s -WAVE STRENGTH FUNCTION RESONANCE

W. M. Good

Daniel Paya¹

Rolf Wagner²

NUCLEAR REACTIONS. ^{43}Ca , ^{47}Ti , ^{49}Ti , ^{53}Cr , ^{57}Fe , ^{63}Cu , ^{65}Cu , measured $\sigma_T(E)$, $E \leq 60$ kev. ^{44}Ca , ^{48}Ti , ^{50}Ti , ^{54}Cr , ^{58}Fe , ^{64}Cu , ^{66}Cu , deduced levels, I^π , level density, resonances, resonance parameters, Γ_n^0/D . Enriched targets.

During the past several years, at least one paper on the s -wave strength function has been published each year.³⁻¹⁰ These works usually have as their objective the fitting of the strength function

in the mass region 85-140, which experiment finds to be anomalously low. The observed strength functions constituting the first resonance at about

¹Permanent address: Commissariat A L'Energie Atomique, Centre D'Etudes Nucleaires de Saclay, Saclay, France.

²Permanent address: Physikalisches Institut der Universitat Basel, Basel, Switzerland.

³Yu. P. Elagin, *Soviet Phys. JETP* 17, 253 (1963).

⁴Yu. P. Elagin, V. A. Lyul'ka, and P. E. Nemirovskii, *Soviet Phys. JETP* 14, 682 (1962).

⁵B. Buck and F. Perey, *Phys. Rev. Letters* 8, 444 (1962).

⁶P. A. Moldauer, *Phys. Rev. Letters* 9, 17 (1962).

⁷T. K. Krueger and B. Margolis, *Nucl. Phys.* 28, 578 (1961).

⁸H. Fiedeldey and W. E. Frahn, *Ann. Phys.* 16, 387 (1961).

⁹A. Sugie, *Phys. Rev. Letters* 4, 286 (1960).

¹⁰A. M. Lane et al., *Phys. Rev. Letters* 2, 424 (1959).

mass 51 peak rather too high, compared with theory, but this has not been taken as serious; the strength in the region of masses above 140 can be accounted for when deformation is taken into account.

The ability of theory to account very well for the first s -wave resonance is a bit surprising when considered in the light of two facts: (1) as the first resonance is spanned, the $f_{7/2}$ shell becomes filled, and the 28- to 50-neutron shell begins to fill; (2) many of the nuclei which had been studied were even-even targets whose resonant level spacings were ≈ 40 kev. For such spacings the condition on I (the energy interval over which the reduced width is averaged) that $D \ll I \ll S/(ds/dE) \ll h^2/2Ma^2$ (ref. 11) can scarcely be met. The even-even compound nuclei which span the first s -wave strength function have not been systematically investigated. These nuclei would be expected to have at least five times the level density of the even-odd compound nuclei. They are ^{43}Ca , ^{47}Ti , ^{49}Ti , ^{53}Cr , ^{57}Fe , and ^{61}Ni , which have, respectively, -4 , -2 , 0 , $+2$, $+4$, and $+6$ neutrons with respect to the closed $f_{7/2}$ shell. The total cross sections of these nuclei have been measured up to 60 kev with the objective of ascertaining what, if any, effect closure of the $f_{7/2}$ shell has on the strength function.

Figure 1 shows the strength functions of these even-even compound nuclei ^{44}Ca , $^{48,50}\text{Ti}$, ^{54}Cr , ^{58}F , and ^{62}Ni ; the odd-odd nuclei ^{46}Si , ^{64}Cu , and ^{66}Cu are also included along with the optical-model prediction as given by Buck and Perey.¹² Table 1 is a listing of individual resonance parameters.

The relatively good agreement between theory and the present experimental results expresses the latter's disagreement with a mass of earlier data indicating a peak strength considerably larger than predicted by theory. At least one of the high values previously obtained was ^{53}Cr , which, as shown in Fig. 1, appears quite "normal."

Insight into the cause of the discrepancy in the case of ^{53}Cr can be obtained from Fig. 5 and from Table 2, where it will be seen that indeed ^{53}Cr has a large strength below 15 kev. More generally, a superficial insight into the relation between the $f_{7/2}$ shell closure and the s -wave strength comes

from the cross sections as shown in Figs. 2-7. The connection appears as a "lumping" of the strength in place of a more nearly uniform distribution. Of course, such "lumping" is a statistical possibility, but when it occurs in so marked a fashion compared with ^{43}Cu and ^{61}Ni , in such a significant region of neutron number, a correlation seems implied which is specifically assumed not to be the case for the distribution function of the majority of widths and spacings. In view of such "lumping" it seems a bit more significant that in the interval 0 to 60 kev the "optical strength" is nevertheless exhibited.

Finally, ^{47}Ti and ^{49}Ti are particularly interesting, since in these two cases of 26 and 28 neutrons in the compound nucleus, the proton number remains constant. A similarity seems to appear (Figs. 3 and 4) between the resonances of $^{49}\text{Ti} + n$ and the first seven resonances in $^{47}\text{Ti} + n$; the resemblance in appearance is matched in Table 2 by a matching in the strengths of these same resonances. The large value for the strength of $^{47}\text{Ti} + n$ (Fig. 1) arises from the large strength that seems to appear at an energy greater than about 30 kev.

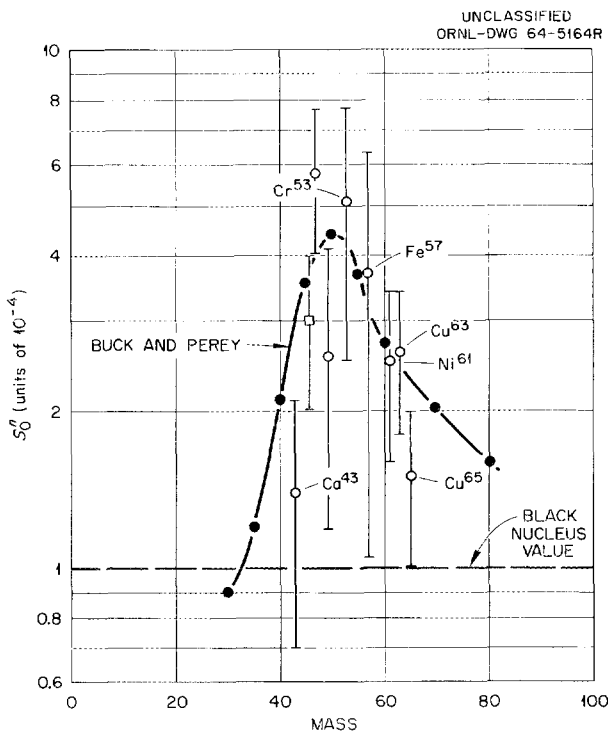


Fig. 1. Strength Function of Nuclei as a Function of Mass of Target in the Region of the First s -Wave Resonance.

¹¹A. M. Lane and R. G. Thomas, *Rev. Mod. Phys.* 30, 309 (1958).

¹²B. Buck and F. Perey, *Phys. Rev. Letters* 8, 444 (1962).

Table 1. Resonance Parameters

	E_0 (kev)	Γ_n (ev)	Γ_n^0 (ev)	J		E_0 (kev)	Γ_n (ev)	Γ_n^0 (ev)	J
^{43}Ca	4.36	49	0.74		^{53}Cr	3.6	157	2.62	
	5.23	37	0.51			4.2	445	6.86	
	8.70	157	1.68			5.4	212	2.88	
	13.80	147	1.25			6.6	357	4.39	
	18.9	162	1.18			8.0	1073	10.7	
	21.0	54	0.37			10.5	224	2.20	
	22.5	109	0.73			19.3	132	0.95	
	26.9	204	1.24			25.3	237	1.49	
	29.2	89	0.52			26.4	350	2.15	
	30.6	60	0.34			28.8	555	3.27	
36.5	299	1.57							
^{47}Ti	2.98	161	2.95		^{57}Fe	3.87	177	2.85	0
	8.15	104	1.15			6.10	396	5.07	1
	10.4	99	0.99			28.7	3018	17.8	1
	11.9	80	0.73			40.5	1258	4.95	
	12.6	73	0.65		45.5	404	1.60		
	16.0	160	1.26		^{61}Ni	6.97	23	0.28	
	26.6	1168	7.16			7.37	238	2.79	
	29.6	220	1.28			12.4	67.7	0.61	
	32.0	848	4.74			13.3	75.9	0.66	
	36.2	394	2.07			13.7	13.0	0.11	
	37.1	365	1.90			16.3	411	3.21	
	39.8	900	4.52			17.5	174	1.32	
	42.0	580	2.82			18.3	181	1.34	
	43.2	1080	5.21			23.8	100	0.64	
	45.9	1125	5.25			28.2	236	1.40	
48.6	493	2.24		30.2		423	2.43		
50.9	805	3.58		31.6	392	2.20			
52.1	952	4.17		32.7	120	0.66			
54.7	476	2.03		33.8	123	0.67			
56.9	1438	6.01		36.0	294	1.55			
^{49}Ti	3.62	162	2.7		40.0	243	1.21		
	8.08	145	1.6		42.2	133	0.65		
	18.2	183	1.36		44.0	169	0.80		
	20.9	95	0.65		48.4	83	0.38		
	22.1	716	4.80		^{63}Cu	2.63	6.9	0.13	
	26.8	462	2.82			4.80	8.8	0.13	
	29.2	173	1.16			5.31	28.2	0.39	
	31.2	1228	6.94			5.79	13.4	0.18	
	35.8	119	0.63			7.64	8.5	0.10	
	37.9	1973	10.14			7.98	69.3	0.77	

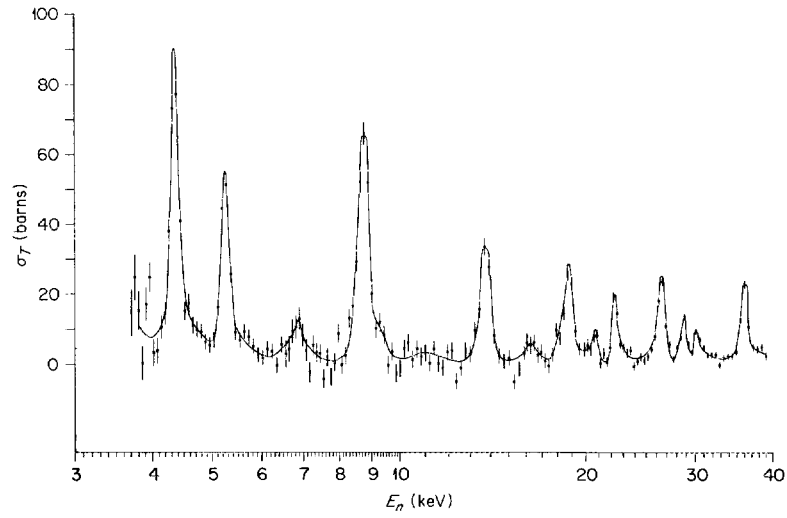
Table 1 (continued)

	E_0 (keV)	Γ_n (eV)	Γ_n^0 (eV)	J		E_0 (keV)	Γ_n (eV)	Γ_n^0 (eV)	J
^{63}Cu	9.21	425	0.44		^{65}Cu	2.5	23.2	0.46	
	9.95	60.8	0.61			3.87	19.7	0.32	
	10.9	67.6	0.65			4.45	15.4	0.23	
	12.4	13.5	0.12			6.45	30.0	0.37	
	13.0	67.2	0.59			7.65	29.8	0.34	
	13.7	49.3	0.42			7.92	155	1.74	
	14.9	34.7	0.28			9.85			
	15.6	22.1	0.18			13.2	72.4	0.63	
	16.1	13.8	0.10			14.2	51.6	0.43	
	17.8	195.8	1.47			15.2	9.6	0.08	
	19.4					15.9	43.9	0.35	
	20.9	302.5	2.09			17.8	296	2.22	
	22.7	143	0.95			19.8	194	1.37	
	24.8	75.5	0.48			21.8	27.4	0.18	
	25.6	207	1.29			24.1	84	0.54	
	26.5	121	0.74			25.0	256	1.62	
	28.2	51.5	0.31			34.9	324	1.73	
	29.3	242	1.41			39.7	249	1.25	
	31.2	96	0.54			43.5	224	1.07	
	33.2	325	1.78			50.8	70	0.31	
36.4	308	1.61		54.2	132	0.57			
42.2	546	2.66		58	320	1.33			

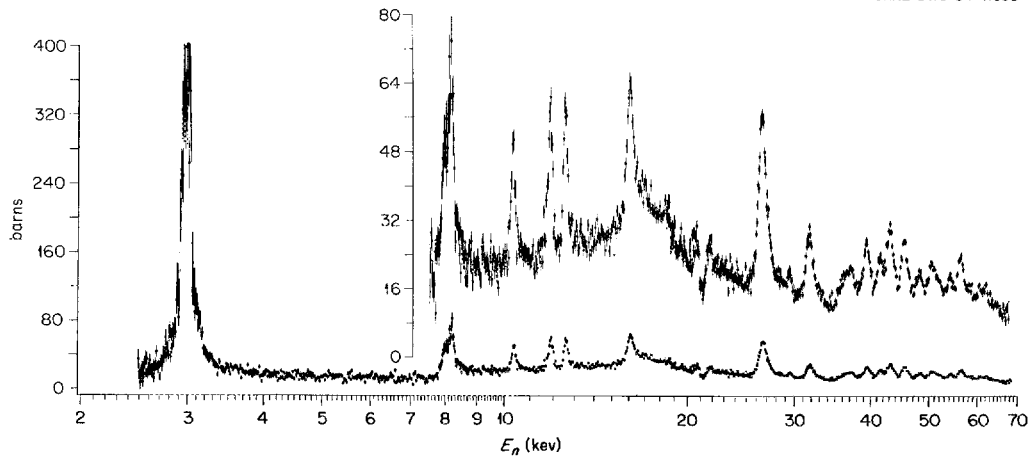
Table 2. Strength Functions
and Average Level Spacings

Isotope	ΔE (keV)	S_n^0 (10^{-4})	\bar{D} (keV)
^{43}Ca	0-36.5	1.4 ± 0.7	13.3 ± 0.6
^{47}Ti	0-57	5.8 ± 2	2.6 ± 0.4
	0-27	2.79 ± 1	
	27-57	8.1 ± 3	
^{49}Ti	0-60	2.64 ± 1.5	55.6 ± 1.0
^{53}Cr	0-40	5.1 ± 2.6	3.0 ± 0.7
	3-15	12.4 ± 8	
	15-40	1.6 ± 1.3	
^{57}Fe	0-55	3.7 ± 2.6	10 ± 3
^{61}Ni	0-50	2.5 ± 0.9	2.4 ± 0.6
^{63}Cu	0-60	2.7 ± 0.8	1.2 ± 0.2
^{65}Cu	0-60	1.5 ± 0.5	1.67 ± 0.3

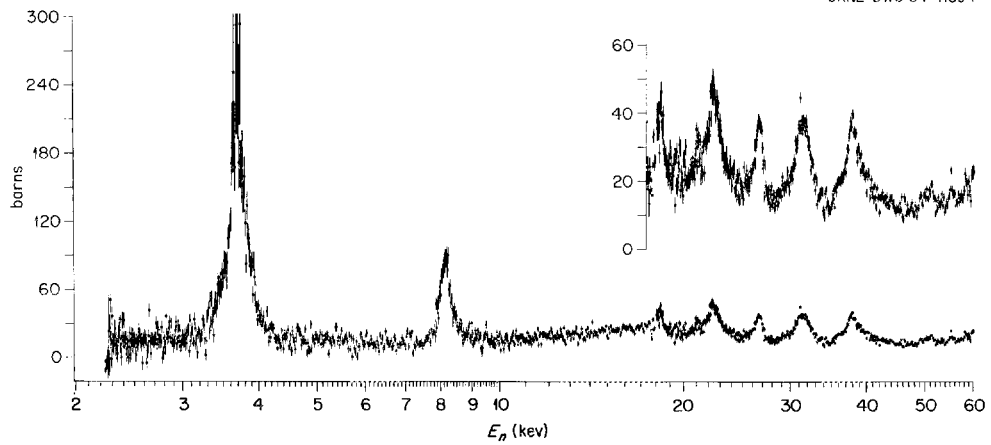
ORNL-DWG 64-5170

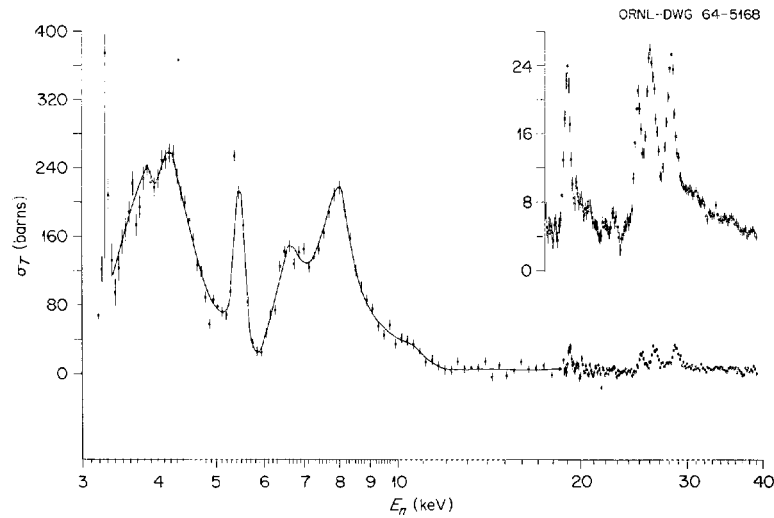
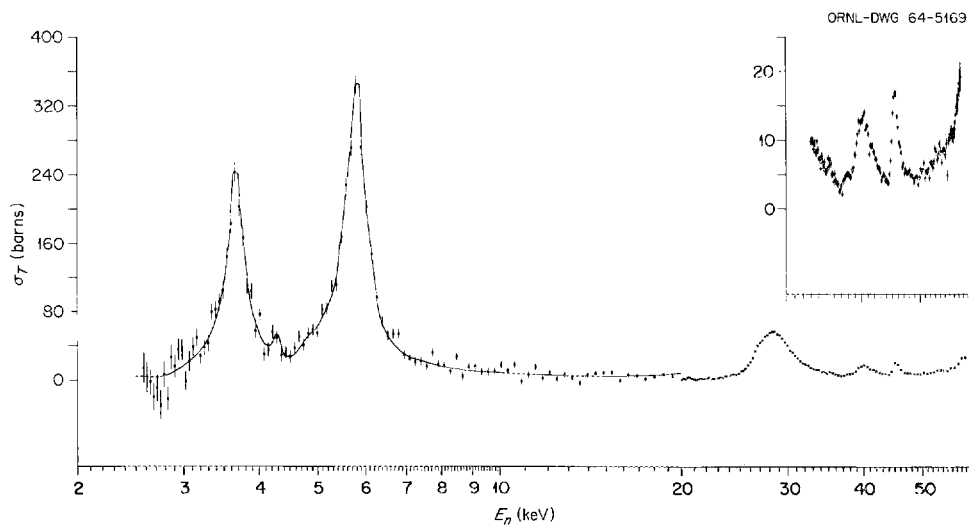
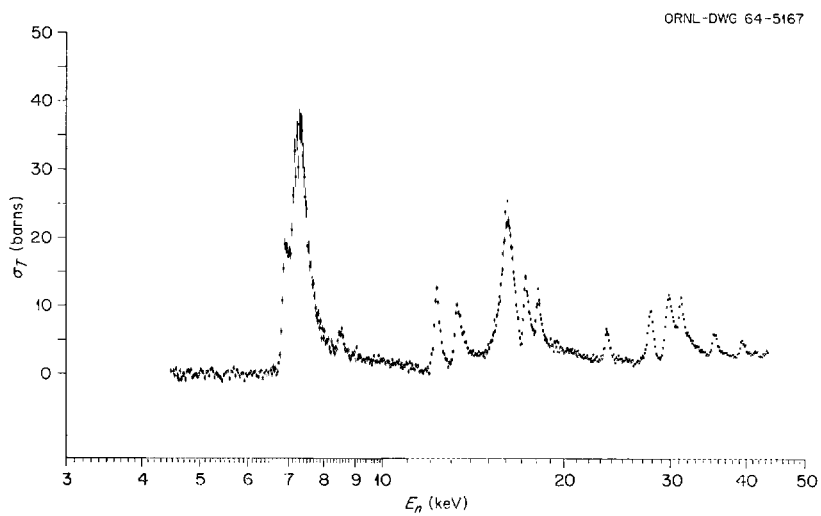
Fig. 2. Total Cross Section of ^{43}Ca .

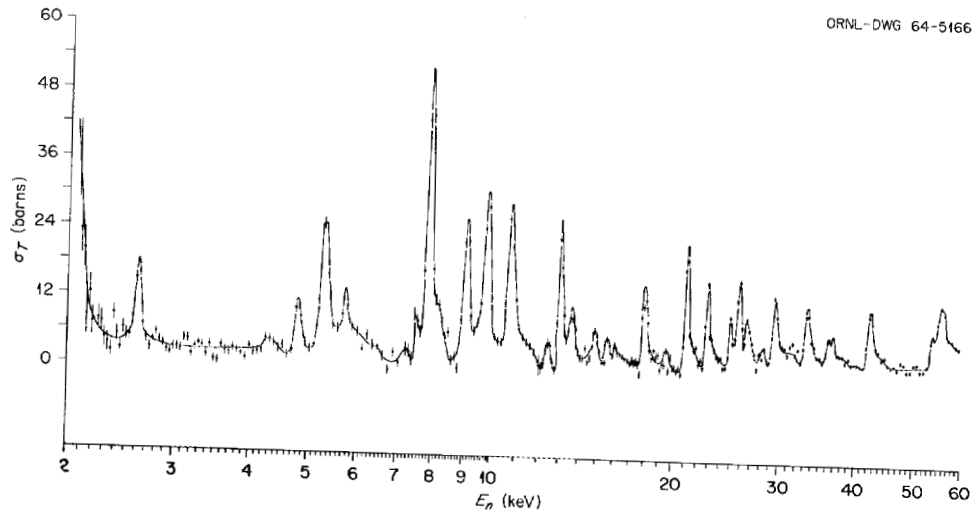
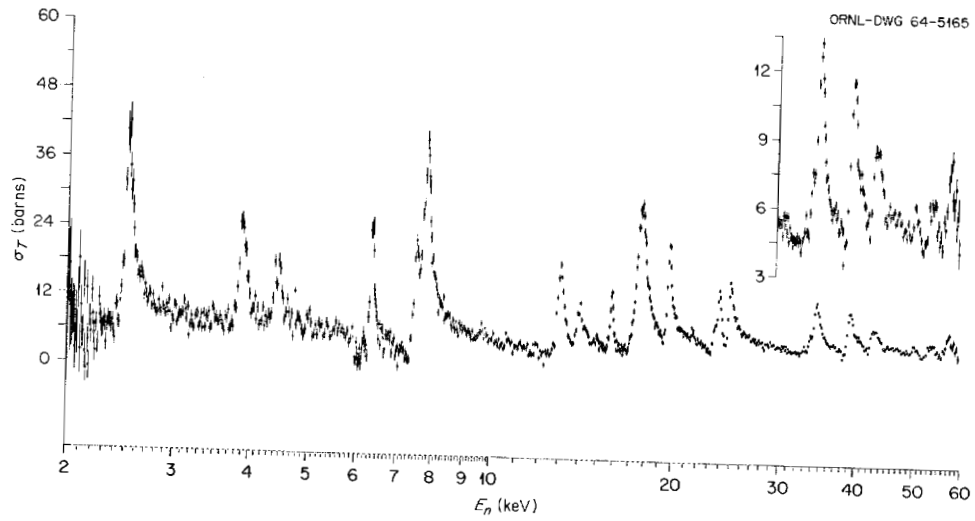
ORNL-DWG 64-11693

Fig. 3. Total Cross Section of ^{47}Ti .

ORNL-DWG 64-11694

Fig. 4. Total Cross Section of ^{49}Ti .

Fig. 5. Total Cross Section of ^{53}Cr .Fig. 6. Total Cross Section of ^{57}Fe .Fig. 7. Total Cross Section of ^{61}Ni .

Fig. 8. Total Cross Section of ^{63}Cu .Fig. 9. Total Cross Section of ^{65}Cu .

A STUDY OF THE GAMMA-RAY SPECTRA EMITTED IN THE RESONANCE CAPTURE OF NEUTRONS BY $^{19}\text{F}^1$

J. R. Bird²

J. A. Biggerstaff

J. H. Gibbons

W. M. Good

NUCLEAR REACTIONS. $^{19}\text{F}(\rho, \gamma)$, measured $\sigma(E, E_\gamma)$, $E \leq 80$ kev. ^{20}F , deduced relative intensities, γ -reduced widths. Natural target.

Gamma-ray spectra have been measured at the 27-kev (2^-) and the 49-kev (1^-) resonances of $^{19}\text{F}(n, \gamma)^{20}\text{F}$. The $E1$ transition to ground is virtually absent at both resonances, while the

other $E1$'s have strengths that appear normal when compared with heavier nuclei in which the radiation widths are proportional to level spacing. A description is given of the two-parameter instrument by means of which it is possible to simultaneously measure the neutron energy (flight time) and gamma-ray pulse-height spectra for radiative neutron capture.

¹Abstract of paper submitted for publication in the *Physical Review*.

²Present address: Australian Atomic Energy Commission, Sutherland, New South Wales, Australia.

A STUDY OF THE RESONANCE STRUCTURE OF THE EVEN ZIRCONIUM ISOTOPES AT BELOW 60-kev NEUTRON ENERGY

J. A. Biggerstaff

W. M. Good

H. J. Kim

NUCLEAR REACTIONS. ^{90}Zr , ^{92}Zr , ^{94}Zr , ^{96}Zr , measured $\sigma_n(E)$, $E \leq 60$ kev. ^{91}Zr , ^{93}Zr , ^{95}Zr , ^{97}Zr , deduced levels, level density, resonances, resonance parameters I_n^0/D . Enriched targets.

In the previous annual report,¹ we reported on an investigation into the neutron total cross sections and strength functions of the isotopes of zirconium. The results of these investigations indicated a large average strength (1.5×10^{-4}) compared with the value $\approx 0.3 \times 10^{-4}$ exhibited by other nuclei of mass greater than 90. Furthermore, the data were such as to leave in doubt the character of the cross sections between resonances, that is, small resonances were suggested, but the statistics were too poor to reveal anything about their size or density.

Measurements were therefore made with increased sample thicknesses for the purpose of (1) confirming the previous results, (2) extending the measurements to higher energy, and (3) im-

proving between-resonance statistics by employing thicker samples, especially in the case of ^{96}Zr .

The cross-section results for $^{90,92,94,96}\text{Zr}$, including both the 1963 and 1964 measurements, are shown in Figs. 1, 2, 3, and 4. The individual resonance parameters are listed in Table 1, and the statistical parameters are shown in Table 2.

Since the report of our measurements on zirconium a year ago, Moskalev *et al.*² have published results of similar measurements. In Tables 1 and 2 the various parameters that they obtained are given for comparison. It will be seen that in energy ranges common to the two experiments, the agreement is good, and furthermore there is agreement with the results quoted a year ago. However, by contrast with the agreements just described, there

¹J. A. Biggerstaff, W. M. Good, and H. Kim, *Phys. Div. Ann. Progr. Rept. Jan. 31, 1964*, ORNL-3582, p. 82.

²S. S. Moskalev, H. V. Muradian, and Yu. V. Adamchuk, *Nucl. Phys.* **53**, 667 (1964).

is also shown in Table 2 what appears to be a significant rise in the strength at higher energy. Since the values quoted a year ago were for an intermediate range of energy, the dependence on energy suggested by Table 2 partly accounts for the somewhat higher value of 1.5 quoted last year. At the energies extending on up to 40 to 60 keV, the strength for all the zirconium isotopes taken together reaches the surprisingly high value of $2.5 \pm 0.3 \times 10^{-4}$, a value considerably higher than predicted by the optical models.

The level spacings obtained from the present set of data and the level spacings obtained by

Moskalev *et al.* both show a decrease in level spacing with neutron excess. The precise figures do not agree so well in this case as in the strength function case; however, the average level spacings are derived from entirely different energy intervals in the two experiments. It may be significant in the case of ^{96}Zr that the number of levels with $E < E_i$ vs E_i cannot be fitted by a single straight line, but can be fitted rather well by two such lines. A discussion of these results can be found in a forthcoming publication, now in rough draft.

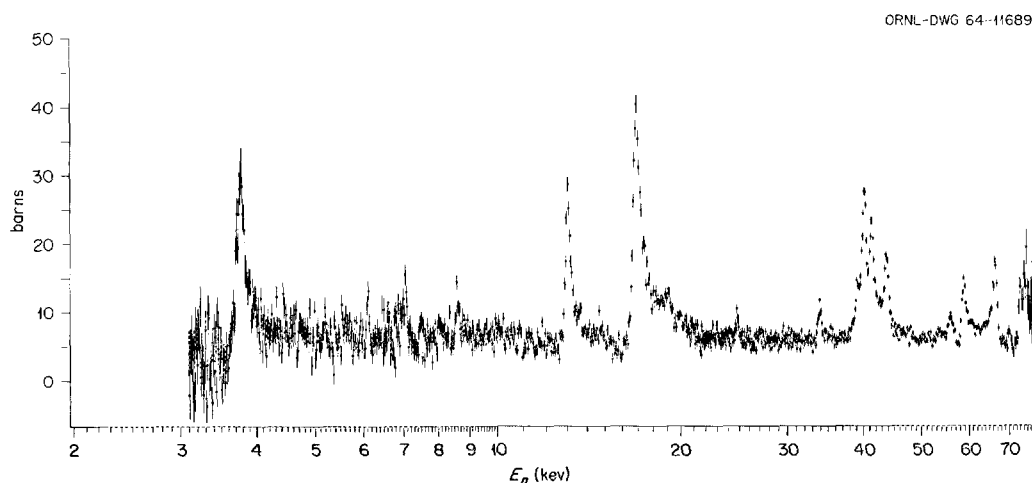


Fig. 1. Total Cross Section of ^{90}Zr .

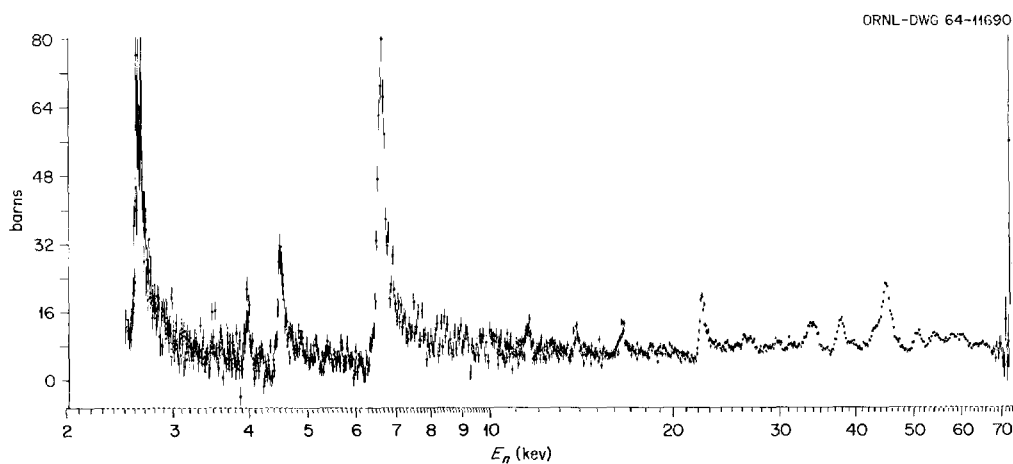


Fig. 2. Total Cross Section of ^{92}Zr .

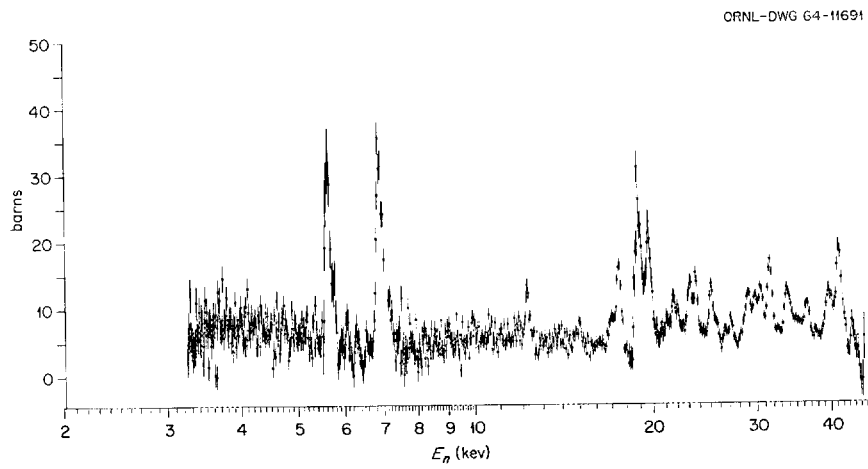


Fig. 3. Total Cross Section of ^{94}Zr .

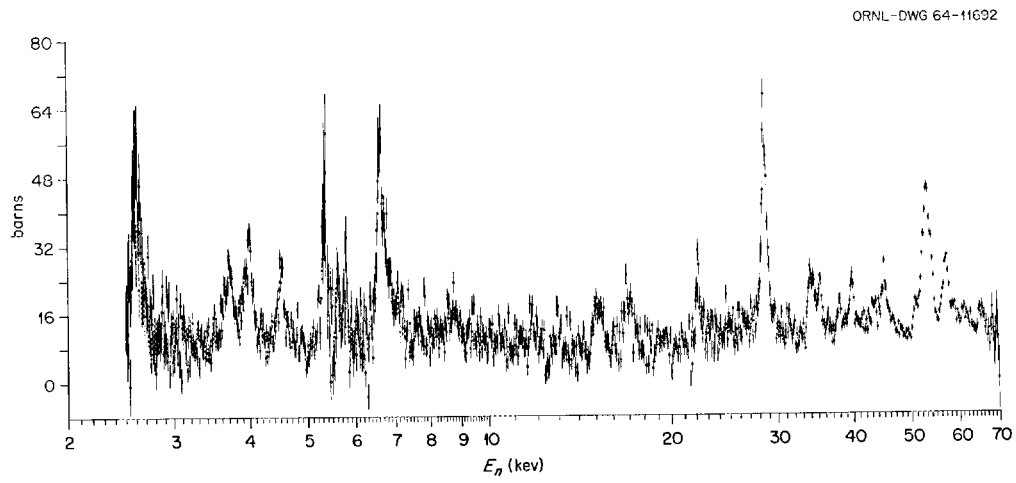


Fig. 4. Total Cross Section of ^{96}Zr .

Table 1. Resonance Parameters for the Even Isotopes of Zirconium

The errors in the "Present Experiment" columns are representative errors based upon analysis of thick and thin sample data

Isotope	E_0 (kev)		Γ_n (ev)		Γ_n^o (ev)	
	Present Experiment	Reference ^a	Present Experiment	Reference ^a	Present Experiment	Reference ^a
⁹⁰ Zr	3.8 ± 0.06	3.91 ± 0.025	14 ± 3	13.6 ± 0.5	0.245 ± 0.05	0.22 ± 0.08
	6.9 ± 0.03		8 ± 1		0.095 ± 0.02	
	7.9 ± 0.05		9 ± 1		0.10 ± 0.02	
	13.3 ± 0.1	13.67 ± 0.16	69 ± 9	65 ± 15	0.595 ± 0.08	0.56 ± 0.13
	17.2 ± 0.1	17.85 ± 0.25	227 ± 17	200 ± 70	1.795 ± 0.2	1.50 ± 0.52
	34.7 ± 0.1		89		0.84	
	40.1 ± 0.1		94		0.47	
	41.6		362		1.79	
	42.4 ± 0.2		342		1.68	
	44.1 ± 1		320		1.03	
	56		126		0.54	
	59		310		1.29	
	68		563		2.20	
	⁹² Zr	2.7 ± 0.06	2.72 ± 0.02	27 ± 4	14 ± 2	0.517 ± 0.1
4.10 ± 0.06		4.15 ± 0.03	6 ± 3	3.5 ± 0.5	0.092 ± 0.05	0.055 ± 0.008
4.71 ± 0.05		4.66 ± 0.03	21 ± 4	10 ± 4	0.321 ± 0.06	0.15 ± 0.06
6.88 ± 0.02		6.88 ± 0.06	86 ± 20	80 ± 10	1.05 ± 0.3	0.96 ± 0.11
12.1			25		0.23	
14.5			38		0.32	
17.2			38		0.30	
23.1			121		0.81	
27.0						
31.2						
34.3			217		1.19	
39.2			208		1.07	
44.7			186		0.90	
46.8			607		2.70	
52.0						
⁹⁴ Zr	5.7 ± 0.1	5.87 ± 0.06	22.1	27 ± 7	0.294	0.35 ± 0.09
	6.98 ± 0.2	7.22 ± 0.06	30.4	72 ± 8	0.367	0.85 ± 0.10
	12.7	12.80 ± 0.16	28.6	20 ± 7	0.27	0.175 ± 0.06
	15.5		13.9		0.11	
	17.7		22.2		0.17	
	17.95 ± 0.2		65 ± 8		0.487 ± 0.08	
	19.4 ± 0.5	19.86 ± 0.27	107 ± 9	125 ± 40	0.778 ± 0.09	0.9 ± 0.3
	20.2 ± 0.2		85		0.61	
	21.7					
	23.1		50		0.32	
23.7		43.5		0.28		

^aS. S. Moskalev, H. V. Muradian, and Yu. V. Adamchuk, *Nucl. Phys.* **53**, 667 (1964).

Table 1 (continued)

Isotope	E_0 (kev)		I_n (ev)		I_n^0 (ev)	
	Present Experiment	Reference ^a	Present Experiment	Reference ^a	Present Experiment	Reference ^a
⁹⁴ Zr	25.1		57		0.36	
	27.0					
	29.0		57		0.34	
	29.8		57		0.34	
	30.2		78		0.45	
	31.8		134		0.75	
	33.8		130		0.71	
	36.3		69		0.36	
	40.0		145		0.73	
	41.6		267		1.29	
	43.7					
⁹⁶ Zr		2.38 ± 0.015		1.5 ± 0.3		0.03 ± 0.006
	2.68		12		0.24	
	3.85 ± 0.06	3.84 ± 0.04	7 ± 1.1	4.5 ± 1	0.12 ± 0.01	0.07 ± 0.016
	4.11 ± 0.02	4.15 ± 0.03	14 ± 1.1	12.5 ± 2	0.21 ± 0.01	0.195 ± 0.032
	4.61 ± 0.01		10.8 ± 3		0.158 ± 0.02	
	5.48 ± 0.1	5.51 ± 0.05	15.6 ± 3	16.0 ± 8	0.215 ± 0.05	0.215 ± 0.110
	5.84 ± 0.07		4		0.05	
	5.97		4		0.05	
	6.80		22		0.27	
	8.96					
	15.45					
	17.51					
	22.76		86		0.58	
	29.4		402		2.39	
	34.5		143		0.79	
	36.1		93		0.50	
	37.2		43		0.23	
	38.9		96		0.49	
	40.7		180		0.91	
	45.8		288		1.36	
	51.6		124		0.55	
54.2		1170		5.11		
58.3		558		2.35		

^aS. S. Moskalev, H. V. Muradian, and Yu. V. Adamchuk, *Nucl. Phys.* **53**, 667 (1964).

Table 2. Strength Functions and Average Level Spacings of the Even Isotopes of Zirconium
 The errors in the "Present Experiment" columns are based upon Porter-Thomas distribution
 of level widths and Wigner Distribution of level spacings

Isotope	ΔE (kev)	$S_n^o = \frac{\sum I_n^o}{\Delta E}$		\bar{D} (kev)	
		Present Experiment	Reference ^a	Present Experiment	Reference ^a
		$\times 10^{-4}$	$\times 10^{-4}$		
⁹⁰ Zr	0-28	1.01 ± 0.7	0.85 ± 0.65		4.5 ± 1.6
	28-70	2.46 ± 1.2			
	0-70	1.81 ± 0.9		5.0 ± 1.0	
⁹² Zr	0-12	1.20 ± 0.9	1.2 ± 0.8		1.2 ± 0.4
	12-52	1.82 ± 0.9			
	0-52	1.75 ± 0.8		3.3 ± 0.7	
⁹⁴ Zr	0-21	1.18 ± 1	1.1 ± 0.8		2.4 ± 0.9
	21-44	2.84 ± 1			
	0-44	2.24 ± 1		1.7 ± 0.3	
⁹⁶ Zr	0-5.8	1.28 ± 1	0.9 ± 0.6	0.750 ± 0.2	1.0 ± 0.3
	5.8-58	2.93 ± 1		4.12 ± 0.8	
	0-58	2.79 ± 1			

^aS. S. Moskalev, H. V. Muradian, and Yu. V. Adamchuk, *Nucl. Phys.* **53**, 667 (1964).

NEUTRON CAPTURE DATA AT STELLAR TEMPERATURES¹

R. L. Macklin

J. H. Gibbons

Neutron capture cross sections are averaged over Maxwell-Boltzmann neutron distributions for temperatures pertinent to slow nucleosynthesis (s process) in red giant stars. Such cross sections, together with isotopic abundances, provide the

¹Abstract of published paper: *Rev. Mod. Phys.* **37**, 166 (1965).

major quantitative experimental tests of the theory. The cross sections are tabulated at convenient intervals from $kT = 5$ kev to $kT = 90$ kev where data are available. In many cases it has been possible to supplement the often fragmentary (as of June 1964) data with evidence from nuclear systematics.

RESONANCE NEUTRON CAPTURE AND TRANSMISSION IN SULFUR, IRON, AND LEAD¹

R. L. Macklin

P. J. Pasma²

J. H. Gibbons

NUCLEAR REACTIONS. Targets ^{32}S , ^{56}Fe , $^{206,7,8}\text{Pb}$, (n, γ and total), $E = 10\text{--}80$ kev. Measured σ_{nT} , σ_{nA} . Deduced resonances, resonance parameters, I , I_γ , J , π , level densities (for $l = 0, 1$ separately), effective nuclear radii. Enriched and natural targets.

Resonances in both the capture and total cross sections for ^{32}S , ^{56}Fe , ^{206}Pb , ^{207}Pb , and ^{208}Pb were investigated in the energy range from 10 to 80 kev. Total and radiative widths, and in some cases spins and/or parities, were assigned, and isotopic identifications of resonances were made. Previously unknown resonances, mostly due to

$l > 0$ neutrons, were found in all of these nuclei. The p -wave level density for ^{206}Pb and ^{207}Pb was found to be more than twice as high as one would expect from the number of observed s resonances. The total radiative widths for an $l_n = 0$ vs two $l_n = 1$ resonances for ^{207}Pb targets differed by a factor of 10. The effective nuclear radius, R' , was found to be 8.5 ± 0.2 fermis (^{206}Pb), 9.5 ± 0.3 fermis (^{207}Pb), and 8.4 ± 0.3 fermis (^{208}Pb), giving an average of 8.8 ± 0.3 fermis, which is in good agreement with an optical-model prediction of 8.7 fermis.

¹Abstract of published paper: *Phys. Rev.* **136**, B695 (1964).

²Visiting scientist from Natuurkundig Laboratorium, Rijks-Universiteit, Groningen, The Netherlands.

THE INTERACTION OF 350-keV POLARIZED NEUTRONS WITH ORIENTED ^{165}Ho NUCLEI¹

R. Wagner²

P. D. Miller

T. Tamura

H. Marshak³

NUCLEAR REACTIONS. $^{165}\text{Ho}(n)$, $E_n = 350$ kev: measured $\sigma_T(\theta, n$ polarization).

The interaction of polarized and unpolarized 350-keV neutrons with oriented and unoriented ^{165}Ho nuclei was investigated in order to study the effect of nuclear deformation and to search for a possible spin-spin interaction. The ORNL 3-mv pulsed and bunched Van de Graaff proton beam was used in conjunction with a time-of-flight spectrometer. The $^7\text{Li}(p, n)$ reaction at a laboratory angle of 51° provided a source of 55% polarized 350-keV neutrons. Using the NBS transportable ^3He refrigerator, a single crystal of ^{165}Ho metal was cooled to 0.34°K , and a nuclear polarization of approximately 15% was obtained with a super-

conducting split solenoid. The differential cross section for unpolarized 350-keV neutrons, elastically scattered from unoriented ^{165}Ho nuclei, was measured in a cylindrical geometry and is in good agreement with the results of a coupled-channel calculation. The total cross section of unoriented ^{165}Ho was measured between 300 and 400 kev. A coupled-channel calculation of the total cross section using the same optical-model parameters as those that fitted the angular distribution is found to agree very well with these data. To investigate the spin-spin interaction, measurements were made of the transmitted intensities with the target nuclei polarized alternately parallel and antiparallel to the direction of neutron polarization. The observed change in intensity, $(-0.11 \pm 0.32)\%$, and the observed total cross section of 7.94 barns imply a change in cross section of $(+30 \pm 85)$ mb, where the plus sign corresponds to a larger cross section for the

¹Abstract of paper to be submitted to the *Physical Review*. A preliminary account has been published: *Phys. Letters* **10**, 316 (1964).

²Now at University of Basel, Basel, Switzerland.

³National Bureau of Standards, Washington, D. C.

parallel orientation. Comparison of this result with that of the coupled-channel calculation indicates that if the spin-spin interaction in the optical-model potential is written as $-V_{ss}(\vec{\sigma} \cdot \vec{I})$ times a Saxon form factor, then V_{ss} lies between -130 and $+280$ kev. Since the ^{165}Ho nucleus is highly deformed, a transmission measurement was made to determine the change in cross section between a highly oriented and a nearly unoriented

target. The transmission of the target decreased by $(1.3 \pm 0.4)\%$ for the higher orientation value, which corresponds to a cross-section increase of 350 ± 100 mb. This deformation effect on the total cross section is also in good agreement with that derived from the coupled-channel calculation. The deformation parameter, β , used in the optical-model potential was $+0.3$, in agreement with other measurements.

METHOD FOR OBTAINING BURSTS OF POLARIZED NEUTRONS OF ENERGY 10-700 kev

J. W. T. Dabbs

J. A. Harvey

As first suggested by Schwinger,¹ fast neutrons can be polarized by scattering from helium at $\sim 90^\circ$ (c.m.) and might be moderated while retaining the polarization.

In considering the use of the proposed ORNL electron linear accelerator, the observation was made that the energy at which most neutrons will be produced in a tungsten or uranium target agrees almost exactly with the peak in both polarization and cross section for scattering of neutrons through a lab angle of $90 \pm 15^\circ$ from helium, namely ~ 1.2 Mev. The calculated polarization of such a scattered beam is ~ 50 - 60% , with only slight dependence on angle, and the effective intensity is $\sim 0.5\%$ of that without the scattering (solid angle factors included). The scattering requires ~ 1 cm thickness of liquid helium at 4.2°K with a heat input expected to evaporate ~ 1 liter of liquid helium per hour at the expected neutron intensity from the proposed linac. The median neutron energy after a single 90° scattering from ^4He is approximately 700 kev.

Such a polarized, scattered beam can be moderated to lower energies without appreciable loss of polarization by a spin-zero moderator which has sufficiently small differences between the two p -wave and between the two d -wave phase shifts. These requirements appear to be met by a moderator of ^{12}C in the form of a graphite block ~ 10 cm on a side. The "slowing-down power" of carbon is only about $1/20$ that of hydrogen; thus a severe loss of intensity occurs at lower energies

because of the high escape probability and the large number of scatterings required to reach the lower energies. In spite of this, the neutron intensity appears usable down to about 10 kev.

A major problem, that of wall backscattering into the moderator, seems to have been essentially solved in the basic design of the proposed linac accelerator facility, which has a 10-ft-diam by 10-ft-high evacuated target room. With the addition of suitable wall treatment to increase the neutron absorption, a 10% background appears feasible on the basis of preliminary estimates. It is not expected that the method described here would be applicable to accelerators not having an evacuated target room, but clever use of shielding might permit a reduction in background to a usable level. Calculations have not been made on this, however.

The estimated intensities as a function of neutron energy for both graphite and hydrogen moderators are given in Table 1. The $N(E_n)$ are the numbers of neutrons that escape from the moderator in the stated energy interval for each neutron incident on the moderator, and are based on a Monte Carlo calculation which was performed by J. G. Sullivan and A. M. Craig, Jr., of the ORNL Mathematics Division. The values of \bar{L} given in Table 1 are the averages over 1000 neutrons of the time delay before escape, converted to a length at the final velocity: that is,

$$L = \sum_{i=1}^t \frac{l_i}{\sqrt{E_i}} \sqrt{E_f},$$

¹J. Schwinger, *Phys. Rev.* **69**, 681 (1946).

where l_i is the actual path length associated with the i th trajectory within the moderator. The variances in the \bar{L} values are denoted by (ΔL) . In the table, ΔL thus represents the effective thickness of the moderator and determines the limit on resolution due to the source using this method. Detailed Monte Carlo calculations of the polarization after moderation by ^{12}C are in progress but have not yet been completed.

Since the inception of this approach, a clearly superior method in the energy range 0–10 keV has been demonstrated by Draghicescu *et al.*² Their method would, in the linac case, consist of passing H_2 -moderated neutrons through a dynamically polarized proton target.³ Their method has the advantage of higher intensity, since the values in

the lower half of Table 1 would apply to the intensity incident on the polarizer. The intensity loss associated with the liquid helium single scattering (factor 200) would not apply; a loss of a factor of 10 because of the small size of the polarizer⁴ and a factor of 5 for transmission loss in the polarizer gives an overall factor of ~ 4 in favor of their method in addition to the intensity factors between the upper and lower halves of Table 1. The polarizations expected from the two methods are rather comparable. It would appear that the two methods are complementary with respect to energy range and that together they will provide means for obtaining bursts of polarized neutrons over the entire range 0–700 keV with only slow variations of polarization with energy.

²P. Draghicescu *et al.*, *Phys. Letters* **12**, 334 (1964).

³See, e.g., C. D. Jeffries, *Dynamic Nuclear Polarization*, Interscience, New York, 1963.

⁴We wish to thank A. Michaudon for pointing this out, and for an illuminating discussion regarding polarization losses during moderation.

Table 1. Neutron Moderation; Monte Carlo Calculations
Based on 1000 neutrons

ΔE	$N(\Delta E)^a$	\bar{L}^b (cm)	ΔL^c (cm)	No. Collisions in ΔE (av)
$E_0 = 700$ keV; Graphite $10 \times 10 \times 8$ cm				
700–100 keV	0.978	5.76	3.75	13
100–10 keV	0.021	12.0	4.6	14
10–1 keV	0.0009	14.0	4.9	14
1–0.1 keV	0.00002	14.0	5.7	13
$E_0 = 1000$ keV; Water $10 \times 10 \times 2$ cm				
1000–100 keV	0.822	2.44	0.74	3.4
100–10 keV	0.087	1.78	1.51	2.3
10–1 keV	0.044	1.43	1.46	2.2
1–0.1 keV	0.021	1.37	1.56	2.0
100–10 eV	0.012	1.27	1.60	2.0
~ 1 eV	0.008	0.95	1.06	3.2

^a $N(\Delta E)$ is fraction of neutrons escaping within ΔE .

^b \bar{L} is effective source distance behind exit face of moderator.

^c ΔL is standard deviation in \bar{L} .

DIFFERENTIAL SCATTERING OF NEUTRONS FROM ^{16}O

C. H. Johnson

J. L. Fowler

NUCLEAR REACTIONS. $^{16}\text{O}(n, n)$, $E_n = 2.25\text{--}4.00$ Mev; measured $\sigma(\theta)$. ^{17}O , deduced resonance parameters, phase shifts.

The recent development of the idea of intermediate states has brought a renewed interest in the spectroscopy of such nuclei as ^{17}O , where relatively pure intermediate states are expected. Previously we had measured differential cross sections in the 3- to 4-Mev neutron energy region by scattering $T(p, n)$ neutrons from beryllium oxide and beryllium.¹ Since a preliminary phase-shift analysis of this data revealed a $3/2^+$ resonance of

¹C. H. Johnson and J. L. Fowler, *Bull. Am. Phys. Soc.* **9**, 348 (1964).

considerable theoretical interest, it was desirable to investigate this region in greater detail with improved accuracy.

Figure 1 shows the apparatus for the improved experiment. The sample is liquid oxygen contained in a 1-mil-wall Dewar flask which was designed to minimize background scattering. The inner wall was only 1 mil thick. The outer wall, which was under atmospheric pressure, was 10 mils of stainless steel; it has to be work-hardened to withstand the pressure. An identical Dewar

ORNL-LR-DWG 67369R2

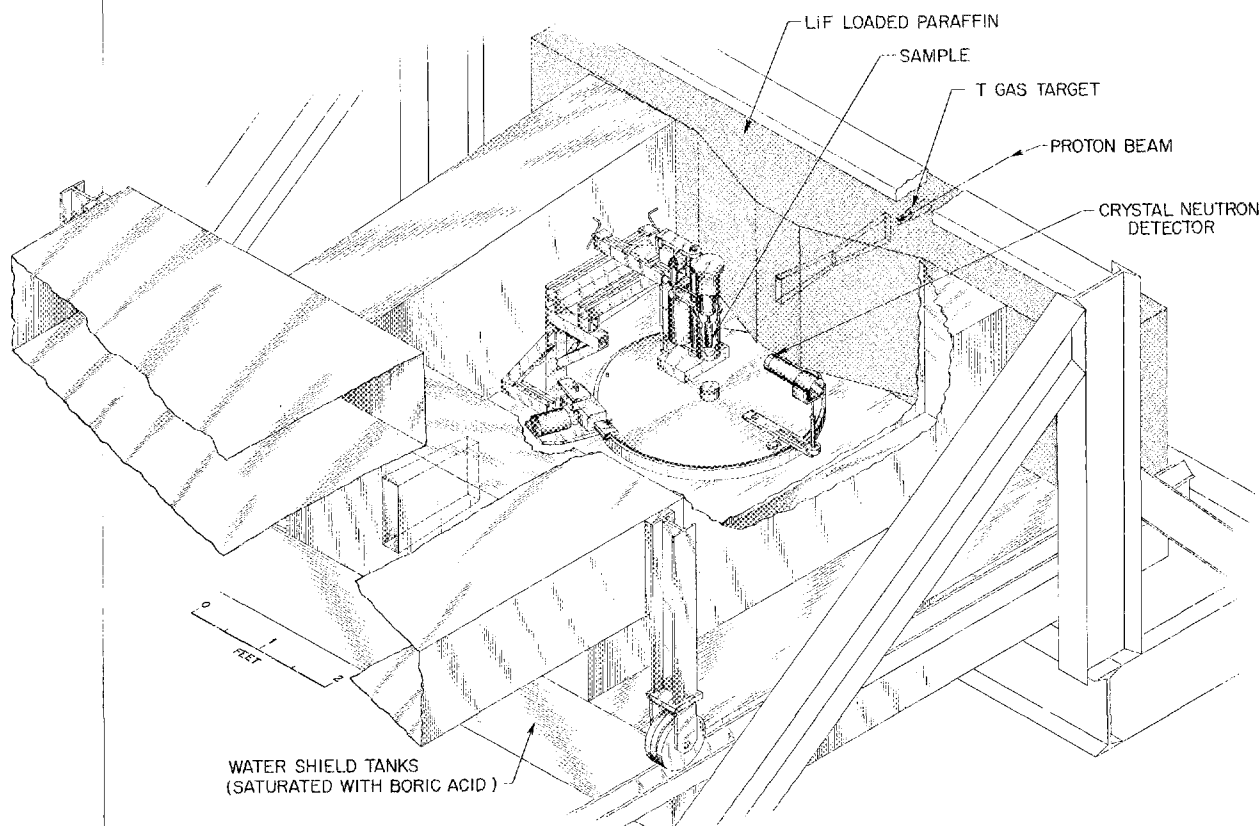


Fig. 1. Apparatus for Measuring the Scattering of Neutrons from Liquid Oxygen.

flask was rotated into the neutron beam to evaluate background. We detected T(p,n) neutrons scattered from the sample with a stilbene crystal from which pulses due to gamma rays are depressed by pulse-shape discrimination. Both the stilbene crystal and the sample can be rotated by remote control, and their position can be noted in the control room. Since we calibrated the neutron detector in the 0° neutron beam with the sample out, the measurements allowed us to calculate absolute cross sections.

Figure 2 shows our results together with data of others up to 3.55 Mev. Our data have been corrected for multiple scattering and angular resolution. The solid line through the points is the result of a least-squares phase-shift fit to the data, with the phase shifts which give the fit shown on the left-hand side. We took a FORTRAN code,² written to compute differential cross sections for neutron scattering from 0-spin nuclei

²J. L. Fowler, J. Agnew, and M. J. Mader, *Bull. Am. Phys. Soc.* **8**, 549 (1963).

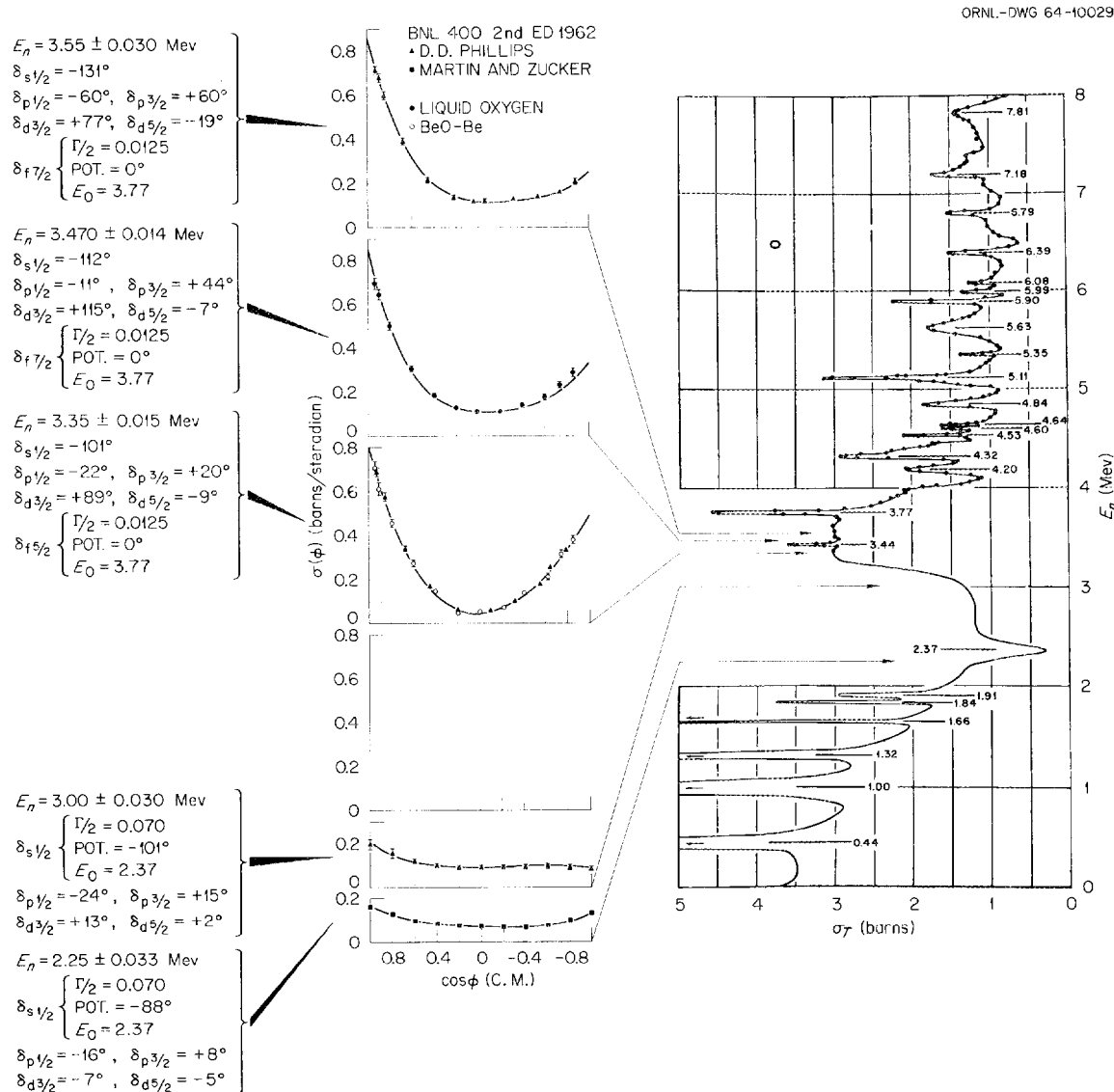


Fig. 2. Center-of-Mass Differential Cross Sections for Scattering of 2.25- to 3.55-Mev Neutrons from Oxygen.

as a function of phase shifts, and incorporated it into a search routine to obtain a fit to the experimental data. The resulting combined code, which averages the theoretical curves over the energy spread of the experimental measurements, uses matrix operations to adjust several phase shifts simultaneously in order to arrive at a minimum in the sum of the weighted square of the deviations between experimental points and

theoretical values. The 3.55-Mev curve illustrates a difficulty of phase-shift analysis. Another set of phase shifts appear in Fig. 4 and give practically an identical fit but are much more consistent with the neighboring phase shifts.

Figure 3 shows an extension of the data to 3.77 Mev. As can be seen by taking the 3.77-Mev resonance as $f_{5/2}$ and allowing for a $d_{5/2}$ potential phase shift, we get an excellent fit to the data.

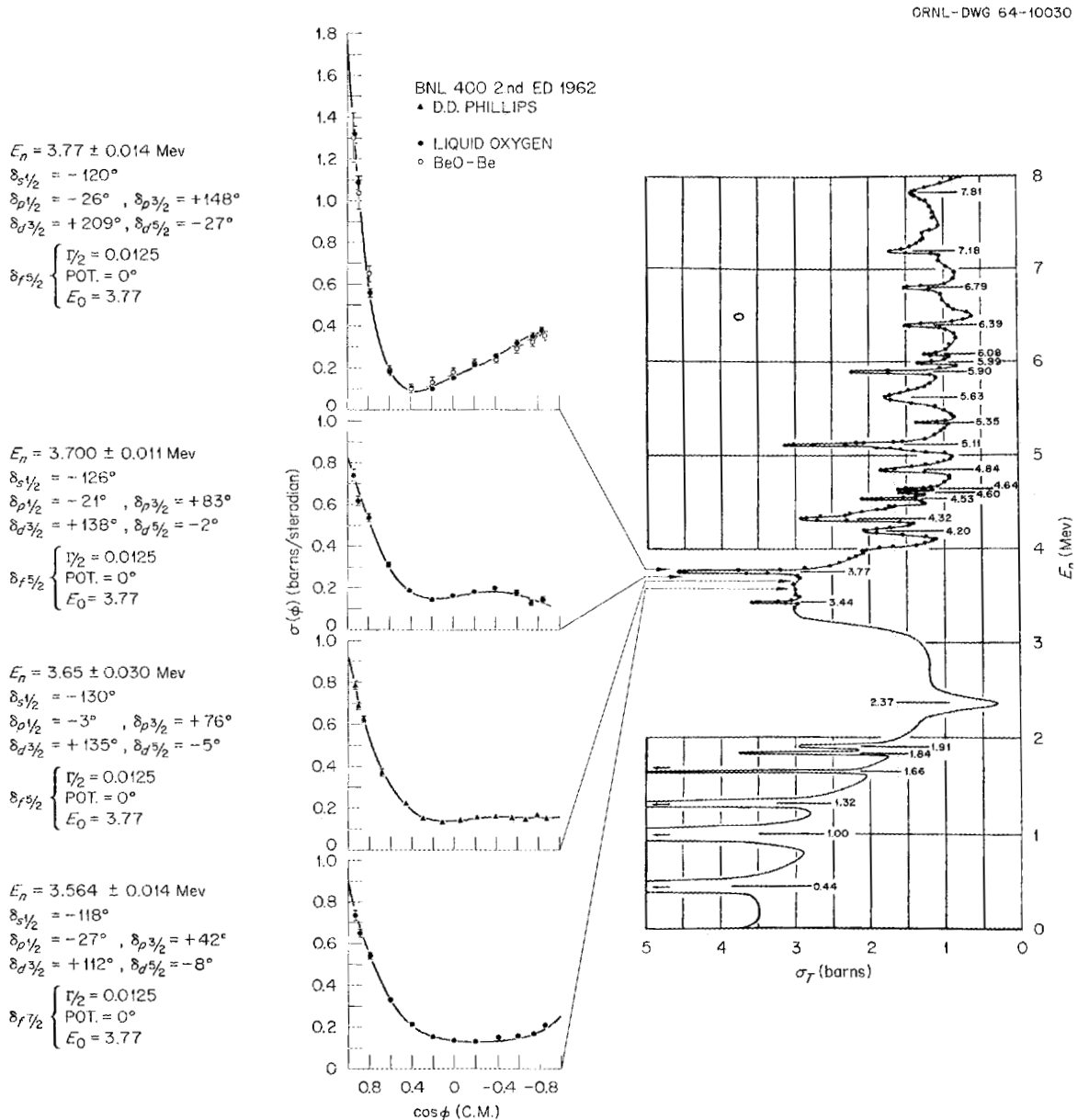


Fig. 3. Center-of-Mass Differential Cross Sections for Scattering of 3.564- to 3.77-Mev Neutrons from Oxygen.

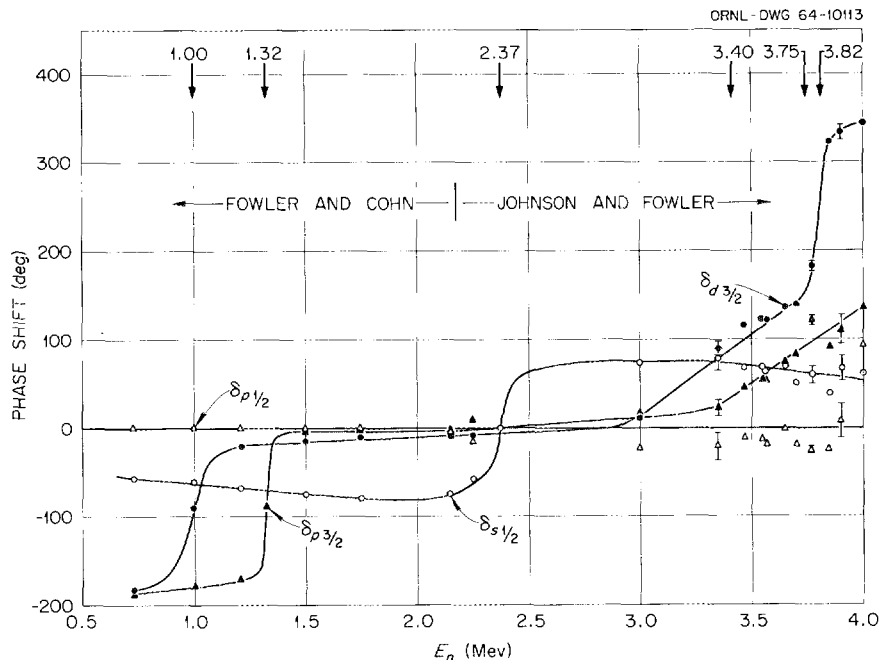


Fig. 4. Results of Phase-Shift Analysis of Differential Scattering of Neutrons from ^{16}O .

Since ^{16}O proton scattering data have a resonance corresponding to an $f_{7/2}$ level at about this excitation energy in the mirror nucleus,³ we have recently measured the total neutron cross section of ^{16}O in this energy region with 5-keV resolution. We find the 3.77-MeV resonance is indeed a $5/2$ resonance in agreement with the results of Fossan *et al.*,⁴ but we obtained a width of 20 keV, slightly less than the 22-keV⁵ and the 25-keV⁴ widths reported in the literature for this resonance.

Figure 4 shows the phase shifts as a function of neutron energy and includes results at lower energy from a previous analysis.⁶ For an estimate of the uncertainties in these phase shifts,⁷ we take cross-section values from a theoretical curve given by the set of phase shifts shown on the left of the figure and alter these values by errors selected in a random fashion but with the same standard deviation as the experimental errors.

Thus we obtain a set of points to be fitted with the original code. We repeat this procedure a number of times and calculate the standard deviation of the resulting phase shifts. At 3 MeV the uncertainties in the phase shifts range from 1.5 to 3.0° . Other typical phase-shift uncertainties are shown.

This analysis shows a $d_{3/2}$ resonance at 3.40 MeV approximately 500 keV wide, another $d_{3/2}$ resonance at 3.82 MeV 50 keV wide, and a $p_{3/2}$ resonance at 3.75 MeV about 500 keV wide. The broad $d_{3/2}$ resonance corresponds to $\sim 1/2$ of the single-particle limit. There is, of course, already a $d_{3/2}$ resonance with a very large fraction of the single-particle limit at 1 MeV. The $p_{3/2}$ resonance at 3.75 MeV is about $1/5$ of the single-particle limit, and the $f_{5/2}$ resonance at 3.77 MeV is about $1/10$ of this limit.

³S. R. Salisbury and H. T. Richards, *Phys. Rev.* **126**, 2147 (1962).

⁴D. B. Fossan *et al.*, *Phys. Rev.* **123**, 209 (1961).

⁵R. B. Walton, J. D. Clement, and F. Borelli, *Phys. Rev.* **107**, 1065 (1957).

⁶J. L. Fowler and H. O. Cohn, *Phys. Rev.* **109**, 89 (1958).

⁷S. T. Thornton, C. H. Johnson, and J. L. Fowler, *Bull. Southeastern Sect. Am. Phys. Soc.* (1964).

RESONANCE PARAMETERS FOR NEUTRON SCATTERING FROM ^{208}Pb

J. L. Fowler

NUCLEAR REACTIONS. $^{208}\text{Pb}(n)$, enriched target, $E_n = 0.7\text{--}1.9$ Mev; measured $\sigma(E, \theta)$. ^{209}Pb , deduced resonance parameters, phase shifts.

The resonance states observed by scattering neutrons from ^{208}Pb , as shown in Fig. 1, were among the first to be compared with theoretical expectations for intermediate states.¹ Here is plotted the total cross section of ^{208}Pb as measured with ~ 3 -keV energy resolution.² Of the some 85 resonances that occur between 0.7 and 1.9 MeV, about one-third are sufficiently isolated and are resolved so that one can assign values of total angular momentum. Shakin, in 1963, compared the widths of the $J = \frac{1}{2}$ resonances at 1.204, 1.318, 1.354, 1.632, 1.715, and 1.872 with the widths he had calculated for $\frac{1}{2}^+$ resonances under the assumption that these arise from two-particle-one-hole excitations of ^{209}Pb . He found order of magnitude agreement. Of course, from total cross section data, one in general only deduces J values. Angular distributions are necessary to assign l values and parities. Accordingly, the angular distributions of scattered neutrons have been measured at most of the prominent isolated resonances up to 1.76 MeV.³

Before each angular distribution measurement, the resonances had to be relocated. Figure 1 in the previous paper shows a drawing of the shielded region in which the neutron scattering experiment was carried out. Neutrons were produced by the $\text{Li}(p,n)$ reaction in a thin evaporated lithium target instead of the $\text{T}(p,n)$ gas cell indicated in the figure. The stilbene crystal rotated to 0° served as the neutron detector for measuring the transmission of a 72% ^{208}Pb sample located between the source and the front of the paraffin shield. This gave the peak of the resonance. For the angular distributions, the 72% sample was removed and a separated 99.75% ^{208}Pb cylinder was supported in the center of the shielded scattering region. Neutrons were detected at various angles with the stilbene crystal, from which gamma-ray

pulses were suppressed by pulse-shape discrimination. Since the neutron flux incident upon the sample was detected with the stilbene crystal rotated to 0° , the differential cross sections are absolute.

Figure 2 shows a set of differential cross sections plotted as a function of the center-of-mass angle. The data have been corrected for the effects of angular resolution, multiple scattering, and the second group of neutrons from the $\text{Li}(p,n)$ reaction. The arrows indicate the energy positions at which measurements were made as they are related to the total cross section plotted on the right-hand side.

A set of measurements made at the beginning of this experiment at 1.646 MeV is shown as open points. Another run at this energy made months later at the end of the experiment is shown as the closed points. There is agreement within the accuracy of the measurements. The phase shifts and resonance parameters listed beside each curve yield the solid curves. These result from a least-squares fit to the experimental points.⁴ One starts with a set of trial phase shifts extrapolated from lower energies. These phase shifts were adjusted by a nonlinear least-squares fitting code, which averages the Breit-Wigner resonance over the energy spread of the measurements to give the fits as shown. In this energy region, one sees a $d_{3/2}$ resonance at 1.600 MeV and a $p_{3/2}$ resonance at 1.620 MeV. The peak at 1.632 MeV is a $p_{1/2}$ resonance. One looks for a least-squares fit which, within the fitting errors, gives the non-resonant phase shifts as a satisfactory extrapolation from the values at lower energies.

Figure 3 shows the results up to 1.761 MeV. This covers the highest-angular-momentum resonances observed up to 1.9 MeV: $J = \frac{7}{2}$ at 1.749 and 1.761 MeV. These turn out to be both $f_{7/2}$ resonances. Attempts to fit them (particularly the 1.761-MeV peak) as $g_{7/2}$ resonances were without

¹Carl Shakin, *Ann. Phys.* **22**, 373 (1963).

²J. L. Fowler and E. C. Campbell, *Phys. Rev.* **127**, 2192 (1962).

³J. L. Fowler, *Bull. Am. Phys. Soc.* **10**, 12 (1965).

⁴J. L. Fowler, John Agnew, and Mary J. Mader, *Bull. Am. Phys. Soc.* **8**, 549 (1963).

ORNL-LR-DWG 64862R3

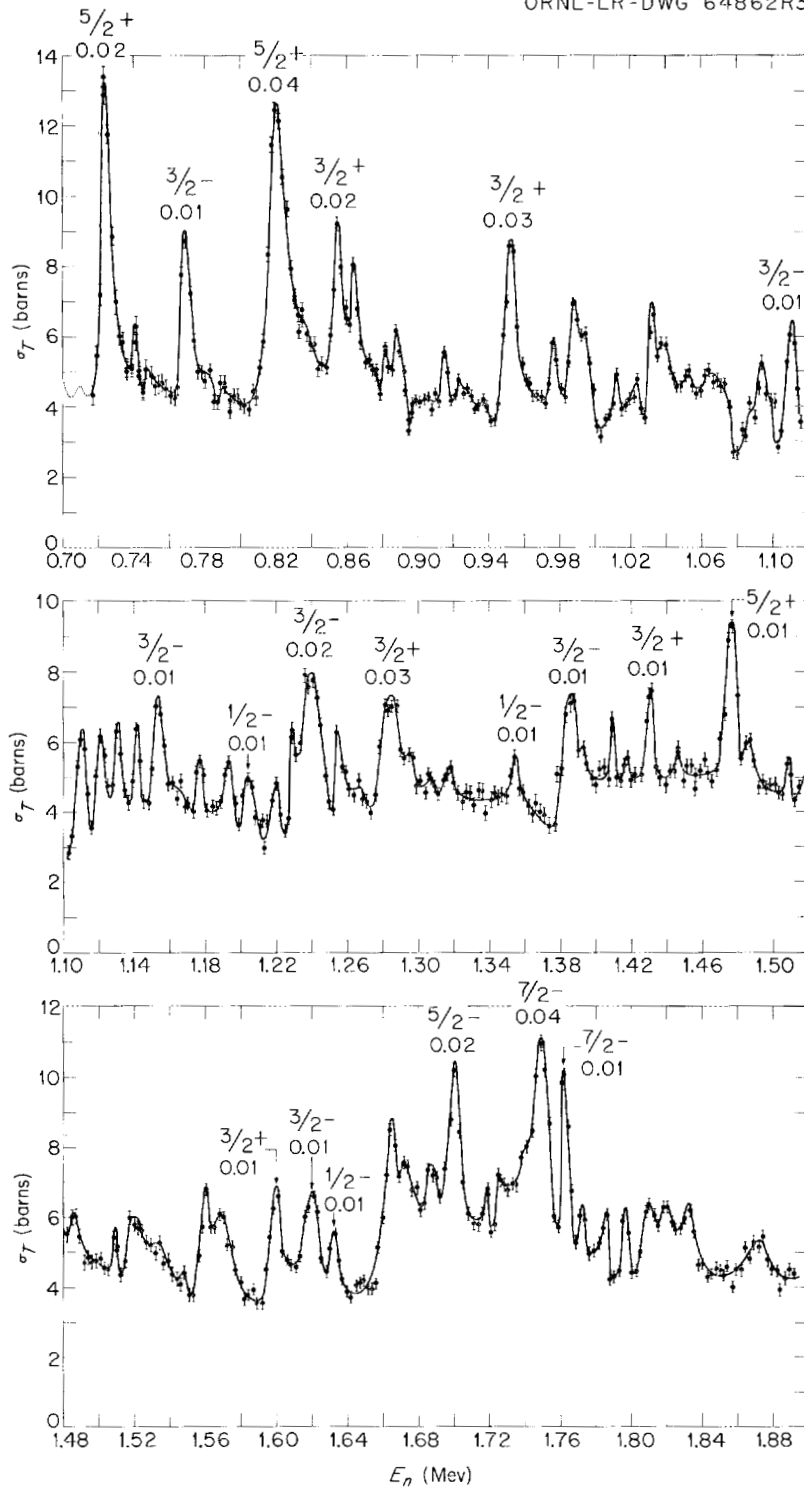


Fig. 1. Total Cross Section of ^{208}Pb with 3-keV Resolution. Listed above prominent isolated resonances are the J -value, parity, and fraction of single particle width.

success. The difference in their appearance arises from the rapidly changing $s_{1/2}$ phase shift, which is going through a resonance in this region. This indicates the broad peak centered around 1.72 Mev is an $s_{1/2}$ resonance. At 1.701 Mev there is an $f_{5/2}$ resonance.

Figure 1 also summarizes the parity assignments. The numbers over the prominent isolated resonances give the J value, parity, and reduced widths in single-particle units. There is only one $s_{1/2}$ resonance in this region— at 1.715 Mev — to be compared with Shakin's calculations of widths of one-hole-two-particle states. There is, however,

an $s_{1/2}$ resonance of $\sim 5\%$ of the single-particle width at 500 kev. There are a number of odd-parity resonances including three f resonances with rather large reduced widths. Since most of the shell-model hole states have odd parity and most of the particles states have even parity, "Doorway" states, that is, one-hole-two-particle states, of odd parities should be plentiful. Also, the coupling of particle states with the 3^- collective state of the ^{208}Pb core would lead to odd-parity states. The spectrum of ^{208}Pb plus a neutron shows a number of candidates for intermediate states.

ORNL-DWG 63-1448R

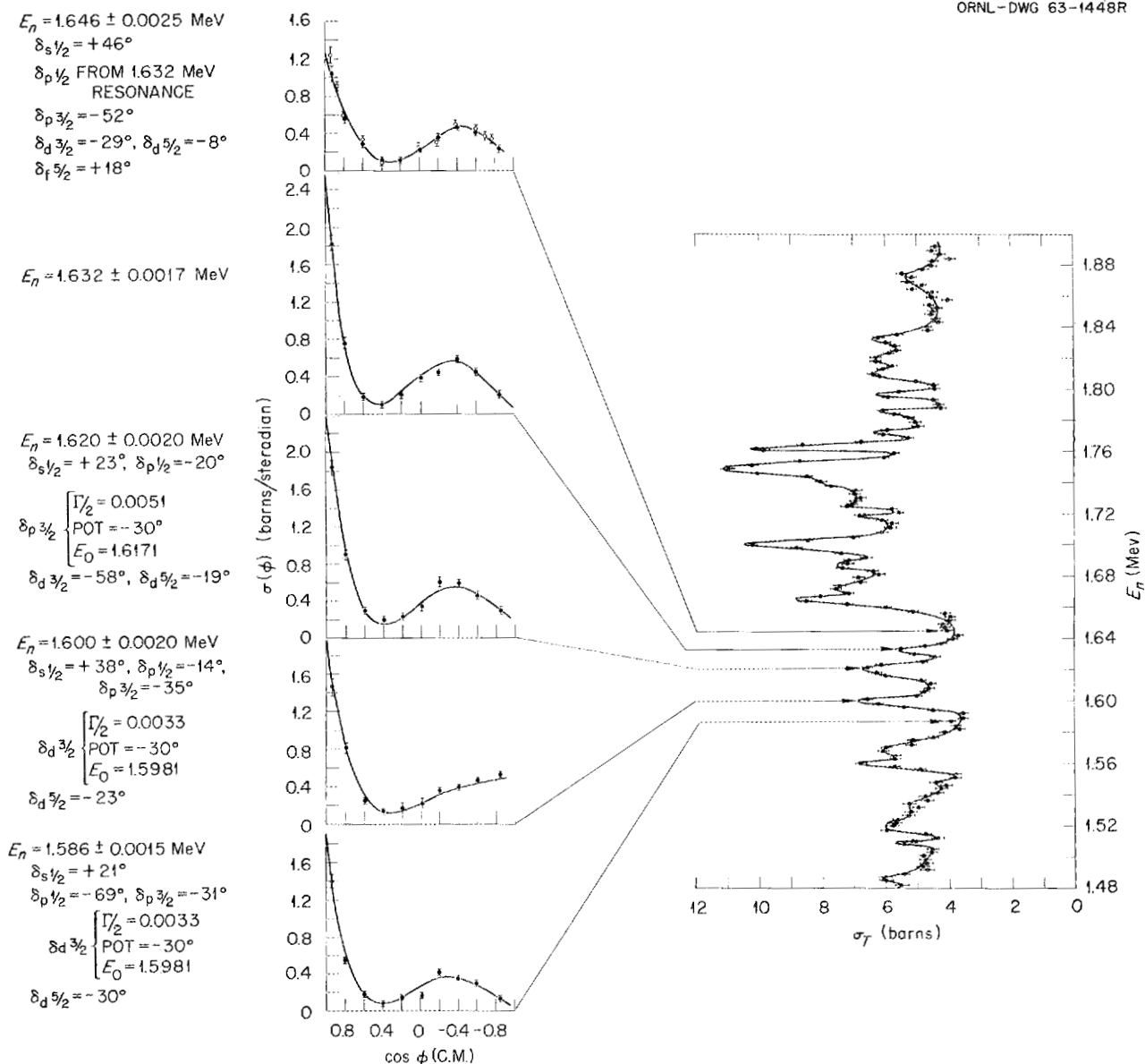


Fig. 2. Differential Cross Sections of ^{208}Pb Neutron Scattering in Center-of-Mass System from 1.586 to 1.646 Mev.

$E_n = 1.761 \pm 0.0013$ MeV
 $\delta_s 1/2 = +151^\circ$
 $\delta_p 1/2 = -37^\circ$; $\delta_p 3/2 = -34^\circ$
 $\delta_d 3/2 = +7^\circ$; $\delta_d 5/2 = -40^\circ$
 $\delta_f 5/2 = -7^\circ$

$\delta_f 7/2 \left\{ \begin{array}{l} \Gamma_{1/2} = 0.0022 \\ \text{POT} = -24^\circ \\ E_0 = 1.760 \end{array} \right.$

$E_n = 1.749 \pm 0.0018$ MeV
 $\delta_s 1/2 = +79^\circ$
 $\delta_p 1/2 = -58^\circ$; $\delta_p 3/2 = -24^\circ$
 $\delta_d 3/2 = +13^\circ$; $\delta_d 5/2 = -38^\circ$
 $\delta_f 5/2 = -9^\circ$

$\delta_f 7/2 \left\{ \begin{array}{l} \Gamma_{1/2} = 0.0053 \\ \text{POT} = +10^\circ \\ E_0 = 1.7499 \end{array} \right.$

$E_n = 1.701 \pm 0.0016$ MeV
 $\delta_s 1/2 = +56^\circ$
 $\delta_p 1/2 = +10^\circ$; $\delta_p 3/2 = -40^\circ$
 $\delta_d 3/2 = -64^\circ$; $\delta_d 5/2 = +11^\circ$

$\delta_f 5/2 \left\{ \begin{array}{l} \Gamma_{1/2} = 0.0033 \\ \text{POT} = 0^\circ \\ E_0 = 1.701 \end{array} \right.$

$\delta_f 7/2 = +10^\circ$

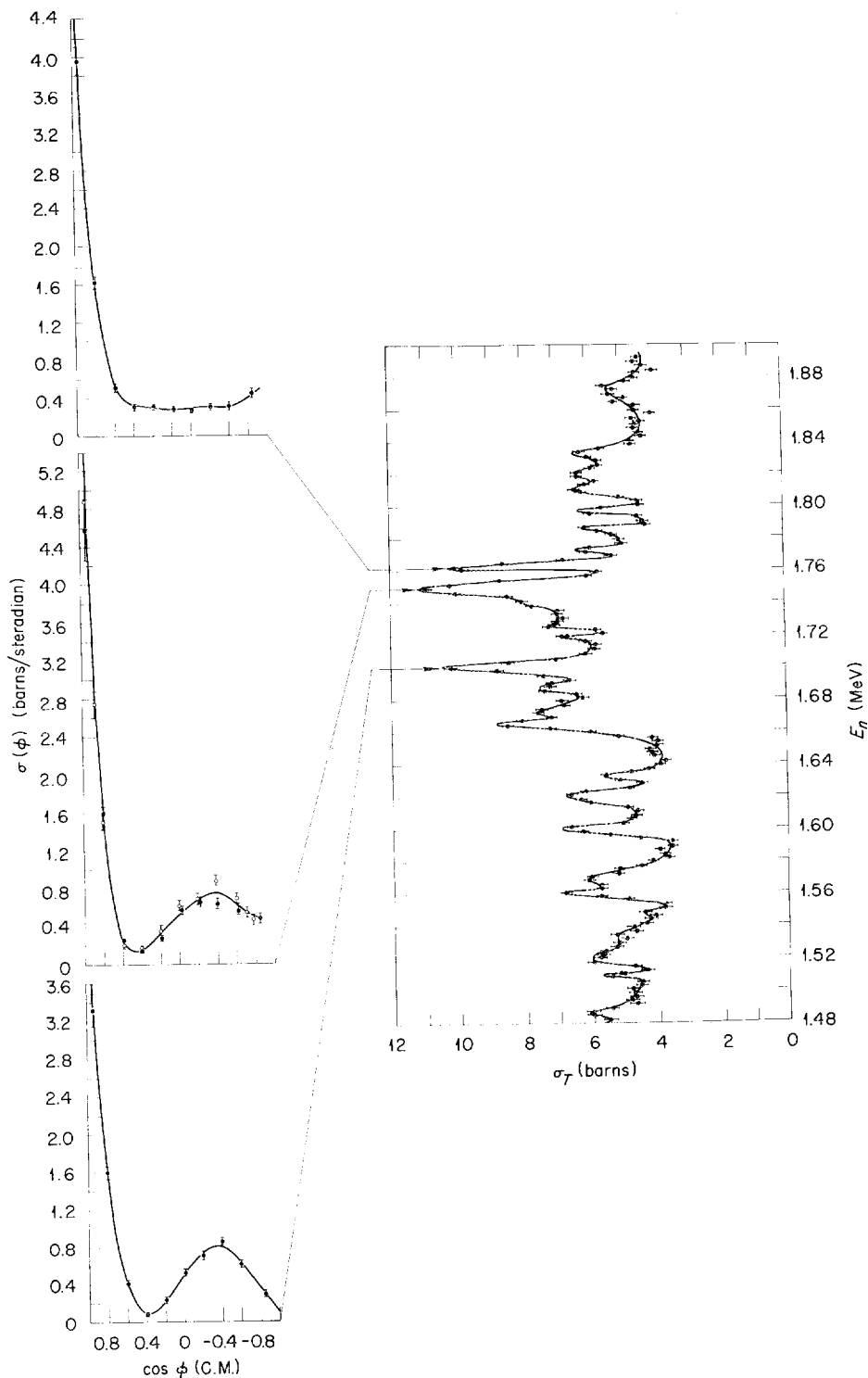


Fig. 3. Differential Cross Sections of ^{208}Pb Neutron Scattering in Center-of-Mass System from 1.701 to 1.761 Mev.

EXCITATION OF COLLECTIVE STATES BY THE INELASTIC SCATTERING OF 14-Mev NEUTRONS¹

P. H. Stelson R. L. Robinson H. J. Kim
J. Rapaport² G. R. Satchler

NUCLEAR REACTIONS. (n, n) , (n, n') ; Bi, Pb, Sb, Sn, Cd, Zn, Ni, Cr, S, P, Si, Al, Mg; $E_n = 14$ Mev, absolute $\sigma(\theta)$, β_2 , β_3 .

Differential cross sections for the inelastic scattering of 14-Mev neutrons to low-lying collective states have been measured for the 13 elements Bi, Pb, Sb, Sn, Cd, Zn, Ni, Cr, S, P, Si, Al, and Mg. The inelastically scattered neutrons were separated from the elastically scattered neutrons by a time-of-flight system which had an energy resolution of 450 keV for

14-Mev neutrons. The absolute cross sections were determined to an accuracy of 20% over the angular range 20 to 130°. The cross sections obtained for excitation of collective quadrupole and octupole states are compared to the distorted-wave theory for direct interactions. It is found that the experimental shapes of the differential cross sections are in reasonable agreement in most cases with those predicted by theory. The nuclear deformation parameters, β_λ , are extracted, and these are compared both to the available electromagnetic β_λ values and to β_λ values obtained from other direct-interaction experiments.

¹Abstract of paper submitted for publication in *Nuclear Physics*.

²Present address: Instituto de Ciencias, Universidad de Chile.

ELASTIC SCATTERING OF 17- TO 21-Mev NEUTRONS FROM ¹²C¹

M. V. Harlow, Jr.² R. L. Robinson B. B. Kinsey³

NUCLEAR REACTIONS. ¹²C(n, n), $E_n = 17-21$ Mev; measured $\sigma_T(E)$, $\sigma(E, \theta)$. ¹³C, deduced level.

A search for a resonance in the yield of elastically scattered 17- to 21-Mev neutrons from ¹²C has been made. The differential cross section has been measured for laboratory angles of 36, 51, 60, 86, 123.5, and 139°. The total cross section was also measured for the same range of neutron energies. In the differential cross sections which were measured at 36, 51, and 60°, a broad peak was present at a laboratory neutron energy of $19.5 \pm$

0.2 Mev. Its total width at half maximum was approximately 1.1 Mev and its height was between 14 and 21% of the value of the continuum. Within the 4.5% statistical error of our measurements, the peak does not appear at 86°. At 123.5 and 139°, the cross section decreases monotonically by a factor of 3 between 17.5 and 20.5 Mev. The total-cross-section data, which exhibit a weak resonance at 19.6 ± 0.2 Mev having a total width at half maximum of about 1.2 Mev, are consistent with the differential-cross-section results. The resonance, which presumably results from a state or states in the compound nucleus ¹³C, appears similar to the known resonance in the yield of elastically scattered 22.5-Mev protons from ¹²C.

¹Abstract of paper submitted for publication in *Nuclear Physics*.

²Present address: Rutherford Laboratory, Harwell, England.

³University of Texas, Austin.

**TOTAL NEUTRON CROSS SECTIONS OF HYDROGEN AND CARBON IN THE
20–30 Mev REGION**

M. L. West II¹

C. M. Jones

H. B. Willard

NUCLEAR REACTIONS. ${}^1\text{H}(n, n)$, ${}^{12}\text{C}(n, n)$, polyethylene and graphite samples, $E_n =$
19.58–30.46 Mev, measured $\sigma_t(E)$.

Precise n - p scattering and polarization measurements in the 0–42 Mev region are needed as an aid to theoretical interpretation of the nucleon-nucleon interaction, since theoretical fits to the present data are not sufficient to describe unambiguously the interaction. Measurements of the n - p differential scattering cross section in the 20–30 Mev region are now in progress at this Laboratory. The total n - p cross section has been measured and will be used to normalize the n - p angular distributions.

The transmissions of polyethylene and carbon were measured to determine their respective total cross sections, and a difference technique was used to extract the hydrogen cross section. Neutrons of the desired energy were produced by bombarding a tritium-zirconium target with deuterons from the ORNL 5.5-Mv Van de Graaff and Tandem accelerators. The deuteron energy calibration was obtained relative to the ${}^7\text{Li}(p, n){}^7\text{Be}$ threshold on the 5.5-Mv accelerator and relative to the ${}^{27}\text{Al}(p, n){}^{27}\text{Si}$ threshold on the Tandem accelerator.

The polyethylene sample was chemically analyzed at ORNL and found to have a hydrogen-to-carbon ratio of $(2.038 \pm 0.020):1$ with no significant impurities. The carbon sample was fabricated from CGB-grade graphite. This is an experimental-grade graphite and is specified to be 99.98% pure. The scatterers were checked by x-ray photography to ensure the absence of voids and other inhomogeneities. These samples were machined in the shape of right cylinders with a diameter of 1 in. Sample length and density were measured to within 0.1%.

Stilbene scintillators served for both the neutron monitor and detector. The detector was located at 0° and 25 in. from the target. Backgrounds measured with zirconium blank were always less than 0.5%, while the background from room scattering was less than 0.6% for all runs. The geometry of this experiment was chosen so that sample alignment was not critical. In all cases corrections for in-scattering were less than 2%.

Preliminary results are presented in Table 1. Corrections have been made for background and in-scattering effects. Neutron energies are known to better than 0.2%. The probable errors have been increased from the statistical error to include estimated maximum values of systematic errors. More exact calculations of these errors and corrections are in progress.

Table 1. The Total Neutron Cross Sections of
Hydrogen and Carbon

E (Mev)	Hydrogen (barns)	Carbon (barns)
19.58	0.498 ± 0.012	1.51 ± 0.04
20.81	0.467 ± 0.012	1.43 ± 0.04
21.93	0.432 ± 0.011	1.34 ± 0.03
26.32	0.329 ± 0.012	1.32 ± 0.05
30.46	0.287 ± 0.011	1.32 ± 0.05

¹Oak Ridge Graduate Fellow from the University of Texas, Austin.

A STUDY OF FLUCTUATING LOW-ENERGY (p,n) REACTION CROSS SECTION¹

H. J. Kim

NUCLEAR REACTIONS. $^{53}\text{Cr}(p,n)^{53}\text{Mn}$, $2.3 < E < 3.1$ Mev, measured $\sigma(E_n)$.

The fluctuations in $^{53}\text{Cr}(p,n)^{53}\text{Mn}$ reaction cross sections were investigated for the incident energy ranges 2.3–2.6 Mev and 2.8–3.1 Mev. The excitation function of the total neutron yield measured with 1-kev energy steps by using a thin target ($30 \mu\text{g}/\text{cm}^2$), the flat-response graphite ball neutron detector, and the 5-Mv Van de Graaff shows very rapid fluctuations of the yields with energy. Besides these fluctuations, no visible systematic energy dependence of the yields is seen within the above energy ranges. Assuming the (p,n) reaction cross section to represent the entire compound-nucleus cross section (i.e., $\Gamma_n \approx \Gamma_{\text{total}}$) and ignoring possible systematic energy dependence of the cross section, the fluctuations are analyzed in terms of the fluctuations of the proton reduced width and the reso-

nance spacing.² The interval cross sections $\alpha(w)$'s, where

$$\alpha(w) = \int_{E-(w/2)}^{E+(w/2)} \sigma_{p,n} dE',$$

have a χ^2 probability distribution, and the probability distribution approaches that of a normal distribution as the internal w increases. The variances of $\alpha(w)$'s are linearly dependent on $1/w$, and this linear dependence implies that the $\alpha(w)$'s are members of a statistical distribution. The information concerning the parameters of the probability distributions of the proton width and the spacing are extracted from the statistical nature of $\alpha(w)$'s.

¹Abstract of published paper: *Phys. Letters* 14, 51 (1965).

²A. M. Lane and J. E. Lynn, AERE-TR-2210 (1957).

CROSS SECTIONS FOR (p,n) REACTIONS IN FIVE ISOTOPES OF TIN

R. L. Kernell¹

C. H. Johnson

NUCLEAR REACTIONS. $^{117}\text{Sn}(p,n)$, $^{119}\text{Sn}(p,n)$, $^{120}\text{Sn}(p,n)$, $^{122}\text{Sn}(p,n)$, $^{124}\text{Sn}(p,n)$,
 $E = 2.5\text{--}5.5$ Mev; measured $\sigma(E)$, Q . Enriched targets.

This report is an extension of (p,n) cross-section measurements initiated to investigate proton strength functions, isotope effects on cross sections, and (p,n) thresholds.² Protons that were accelerated by a Van de Graaff to energies

in the range 2.5 to 5.5 Mev impinged on the target. Neutrons resulting from (p,n) reactions were counted by a 4π flat-response graphite-sphere detector.³

Thin targets were prepared by evaporating isotopically enriched samples onto 10-mil platinum backings. Table 1 lists the five isotopes,

¹Graduate student, University of Tennessee.

²C. H. Johnson, A. Galonsky, and C. N. Inskeep, *Phys. Div. Ann. Progr. Rept. Mar. 25, 1960*, ORNL-2910, p. 25.

³R. L. Macklin, *Nucl. Instr.* 1, 335 (1957).

Table 1. Properties of Targets

Target Nucleus	Abundance (at. %)	Target Thickness at 3 Mev (kev)
^{117}Sn	85.4	265
^{119}Sn	89.8	188
^{120}Sn	98.39	205
^{122}Sn	90.8	196
^{124}Sn	92.8	173

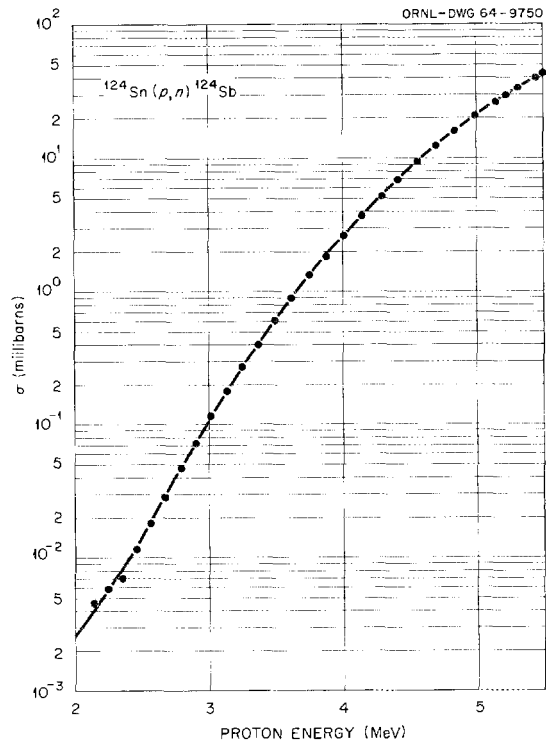
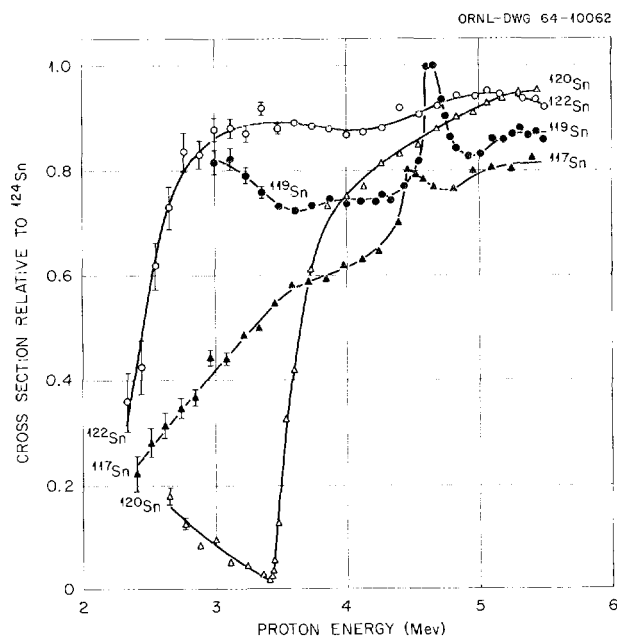
their percentage abundances in the targets, and the target thicknesses at 3 Mev. Target thicknesses were chosen to be many times the level spacings in the compound nuclei but considerably less than the range of proton energies used in the investigation. Hence the observed neutron yields are averaged over resonances.

Figure 1 shows the cross section for ^{124}Sn , the heaviest of the five isotopes studied. The cross section increases from a few thousandths of a millibarn near 2 Mev to 42 mb at 5.5 Mev. Using values of the ^{124}Sn cross section read from the smooth curve shown in Fig. 1, the cross sections of the other isotopes relative to ^{124}Sn were determined. The results are presented in Fig. 2. Values below approximately 3 Mev are uncertain because of relatively high yields from target contaminants. Further work is being conducted with new targets to obtain more accurate cross sections at the lower energies. The peaks at 4.5 Mev on the ^{117}Sn curve and at 4.6 Mev on the ^{119}Sn curve result from isobaric analog states in the compound nuclei. A detailed investigation of these resonances using thin (10 kev) targets is reported elsewhere in this report.⁴

The threshold for $^{120}\text{Sn}(p,n)^{120}\text{Sb}$ was determined to be 3494 ± 7 kev. This corresponds to $Q = -3465 \pm 7$ kev, in good agreement with the value $Q = -3462.9 \pm 7.1$ kev reported by Okano and Nishimura.⁵

⁴C. H. Johnson and R. L. Kernell, "Isobaric Analog States in ^{90}Zr , ^{116}Sb , ^{118}Sb , and ^{120}Sb ."

⁵K. Okano and K. Nishimura, *J. Phys. Soc. Japan* 18, 1563 (1963).

Fig. 1. Cross Sections for the (p,n) Reaction in ^{124}Sn .Fig. 2. Cross Sections for the (p,n) Reaction in ^{117}Sn , ^{119}Sn , ^{120}Sn , and ^{122}Sn Relative to the $^{124}\text{Sn}(p,n)^{124}\text{Sb}$ Cross Section.

An attempt has been made to relate the experimental (p,n) cross section to that predicted by an optical model. Since the protons have energies considerably below the Coulomb barrier for tin, the (p,n) cross section is expected to be essentially equal to the cross section for formation of the compound nucleus. The latter was calculated

using the optical-model parameters of Perey.⁶ A preliminary analysis indicates that the observed cross sections show a larger increase with atomic number than is predicted by the optical model based on these parameters.

⁶F. G. Perey, *Phys. Rev.* **131**, 745 (1963).

ISOBARIC ANALOG STATES IN ^{90}Zr , ^{116}Sb , ^{118}Sb , and ^{120}Sb

C. H. Johnson

R. L. Kernell¹

NUCLEAR REACTIONS. $^{89}\text{Y}(p,n)$, $^{115}\text{Sn}(p,n)$, $^{117}\text{Sn}(p,n)$, $^{119}\text{Sn}(p,n)$, $E = 3.6$ to 5.1 Mev; measured $\sigma(E)$, Q . ^{90}Zr , ^{116}Sb , ^{118}Sb , ^{120}Sb , deduced levels, J , Γ . Enriched targets.

Recently isobaric analog states have been discovered² in highly excited compound nuclei. If a target nucleus (N, Z) is bombarded by protons, the compound nucleus will have many normal states whose isobaric spin $T_0 = (N - Z)/2 - 1/2$ has the same magnitude as the z component. The isobaric analog states have $T = T_0 + 1$ and have large energy spacings similar to the low-lying levels formed with $T = T_0 + 1$ by the target nucleus plus a neutron. The Coulomb interaction of the proton with the rest of the nucleus is responsible for displacing the analog states to high excitations in the compound nucleus. The fact that resonances due to these states are observed not only in proton scattering but also in (p,n) reactions shows that they have impure isobaric spin, and the nature of this mixing with the normal states is of considerable interest. If the (p,n) reaction channel is open, both the scattering and reaction cross sections must be measured in order to determine the partial widths, including the mixing width.

This report is concerned with the measurement of total (p,n) reaction cross sections. Protons

from the 5.5-Mv Van de Graaff bombarded targets of separated isotopes which had been evaporated onto platinum blanks. Neutrons were detected with Macklin's³ flat-response 4π counter. Since measurements were restricted to the (p,n) reaction cross section, only the resonance energies and total widths can be extracted from the data; however, the shapes and peak heights of the resonances allow some further qualitative conclusions.

Figure 1 shows the cross section for $^{89}\text{Y}(p,n)^{89}\text{Zr}$. The smooth curve, labeled σ_c , is the compound-nucleus cross section calculated with Perey's⁴ optical-model parameters but normalized with a multiplicative factor of 0.48 in order to fit the observed (p,n) cross section in the smooth region near 4.9 Mev. The reason for the normalization is that the (p,n) cross section is expected⁵ to be nearly equal to σ_c providing that several neutron channels are open and that the proton energy is well below the top of the Coulomb barrier. It seems reasonable that minor adjustments in the

¹Graduate student, University of Tennessee.

²J. D. Fox, C. F. Moore, and D. Robson, *Phys. Rev. Letters* **12**, 198 (1964).

³R. L. Macklin, *Nucl. Instr.* **1**, 335 (1957).

⁴F. G. Perey, *Phys. Rev.* **131**, 745 (1963).

⁵C. H. Johnson, A. Galonsky, and J. P. Ulrich, *Phys. Rev.* **109**, 1243 (1958).

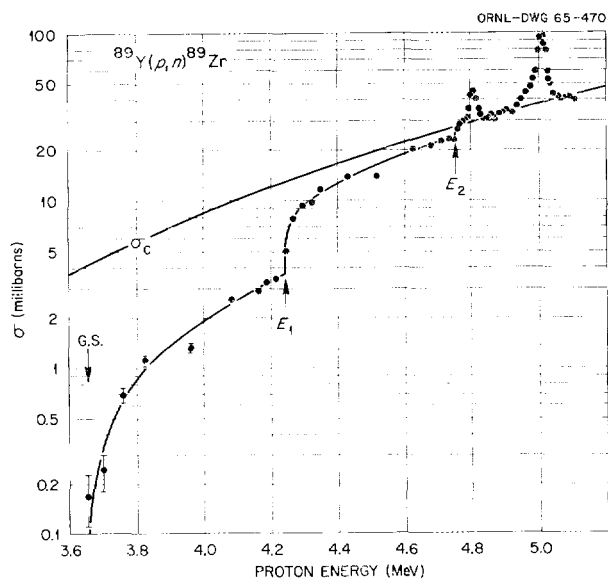


Fig. 1. The $^{89}\text{Y}(p,n)^{89}\text{Zr}$ Cross Section Measured with a Target Which was 6 kev thick at 5 Mev. Thresholds indicated at G.S., E_1 , and E_2 correspond to neutron emission to the ground state and to the first two excited states of ^{89}Zr . The curve labeled σ_c is the compound-nucleus cross section calculated with an optical model and normalized to fit the data near 4.9 Mev.

model parameters can account for the required normalization.

The three thresholds in Fig. 1 are of interest apart from the main topic on analog states. Thresholds G.S. and E_1 to the ground and first excited states of ^{89}Zr have appeared in the literature;^{6,7} however, the threshold E_2 at 4751 ± 7 kev has not been reported. Subtraction of the ground-state threshold⁷ results in an energy of 1084 ± 8 kev for the second excited state in ^{89}Zr . This agrees with other measurements^{8,9} by different methods. The shape of the excitation function near the thresholds is also of interest. The curve above G.S. and E_1 is qualitatively (and perhaps quantitatively) in agreement with Hauser-

⁶C. H. Johnson, C. C. Trail, and A. Galonsky, *Phys. Rev.* **136**, B1719 (1964).

⁷K. Okano and K. Nishimura, *J. Phys. Soc. Japan* **18**, 1563 (1963).

⁸D. B. Lightbody, G. E. Mitchell, and A. Sayres, *Bull. Am. Phys. Soc.* **9**, 651 (1964).

⁹C. D. Goodman *et al.*, *Electronuclear Div. Ann. Progr. Rept. Dec. 31, 1963*, ORNL-3630, p. 21.

Feshbach¹⁰ predictions for transitions to the $\frac{9}{2}^+$ ground state and $\frac{1}{2}^-$ excited state of ^{89}Zr . Now consider the conditions just below the E_2 threshold. All states formed by s - or p -wave protons can decay to the $\frac{1}{2}^-$ state by emission of s - or p -wave neutrons, and 3^- states formed by d -wave protons can decay by p -wave neutrons to the $\frac{9}{2}^+$ ground state. In each case the neutron transmission factors are much ~~less~~ ^{more} than the proton factors, so that the (p,n) cross sections for these channels are nearly equal to the compound-nucleus cross sections. However, 2^- states formed by d -wave protons can emit neutrons only if $l_n \geq 2$; hence the (p,n) cross section should be somewhat less than the compound-nucleus cross section. The fact that the E_2 threshold is observed indicates that just above the threshold, compound 2^- states can emit neutrons with $l_n < 2$. Goodman *et al.*⁹ found from the $^{90}\text{Zr}(p,d)^{89}\text{Zr}$ pickup angular distributions that the new state is either $\frac{1}{2}^-$ or $\frac{3}{2}^-$. If it were $\frac{1}{2}^-$ then a sharp rise in neutron yield would not be expected, but if it is $\frac{3}{2}^-$ a rise would result because 2^- states can decay with s -wave neutrons. The above arguments, based on the very fact that the threshold is observed, indicate that $\frac{3}{2}^-$ is the correct choice. Goodman *et al.*⁹ made theoretical arguments to show that $\frac{1}{2}^-$ is the correct assignment.

In Fig. 1 the resonances at 4804 ± 6 and 5007 ± 6 kev are the 2^- and 3^- analog states which Fox *et al.*² discovered. The shape of these resonances is shown more clearly in Fig. 2, which gives the ratio of the observed cross section to the normalized theoretical σ_c . This ratio has the effect of removing the energy dependence of the Coulomb penetrability and of the geometric factor $\pi\lambda^2$. A slightly better procedure near the resonances would be to use a particular proton partial wave for finding the energy dependence of the resonance ratio; however, since the penetrabilities for all partial waves have nearly the same energy dependence, the ratio shown is a good approximation. The resonances are each about 25 kev wide, considerably broader than the target thickness of 6 kev. Fox *et al.*² reported widths of about 10 kev, and the reason for this discrepancy is not clear. In Fig. 2 curves are shown for Lorentz shapes of the indicated widths averaged over the target thicknesses. Clearly the cross section

¹⁰W. Hauser and H. Feshbach, *Phys. Rev.* **87**, 366 (1952).

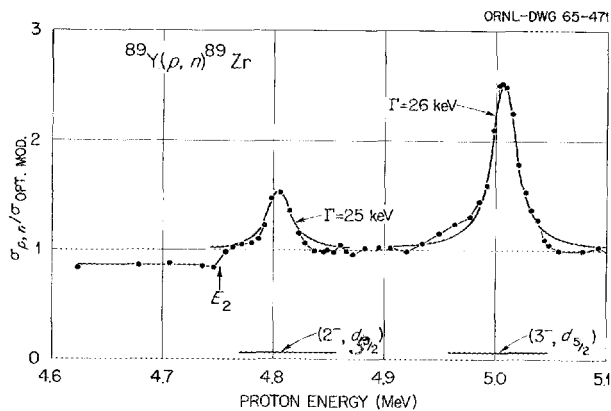


Fig. 2. The $^{89}\text{Y}(p,n)^{89}\text{Zr}$ Cross Section Plotted in a Manner Which Removes the Energy Dependence on Coulomb Penetrability and on $\pi\chi^2$. The ordinate is the ratio of the $^{89}\text{Y}(p,n)^{89}\text{Zr}$ reaction cross section to the cross section labeled σ_c in Fig. 1. The two resonances arise from a 2^- and a 3^- state which are isobaric analogs to low levels in ^{90}Y . Lorentz curves of the indicated widths have been averaged over the target thickness and plotted at the two resonances. In the lower part of the figure are indicated the energy cross sections predicted by the optical model for production of 2^- states by $d_{5/2}$ protons and for 3^- states by $d_{5/2}$ protons in the absence of the resonances.

does not follow the Lorentz shape, and this may be related to the fine structure observed¹¹ at other analog states in this mass region. In the lower part of the figure, below each resonance, are indicated the cross sections that are predicted by the optical model for the partial waves that give rise to the resonances. The resonances rise to 10 to 25 times this "background."

Figure 3 shows resonances in (p,n) reactions in the three odd isotopes of tin. The percentage isotopic abundances for ^{115}Sn , ^{117}Sn , and ^{119}Sn were 11.8, 89.2, and 89.8 respectively. Uncertainties in the cross sections are about $\pm 10\%$ for the two heavier isotopes but about $\pm 25\%$ for ^{115}Sn , which had such poor enrichment. The smooth curves are optical-model⁴ compound-nucleus cross sections normalized by multiplying by 0.70, 0.83, and 0.91 for isotopes 115, 117, and 119 respectively.

¹¹P. Richard *et al.*, *Phys. Rev. Letters* **13**, 343a (1964).

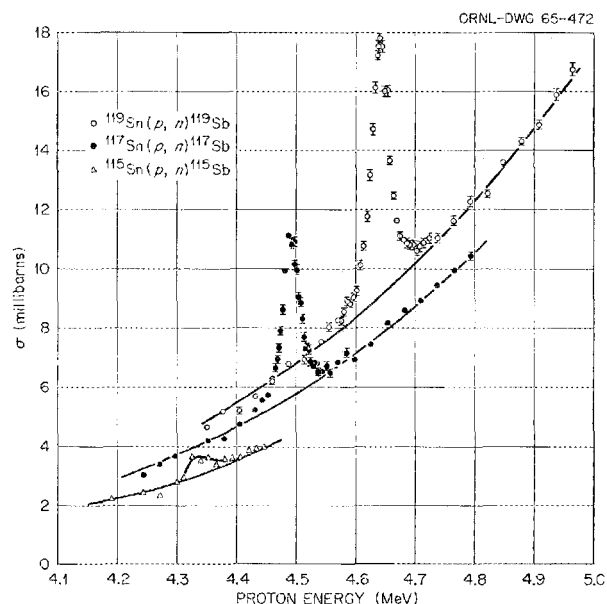


Fig. 3. The (p,n) Cross Sections for the Odd Isotopes of Tin. The target thicknesses were about 10 kev, somewhat narrower than the isobaric analog resonances. The smooth curves are compound-nucleus cross sections calculated from an optical model and normalized to fit the off-resonance cross sections.

Figure 4 gives the ratios of the (p,n) cross section to the normalized compound-nucleus values. As stated above, the plot of the ratios is convenient for studying the shapes of the resonances. The resonant energies for isotopes 115, 117, and 119 are 4330 ± 15 , 4491 ± 6 , and 4642 ± 6 kev respectively, and the corresponding Coulomb displacement energies based on recent¹² neutron separation energies are 13.862 ± 0.018 , 13.772 ± 0.015 , and 13.707 ± 0.015 Mev. These values are in agreement with (although they are about 2% lower than) those reported¹³ for the even isotopes. These energies indicate that the states are the 0^+ analogs to the ground states of ^{116}Sn , ^{118}Sn , and ^{120}Sn .

The resonances for ^{117}Sn and ^{119}Sn are each beautifully symmetric and somewhat broader than

¹²R. A. Damerow, R. R. Ries, and W. H. Johnson, Jr., *Phys. Rev.* **132**, 1673 (1963).

¹³J. A. Becker *et al.*, *Bull. Am. Phys. Soc.* **9**, 107 (1964).

the experimental 10-keV energy resolution. Curves of the Lorentz shape for $\Gamma = 30$ keV were averaged over the experimental resolution and plotted in the figure. The fact that the experimentally observed resonances have nearly a Lorentz shape indicates that the analog state is mixed with a large number of normal states. Off resonances, the ratios are nearly unity, which simply means that the calculated σ_c has about the right energy dependence and that the normalization factor was well chosen.

The lines labeled $(0^+, s_{1/2})$ in the lower part of the figure indicate the optical-model predictions

for forming the 0^+ state by s -wave protons in the absence of the resonance. If one considers the resonance to be of the giant-resonance type, then the s -wave proton strength function must increase by a factor of 40 to 60 at resonance.

Little can be said about the weak resonance in ^{115}Sn . The curve shown is simply an experimental one. The peak is only about 20% above background, and this is consistent with the fact that the neutrons emitted are probably d -wave with only 500 keV energy.

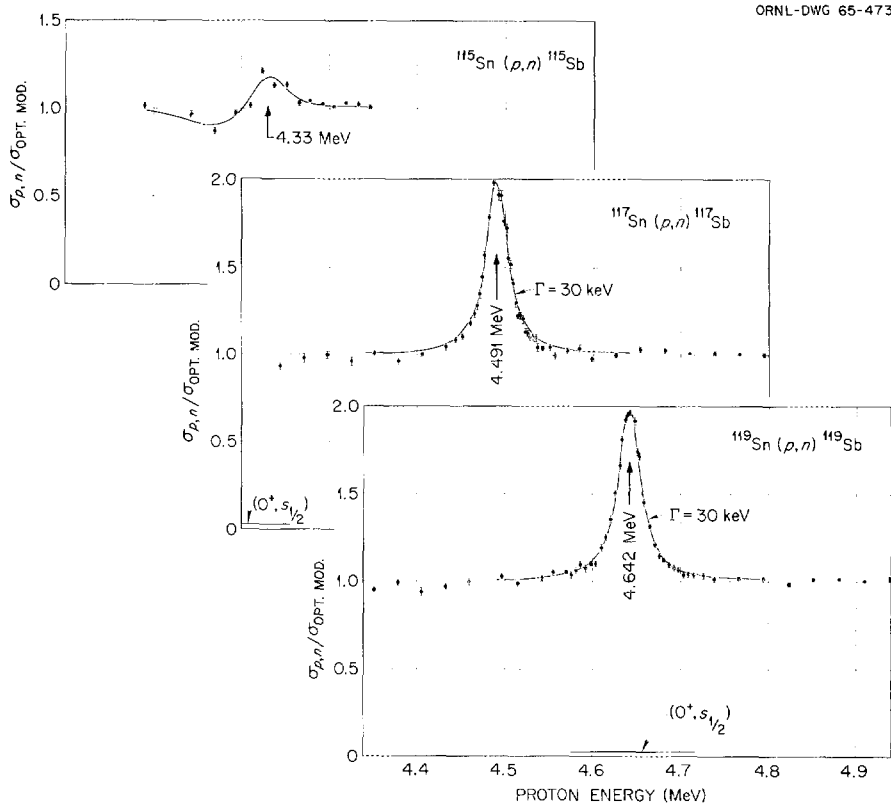


Fig. 4. The Cross Sections for the Tin Isotopes Are Plotted in a Manner Which Removes the Energy Dependence on the Coulomb Penetrability and on $\pi\chi^2$. The ordinate is the observed (p,n) cross section divided by the normalized compound-nucleus cross section in Fig. 3. Curves of the Lorentz shape averaged over the target thicknesses are shown for the two heavier isotopes. The curve through the ^{115}Sn data is simply an experimental one. The lines labeled $(0^+, s_{1/2})$ are the average cross sections for producing 0^+ states by s -wave protons as predicted by an optical model in the absence of the resonance.

ELASTIC AND INELASTIC SCATTERING OF 12- AND 13-Mev PROTONS FROM ^{106}Pd AND ^{108}Pd

R. L. Robinson

J. L. C. Ford, Jr.

P. H. Steison

G. R. Satchler

NUCLEAR REACTIONS. $^{106,108}\text{Pd}(p,p')$, enriched targets, $E_p = 12, 13$ Mev; measured $\sigma(\theta)$. $^{106,108}\text{Pd}$, deduced levels, β_2, β_3 .

The distorted-wave theory for direct nuclear interactions has enjoyed considerable success in explaining proton scattering data for protons with energies greater than 4 Mev above the (p,n) threshold. From a comparison of the predictions of this theory and experimental results, one can deduce spectroscopy factors of the target nuclei and information about the nuclear reaction mechanism. This has led us to undertake a study in which the differential cross sections of protons elastically and inelastically scattered from medium-weight nuclei are measured. The results for the two nuclei ^{106}Pd and ^{108}Pd are reported here.

Protons from the Tandem Van de Graaff accelerator were scattered from self-supporting, ~ 1 mg/cm² foils of the enriched isotopes. The scattered protons were detected by two semiconductor particle detectors which were placed 7 in. from the target and subtended a solid angle of 2.75×10^{-4} steradian. These detectors were suspended from the

top of an 18-in.-diam scattering chamber. The angle between the incident proton beam and the detectors was varied by rotating the top. Data were normalized to the number of elastically scattered protons observed by a detector fixed at 90° relative to the incident beam.

The differential cross sections for 13-Mev protons scattered from ^{106}Pd and 12- and 13-Mev protons scattered from ^{108}Pd have been measured. Representative proton spectra are shown in Figs. 1 and 2. For each target, proton groups were observed which correspond to excitation of the first 2^+ state, the two phonon states, and the octupole state. These states are identified in the figures by spin assignments. Energies determined for the octupole states are 2.08 ± 0.02 Mev in ^{106}Pd and 2.04 ± 0.02 Mev in ^{108}Pd . There was also evidence for several weakly excited levels between 2 and 2.5 Mev in both nuclei.

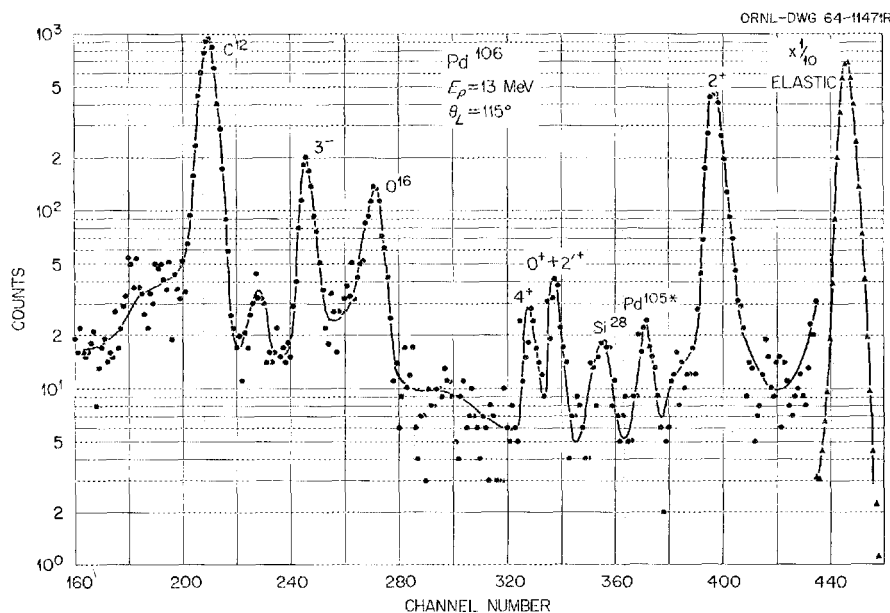


Fig. 1. Spectra of 13-Mev Protons Scattered from a ^{106}Pd Target Through an Angle of 115° .

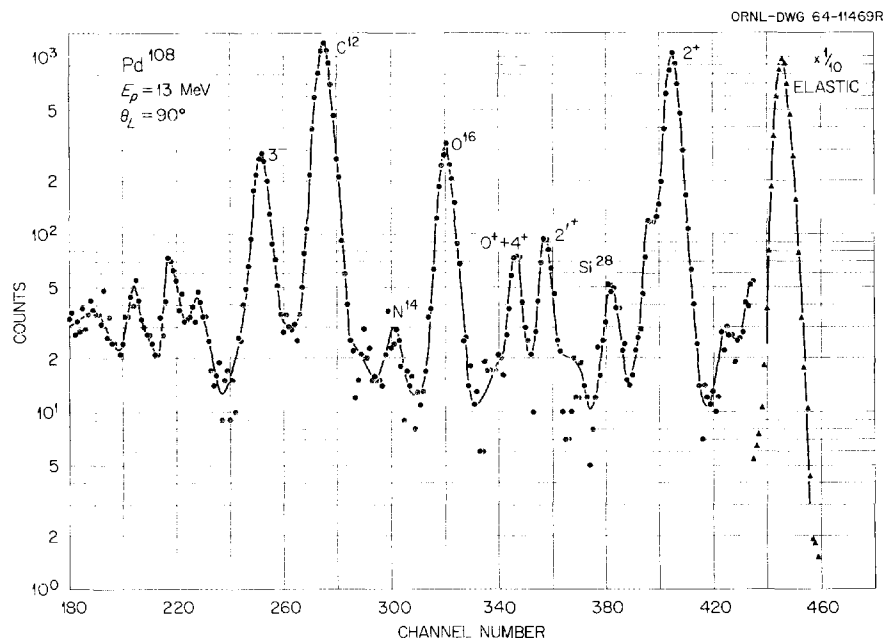


Fig. 2. Spectra of 13-MeV Protons Scattered from a ^{108}Pd Target Through an Angle of 90° .

The elastic differential cross sections divided by the Rutherford cross section are illustrated in Fig. 3. The predictions of the distorted-wave theory are given by the curves in this figure. To obtain the best agreement between the theory and experimental results, the optical-model parameters¹ V and W and the magnitude of the cross sections were treated as free parameters. Values deduced for V and W are listed in Fig. 3. The normalization factors used for the magnitude of the cross sections were also applied to the inelastic differential cross sections. The other parameters in the optical-model potential were taken as $r_0 = 1.2$ fermis, $r'_0 = 1.25$ fermis, $a = 0.7$ fermi, $a' = 0.65$ fermi, and $V_{SO} = 6$ Mev. Equally good fits of the theory to the elastic differential cross sections were obtained if r'_0 was increased to 1.3 fermis. However, the data were poorly fitted for $r'_0 = r_0$.

The differential cross sections for the inelastically scattered proton groups for $E_p = 13$ Mev are given in Fig. 4 for ^{106}Pd and in Fig. 5 for ^{108}Pd . Comparison of the data for excitation of the first 2^+ states with the theoretical prediction gives values for the quadrupole deformation parameter β_2 of 0.25 ± 0.02 for ^{106}Pd and 0.23 ± 0.02 for

^{108}Pd . These are compatible with the β_2 values of 0.226 ± 0.008 and 0.244 ± 0.009 obtained for ^{106}Pd and ^{108}Pd , respectively, from Coulomb excitation studies.² From the cross section for excitation of the octupole states, β_3 's are estimated to be 0.15 ± 0.02 in ^{106}Pd and 0.14 ± 0.02 in ^{108}Pd . These correspond to enhancements over the single-particle estimate of 20 and 17 for the $E3$ transitions from the octupole states to the ground states in ^{106}Pd and ^{108}Pd .

For the theoretical curves shown in Figs. 4 and 5, both the real and the imaginary parts of the optical-model potential were taken as nonspherical. This assumption gave noticeably better fits to the differential cross sections for excitation of the octupole states than if only the real part of the potential was taken as nonspherical. The theoretical curves in Figs. 4 and 5 also include contributions due to Coulomb excitation.

Since excitation of the two phonon levels cannot be treated by the first-order distorted-wave approximation, no effort has yet been made to fit their differential cross sections. The curves shown with these cross sections in Figs. 4 and 5 are only visual fits of the experimental points and have no theoretical significance.

¹Definition of the parameters in the optical-model potential can be found in the paper: F. G. Percy, *Phys. Rev.* 131, 745 (1963).

²P. H. Stelson and F. K. McGowan, *Phys. Rev.* 110, 489 (1958).

Fig. 3. Differential Cross Sections Divided by the Rutherford Cross Section for 13-Mev Protons Elastically Scattered from ^{106}Pd and 12- and 13-Mev Protons Scattered from ^{108}Pd .

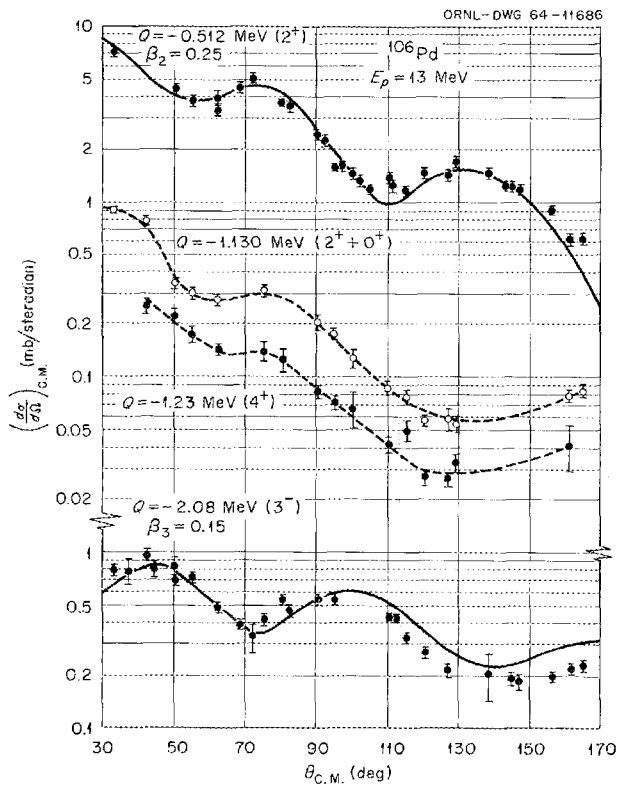
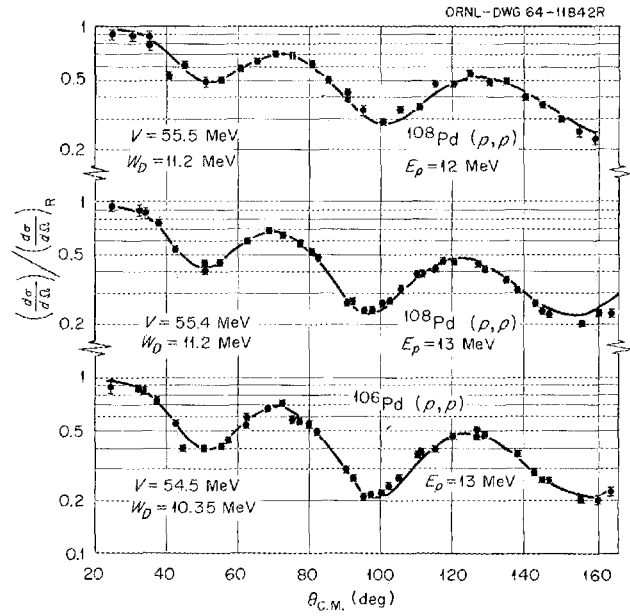


Fig. 4. Differential Cross Sections for Excitation of the 0.512 Quadrupole State, the 1.13 (2^+ and 0^+) and 1.23 (4^+) Two Phonon States, and the 2.08-Mev Octupole State in ^{106}Pd by the Inelastic Scattering of 13-Mev Protons.

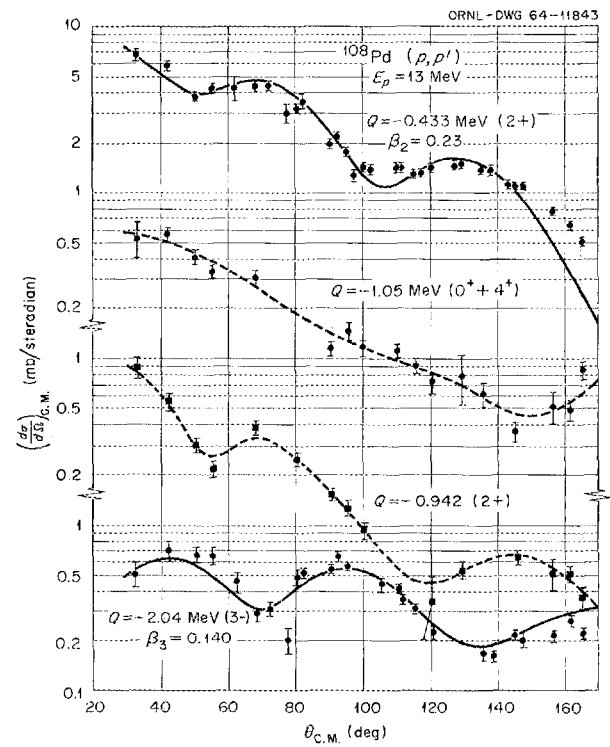


Fig. 5. Differential Cross Sections for Excitation of the 0.433 Quadrupole State, the 0.942 (2^+) and 1.05 (0^+ and 4^+) Two Phonon States, and the 2.04-Mev Octupole State in ^{108}Pd by the Inelastic Scattering of 13-Mev Protons.

SEQUENTIAL EMISSION IN THE REACTION ${}^7\text{Li}(d,n)2\alpha$ ¹

C. M. Jones C. H. Johnson
 J. K. Bair H. B. Willard
 Mark Reeves III²

NUCLEAR REACTIONS. ${}^7\text{Li}(d,2\alpha)$; measured $\sigma(E; E_{\alpha_1}, E_{\alpha_2}, \theta_{\alpha_1}, \theta_{\alpha_2}, \phi_{\alpha_1}, \phi_{\alpha_2})$.
 Deduced reaction mechanism. Enriched target.

The reaction ${}^7\text{Li}(d,n)2\alpha$ has been studied by observing the two emitted alpha particles in coin-

cidence. A number of three-dimensional correlation spectra have been measured at deuteron bombarding energies between 2.0 and 7 Mev. The structure observed in these spectra is consistent with the assumption that the reaction proceeds primarily through a sequential mechanism via the intermediate nuclei ${}^5\text{He}$ and ${}^8\text{Be}$.

¹Abstract of paper presented at Topical Conference on Correlations of Particles Emitted in Nuclear Reactions, Gatlinburg, Tenn., October 15-17, 1964. (Proceedings of conference will be published in *Reviews of Modern Physics*.)

²Now a graduate fellow at the University of Tennessee, Knoxville.

Q VALUES OF THREE-BODY NUCLEAR REACTIONS¹

Mark Reeves III²

The Q values for nuclear reactions having three particles in the final state and the FORTRAN

program from which these values were calculated are presented. Protons, deuterons, ${}^3\text{He}$ ions, and ${}^4\text{He}$ ions are considered as projectiles, and all stable nuclides for which $3 < Z < 20$ are used as targets.

¹Abstract of ORNL-TM-938.

²Now a graduate fellow at the University of Tennessee, Knoxville.

${}^{15}\text{N}({}^3\text{He},p){}^{17}\text{O}$ AND ${}^{15}\text{N}({}^3\text{He},d){}^{16}\text{O}$ REACTIONS AND INTERMEDIATE RESONANCES

K. K. Seth¹ G. Walter¹ P. D. Miller
 J. A. Biggerstaff G. R. Satchler

NUCLEAR REACTIONS. ${}^{15}\text{N}({}^3\text{He},d){}^{16}\text{O}$, ${}^{15}\text{N}({}^3\text{He},p){}^{17}\text{O}$ reactions. Angular distribution at $E_{{}^3\text{He}} = 6.41$ Mev. Deduced character of states in residual nuclei.

One of the most intriguing aspects of the nuclear reaction mechanism problem is the transition from the relatively straightforward mechanism, usually referred to as the direct interaction, to the chaotic situation represented by the compound-nucleus

interaction. Recently, Block and Feshbach² proposed the concept that three quasi-particle intermediate states in the reaction play the dominant role of being the doorways to compound-nucleus formation. They called these states doorway

¹Northwestern University, Evanston, Ill.

²B. Block and H. Feshbach, *Ann. Phys. (N.Y.)* 23, 47 (1963).

states. Lemmer,³ Shakin,⁴ and a number of other workers at MIT, notably Kerman, Rodberg, and Young⁵ have made significant contributions to the development of this idea.

The intermediate state comes about as follows. In the simplest interaction between an incoming particle and the target nucleus, the particle sees what is essentially the real nuclear potential. The next stage of involvement consists of a two-body interaction between the incident particle and a nucleon of the target nucleus. The interacting particle is raised to a higher level and leaves a hole behind. This three-quasi-particle structure subsequently either leads to more complicated five-quasi-particle excitations, seven-quasi-particle excitations, and so on until the compound-nucleus limit is reached, or else it may dissolve back to the single particle in a potential well with the particle escaping. There is no doubt that a process somewhat similar to this takes place. However, the significant question is: How important is the doorway step? In clearer terms, does the doorway state live long enough to give rise to a "narrow-enough-to-be-observed" structure, or is the lifetime so small and the width consequently so large that the structure is wiped out?

Indirect proofs of the existence of intermediate resonances have been provided by the work of Glasgow and Foster⁶ ($\bar{\sigma}_p$), Langsdorf *et al.*⁷ [$\sigma_{el}(\theta)$], and Seth⁸ ($\bar{\sigma}_p$). A more direct confirmation of the idea is, however, sorely needed.

For light nuclei, this elucidation would consist of the observation of individual states which could be ascribed to a two-particle-one-hole nature. With this in mind, Lemmer suggested the $^{15}\text{N}(^3\text{He},p)^{17}\text{O}$ experiment to us. It is to be expected that in this reaction strong enhancement of two-particle-one-hole states will be observed, since the ^{15}N ground-state (GS) configuration is $(p_{1/2})^{-1}$, and the reaction is a two-particle transfer reaction.

Doubly charged ^3He ions of about 6.4 Mev were incident on an isotopically pure ^{15}N gas target

³R. H. Lemmer, *Phys. Letters* **4**, 205 (1963).

⁴R. H. Lemmer and C. M. Shakin, *Ann. Phys. (N.Y.)* **27**, 13 (1964).

⁵A. K. Kerman, L. S. Rodberg, and J. E. Young, *Phys. Rev. Letters* **11**, 422 (1963).

⁶D. W. Glasgow and D. G. Foster, *Bull. Am. Phys. Soc.* **8**, 321 (1963).

⁷A. Langsdorf, R. O. Lane, and J. E. Monahan, *Phys. Rev.* **107**, 1077 (1957).

⁸K. K. Seth, to be published in *Physics Letters*.

confined in a small scattering chamber. Solid-state detectors were employed. A typical pulse-height spectrum is illustrated in Fig. 1. It may be noted that groups from the reactions $^{15}\text{N}(^3\text{He},\alpha)^{14}\text{N}$ and $^{15}\text{N}(^3\text{He},d)^{16}\text{O}$ are also observed. To be particularly noted are the strong proton groups corresponding to excitations of the 8th, 18th, and ~ 35 th excited states of ^{17}O . The elastic-scattering angular distribution is shown in Fig. 2. The ordinate scale is based on the observation that $\sigma(\theta)/\sigma_r(\theta) \sim 0.66 \pm 0.02$ at $\theta_{\text{c.m.}} = 36^\circ$ for all reasonable choices of an optical potential for ^3He . Once this is accepted, all of our relative angular distributions acquire absolute cross-section scales. The optical-model fit to the elastic-scattering data is entirely satisfactory, considering the statistical accuracy of the data.

$^{15}\text{N}(^3\text{He},d)^{16}\text{O}$

A number of significant observations can be made about this reaction.

1. While a weak ground-state transition (to 0^+) was observed, transitions to the second 0^+ and the 2^+ excited states were not observed, and an upper limit of 5% of the yield of the 6.14-Mev (3^-) state can be placed for them.
2. Strong transitions to all three negative parity states, 6.14 Mev (3^-), 7.12 Mev (1^-), and 8.88 Mev (2^-), were observed. These are all about 20 to 30 times stronger than the ground-state transition. These two observations conclusively prove that these negative parity states have large parentage in the $(p_{1/2})^{-1}$ ground state of ^{15}N . It has long been thought that the negative parity states of ^{16}O are one-particle-one-hole states. Elliott and Flowers,⁹ and more recently Brown *et al.*¹⁰ and Gillet,¹¹ have developed this picture in detail. A striking confirmation of this interpretation is provided in Fig. 3. Here, along with the observed angular distributions, are shown results of distorted-wave Born approximation (DWBA) calculations, using the particle-hole wave functions of Gillet.

⁹J. P. Elliott and B. Flowers, *Proc. Roy. Soc. (London)* **A229**, 536 (1955).

¹⁰G. E. Brown, J. A. Evans, and D. J. Thouless, *Nucl. Phys.* **45**, 164 (1963).

¹¹V. Gillet and N. Vinh Mau, *Nucl. Phys.* **54**, 321 (1964).

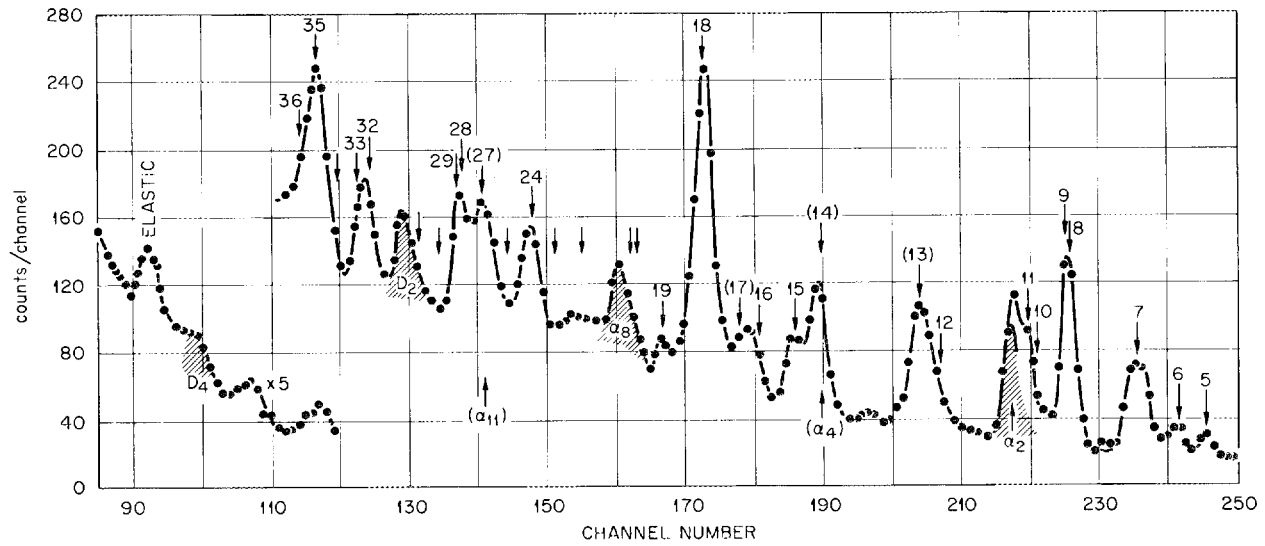
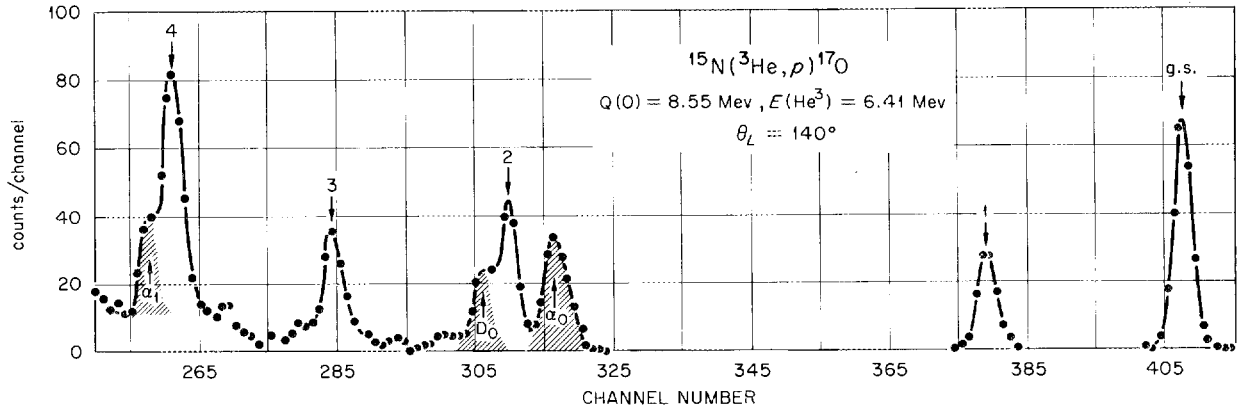


Fig. 1. Pulse-Height Spectrum at $\theta_L = 140^\circ$ Resulting from the Bombardment of ^{15}N by 6.41-Mev ^3He .

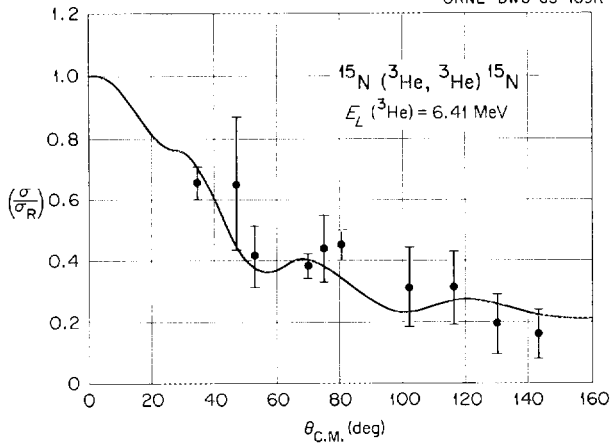


Fig. 2. $^{15}\text{N}(^3\text{He}, ^3\text{He})^{15}\text{N}$ Elastic Scattering Angular Distribution at $E = 6.41 \text{ Mev}$ with an Optical-Model Fit to the Data.

Notice that for all three negative parity states the predicted angular distributions are in good agreement with the data both qualitatively and quantitatively. It is worth noting that these curves were obtained without any attempt at fitting the data; that is, Gillet's spectroscopic factors were used with the DWBA code. It is also noteworthy that both the calculated and the experimental cross sections are absolute. Finite-range and nonlocality effects have not been included in these calculations, but the insensitivity of the results to use of a radial cutoff suggests that these effects are small. Spin-orbit coupling is expected to have little effect also. The spectroscopic factors obtained from the wave functions of Gillet's random phase approximation—number one (RPA1) were:

$$|3^- \rangle = 0.934 |p_{1/2}^{-1} d_{5/2} \rangle + \dots,$$

$$|1^- \rangle = 0.613 |p_{1/2}^{-1} s_{1/2} \rangle + 0.433 |p_{1/2}^{-1} - d_{3/2} \rangle + \dots,$$

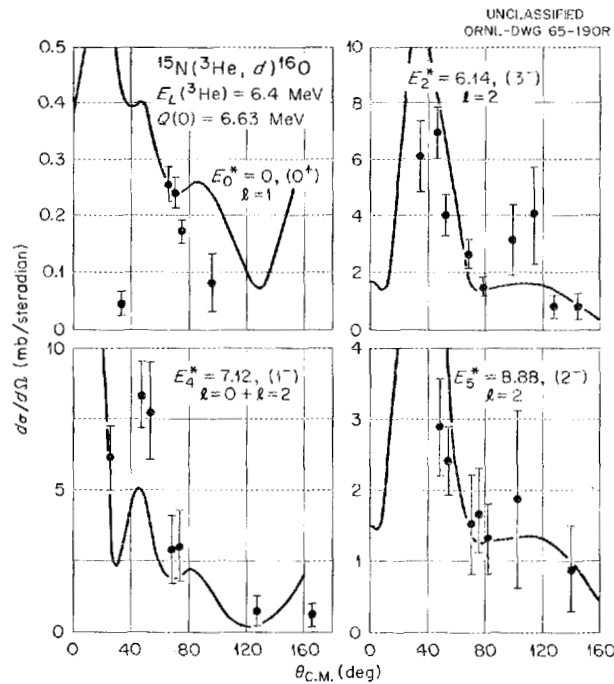


Fig. 3. $^{15}\text{N}(^3\text{He},d)^{16}\text{O}$ Angular Distributions to the Ground State and Negative Parity Excited States of ^{16}O . Distorted-wave Born approximation predictions as discussed in the text are shown.

$$|2^- \rangle = 0.965 |p_{1/2}^{-1} d_{5/2} \rangle + \dots,$$

where other configurations do not contribute if ^{15}N is in a pure $p_{1/2}$ -hole state.

$^{15}\text{N}(^3\text{He},p)^{17}\text{O}$

Figures 4 and 5 show our observed angular distributions. Unfortunately, we have neither spectroscopic factors nor results of DWBA calculations to report here.

As illustrated in Table 1, the following observations can, however, be made:

1. The relative cross sections reduced by $[(2J + 1)\sigma_{\text{GS}}]^{-1}$ for the three positive parity states are 1.00, 1.4, and 0.69, while those for the negative parity states are 2.4, 1.4, 1.4, 1.9, and 2.2. Thus the average of the reduced yields of the negative parity states is approximately twice as large as that of the positive parity states, strongly indicating the altogether different parentage of the negative parity states.
2. The reduced yields of the five adjoining negative parity states are 2.4 ($\frac{1}{2}^-$), 1.4 ($\frac{5}{2}^-$), 1.4 ($\frac{3}{2}^-$), 1.9 ($\frac{3}{2}^-$), and 2.2 ($\frac{7}{2}^-$). Their approximate equality strongly suggests a common parentage for them and is strongly reminiscent of the near equality of the $E2$ transition strengths in the levels of the same vibrational band. These observations suggest an even simpler picture than the (two-particle—one-hole) states we started to look for. One wonders if indeed these states do not represent (vibration + one particle) states with the particle being in a $d_{5/2}$ or $s_{1/2}$ state and the vibration being one of the 3^- , 1^- , or 2^- states in ^{16}O .

Indeed, some time ago, Brown, Evans, and Thouless¹⁰ suggested precisely this nature for the ^{17}O states. The three strongest groups (all about four times as strong as the positive parity levels) are E_8 (5.70 Mev, $\frac{7}{2}^-$), E_{18} (7.37 Mev, $\frac{5}{2}^-$), and E_{35} (9.16 Mev, ...). We tentatively regard these as the "center of gravity" of the set of levels having different J but all consisting of the same vibration and the same particle. The results of this picture are displayed in Table 2. In the first column the vibrational excitation of ^{16}O is given. In the second column the assumed

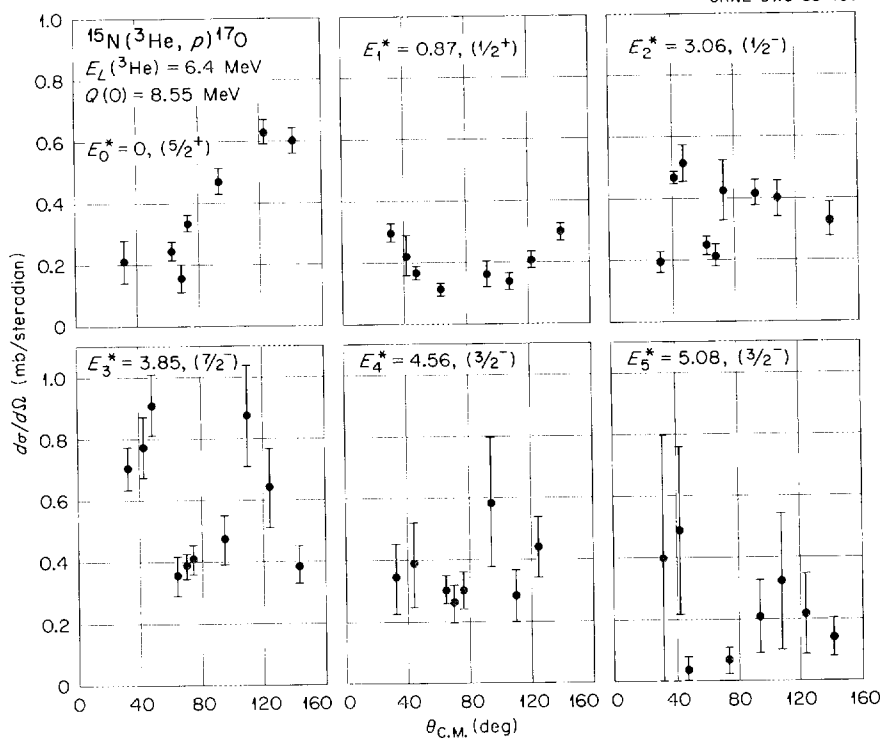
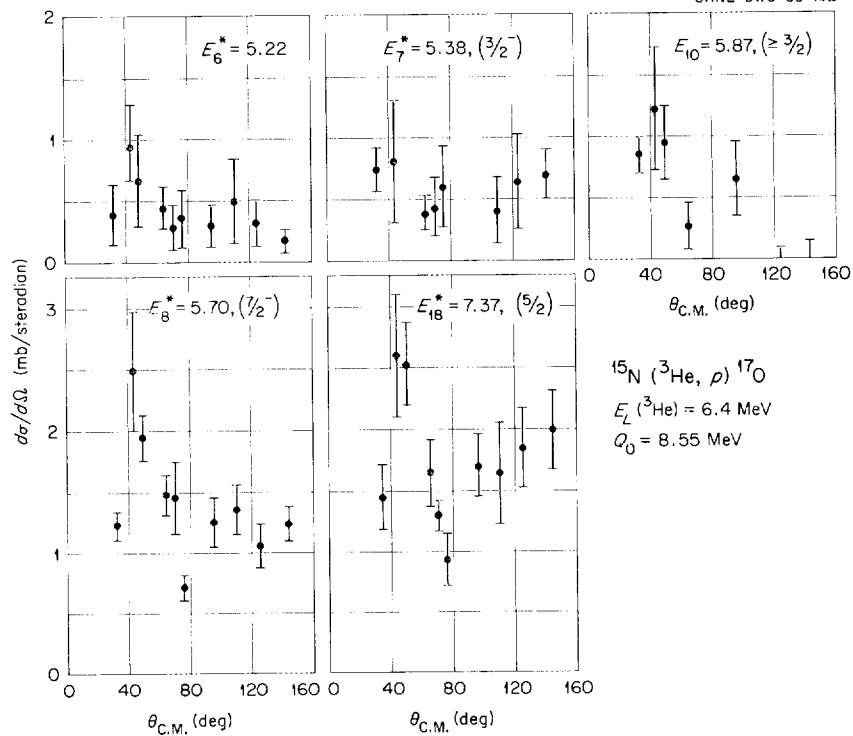
UNCLASSIFIED
ORNL-DWG 65-191Fig. 4. $^{15}\text{N}(^3\text{He},p)^{17}\text{O}$ Angular Distributions to the Ground and First Five Excited States of ^{17}O .UNCLASSIFIED
ORNL-DWG 65-192Fig. 5. $^{15}\text{N}(^3\text{He},p)^{17}\text{O}$ Angular Distributions to the Higher Excited States of ^{17}O .

Table 1. Experimental Cross Sections and Reduced Yields for Formation of States in ^{17}O

States	GS	1	2	3	4	5	6	7	8	9	10	18	35
Energies* (Mev)	0	0.87	3.06	3.85	4.56	5.08	5.22	5.38	5.70	5.73	5.87	7.38	9.16
$J(\pi)$	$5/2^+$	$1/2^+$	$1/2^-$	$5/2^-$	$3/2^-$	$3/2^+$		$3/2^-$	$7/2^-$		$\geq 3/2$	$5/2$	
$2J+1$	6	2	2	6	4	4		4	8		≥ 4	6	
$\sigma(^3\text{He},p)$ (mb)	5.17	2.43	4.20	7.21	4.86	2.39	4.18	6.66	15.5		5.06	20.7	(23.9)
$\sigma/(2J+1)$ (relative)	1.00	1.4	<u>2.4</u>	<u>1.4</u>	<u>1.4</u>	0.69		<u>1.9</u>	<u>2.2</u>		<u>≤ 1.5</u>	<u>4.0</u>	

single-particle configuration is given with the excitation energy relative to the ground state of ^{17}O . The third column is simply the sum of the first two, and the fourth column is the observed excitation energy. The defect (difference between third and fourth columns) represents the *difference* between the coupling strength of an odd neutron to the ground state of ^{16}O and the coupling strength of an odd neutron to a vibrational state of ^{16}O . All energy values are in Mev.

The defect appears to be relatively small and constant. While we do not claim that this is a complete analysis, it nevertheless suggests a self-consistent picture of strong vibrational excitations which are modified but little by the odd-particle coupling.

It is interesting to compare these data with those of Cerny¹² on the $^{15}\text{N}(\alpha,d)^{17}\text{O}$ reaction. The experiment is qualitatively comparable to ours even though it was done at 45 Mev. As Fig. 6 illustrates, the spectra are remarkably similar. Cerny observed what he called three strong groups at 5.7, 7.6, and 9.0 Mev excitation in ^{17}O . This result is exactly the same as ours, except that with 400-kev resolution he actually saw the "center

Table 2. Comparison of Observed Excitation Energies in ^{17}O with the Prediction of the (Vibration + One Particle) Model

Vibration	Particle	Predicted E^*	Observed E^*	Defect
3^- (6.14)	$d_{5/2}$ (0)	6.14	5.70	0.44
1^- (7.12)	$s_{1/2}$ (0.87)	7.99	7.37	0.62
2^- (8.88)	$s_{1/2}$ (0.87)	9.75	9.16	0.59

of gravity" of a group of levels that we resolve. (Incidentally, this verifies our center locations.) Unfortunately, Cerny proposed a $(d_{5/2})^2$ explanation for two of these states, which does not agree with our conclusions.

¹²J. Cerny III, *Two-Nucleon Transfer Reactions in the Light Elements* (Thesis), 1961, UCRL-9714.

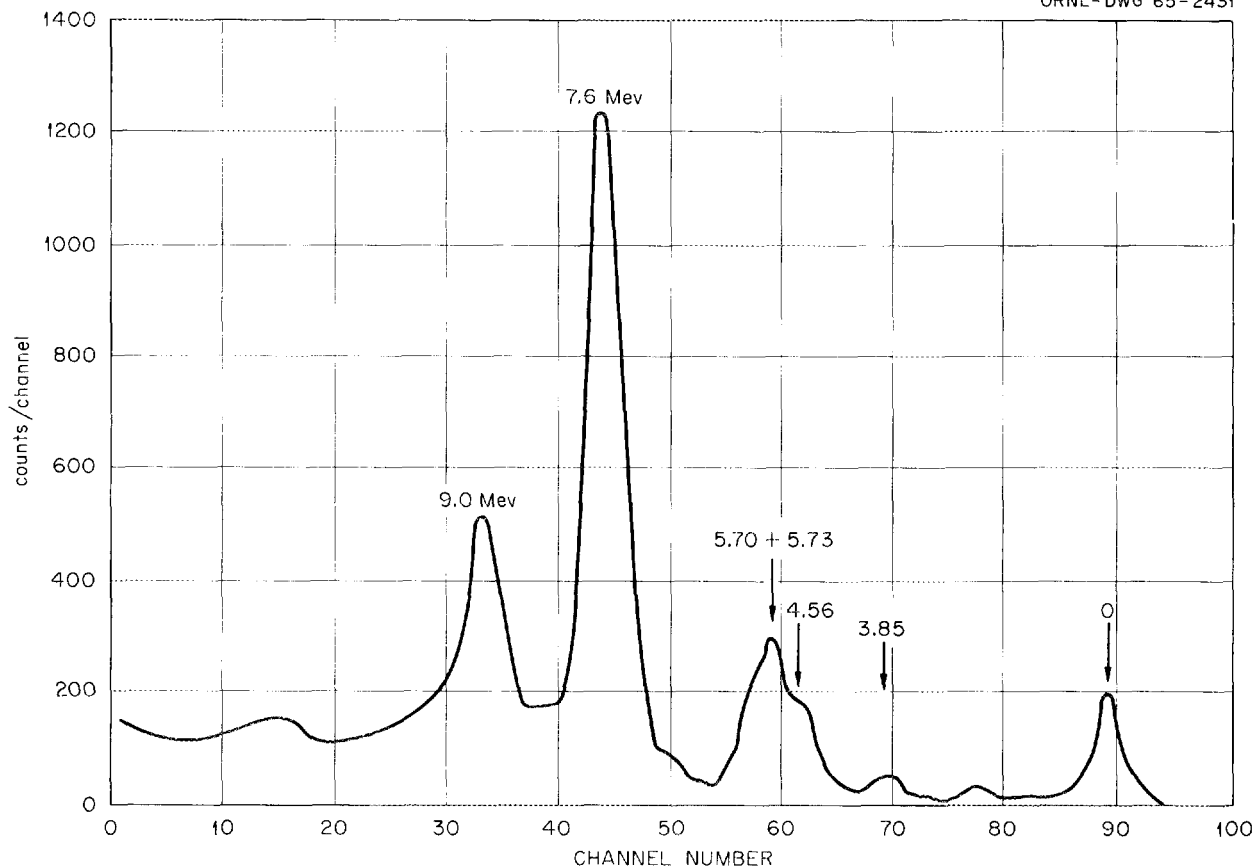


Fig. 6. Deuteron Energy Spectrum at 15° (lab) for the Reaction $^{15}\text{N}(\alpha, d)^{17}\text{O}$. This data is from ref. 12.

TOTAL CROSS SECTION FOR $^9\text{Be}(\alpha, n)^1$

J. H. Gibbons

R. L. Macklin

NUCLEAR REACTIONS. $^9\text{Be}(\alpha, n)$, $E = 1.7\text{--}10.5$ Mev; measured $\sigma(E)$. Nucleus ^{13}C deduced levels, 1^1 . Other than ^{12}C , $^{12}\text{C}^*$ final states dominant near $E_\alpha = 10$ Mev. Natural target.

The absolute total (4π) neutron yield from $^9\text{Be}(\alpha, n)$ has been measured for alpha energies from 1.7 to 10.5 Mev by extension of earlier measurements. In addition to previously reported states in ^{13}C ,

resonance peaks are observed corresponding to E_{ex} of 15.3 and 17.0 Mev. The widths for resonances at $E_\alpha = 1.92, 2.25,$ and 2.58 Mev are 0.2, 0.4, and 0.3 Mev respectively. Near $E_\alpha = 10$ Mev, reactions leading to states in ^{12}C apparently account for $<30\%$ of the observed cross section.

¹Abstract of paper accepted by the *Physical Review*.

TOTAL NEUTRON YIELD FROM THE REACTION $^{14}\text{C}(\alpha, n)^{17}\text{O}$ ¹

J. K. Bair

J. L. C. Ford, Jr.

C. M. Jones

NUCLEAR REACTIONS. $^{14}\text{C}(\alpha, n)$; measured $\sigma(E)$. ^{18}O deduced levels, Γ .

The total neutron yield of the reaction $^{14}\text{C}(\alpha, n)^{17}\text{O}$ has been measured in the alpha-particle bombarding energy range 2.5 to 5.1 Mev. Six new levels were

observed in the compound ^{18}O nucleus at bombarding energies of 4.030 ± 0.015 , 4.07 ± 0.03 , 4.17 ± 0.03 , 4.434 ± 0.010 , 4.70 ± 0.4 , and 5.004 ± 0.010 Mev. These correspond to excitation energies of 9.361, 9.39, 9.47, 9.675, 9.88, and 10.119 Mev. The experimental widths varied from 21 to 200 kev.

¹Abstract of paper to be submitted to the *Physical Review*.

COULOMB EXCITATION OF VIBRATIONAL TRIPLET STATES AND OCTUPOLE STATES IN THE EVEN CADMIUM NUCLEI¹

F. K. McGowan

P. H. Stelson

R. L. Robinson

J. L. C. Ford, Jr.

NUCLEAR REACTIONS. $^{110,112,114,116}\text{Cd}(^{16}\text{O}, ^{16}\text{O}'\gamma)$, $^{110,112,114,116}\text{Cd}(\alpha, \alpha'\gamma)$, enriched targets, $E_{^{16}\text{O}} = 42-49$ Mev, $E_{\alpha} = 9-10.9$ Mev; measured γ , $\gamma\gamma$ spectra. $^{110,112,114,116}\text{Cd}$, deduced levels, J , π , $B(E2)$, $B(E3)$.

Oxygen-16 ions with energies of 42 to 49 Mev have been used to Coulomb-excite higher states in the even cadmium isotopes. Double $E2$ excitation of the 0^+ state at 1133 kev in ^{114}Cd has been observed. The $E2$ transition between the excited 0^+ state and the first 2^+ state is strongly enhanced; that is, $B(E2, 0^+ \rightarrow 2)/B(E2, 2 \rightarrow 0) = 0.85 \pm 0.17$. The second 2^+ state and the 4^+ state in ^{116}Cd are degenerate to within 5 kev at 1222 kev excitation. The values obtained for the ratio $B(E2, 4 \rightarrow 2)/B(E2, 2 \rightarrow 0)$ are 1.42 ± 0.19 , $1.82 \pm$

0.23 , 1.80 ± 0.23 , and 1.63 ± 0.36 , respectively, for ^{110}Cd , ^{112}Cd , ^{114}Cd , and ^{116}Cd . States at 2051 ± 16 , 1968 ± 16 , 1945 ± 16 , and 1900 ± 16 kev are excited in ^{110}Cd , ^{112}Cd , ^{114}Cd , and ^{116}Cd respectively. If these states are interpreted to be the result of direct $E3$ Coulomb excitation, the $B(E3, 0 \rightarrow 3)$ are 10.3, 10.6, 9.0, and 7.5×10^{-74} $e^2\text{cm}^6$, with an accuracy of $\pm 20\%$, provided the branching ratio of cascades to crossover from the 3^- state is large compared with unity. These $B(E3)$ values represent enhancements of 13 to 20. They are 3 to 6 times smaller than the results derived from yield measurements with 14- to 15-Mev alpha particles at Copenhagen.

¹Abstract of paper submitted to *Nuclear Physics*.

LOW-LYING LEVELS IN ^{75}As R. L. Robinson
F. K. McGowanJ. L. C. Ford, Jr.
P. H. Stelson

NUCLEAR REACTIONS. $^{75}\text{As}(\alpha, \alpha'\gamma)$, $E_\alpha = 3.5\text{--}8.1$ Mev, $^{75}\text{As}(^{16}\text{O}, ^{16}\text{O}'\gamma)$, $E_{^{16}\text{O}} = 36\text{--}38$ Mev; measured E_γ , I_γ , $\gamma\gamma$ spectra, $\gamma^{16}\text{O}$ spectra, $\gamma(\theta)$. ^{75}As , deduced levels, J , π , $B(E2)$, $B(M1)$, δ , $\tau_{1/2}$.

Although extensive studies have been made of the low-lying levels in ^{75}As through the investigation of the gamma rays and the conversion electrons following the decays of the radioactive nuclei ^{75}Ge and ^{75}Se ,¹ many of the level properties have not been established. In order to achieve an understanding of the nature of the nucleus when in these excited modes, it is necessary to ascertain the properties of these levels. Coulomb excitation of ^{75}As provides a means of reducing the number of unknowns.

Coulomb excitation has been effected by bombarding a thick arsenic target with helium and oxygen ions. A description of the experimental arrangement for study of gamma rays resulting from this bom-

bardment can be found in earlier publications.² Two new techniques have been added during the past year: (1) gamma-ray spectra were taken with a lithium-drifted germanium detector as well as with the conventional NaI crystal, and (2) gamma-ray spectra were taken in coincidence with back-scattered bombarding particles.

Examples of the spectra are given in Figs. 1--4. The contrast between Figs. 1 and 2 demonstrates the greatly improved resolution of the lithium-drifted germanium detector over the NaI crystal. The narrowness of the peaks in the spectrum, as measured with the germanium detector, not only makes possible observation of additional gamma-ray transitions but also enables one to determine energies to

¹Nuclear Data Sheets, Nuclear Data Group, Oak Ridge National Laboratory; M. de Cr6es and G. B6ckstr6m, *Arkiv Fysik* **16**, 567 (1960); W. F. Edwards and C. J. Gallagher, Jr., *Nucl. Phys.* **26**, 649 (1961).

²P. H. Stelson and F. K. McGowan, *Phys. Rev.* **110**, 489 (1958); F. K. McGowan and P. H. Stelson, *Phys. Rev.* **106**, 522 (1957).

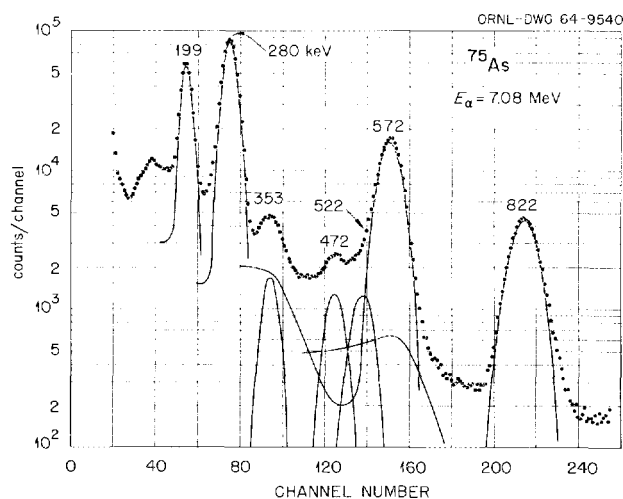


Fig. 1. Gamma-Ray Spectrum for 7.08-Mev Alpha Particles on a Target of As as Measured with a 3 in. x 3 in. NaI Crystal.

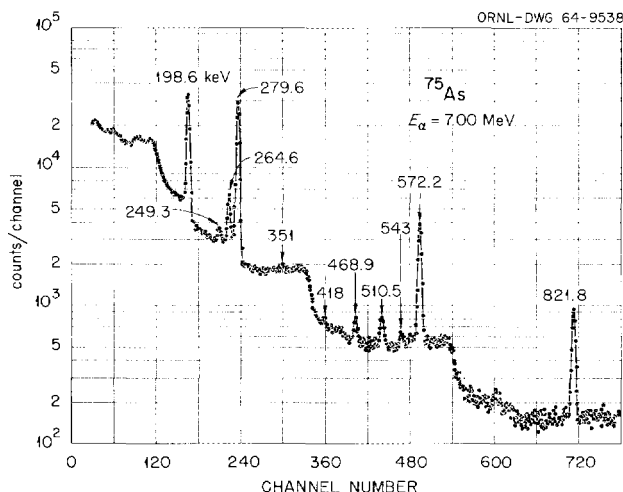


Fig. 2. Gamma-Ray Spectrum for 7.00-Mev Alpha Particles on a Target of As as Measured with a Lithium-Drifted Germanium Detector. The volume of this detector is about 0.2 cm^3 .

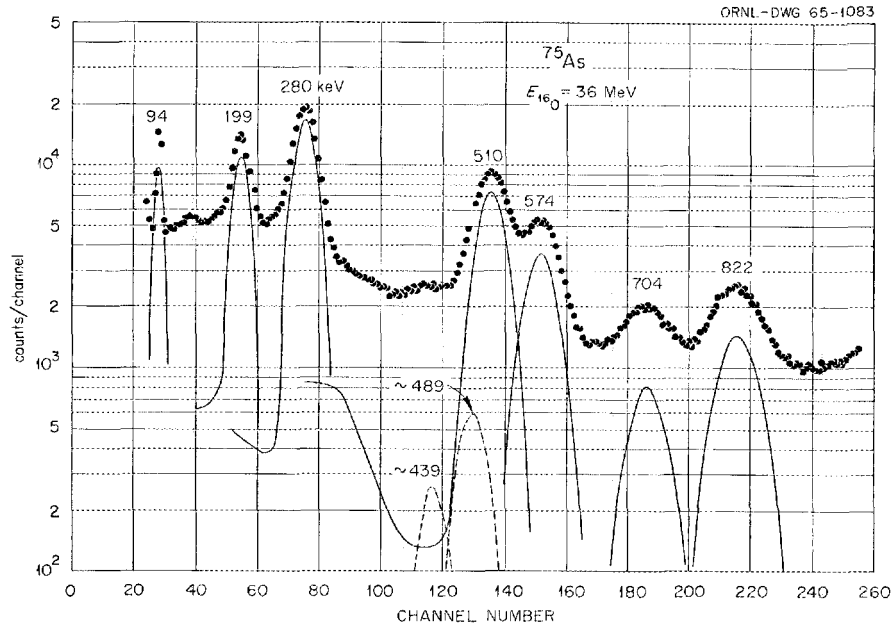


Fig. 3. Gamma-Ray Spectrum for 36-Mev Oxygen Ions on a Target of As.

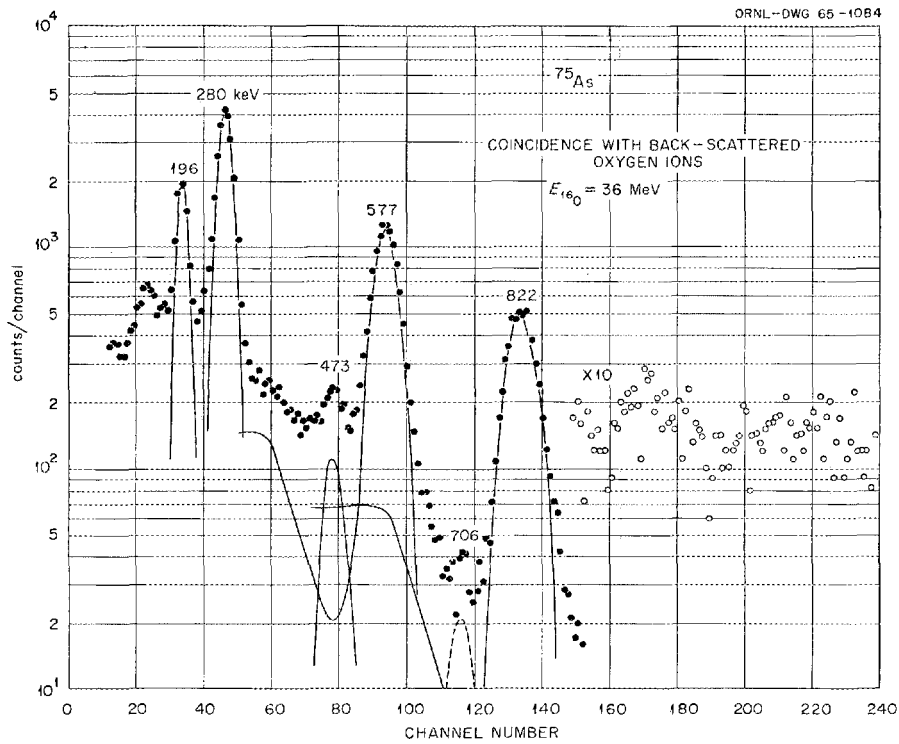


Fig. 4. Spectrum of Gamma Rays in Coincidence with 36-Mev Oxygen Ions Back-Scattered from an As Target.

a few tenths of a kev. Figures 3 and 4 illustrate the improvement achieved in a spectrum by observing only gamma rays which are in coincidence with the back-scattered particles. Also note in Figs. 1 and 3 that, at least for this target, a "cleaner" spectrum is obtained when the target is bombarded with helium ions than when bombarded with oxygen ions. The peak at 353 kev in Fig. 1 is from the reaction $^{18}\text{O}(\alpha, n)^{21}\text{Ne}$. Oxygen results from the oxidation of the arsenic metal target. The amount present was estimated from a comparison of the magnitudes of the 353-kev gamma ray as observed with the arsenic target and with a GeO_2 target.

From the gamma-ray yields determined from spectra taken at 11 alpha-particle energies between 3.5 and 8.1 Mev and at two oxygen ion energies (36 and 38 Mev), it is established that levels at 199, 280, 469, 572, and 822 kev are populated via the $E2$ Coulomb excitation process. Spectra were also measured in coincidence with the 199- and 280-kev gamma rays for four alpha-particle energies and one oxygen ion energy. These spectra reveal three cascade transitions with energies of 296, 418, and 543 kev. Their positions are shown in the level diagram in Fig. 5. The yields found for the 418-kev gamma ray indicate that there is a level at 617 kev populated by the $E2$ Coulomb excitation process.

Coulomb excitation of the known 265-kev level shown in Fig. 5 is inferred from the presence of a 264.6-kev peak in the spectrum measured with the lithium-drifted germanium detector (see Fig. 2).

Similarly, the 249.3-kev transition, which fits energetically between the 822- and the 572-kev levels, was only seen in this spectrum. The dashed lines in Fig. 5 are for transitions not observed in the present study. Their intensities are taken from earlier investigations.¹

The reduced $E2$ transition probabilities for excitation, $B(E2)_{\text{ex}}$, deduced from the gamma-ray yields, are given in Table 1. Corrections for the gamma-ray branching ratios, which are given above the levels in Fig. 5, for internal conversion, and for oxygen in the target were applied. The latter correction was 3 to 14% for the metal arsenic target. To check this correction, spectra were measured when a thick target of As_2O_3 (a target in which the amount of oxygen was known) was bombarded with 4.0- and 4.5-Mev alpha particles. The $B(E2)_{\text{ex}}$'s obtained from these runs are shown in the last column in Table 1 and are seen to agree with those found when the metal arsenic target was used.

Angular anisotropies for the strongest transitions were measured relative to the direction of the incident beam for $E_\alpha = 3.5, 5.1,$ and 7.1 Mev. The data were fitted to the equation

$$W(\theta) = 1 + a_2 g_2 A_2 P_2(\cos \theta),$$

where a_2 and g_2 are, respectively, the thick-target particle parameter and the correction for the finite angular resolution of the detector. Table 2 contains average A_2 's along with the level spins which are

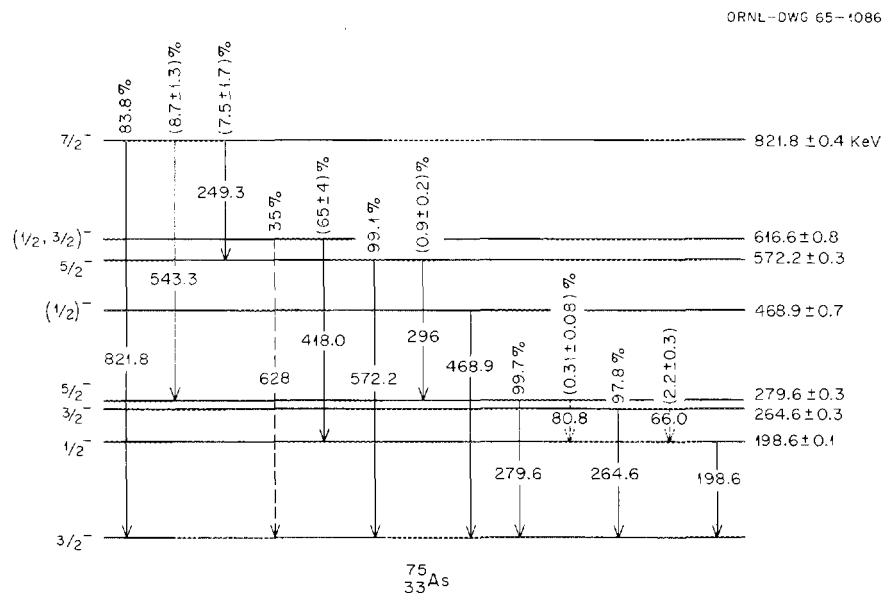


Fig. 5. Energy-Level Diagram of Coulomb Excited Levels in ^{75}As .

consistent with these coefficients. The level spins which are compatible with all experimental results are given in the level scheme in Fig. 5. Since the levels are all populated by the $E2$ Coulomb

excitation process, their parities are identical to the parity of the ground state.

Table 3 summarizes the known properties of the Coulomb-excited levels and the gamma rays originating at these levels. The value taken for the single-particle $B(E2)$ is $B(E2)_{sp} = e^2/4\pi | \frac{3}{5} R_0^2 |^2$, with $R_0 = 1.2 \times 10^{-13} A^{1/3}$ cm. The single-particle estimate for the reduced $M1$ transition probability, $B(M1)$, is approximately $(e\hbar/2Mc)^2$.

Table 1. The $B(E2)_{ex}$'s of Levels in ^{75}As

Level (kev)	$B(E2)_{ex} \times 10^{50}$ ($e^2\text{cm}^4$)		
	^4He on As	^{16}O on As	^4He on As_2O_3
198.6	1.59 ± 0.14	1.61 ± 0.19	1.63 ± 0.17
264.6	0.54 ± 0.07		
279.6	4.4 ± 0.5	4.4 ± 0.6	4.5 ± 0.5
468.9	0.33 ± 0.03	0.44 ± 0.08	
572.2	7.4 ± 0.7	6.8 ± 1.0	7.2 ± 0.9
616.6	0.120 ± 0.021	0.109 ± 0.036	
821.8	11.3 ± 1.1	10.4 ± 1.4	

Table 2. Experimental Angular Distribution Coefficients

E_γ	A_2	Possible Spin
198.6	-0.005 ± 0.016	1/2, 3/2, 5/2
279.6	-0.191 ± 0.010	5/2
572.2	$+0.064 \pm 0.014$	5/2
821.8	$+0.22 \pm 0.02$	7/2

Table 3. Level and Gamma-Ray Properties

Level (kev)	E_γ (kev)	$B(E2)_{ex} \times 10^{50}$ ($e^2\text{cm}^4$)	I_f	$B(E2)_d \times 10^{50}$ ($e^2\text{cm}^4$)	$\frac{B(E2)_d}{B(E2)_{sp}}$	$\delta = (E2/M1)^{1/2}$	$\frac{B(M1) \times 10^2}{(e\hbar/2Mc)^2}$	$T_{1/2}$ (sec)
198.6	198.6 ± 0.1^a	1.61 ± 0.14	1/2	3.22 ± 0.28	17	$ 0.43 \pm 0.04 $	0.47 ± 0.06	$(9.0 \pm 1.0) \times 10^{-10}^b$
264.6	264.6 ± 0.3	0.54 ± 0.07	3/2	0.54 ± 0.07	2.9	$ 0.037 \pm 0.003 $	20 ± 2	$(1.09 \pm 0.07) \times 10^{-11}^c$
264.6	66 ± 0.1^a					$< 0.045 $	28 ± 5^d	
279.6	279.6 ± 0.3	4.5 ± 0.4	5/2	3.0 ± 0.3	16	-0.47 ± 0.08	0.74 ± 0.14	$(2.0 \pm 0.3) \times 10^{-10}$
279.6	80.8 ± 0.1^a			9.8 ± 2.8	52	∞		
468.9	468.9 ± 0.7	0.35 ± 0.03	1/2	0.70 ± 0.06	3.7			
572.2	572.2 ± 0.3	7.2 ± 0.7	5/2	4.8 ± 0.5	25	$+0.39 \pm 0.05$	7.5 ± 1.9	$(2.4 \pm 0.6) \times 10^{-12}$
572.2	296 ± 4						<0.9	
616.6	628 ± 5^e	0.116 ± 0.019	1/2, 3/2	0.23, 0.12	1.2, 0.6			
616.6	418.0 ± 0.7							
821.8	821.8 ± 0.4	10.9 ± 1.0	7/2	5.5 ± 0.5	29	∞		$(2.3 \pm 0.2) \times 10^{-12}$
821.8	543.3 ± 1.2						<1	
821.8	249.3 ± 0.5						8 ± 3^d	

^aRef. 1.

^bE. N. Shipley, F. J. Lynch, and R. E. Holland, *Bull. Am. Phys. Soc.* 4, 404 (1959).

^cF. R. Metzger, *Phys. Rev.* 127, 220 (1962).

^dAssumed $B(E2) < 100 B(E2)_{sp}$.

^eA. W. Schardt and J. P. Welker, *Phys. Rev.* 99, 810 (1955).

GAMMA-RAY SPECTROSCOPY WITH A LITHIUM-DRIFTED GERMANIUM DETECTOR

R. L. Robinson P. H. Stelson F. K. McGowan
 J. L. C. Ford, Jr. W. T. Milner

The energies of gamma rays from about 50 nuclides have been determined to within a few tenths of a kev by means of a lithium-drifted germanium detector. This accuracy is about an order of magnitude better than has generally been achieved with the NaI crystal, due principally to the superior resolution of the germanium detector. For example, the width of a peak of a 320-kev gamma ray is 3.7 kev as measured with our germanium detector and 31 kev as measured with an NaI crystal. A second advantage of the germanium semiconductor over the scintillation spectrometer in energy determinations is that its energy response is linear. Furthermore, the gain stability of a germanium detector is better than that of an NaI detector.

Although data were obtained with a variety of instrumentation, the electronics for the greater part consisted of a Tennelec 100C preamplifier, a Tennelec TC-200 amplifier, and an 800-channel Victoreen analyzer. The detector, which had an active volume of 0.2 cm³, was vacuum packed in a thin-walled aluminum container.¹ It was connected to the preamplifier via a special, low-

¹Fabricated by R. J. Fox of the Instrumentation and Controls Division.

Table 1. Energies of Calibration Gamma Rays

Isotope	E_{γ} (kev)
²⁰³ Hg	279.12 ± 0.05
¹⁹⁸ Au	411.76 ± 0.03
Annihilation radiation	510.976 ± 0.007
²⁰⁷ Bi	569.6 ± 0.5
¹³⁷ Cs	661.62 ± 0.15
⁸⁸ Y	898.4 ± 0.4
²⁰⁷ Bi	1063.7 ± 0.3
⁶⁰ Co	1173.0 ± 0.2
⁶⁰ Co	1332.7 ± 0.2

capacitance, 6-in.-long connector. This permitted submersing the detector into a Dewar flask containing a 30-hr supply of liquid nitrogen. The total input capacitance, which needs to be a minimum to optimize the intrinsic resolution, was 10 pf. The linearity of the electronic system was checked by replacing the detector with a signal generator capable at maximum output of producing pulses with an amplitude known to 1 part in 10⁵.² Gamma-ray energies were determined by measuring the transition in question with two or more radioactive sources producing gamma rays of known energies. The calibration sources are listed in Table 1. Errors assigned to the measured energies incorporate statistically the uncertainties in the energies of the calibration lines and in the reading errors of the peaks in the spectra.

Table 2 lists energy values estimated by this method for gamma rays which are frequently used as energy standards but which had greater uncertainties than those listed in Table 1. Table 3 contains energies found for gamma rays resulting from the decay of the radioactive nuclei ¹⁰²Rh and ¹⁰⁶Rh. In both nuclei, two near-lying transitions between two members of the "two-phonon" states and the first 2⁺ state were resolved. These can be seen

²We are indebted to J. A. Biggerstaff for the use of a precision pulser which he designed.

Table 2. Energies Determined for Transitions Frequently Used as Calibrations

Isotope	E_{γ} (kev)
⁵¹ Cr	319.8 ± 0.3
⁷ Be	477.4 ± 0.2
⁵⁴ Mn	835.0 ± 0.3
⁶⁵ Zn	1115.6 ± 0.4
²² Na	1274.6 ± 0.3
⁸⁸ Y	1836.2 ± 0.3

Table 3. Energies of the Prominent ^{106}Rh and ^{102}Rh Gamma Rays

E_{γ} , ^{106}Rh (keV)	E_{γ} , ^{102}Rh (keV)
511.6 ± 0.5	418.2 ± 0.5
616.2 ± 0.9	475.2 ± 0.5
622.2 ± 0.5	628.1 ± 0.5
873.5 ± 0.7	631.6 ± 0.5
1049.8 ± 0.7	698.0 ± 0.5
1127.4 ± 0.7	767.6 ± 0.5
1562.5 ± 1.1	1047.2 ± 0.7
	1103.3 ± 0.7
	1113.2 ± 0.7

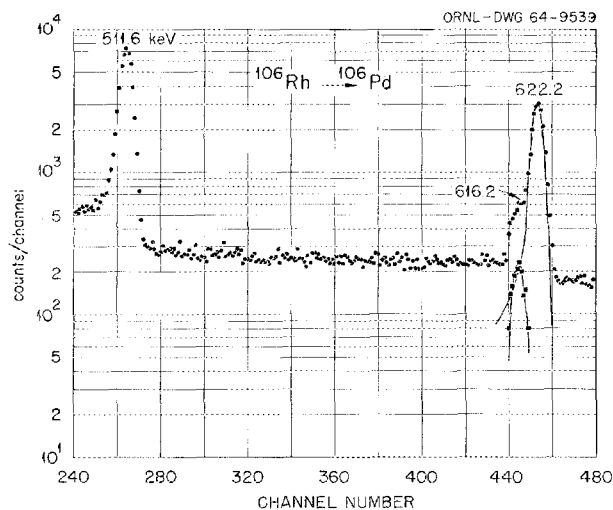


Fig. 1. Spectrum of Gamma Rays Between 500 and 640 keV from ^{106}Rh .

for ^{106}Rh in Fig. 1 at 622.2 and 616.2 keV. The ratio of their intensities was estimated as 14 ± 2 . In ^{102}Rh the gamma rays of the doublet have energies of 631.6 and 628.1 keV and an intensity ratio of 10 ± 2 . Figure 2 illustrates the gamma-ray spectrum of ^{102}Rh . The observed transitions fit energetically into a decay scheme (see Fig. 2) proposed by McGowan and Stelson.³

³F. K. McGowan and P. H. Stelson, *Phys. Rev.* **123**, 2131 (1961).

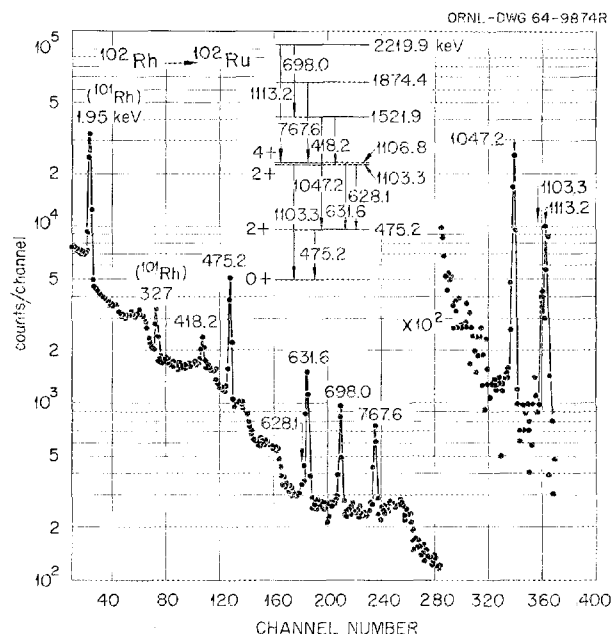


Fig. 2. Gamma-Ray Spectrum of ^{102}Rh .

Table 4 contains energies determined for gamma rays resulting from Coulomb excitation. They were induced by bombarding thick targets of the enriched isotopes with 7- to 9-MeV alpha particles. In several spectra a line due to the $^{18}\text{O}(\alpha, n)^{21}\text{Ne}$ reaction was observed. From this, the energy for the first excited level of ^{21}Ne was estimated as 350.2 ± 0.8 keV.

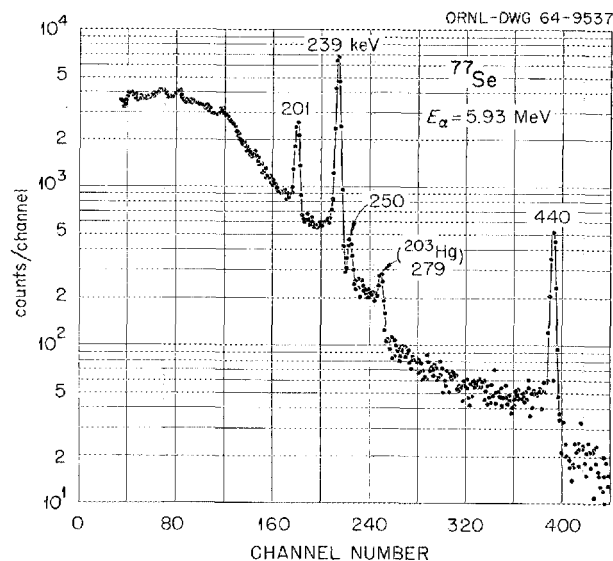
The spectrum of gamma rays from Coulomb-excited ^{77}Se is illustrated in Fig. 3. In our previous Coulomb-excitation investigation of this nucleus,⁴ the presence of the weak 250-keV transition could only be inferred from gamma-gamma coincidence results, and its intensity could only be deduced in an indirect manner. Here, the transition is clearly resolvable from the strong 239-keV gamma ray. From the ratio of the intensities of the 250- to the 239-keV gamma rays (0.035 ± 0.007), a new estimate of $(0.97 \pm 0.23) \times 10^{-50} e^2\text{cm}^4$ was determined for the $B(E2)_{\text{ex}}$ of the 250-keV level. This is about twice that predicted by the single-particle estimate.

⁴R. L. Robinson, F. K. McGowan, and P. H. Stelson, *Phys. Rev.* **125**, 1373 (1962).

Table 4. Energies of Gamma Rays Resulting from Coulomb Excitation

Isotope	E_{γ} (keV)	Isotope	E_{γ} (keV)
$^{48}_{22}\text{Ti}$	983.1 \pm 1.5	^{108}Pd	433.9 \pm 0.2
$^{50}_{24}\text{Cr}$	783.1 \pm 0.4	^{110}Pd	373.8 \pm 0.3
$^{56}_{26}\text{Fe}$	846.8 \pm 0.6	$^{106}_{48}\text{Cd}$	632.8 \pm 0.2
$^{64}_{30}\text{Zn}$	991.7 \pm 0.7	^{108}Cd	633.2 \pm 0.2
^{66}Zn	1039.2 \pm 0.9	^{112}Cd	617.4 \pm 0.3
^{68}Zn	1077.6 \pm 0.8	^{114}Cd	558.5 \pm 0.3
^{70}Zn	883.7 \pm 0.7	^{116}Cd	513.1 \pm 0.2
$^{70}_{32}\text{Ge}$	1039.8 \pm 0.7	$^{112}_{50}\text{Sn}$	1257.3 \pm 0.9
^{72}Ge	834.8 \pm 0.6	^{116}Sn	1293.3 \pm 0.8
^{74}Ge	596.0 \pm 0.3	^{117}Sn	861.4 \pm 0.6
^{76}Ge	563.2 \pm 0.3		1004.3 \pm 0.8
$^{77}_{34}\text{Se}$	200.7 \pm 1.0	^{118}Sn	1230.2 \pm 0.9
	239.1 \pm 1.0	$^{119}_{50}\text{Sn}$	898.4 \pm 0.6
	250.1 \pm 1.0		921.6 \pm 0.6
	439.9 \pm 1.0	^{120}Sn	1171.5 \pm 1.0
$^{79}_{35}\text{Br}$	217.5 \pm 1.0	^{122}Sn	1140.2 \pm 1.0
	262.0 \pm 1.0	^{124}Sn	1131.4 \pm 0.9
	306.5 \pm 1.0	$^{121}_{51}\text{Sb}$	572.8 \pm 0.4
	522.2 \pm 2.0	^{123}Sb	160.2 \pm 0.3
$^{94}_{42}\text{Mo}$	871.1 \pm 0.7		381.6 \pm 0.3
^{96}Mo	778.5 \pm 0.6		542.4 \pm 1.1
^{98}Mo	786.8 \pm 0.4	$^{122}_{52}\text{Te}$	564.4 \pm 0.9
^{100}Mo	535.5 \pm 0.3	^{124}Te	602.8 \pm 0.8
$^{96}_{44}\text{Ru}$	832.6 \pm 0.6	^{126}Te	666.5 \pm 0.8
^{100}Ru	539.6 \pm 0.3	^{128}Te	743.2 \pm 0.8
^{104}Ru	357.7 \pm 0.3	^{130}Te	839.9 \pm 0.8
$^{104}_{46}\text{Pd}$	555.5 \pm 0.4	$^{195}_{78}\text{Pt}$	98.9 \pm 0.5
^{106}Pd	511.7 \pm 0.3		139.8 \pm 0.4
			211.2 \pm 0.3
			239.0 \pm 0.3

Fig. 3. Spectrum of Gamma Rays from Coulomb Excitation of ^{77}Se .



DECAY OF $^{79}\text{Kr} \rightarrow ^{79}\text{Br}$

R. L. Robinson

RADIOACTIVITY. ^{79}Kr [from $^{79}\text{Br}(p,n)$], measured E_γ , I_γ , $\gamma\gamma$ spectra. ^{79}Br deduced levels, $\log ft$, J , π . Natural target.

From our Coulomb excitation studies,¹ it was possible to establish the reduced $E2$ transition probabilities for excitation, $B(E2)_{ex}$, for seven low-lying levels of ^{79}Br . However, the $B(E2)_d$ and $B(M1)_d$ for the majority of gamma rays could not be ascertained because of insufficient knowledge of level spins and gamma-ray multipole admixtures. In principle, the situation could be clarified through the measurement of the directional angular correlations of coincident gamma rays from levels of ^{79}Br . An investigation of gamma rays

from the decay of ^{79}Kr provides the best method of procuring this type of data; thus such a study was initiated. Unfortunately, because of the complexity of the decay, the original goal has not yet been achieved. However, information was obtained about the levels populated through the decay of ^{79}Kr and the branching ratios of gamma rays from these levels.

Four samples of ^{79}Kr were produced by bombarding KBr with an $\sim 8\text{-}\mu\text{a}$ beam of 4.1-Mev protons from 4 to 12 hr. To eliminate the contributions from activities with short lifetimes, gamma-ray studies were not undertaken until several hours after the completion of a bombardment. No chemistry was performed. A typical singles gamma-ray

¹R. L. Robinson, F. K. McGowan, and P. H. Stelson, *Bull. Am. Phys. Soc.* **8**, 60 (1963); and private communication.

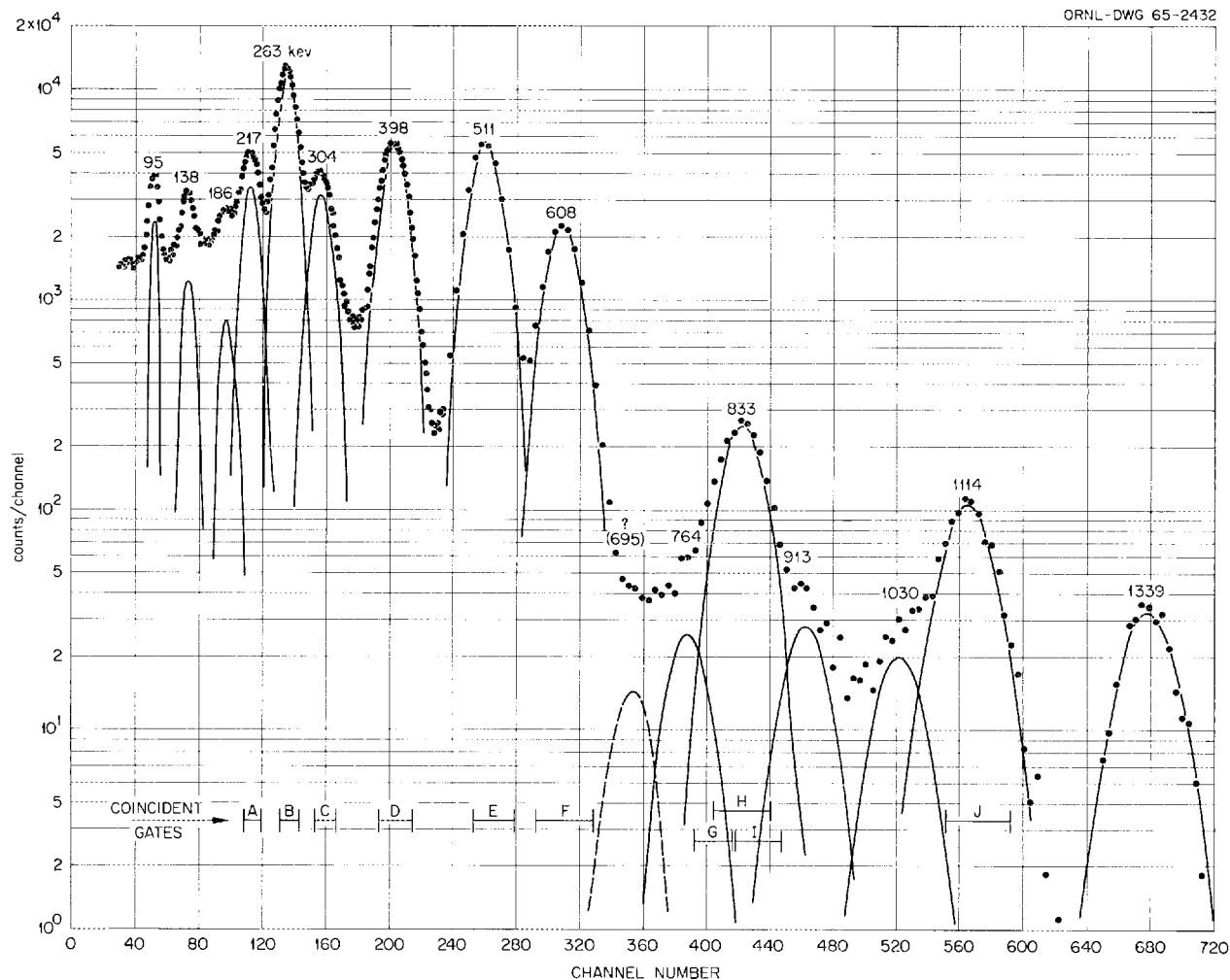


Fig. 1. Gamma-Ray Spectrum of ^{79}Kr as Measured with an NaI Crystal. The segments labeled A through J in the lower part of the figure indicate the gates used in the gamma-gamma coincidence studies.

spectrum as taken with a 3- by 3-in. NaI crystal is shown in Fig. 1. The rate of decay of the 12 strongest peaks was followed over a period of up to 300 hr. All but the peaks at 95, 186, and 1114 keV were found to have half-lives consistent with the 35-hr half-life reported for ^{79}Kr .²

Singles spectra were also taken with a lithium-drifted germanium detector which had an active volume of 0.2 cm^3 . As can be seen from one of these spectra, which is illustrated in Fig. 2,

additional gamma rays were revealed. Energies of the gamma rays in this figure were determined to approximately 1 keV.

Ten gamma-gamma coincidence spectra were measured. The energy intervals of the gating gamma rays are shown in the lower part of Fig. 1. Gamma-ray intensities were deduced from these spectra and also from the singles spectrum in the figure. The relative intensities of members of three doublets at 207.5-217.1, 299.2-306.8, and 389.5-398.0 keV, which could not be resolved in the singles scintillation spectrum, were estimated from the spectrum as measured with the germanium detector.

²Nuclear Data Sheets, National Academy of Science -- National Research Council, Washington, D. C.

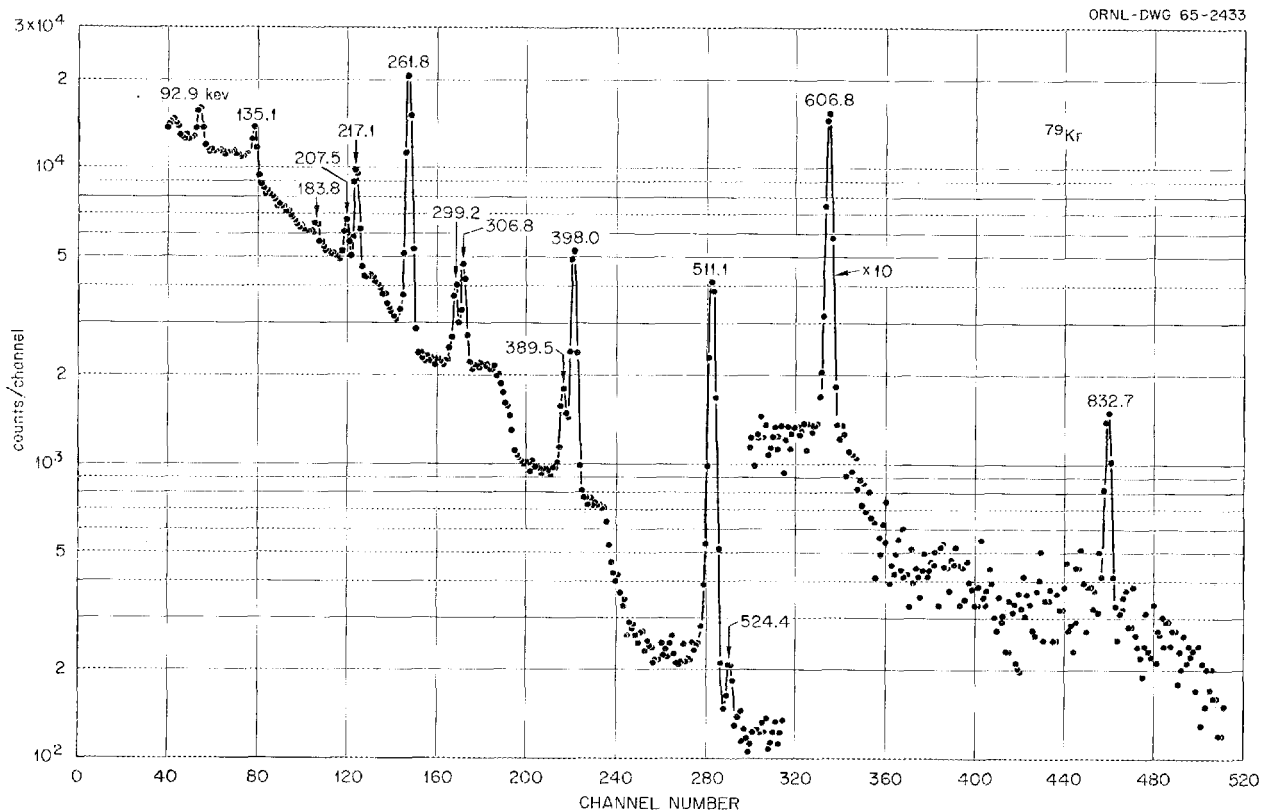


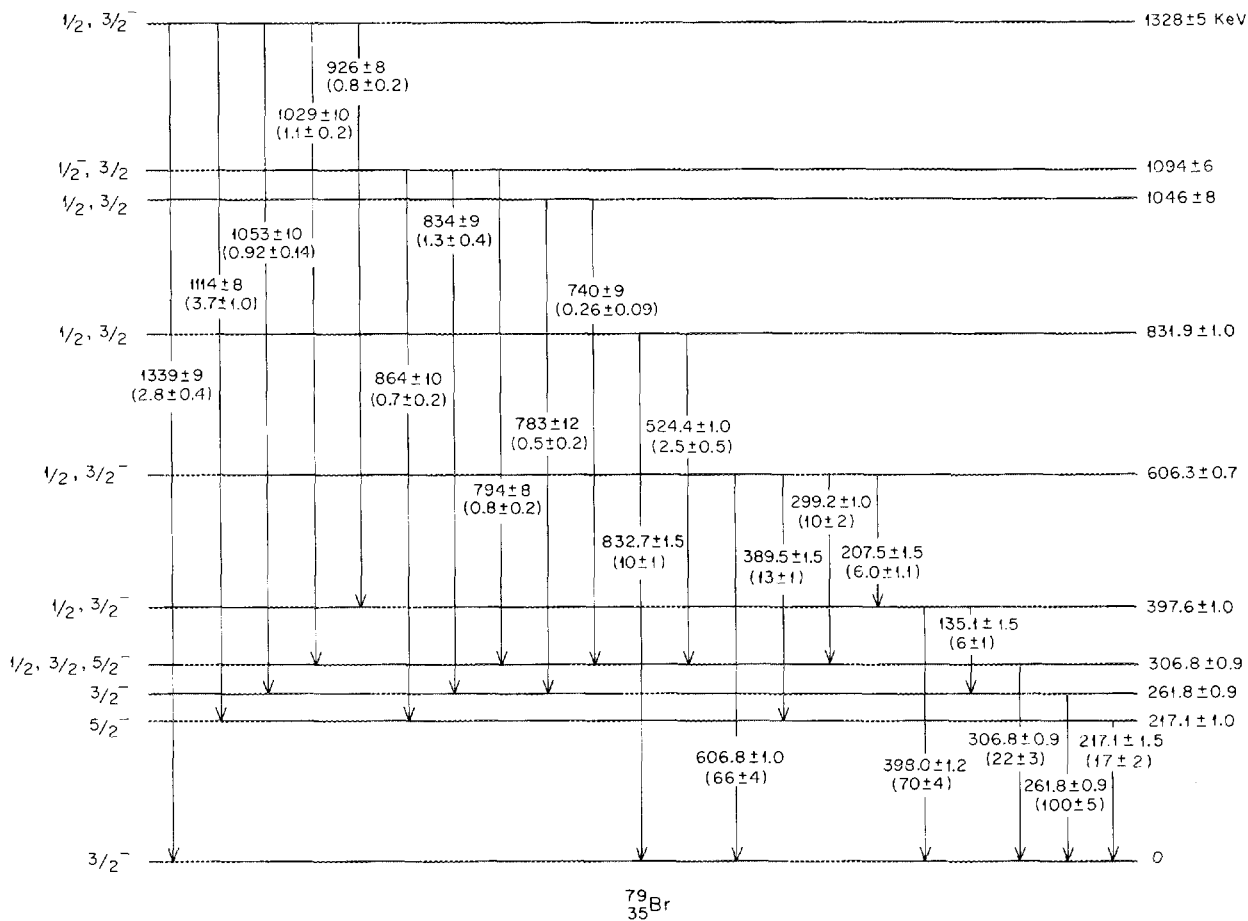
Fig. 2. Gamma-Ray Spectrum of ^{79}Kr as Measured with a Lithium-Drifted Germanium Detector.

A proposed decay scheme consistent with the present investigation is given in Fig. 3. The pair of numbers associated with each transition gives its energy in keV and the relative intensity as normalized to 100 for the 261.8-keV gamma ray. The spins and parities shown for the levels below 700 keV are those obtained in previous investigations.^{1,2} If the energy difference between ^{79}Kr and ^{79}Br is taken as 1620 keV,² the $\log ft$ values for decay by electron capture to the 1328-, 1094-, 1046-, and 831.9-keV levels are, respectively, 5.8, 6.8, 7.5, and 6.4. Since the ground-state spin of ^{79}Kr is $\frac{1}{2}$, the $\log ft$ values established that the spins of these states are $\frac{1}{2}$ or $\frac{3}{2}$. The low value of the $\log ft$ associated with population of the 1328-keV state indicates that its parity is the same as the ground state of ^{79}Kr (i.e., odd). Spin $\frac{3}{2}$ is slightly favored over $\frac{1}{2}$ for the 1328-keV state because gamma rays with similar intensities from

this level terminate at spin $\frac{3}{2}$ and spin $\frac{5}{2}$ states. An assignment of $\frac{1}{2}^+$ for the 1094-keV level can be ruled out, since an $M2$ transition would not be as intense as the 864-keV gamma ray was found to be.

Three other levels are known to exist in ^{79}Br below 1.5 MeV which are not included in Fig. 3. Two, with energies of 526 and 765 keV, were disclosed through Coulomb excitation studies,¹ and a third, a $\frac{9}{2}^+$ isomeric state at 208 keV, was located through (p,γ) studies.³ There are a number of indications in the present investigation that the complexity of the ^{79}Kr decay is considerably greater than shown in Fig. 3. However, a more thorough investigation is needed to establish the reality of weak transitions and other levels.

³A. Goodman and A. W. Schardt, *Bull. Am. Phys. Soc.* 4, 56 (1959).

Fig. 3. Energy-Level Diagram for ^{79}Br .INTERNAL BREMSSTRAHLUNG FROM $^6\text{He}^1$ J. K. Bienlein²

Frances Pleasonton

RADIOACTIVITY. ^6He measured shape of internal bremsstrahlung spectrum.

The spectrum of internal bremsstrahlung from the super-allowed beta emitter ^6He has been measured, using a sodium iodide scintillation spectrometer. The shape of the experimental spectrum agrees

with the theory of Knipp, Uhlenbeck, and Bloch for energies greater than 0.3 Mev. In this decay, Coulomb corrections are of little significance; thus the results can be interpreted as confirming the fundamental concept of internal bremsstrahlung as a process in which the electron exists first in a virtual state and then goes to its final state by emitting a photon.

¹Abstract of paper submitted to *Nuclear Physics*.

²Present address: CERN, Geneva, Switzerland; permanent address: Universitat Erlangen, Erlangen, Germany.

INTERNAL BREMSSTRAHLUNG ACCOMPANYING THE BETA DECAY OF ^{42}K ¹J. K. Bienlein²

Frances Pleasonton

RADIOACTIVITY. ^{42}K . Measured total yield of internal bremsstrahlung in the beta decay of $^{42}\text{K} \rightarrow ^{42}\text{Ca}$.

The total yield of internal bremsstrahlung in the decay of $^{42}\text{K} \rightarrow ^{42}\text{Ca}$ was measured with an NaI

scintillation spectrometer. The experimental results are higher than the yields predicted by theory. Over the internal bremsstrahlung energy range from 100 to 400 keV, the ratio of experiment to theory decreases from about 5 to 3 (Knipp, Uhlenbeck, and Bloch) or from about 3 to 2 (Felsner).

¹Abstract of paper to be published in the *Proceedings of the International Conference on Nuclear Physics, Paris, 1964*, sponsored by IUPAP, UNESCO, and Societe Francaise.

²Presently at CERN, Geneva, Switzerland.

SOME HEAVY-ION STOPPING POWERS

C. D. Moak

M. D. Brown¹

The discovery of energy compounding through continuous stripping in the second stage of the Tandem Van de Graaff Accelerator has produced a source of heavy ions of accurately known energies, closely simulating fission fragments, and having the useful property of a series of lines of different energies ranging from 10 to 100 MeV.² The spectrum of the lines observed is illustrated for bromine in Fig. 1 and for iodine in Fig. 2. It should be noted that the width of the lines shown in these figures is characteristic of the solid-state detector used; the lines would be quite sharp for a perfect detector.³ A feature of the bromine spectrum is that both ^{79}Br and ^{81}Br contribute to give a double peak. Since Fig. 1 was made, a technique has been devised whereby either ^{79}Br or ^{81}Br can be suppressed at the accelerator ion source.

Stopping powers of several materials have been measured by placing foils of known thicknesses in front of the detector and measuring the shifts of the various peaks. Foils of Be, C, Al, Ni, Ag, and Au were prepared by evaporation onto very thin carbon films. The resulting foils are thought to be reasonably polycrystalline, but no information as to crystal size is available for the foils used. Foil thicknesses were measured by obtaining alpha-particle energy-loss data for each foil and converting these to thickness with the aid of alpha-particle stopping-power curves provided by Whaling.⁴

The curves shown in Figs. 3 and 4 illustrate the results obtained. Experimental errors are thought to be mostly systematic in that alpha-particle stopping-power errors would be contained in the results, as well as any systematic errors contained in the procedure for foil thickness measurement. Total experimental error is believed to be $\pm 10\%$ for the final results shown in Figs. 3 and 4.

¹Graduate student, University of Tennessee, Knoxville.

²C. D. Moak *et al.*, *Rev. Sci. Instr.* **34**, 853 (1963).

³F. J. Walter *et al.*, *Bull. Am. Phys. Soc.* **8**, 39 (1963).

⁴W. Whaling, private communication.

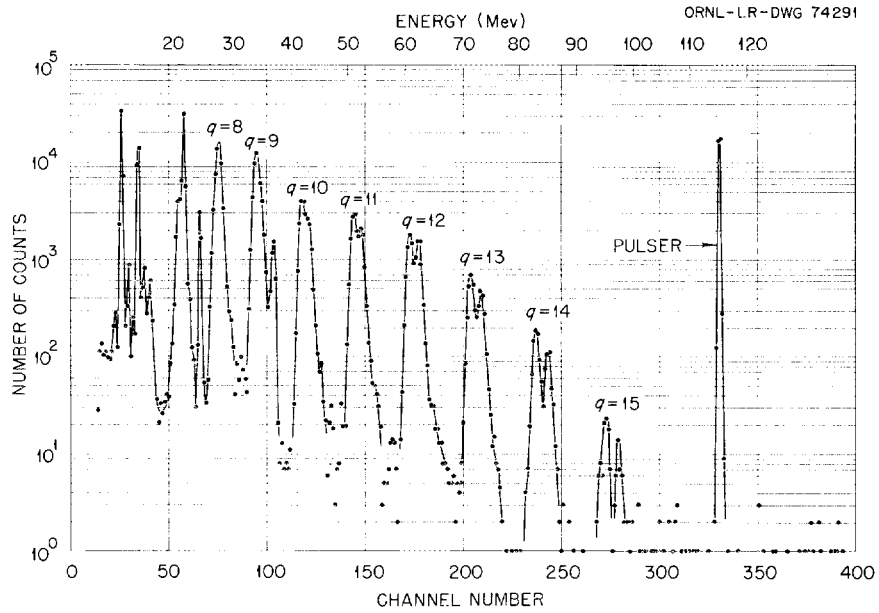


Fig. 1. Pulse-Height Spectrum of Bromine Ions from the Oak Ridge Tandem Van de Graaff Accelerator. The ions are deflected through a 90° analyzing magnet onto a silicon surface barrier detector.

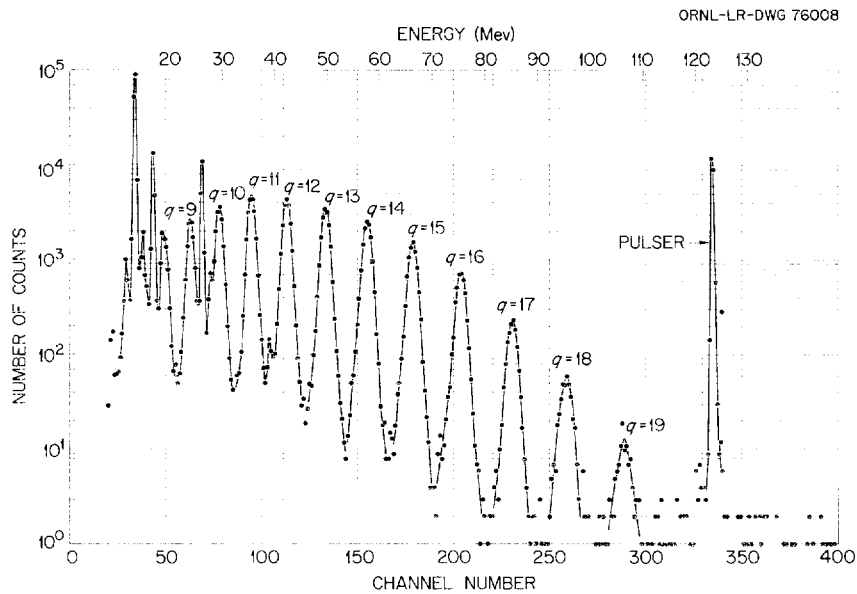


Fig. 2. Pulse-Height Spectrum of Iodine Ions from the Oak Ridge Tandem Van de Graaff Accelerator. The ions are deflected through a 90° analyzing magnet onto a silicon surface barrier detector.

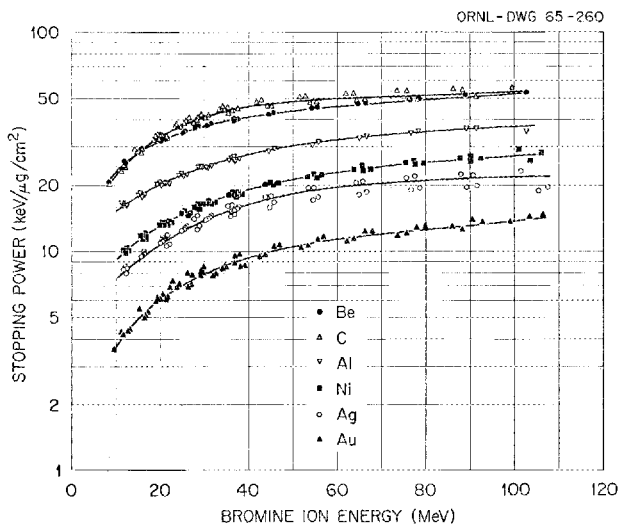


Fig. 3. Bromine Ion Stopping Powers.

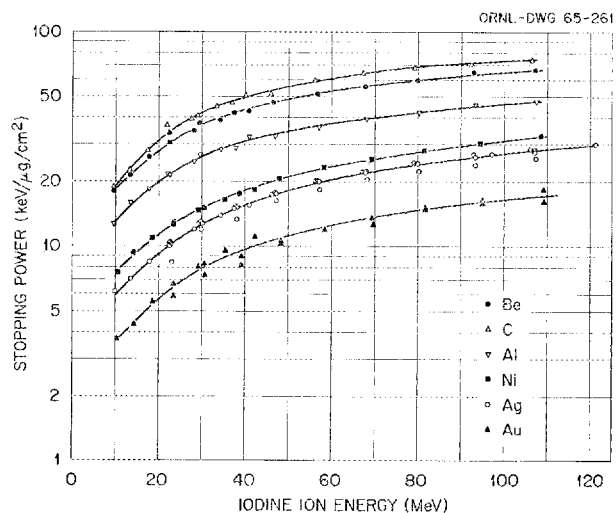


Fig. 4. Iodine Ion Stopping Powers.

RESPONSE OF GERMANIUM AND SILICON DETECTORS TO ENERGETIC BROMINE AND IODINE IONS

W. W. Walker¹

C. D. Moak

J. W. T. Dabbs

In silicon semiconductor detectors, a "pulse-height defect" of several Mev (equivalent) at energies of ~ 50 to 100 Mev for heavy ions and fission fragments, together with rather poor resolution (~ 1 Mev full width at half maximum) for such particles, has been known for some time.² The mechanisms responsible for these deviations from the ideal response are unknown. In view of this, it seemed desirable to study the behavior of germanium semiconductor detectors in the hope that a comparison with silicon detectors might provide a clue toward understanding these effects.

We have therefore fabricated a number of germanium surface-barrier detectors and exposed them to energetic ^{79}Br and ^{127}I ions from the Tandem Van de Graaff Accelerator, to spontaneous fission fragments from ^{252}Cf , and to alpha particles from

^{241}Am and ^{252}Cf . The fabrication technique was essentially the same as that used previously for silicon: Wafers $\frac{1}{4}$ in. in diameter by 1 mm thick were cut from a large slice of *n*-type germanium (G-5-6; 45.6 ohm-cm at 294°K, 25.8 ohm-cm at 77°K; 1.1×10^{13} net donor impurities per cm^3). After lapping with 1850-mesh Al_2O_3 , the wafers were etched (all surfaces) in modified CP-4 (4.5 acetic acid, 5HNO₃, 3HF) for a period of 1 to 6 min, followed by removal to a 5-cm³ H₂O bath for 15 to 90 min, where a very slow etching action continued. After rinsing and drying, the wafers were mounted in lavite rings³ with a low-temperature epoxy.⁴ Two wafers were given a 10-min soak in 80°C, 1% sodium dichromate solution. Only one of these was of acceptable quality, however. The detectors had active areas of 2 to 6 mm². After

¹1964 summer research participant from the University of Alabama.

²F. J. Walter *et al.*, *Bull. Am. Phys. Soc.* **8**, 39 (1963); H. W. Schmitt *et al.*, *Proc. Intern. Conf. Phys. Chem. Fission, Salzburg, March 1965*, IAEA, Vienna, 1965.

³R. J. Fox, *Semiconductor Nuclear Particle Detectors*, ed. by J. W. T. Dabbs and F. J. Walter, NAS-NRC Publication 871 (1961).

⁴Grodan "Hivac No. 1" containing 1.8 g per g of resin "X-16" filler.

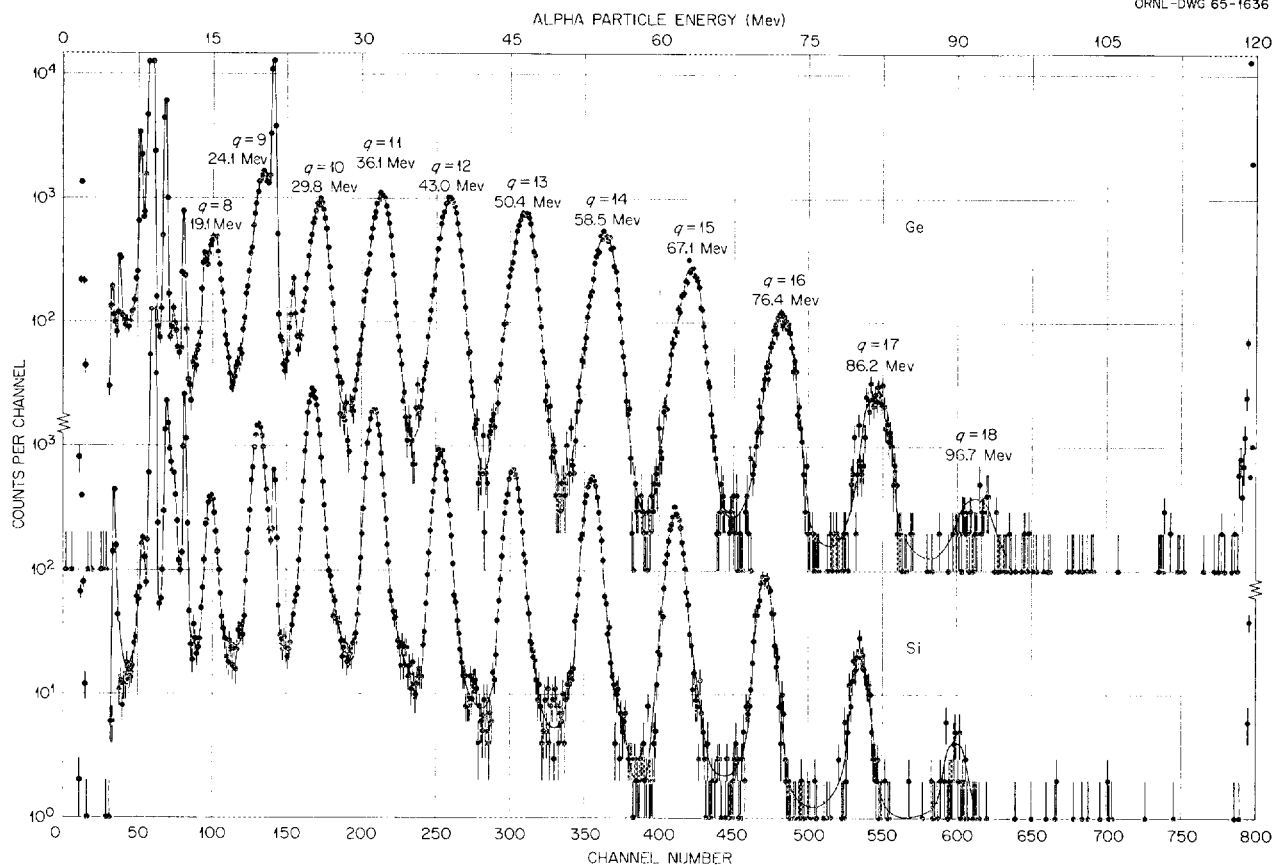


Fig. 1. Pulse-Height Spectrum of ^{127}I Ions; (a) Taken with Ge Surface Barrier Detector at 77°K , and (b) Taken with an Si Surface Barrier Detector at 300°K .

evaporating gold ($\sim 50 \mu\text{g}/\text{cm}^2$) on both sides, the detectors were tested for alpha-particle resolution. Rather surprisingly, seven of ten detectors fabricated gave good alpha-particle resolutions. Two had resolutions of $\sim 20 \text{ keV}$ (full width at half maximum) for alpha particles at 77°K .

For purposes of comparison, several silicon detectors were studied along with the germanium detectors. The silicon detectors used were prepared by the sodium dichromate method, which had been shown to produce good results for fission fragments.⁵

Pulse-height spectra for the two types of detector are shown in Fig. 1. Clearly the germanium detector has poorer resolution, but it may be that different surface treatments would produce better results. Curves of pulse height vs energy for

bromine and iodine ions for germanium detectors are shown in Fig. 2. The horizontal lines shown crossing the curves correspond to the pulse-height locations of heavy and light fragment peaks from spontaneous ^{252}Cf fission.

Analysis of the response curves for the six germanium detectors tested shows some variation in both "pulse-height defect" and in the slope. As with silicon detectors, the defects are larger for iodine ions than for bromine ions, and in the case of iodine ions, the slope differs from the slope of the extrapolated alpha-particle response by a significant amount.

It would seem that these experiments indicate that detector resolution and detector "pulse-height defect" are not necessarily related, since variations of resolution without variation of "pulse-height defect" have been observed. It may be that further improvements in resolution are to be found through improvements in fabrication technique.

⁵F. J. Walter, *IRE Trans. Nucl. Sci.* 11(3), 232 (1964).

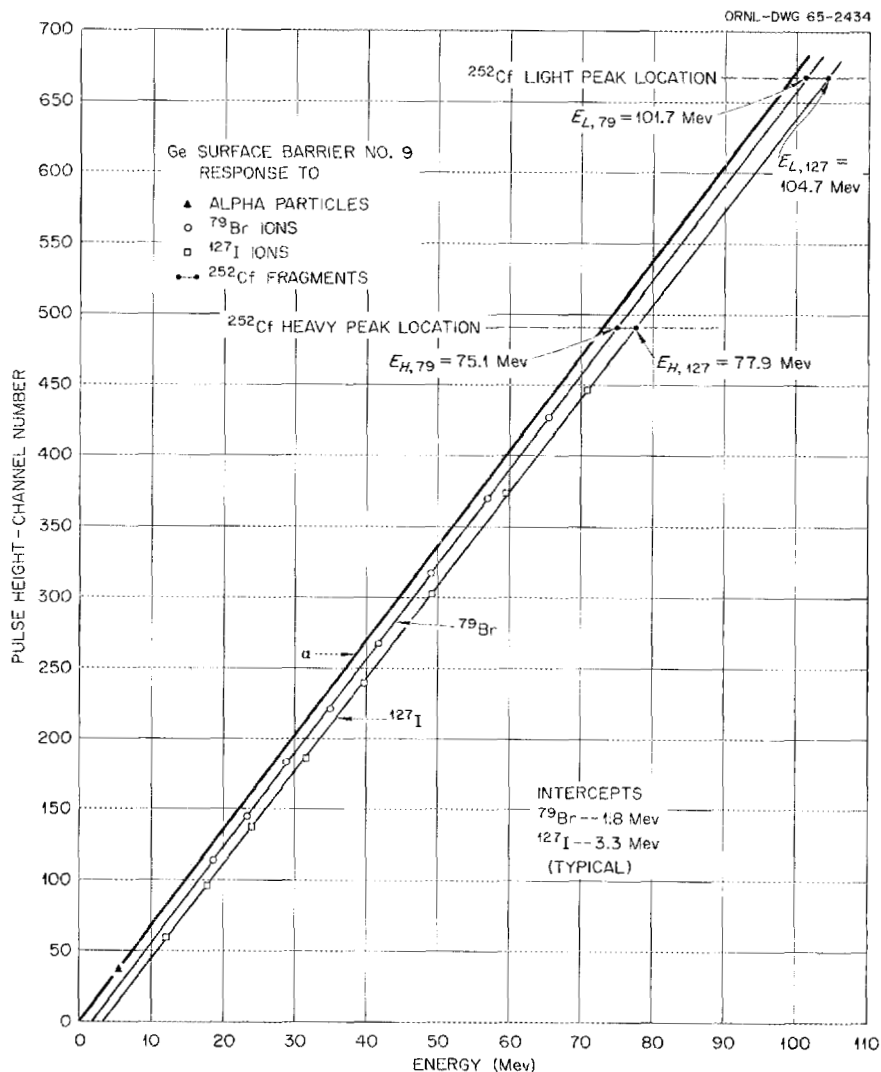


Fig. 2. Pulse Height vs Energy; ⁷⁹Br and ¹²⁷I Ions on 77°K Ge Detector. Horizontal lines are pulse height locations of heavy and light fragment peaks from spontaneous ²⁵²Cf fission.

FISSION OF ORIENTED NUCLEI

J. W. T. Dabbs G. W. Parker¹

During this report period the cryostat modifications mentioned in the last report² have been

¹Reactor Chemistry Division.

²J. W. T. Dabbs, F. J. Walter, and G. W. Parker, *Phys. Div. Ann. Progr. Rept. Jan. 31, 1964*, ORNL-3582, pp. 121-26.

completed, and the apparatus has been returned to the ORR. A number of unexpected difficulties appeared, however, and much time and effort have been required to resolve them. These primarily revolve around the attempt to increase the counting rates by approximately an order of magnitude.

Three major difficulties appeared, as follows:

1. The rotating counter arrangement was found to operate at a much higher temperature than expected because of the difficulty in making an adequate flexible braid heat shunt from the rotating counter assembly to liquid-nitrogen temperatures. This situation has been improved to the point that the temperature of the detectors is $\sim 89^\circ\text{K}$ (with the N_2 bath at 81°K under delivery pressure). At this temperature, radiant heat from the detectors is 46% higher than previously.
2. The sample container surface exposed to radiant heat from the detectors is now 30 cm^2 compared with 3 cm^2 previously. The total heat input from radiation is thus ~ 15 times larger than before. It has been found necessary to evaporate gold on the exposed surfaces to reduce their absorptivity; even in these circumstances a heat input of more than 0.5 mw is obtained. After considerable improvement in the efficiency of the ^3He refrigerator, a temperature of 0.50 to 0.51°K appears to be the limit attainable in the present apparatus. The evaporating ^3He has a temperature of 0.42°K . A "Kapitza resistance" occasioned by the acoustical impedance mismatch for phonons crossing the metal-helium boundaries is probably responsible for the observed temperature difference.
3. The area of the thin ($225\text{ }\mu\text{g}/\text{cm}^2$) nickel window has been enlarged from 3 cm^2 to 27 cm^2 ; this order of magnitude increase in area has made the task of fabricating gas-tight windows much more difficult. It has been found necessary to obtain nickel foil from one supplier³

and have a nickel mesh of 20 lines per inch and 92% transmission electroformed (electroplated through a photoresist pattern) onto the surface by another supplier.⁴ The foils are backed with ~ 0.5 -mil copper, which is etched away after mounting.⁵ The inner side of the foil is then wetted with a 1 wt % solution of VYNS (polyvinyl chloride-acetate copolymer; $\sim 85\%$ chloride, 15% acetate) resin in cyclohexanone, and the excess drained off. Upon evaporation of the solvent, the resin makes a thin coating (estimated $40\text{ }\mu\text{g}/\text{cm}^2$) which covers minor pinholes in the foil. Further difficulties with differential shrinkage have required changes in the mounting methods; in particular, soft solder has been used to eliminate the shrinkage associated with epoxy use, although with care an epoxy mounting can be made. Following a leak detector test at 77°K , the window and support can are coated with evaporated gold to reduce the absorptivity as described above. A coating of $\sim 50\text{ }\mu\text{g}/\text{cm}^2$ is applied over the window area itself; a heavier coating is used over the can surfaces and any exposed epoxy or solder used in mounting.

The observed counting rates are indeed increased by a factor of ~ 9 , and all the electronic apparatus is in satisfactory operation. Data obtained to date, however, are insufficient to justify presentation here.

The assistance of W. W. Walker during a portion of his summer visit is gratefully acknowledged.

³Chromium Corporation of America, Waterbury, Conn. (Grade D Ni foil, 0.000010 in. thick).

⁴Buckbee-Mears Co., 245 E. 6th St., St. Paul, Minn.

⁵The selective etchant used is composed of CCl_3COOH , 100 g/liter and NH_4OH , 500 ml/liter.

FISSION FRAGMENT ENERGY CORRELATION EXPERIMENTS

H. W. Schmitt

J. H. Neiler¹F. J. Walter²

NUCLEAR FISSION. ²⁵²Cf and ²³⁵U, measured correlated fragment energies, deduced mass and energy distributions, mass-energy correlations.

Introduction

In order to understand the fission process, it is essential that details of the mass and energy distributions and mass-energy correlations in fission at low excitation energies be known. Further, it is necessary to obtain the absolute fragment energies as accurately as possible in order that valid, quantitative calculations of the parameters derived from these quantities may be made. An error of only 2% in total fragment kinetic energy, for example, is magnified to 20% or more in deduced fragment excitation energies.

Over the past several years, we have carried out fragment energy correlation experiments for a number of cases, including spontaneous fission of ²⁵²Cf; thermal-neutron-induced fission of ²³⁵U,^{3,4} ²³⁹Pu,^{5,6} and ²⁴¹Pu;⁶ resonance-neutron fission of ²³⁹Pu;⁵ and proton-induced fission of ²²⁶Ra.⁷ We have used many of the same techniques in studies of ternary fission³ and of prompt gamma rays accompanying fission.⁸ Previous reports have included descriptions of these experiments⁹ and have given partial results.³⁻⁸ It is only within the past year, however, that we have developed an accurate absolute energy

calibration for semiconductor detectors for fission fragments. This development was possible through a series of experiments^{10,11} with fission fragments and with heavy ions (⁷⁹Br, ⁸¹Br, and ¹²⁷I) accelerated in the Tandem Van de Graaff, together with a measurement of correlated energies and velocities of the heavy ions and ²⁵²Cf spontaneous fission fragments.¹²

Thus we are now able to analyze our energy correlation data with a proper absolute energy calibration. This work has been in progress for the past few months, and it is our purpose in this report to review the experiments briefly, to outline the present analysis, and to give the results as far as they have been carried for ²⁵²Cf spontaneous fission and ²³⁵U thermal-neutron fission. Although we have carried out some preliminary calculations which appear promising for future interpretation of the data, we shall postpone discussions along these lines until all the experimental data have been analyzed in detail.

Method and Apparatus

A description of the method and apparatus used in the ²³⁵U experiment is contained in an earlier publication.⁹ We have modified the logic circuitry

¹Present address: Oak Ridge Technical Enterprises Corp., Oak Ridge, Tenn.

²Present address: Radiation Instruments Development Laboratory, Oak Ridge, Tenn.

³H. W. Schmitt *et al.*, *Phys. Rev. Letters* **9**, 427 (1962).

⁴F. J. Walter *et al.*, *Phys. Div. Ann. Progr. Rept. Jan. 31, 1962*, ORNL-3268, p. 54.

⁵F. J. Walter *et al.*, *Phys. Div. Ann. Progr. Rept. Jan. 31, 1963*, ORNL-3425, p. 79.

⁶F. J. Walter, H. W. Schmitt, and J. H. Neiler, *Phys. Rev.* **133**, B1500 (1964).

⁷H. W. Schmitt, J. W. T. Dabbs, and P. D. Miller, *Proceedings of IAEA Symposium on the Physics and Chemistry of Fission, Salzburg, Austria, 1965*, to be published. (See also "Correlated Fragment Energy Measurements and Mass-vs-Angle Correlations in ²²⁶Ra: p Fission," this report.)

⁸H. Maier-Leibnitz, H. W. Schmitt, and P. Armbruster, *Proceedings of IAEA Symposium on the Physics and Chemistry of Fission, Salzburg, Austria, 1965*, to be published. (See "Average Number and Energy of Gamma Rays Emitted as a Function of Fragment Mass in ²³⁵U, Thermal-Neutron-Induced Fission," this report.)

⁹C. W. Williams *et al.*, *Nucl. Instr. Methods* **29**, 205 (1964).

¹⁰C. D. Moak *et al.*, *Rev. Sci. Instr.* **34**, 853 (1963).

¹¹H. W. Schmitt *et al.*, *Proceedings of IAEA Symposium on the Physics and Chemistry of Fission, Salzburg, Austria, 1965*, to be published. (See "Absolute Energy Calibration of Solid State Detectors for Fission Fragments and Heavy Ions," this report.)

¹²H. W. Schmitt, W. E. Kiker, and C. W. Williams, *Phys. Rev.* **137**, B837 (1965).

somewhat, and a block diagram of our present system is shown in Fig. 1. This system was used for the ^{252}Cf experiment. The linear circuitry indicated in Fig. 1 is self-explanatory. All units were connected into the system throughout the runs; periodic checks of stability and linearity of the system were made with the pulser. The function of the inspector circuit was to reject pileup pulses, that is, pulses resulting from the near superposition of a fission-fragment pulse with an accidental scattered-proton or natural alpha-particle pulse. Pairs of pulses in either detector whose time separations were in the range of 20 nsec to 2 μsec were detected by the inspector circuit, and the anticoincidence signals generated in such cases served to reject these events. When no pileup occurred, the two coincident fission-fragment pulse heights (channel numbers) were recorded event by event on punched paper tape; the data were sorted, summed, and otherwise processed by means of a digital computer.

The fissile deposit and backing are both relatively thin and uniform. In the present experiment the ^{252}Cf spontaneous fission source was

deposited by the self-transfer method (see Acknowledgments) onto a thin film of aluminum oxide in which the energy loss for fission fragments was $\lesssim 4$ Mev. The source strength was $\sim 3 \times 10^5$ fissions/min, and the ^{252}Cf deposit was about 1 cm^2 in area. The ^{235}U target was prepared by vacuum evaporation of $^{235}\text{UF}_4$ onto a carbon film about $20 \mu\text{g}/\text{cm}^2$ thick, for which the fragment energy loss was $\lesssim 3$ Mev. The deposit thickness was about $20 \mu\text{g}/\text{cm}^2$, and the area was about 1 cm^2 . The sample was $>99\%$ pure, and only a fraction of a percent of the impurity content consisted of other thermally fissionable materials. The neutron beam from the ORR was collimated so that no part of the beam struck the target mounting frame, detectors, or any other parts inside the chamber.

The fragments were collimated with rounded (i.e., doughnut-shaped) collimators. There are generally edge effects associated with solid-state detectors; these may occur at the edge of the silicon itself, where possible lower electric fields may give rise to reduced pulse heights, or at the inside edge of a protective layer (usually epoxy), where some of the fragments may be degraded in

ORNL-DWG 65-367

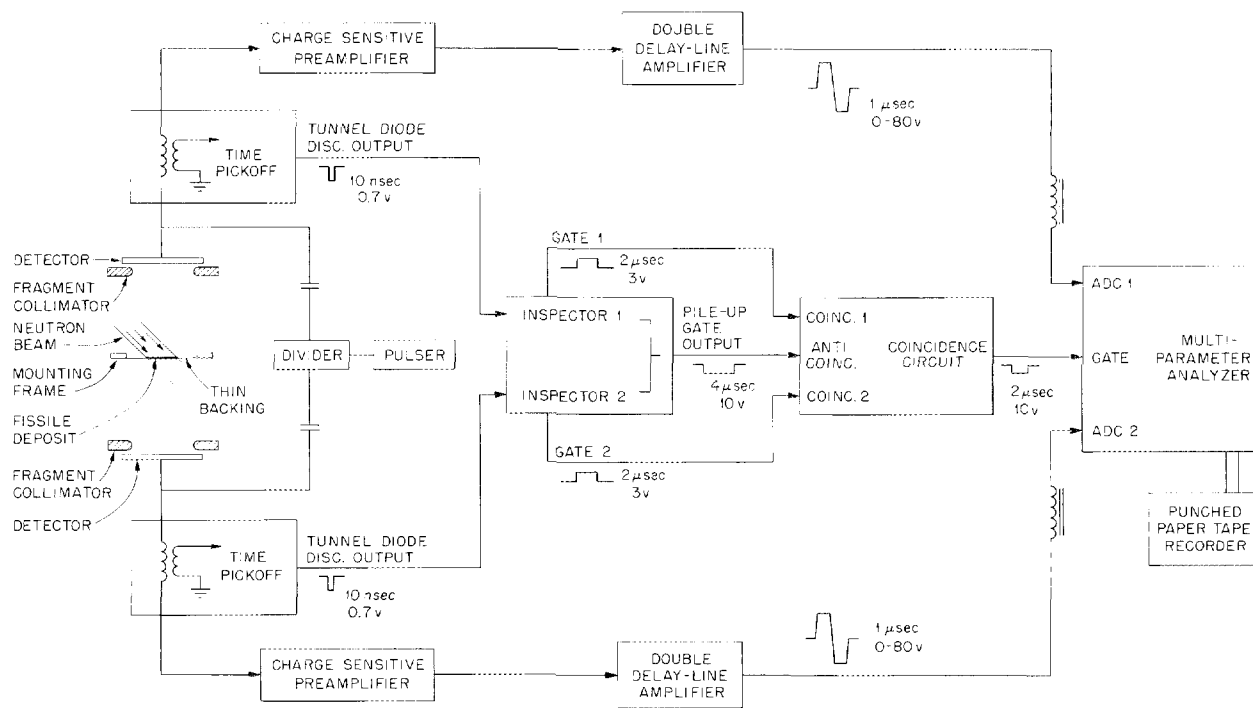


Fig. 1. Schematic Diagram of Source and Detector Arrangement and Block Diagram of Electronic Equipment for Fission-Fragment Energy Correlation Experiments.

energy before entering the silicon. The rounded, "doughnut-like" shape of the collimator minimizes the number of degraded and accidentally scattered fragments which are detected, provided the effective collimator surface area available to small-angle scattering¹³ is kept as small as possible while maintaining a radius large enough to completely stop the fragments incident at larger angles. Accordingly, we have used $\frac{1}{8}$ -in.-thick aluminum collimators, carefully rounded, with circular apertures of 3.5 to 3.8 cm² area — slightly smaller than the total effective detector area. In this arrangement, low-energy pulses due to tailing effects were almost completely absent. (These effects are not so important for light particles such as protons or alpha particles, and the problem of collimation is different in those cases.)

The detectors were surface-barrier detectors, ~ 4 cm² in area, matched as closely as possible. They were fabricated from ~ 500 -ohm-cm *n*-type silicon, and the front electrode of each detector consisted of a vacuum-evaporated gold film about 40 $\mu\text{g}/\text{cm}^2$ thick. The pulse-height response of these detectors was found to saturate satisfactorily (i.e., the same pulse heights and peak-to-valley ratios were obtained) for bias voltages between 50 and 150 v. A bias voltage of ~ 100 v was maintained throughout the experiments. The detectors exhibited alpha-particle resolutions of < 60 keV when tested with a standard low-noise, charge-sensitive amplifier.

Analysis

Neutron Emission. — It is necessary first to establish the relation between the initial and final energies of a fragment, with respect to neutron emission. For this purpose we consider a single fragment of initial mass m^* , final mass m after emission of ν neutrons, and initial and final energies E^* and E respectively. (We use the asterisk to refer to the excited, pre-neutron-emission fragments.) The neutrons are assumed to be emitted after the fragment has been fully accelerated. The angular distribution of the neutrons in the fragment center-of-mass system is assumed

to be isotropic. It is then easily shown that

$$\langle E \rangle = (m/m^*)E^* + E_R, \quad (1)$$

where E_R is the center-of-mass recoil energy of the fragment. The energy E_R is of the order of 0.1 MeV or less and is negligible, for most purposes, compared with the first term of Eq. (1).

To analyze the energy correlation experiments, we assume that mass and linear momentum are rigorously conserved before neutron emission. That is,

$$m_1^*E_1^* = m_2^*E_2^*, \quad (2)$$

$$m_1^* + m_2^* = A, \quad (3)$$

where the subscripts refer to fragments 1 and 2, and A is the mass of the fissioning nucleus. If we note that

$$m_i = m_i^* - \nu_i \quad (i = 1, 2), \quad (4)$$

then it is easily shown that the mass m_1^* is related to the measured energies as follows:

$$m_1^* = \frac{AE_2}{E_2 + E_1(1 + \xi_1)}, \quad (5)$$

where

$$\xi_1 = \nu_1/m_1 - \nu_2/m_2. \quad (6)$$

The equations for m_2^* are obtained by interchanging subscripts.

In most energy correlation experiments the values of ν_1 and ν_2 are not known as functions of both mass and energy, as would be required in Eqs. (5) and (6). Thus it appears most reasonable at present to analyze the energy correlation data according to simple, though slightly incorrect, relations and then to correct the functions and distributions of interest as accurately as possible for effects of neutron emission.

Data Processing and Analysis. — We write the following equations:

$$\mu_1 E_1 = \mu_2 E_2, \quad (7)$$

$$\mu_1 + \mu_2 = A, \quad (8)$$

¹³D. Engelkemeir and G. N. Walton, AERE-R 4716 (1964), unpublished.

where now the μ_i are "pseudo-masses" of the fragments and are obtained from the measured energies E_1 and E_2 as indicated. These quantities are not expected to differ greatly (< 2 amu) from the correct masses m_i^* , inasmuch as both fragments emit neutrons, and the error is to some extent canceled by the use of E_1 and E_2 in Eq. (7). It is readily shown that m_1^* is related to μ_1 and μ_2 through the equation

$$m_1^* = \mu_1 \left(1 - \frac{E_1}{E_1 + E_2} \xi_1 \right). \quad (9)$$

Expressing μ_1 solely in terms of the m_i^* and ν_i , we have

$$\mu_1 = m_1^* \left(1 + \frac{m_2^*}{A} \xi_1 \right). \quad (10)$$

The energies of Eqs. (7) and (9) are obtained with the aid of the mass-dependent pulse-height calibration equations for the particular detectors used in the experiment. It is sufficiently accurate to use the μ_i in the calibration equations, inasmuch as the coefficients of the mass-dependent terms are small enough so that errors in mass up to a few atomic mass units give rise to errors in energy of only ~ 0.2 Mev or less.

Detailed total kinetic energy distributions as a function of fragment mass (or mass distributions as a function of total kinetic energy) are required for study and comparison in theoretical approaches to fission. Thus we transform the data in the original pulse-height vs pulse-height matrix $N(x_1, x_2)$ to a pseudo-mass vs total kinetic energy matrix $\bar{N}(\mu_1, E_k)$ by means of the equation

$$N(\mu_1, E_k) = N(x_1, x_2) J \begin{pmatrix} x_1 & x_2 \\ m_1 & E_k \end{pmatrix}, \quad (11)$$

where $E_k = E_1 + E_2$, the total measured kinetic energy of the fragments. The mass-dependent energy calibration equations^{11,12} are

$$E_i = (a_i + a'_i \mu_i) x_i + b_i + b'_i \mu_i \quad (i = 1, 2), \quad (12)$$

and the appropriate equations for the transformation are then

$$x_1(\mu_1, E_k) = \frac{E_k(1 - \mu_1/A) - b'_1 \mu_1 - b_1}{a_1 + a'_1 \mu_1}, \quad (13)$$

$$x_2(\mu_1, E_k) = \frac{\mu_1 E_k/A - b'_2 A + b'_2 \mu_1 - b_2}{a'_2 A - a'_2 \mu_1 + a_2}, \quad (14)$$

$$\left| J \begin{pmatrix} x_1 & x_2 \\ \mu_1 & E_k \end{pmatrix} \right| = \left| (a_1 + a'_1 \mu_1)^{-1} (a_2 + a'_2 A - a'_2 \mu_1)^{-1} \right. \\ \times \left[\left(\frac{\mu_1}{A} \right) \left(\frac{a_1 E_k/A + a_1 b'_1 + a'_1 E_k - b_1 a'_1}{a_1 + a'_1 \mu_1} \right) \right. \\ \left. \left. + \left(1 - \frac{\mu_1}{A} \right) \left(\frac{a_2 E_k/A + a_2 b'_2 + a'_2 E_k - b_2 a'_2}{a_2 + a'_2 A - a'_2 \mu_1} \right) \right] \right|. \quad (15)$$

Although the equations are cumbersome, they are straightforward and have been programmed for computer use. We note in Eq. (11) that the value of $N(x_1, x_2)$ is required at the point x_1, x_2 , corresponding to the chosen values of μ_1, E_k . This quantity is obtained by a quadratic interpolation method described in a previous paper in connection with another experiment.¹²

An alternative to the transformation described in the preceding paragraph for obtaining the array $N(\mu_1, E_k)$ is as follows: The cells (1 channel \times 1 channel) in the data array $N(x_1, x_2)$ are subdivided into a number of smaller cells, and the number of counts in the original unit is divided equally among the smaller units. The coordinates μ_1, E_k are then calculated for the center of each of these smaller subboxes, and the assigned counts are then added to those in the μ_1, E_k interval in which the coordinates fall. We have analyzed the data of the present experiment by this method; each of the original units in the data array were divided into 100 subboxes for this analysis. Although the results of the two methods are in generally good agreement throughout the arrays, we feel (1) that the interpolation method is somewhat better where the statistical uncertainties in the data are small, so that advantage may be taken of the local shapes of the distributions,

and (2) that the "subboxing" calculation is somewhat better in regions where the statistical uncertainties are large and the number of counts is small. The results presented in the next section have been taken from both analyses in accordance with this evaluation, although only small differences would occur if either analysis were used alone.

From the array $N(\mu_1, E_k)$, we may now obtain the distribution of "pseudo-masses," $N(\mu_1)$:

$$N(\mu_1) = \sum_{E_k} N(\mu_1, E_k). \quad (16)$$

Then with a knowledge of the average number of neutrons emitted as a function of fragment mass, $\nu(m_1^*)$, we may obtain the pre-neutron-emission mass distribution, $N(m_1^*)$, from the relation

$$N(m_1^*)dm_1^* = N(\mu_1) \left. \frac{d\mu_1}{dm_1^*} \right| dm_1^*, \quad (17)$$

where, in the present analysis, the derivative is obtained numerically; $N(\mu_1)$ is determined (by interpolation) at the value of μ_1 corresponding to a particular integral value of m_1^* .

Similarly, we obtain the average measured total fragment kinetic energy (post-neutron-emission energy) $\langle E_k \rangle$ as a function of μ_1 from the relation

$$\langle E_k(\mu_1) \rangle = \frac{\sum_{E_k} E_k N(\mu_1, E_k)}{\sum_{E_k} N(\mu_1, E_k)}. \quad (18)$$

Again, from a knowledge of $\nu(m_1^*)$ we determine the value of μ_1 corresponding to a particular m_1^* from Eq. (10); then we obtain the average initial (i.e., pre-neutron-emission) total kinetic energy $\langle E_k^*(m_1^*) \rangle$ from the equation

$$\langle E_k^*(m_1^*) \rangle = \langle E_k(\mu_1) \rangle \left(1 + \frac{\nu_1}{A} \frac{\mu_2}{m_1} + \frac{\nu_2}{A} \frac{\mu_1}{m_2} \right). \quad (19)$$

Mass and Energy Resolution. — The energy resolution inherent in fragment-energy-correlation measurements is determined by the inherent resolution in the detectors and by the distributions in angle of emission, number, and energy of the neutrons emitted. The detector resolution has been measured and is of the order of 1.5 Mev (full width at half maximum, FWHM).^{11,12} The dispersion in

fragment energy due to the effects of neutron emission has been evaluated by Terrell¹⁴ with the assumption that the neutrons are emitted isotropically in the fragment center-of-mass system and that the angle of emission, number, and the energy of the neutrons may be treated as independent variables. In the present case the variance of the detector resolution function, σ_D^2 , is added to the variance due to neutron emission to obtain the total variance σ_E^2 of the single-fragment energy resolution function. The resolutions in mass and total kinetic energy are then obtained in terms of $\sigma_{E_1}^2$ and $\sigma_{E_2}^2$.

Results for ²⁵²Cf Spontaneous Fission

The correlation data array showing $N(x_1, x_2)$ is given in Fig. 2. Data were obtained in 256 × 256 channels. The numbers labeling the contours indicate the number of events per cell (1 channel × 1 channel). Lines of constant total kinetic energy E_k and of constant pseudo-mass μ_1 or μ_2 are included. As indicated in the previous section, a transformation to the array $N(\mu_1, E_k)$ was carried out. This array is shown in Fig. 3; numbers labeling the contours indicate the number of events per Mev per amu.

Complete two-dimensional data giving ν as a function of fragment mass and kinetic energy would be required to construct lines of constant m_1^* or E_k^* in the above arrays or to construct the array $N(m_1^*, E_k^*)$. Such data have been obtained,¹⁵ however, for general application to these and other energy correlation experiments, we have taken the approach indicated in the previous section; that is, we derive the parameters and functions of interest from the $N(\mu_1, E_k)$ array, with the effects of neutron emission included. The relation between μ_1 and m_1^* , based on the average neutron emission data of Bowman *et al.*,¹⁵ is given in Fig. 4.

The fragment mass distribution obtained from the present experiment is shown in Fig. 5. For comparison we show both the "pseudo-mass" distribution $N(\mu)$ and the pre-neutron-emission mass distribution $N(m^*)$ obtained from $N(\mu)$ and

¹⁴J. Terrell, *Phys. Rev.* **127**, 880 (1962).

¹⁵H. R. Bowman *et al.*, *Phys. Rev.* **126**, 2120 (1962); **129**, 2133 (1963).

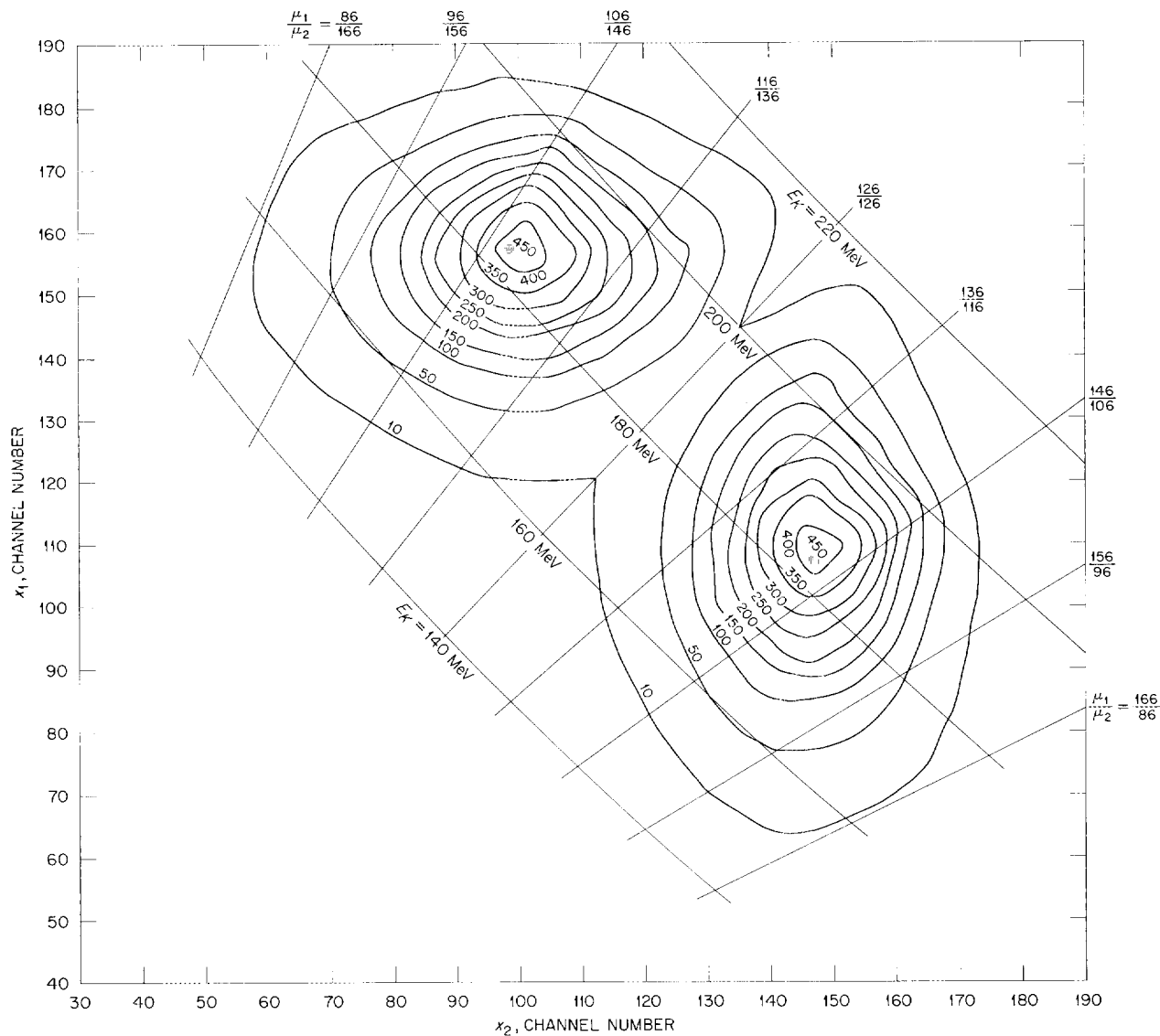


Fig. 2. Data Array $N(x_1, x_2)$ for ^{252}Cf Spontaneous Fission.

$\nu(m^*)$ as indicated in the analysis. The distribution $N(m^*)$ obtained by Whetstone¹⁶ from double velocity measurements is also shown; the distribution obtained by Fraser *et al.*¹⁷ differs only slightly from that of Whetstone. No corrections have been made for resolution in any of the data of Fig. 5. We note that the mass resolution in the present energy correlation experiment is ~ 4 amu

(FWHM), compared with ~ 2 amu (FWHM) for the double velocity experiments. Therefore, some of the fine structure of Whetstone's distribution is not reproduced clearly in our mass distribution, and the valley and wings of the present distribution are slightly higher.

The average kinetic energy as a function of fragment mass is plotted in Fig. 6. For comparison we show the two functions $E_k(\mu)$ and $E_k^*(m^*)$ obtained from the present experiment. Also shown in the figure are the average kinetic energies

¹⁶W. L. Whetstone, *Phys. Rev.* **131**, 1232 (1963).

¹⁷J. S. Fraser *et al.*, *Can. J. Phys.* **41**, 2080 (1963).

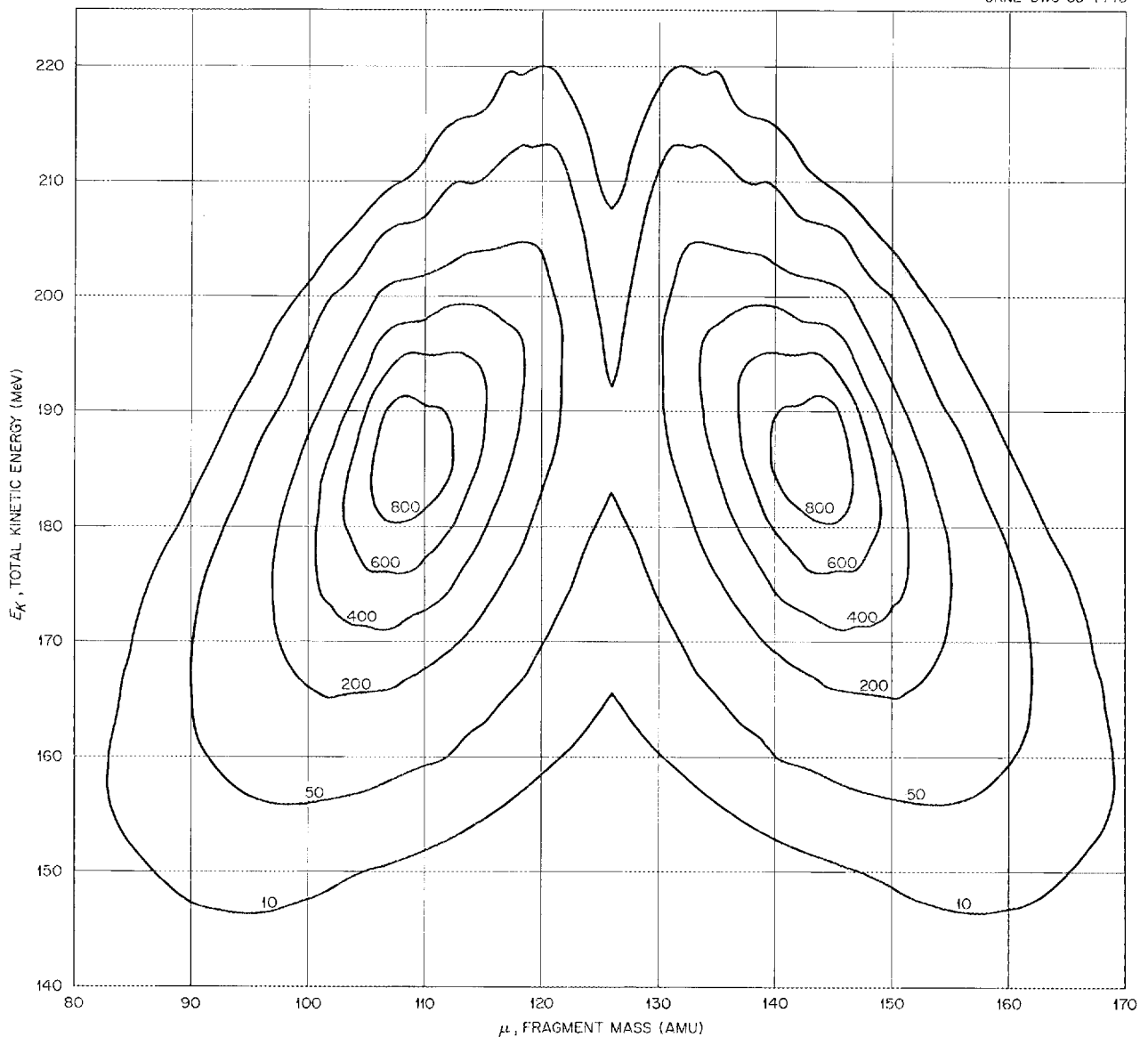


Fig. 3. Mass vs Total Fragment Kinetic Energy Array, $N(\mu, E_k)$, for ^{252}Cf Spontaneous Fission.

$E_k^*(m^*)$ of Whetstone.^{16,18} We note that the agreement in $E_k^*(m^*)$ is within ~ 1 Mev, or 0.7%, throughout, except for points at a few masses at the extreme asymmetric end of the curve and one or two masses just at symmetry. The dis-

¹⁸The data of Fraser *et al.* lie somewhat lower than the curves shown in Fig. 6; the discrepancy, however, is explained by small tailing effects which are possible in that experiment, as discussed by those authors in ref. 17 and private communication (1964).

crepancy seen in the figure in the symmetric region is qualitatively accounted for by the somewhat poorer mass resolution of the present experiment. Also, our more precise energy-velocity correlation experiment on post-neutron-emission ^{252}Cf fission fragments¹² confirms a somewhat lower average total kinetic energy at symmetry than is observed in the present experiment. The small discrepancy in $E_k^*(m^*)$ seen in Fig. 6 for a few masses at extreme asymmetry may arise from otherwise

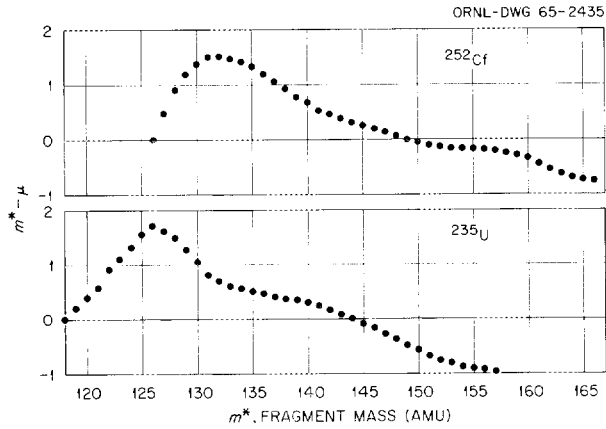


Fig. 4. Relation Between m^* and μ , Plotted as $(m^* - \mu)$ vs m^* , for Two Fission Cases. Calculation is based on $\nu(m)$ given by Bowman *et al.* (ref. 15) for ^{252}Cf and on $\nu'(m)$ given by Apalin *et al.* (ref. 19) for ^{235}U .

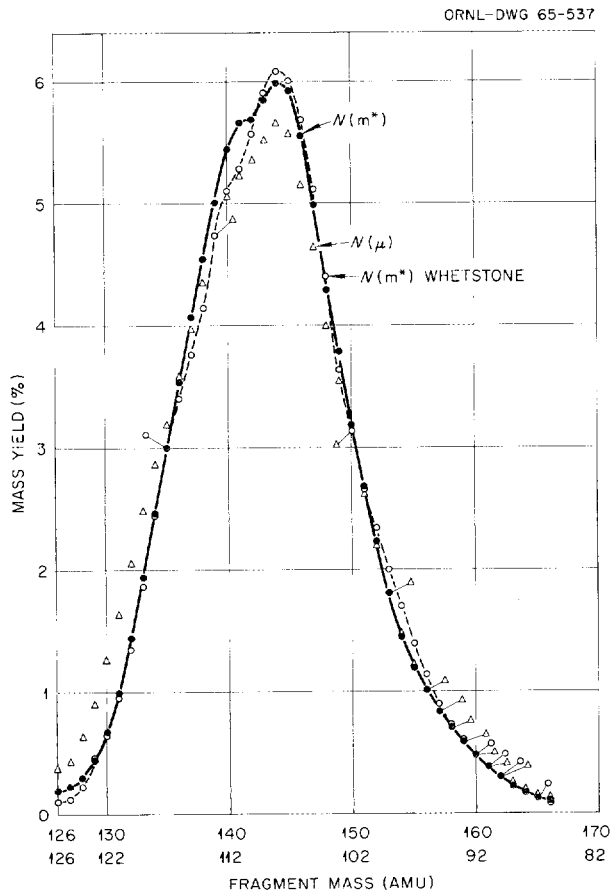


Fig. 5. Fragment Mass Distribution for ^{252}Cf Spontaneous Fission. The distribution $N(\mu)$ is obtained directly from the data; correction for neutron emission yields the distribution $N(m^*)$. The distribution of Whetstone (ref. 16), obtained from double velocity measurements, is shown for comparison. No correction for resolution has been included.

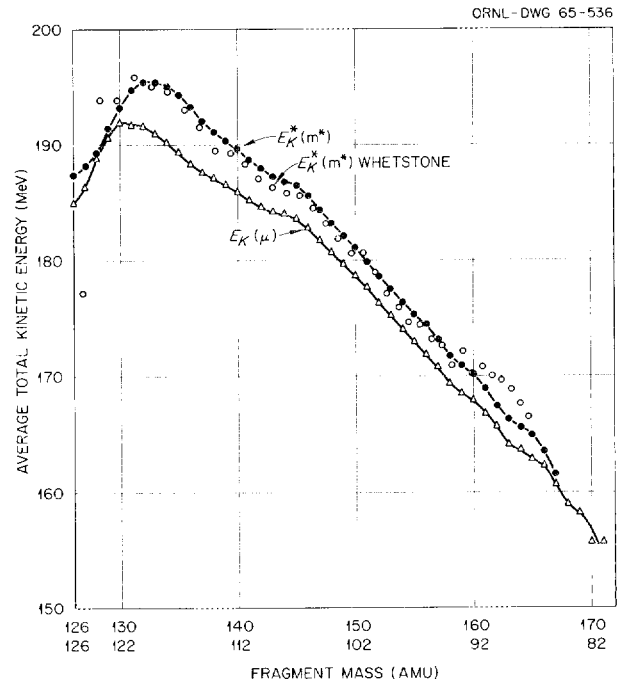


Fig. 6. Average Total Fragment Kinetic Energy as a Function of Mass for ^{252}Cf Spontaneous Fission. The quantity $\langle E_k(\mu) \rangle$ is obtained directly from the data; correction for neutron emission yields the relation $\langle E_k^*(m^*) \rangle$. The double velocity results of Whetstone (ref. 16) are shown for comparison.

negligible experimental effects in either experiment.

The comparisons discussed above and shown in Figs. 5 and 6 demonstrate the necessity of taking into account the effects of neutron emission together with the mass-dependent energy calibration in the analysis of energy correlation experiments, particularly where detailed quantitative results are required. Although an array giving $\nu(m^*, E^*)$ or its equivalent would be required for a complete, more exact analysis of such experiments, the mass distribution $N(m^*)$ and average

kinetic energies $\langle E_k(m^*) \rangle$ seem to be given reasonably accurately by the analysis of the previous section; and we conclude that these results from energy- and velocity-correlation experiments are in good agreement, or where they are not, the differences are understood.

Results for ^{235}U Thermal-Neutron-Induced Fission

The correlation data array showing $N(x_1, x_2)$ for this case is given in Fig. 7. Again, the numbers

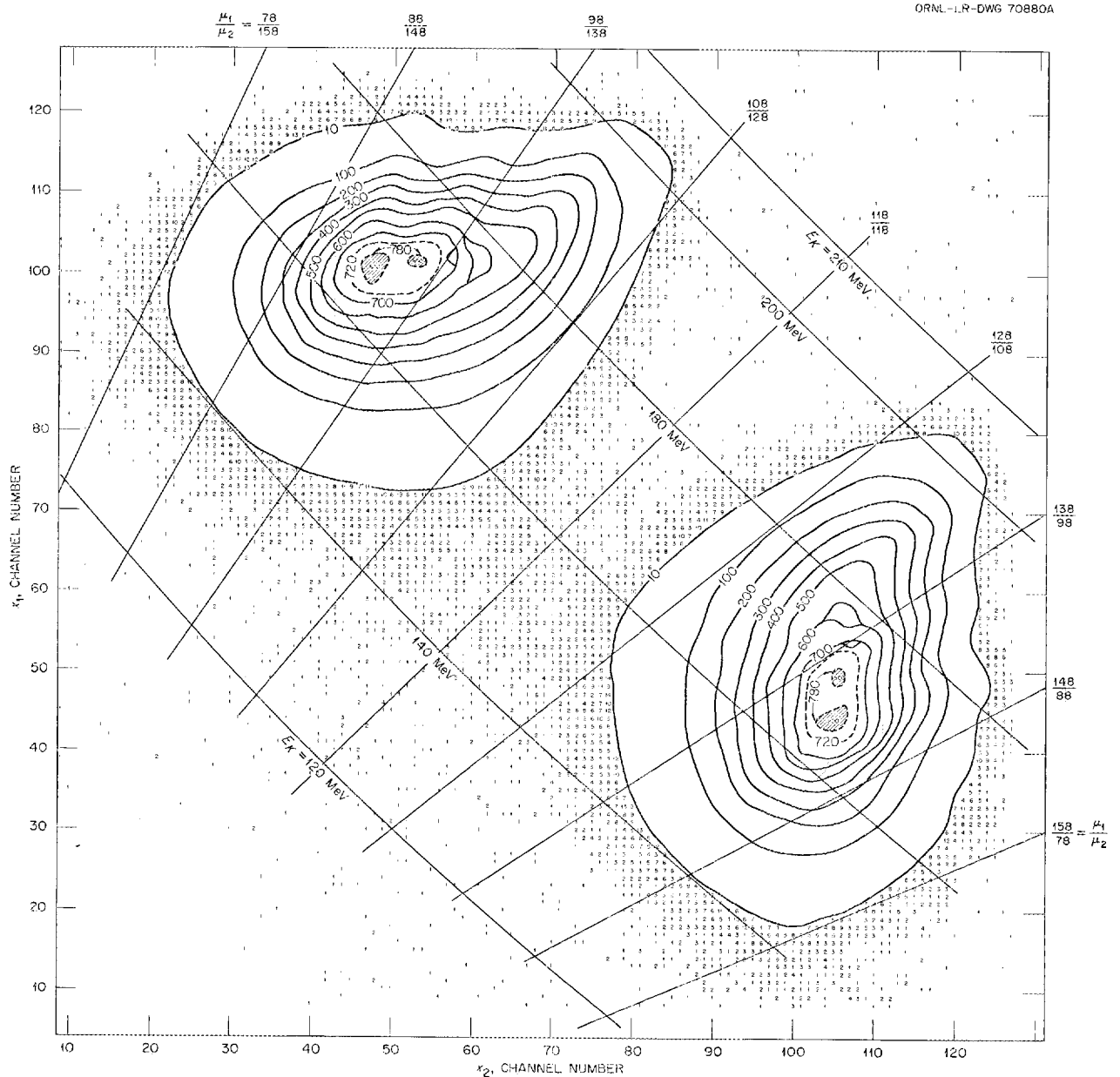


Fig. 7. Data Array $N(x_1, x_2)$ for ^{235}U Thermal-Neutron-Induced Fission.

labeling the contours indicate the number of events per cell (1 channel \times 1 channel), and lines of constant E_k and μ_1/μ_2 are included. Actual numbers have been entered outside the contours labeled 10 in order to show the locations of rarer events.

Transformation to the array $N(\mu_1, E_k)$ yields the contour diagram shown in Fig. 8. The numbers labeling the contours and the numbers entered outside the last contour give the number of events per Mev per amu. The same treatment was carried out for these data as for ^{252}Cf ; the neutron emission data of Apalin¹⁹ were used, and the relation between μ_1 and m_1^* is shown in Fig. 4.

The fragment mass distribution $N(m^*)$ for ^{235}U is shown in Fig. 9; the distribution $N(m^*)$ from the double velocity experiment of Milton and Fraser²⁰ is also shown. Again, no corrections for resolution have been included, and it appears reasonable to account for the observed differences principally in terms of the somewhat poorer mass resolution of the energy correlation experiment.

The average total kinetic energy as a function of fragment mass, $\langle E_k(m^*) \rangle$, is shown in Fig. 10;

¹⁹V. F. Apalin *et al.*, *Nucl. Phys.* **55**, 249 (1964).

²⁰J. C. D. Milton and J. S. Fraser, *Can. J. Phys.* **40**, 1626 (1962).

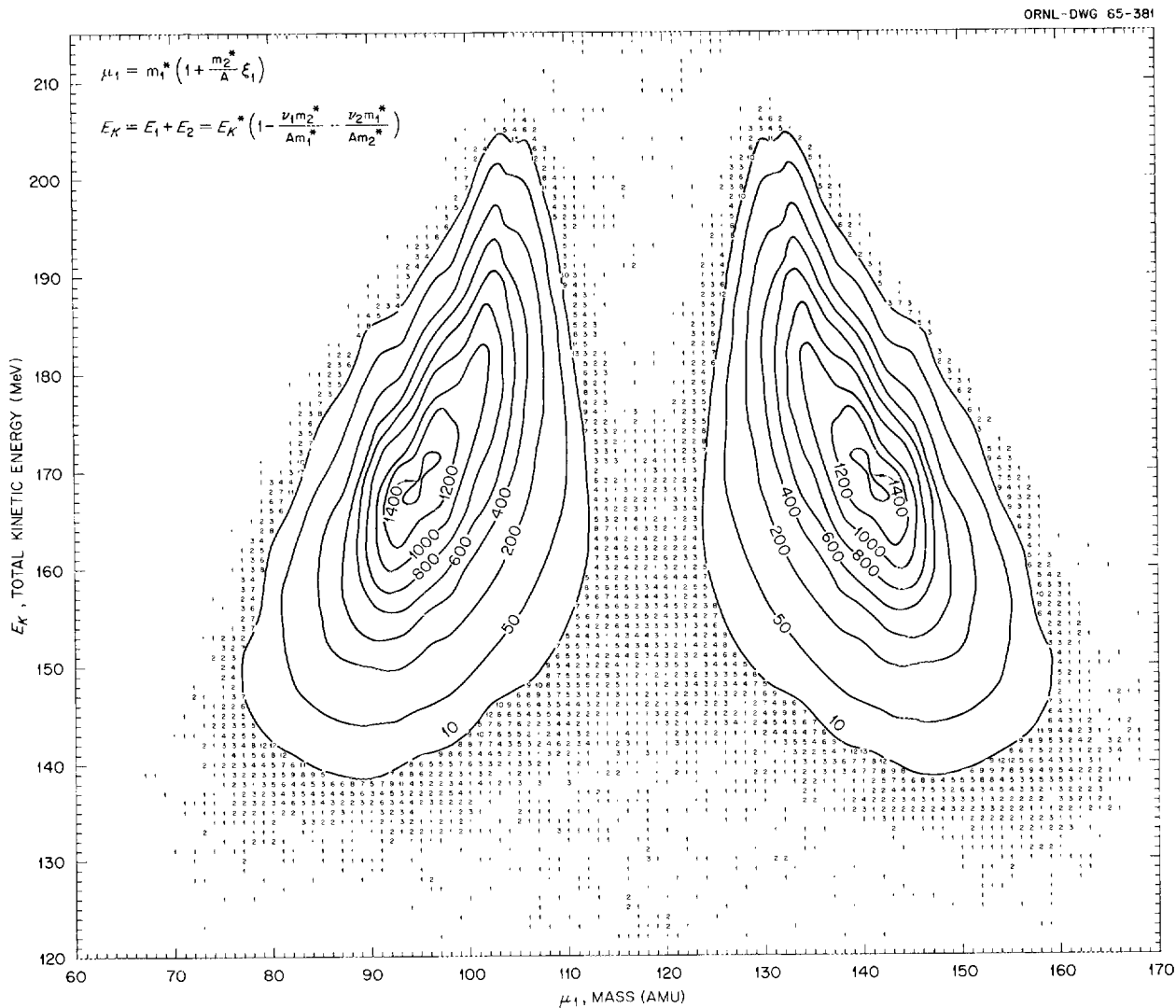


Fig. 8. Mass vs Total Fragment Kinetic Energy Array $N(\mu, E_k)$ for ^{235}U Thermal-Neutron-Induced Fission.

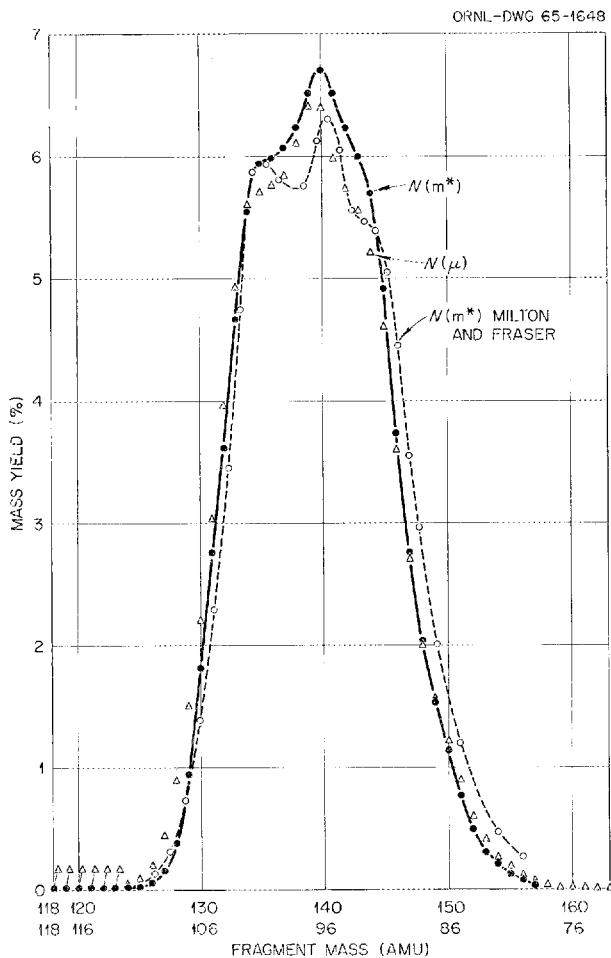


Fig. 9. Fragment Mass Distribution for ^{235}U Thermal-Neutron-Induced Fission. The distribution $N(\mu)$ is obtained directly from the data; correction for neutron emission yields the distribution $N(m^*)$. The distribution of Milton and Fraser (ref. 20), obtained from double velocity measurements, is shown for comparison. No correction for resolution has been included.

as above, corrections for resolution have not been included. Also shown in the figure are the results of Milton and Fraser.²⁰ The discrepancy between the two curves is ~ 4 Mev (two or more times the quoted standard deviations) over most of the mass range; it increases toward symmetry and decreases somewhat for $m^* > 145$ amu. The difference between the two curves may be accounted for on the basis of two considerations: (1) dispersion effects in the present results tend to give kinetic energies which are too high, perhaps by as much as 1 Mev in certain regions; (2) velocity tailing

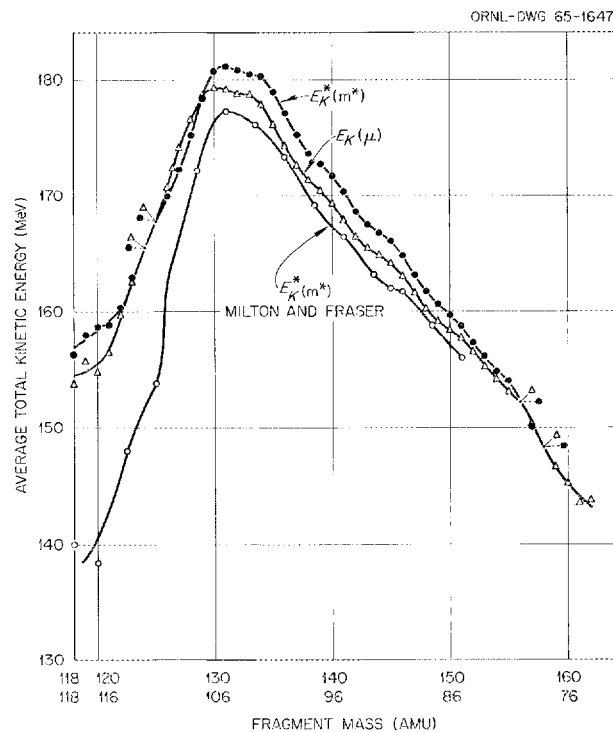


Fig. 10. Average Total Fragment Kinetic Energy as a Function of Mass for ^{235}U Thermal-Neutron-Induced Fission. The quantity $\langle E_k(\mu) \rangle$ is obtained directly from the data; correction for neutron emission yields the relation $\langle E_k^*(m^*) \rangle$. The double velocity results of Milton and Fraser are also shown - see text.

effects (caused by small-angle scattering along the drift tubes) which might be present in the time-of-flight experiments would tend to give kinetic energies which are too low. Quantitative evaluation of the latter effect is difficult; however, a later discussion on this point by Fraser *et al.*¹⁷ and recent measurements by Engelkemeir¹³ indicate its possible importance. Our value for the overall total fragment kinetic energy for ^{235}U is 171.9 ± 1.2 Mev, compared with the value 168.3 ± 1.7 Mev of ref. 20.

Acknowledgments

The authors gratefully acknowledge the preparation of the ^{252}Cf source by S. G. Thompson (UCRL, Berkeley) and that of the ^{235}U target by E. H. Kobisk (Isotopes Division). The assistance of Mary M. Kedl and Mary F. Patterson (Mathematics Division) in the processing of the data is gratefully acknowledged.

CORRELATED FRAGMENT ENERGY MEASUREMENTS AND MASS-vs-ANGLE CORRELATIONS IN $^{226}\text{Ra} + p$ FISSION

H. W. Schmitt

J. W. T. Dabbs

P. D. Miller

NUCLEAR FISSION. ^{226}Ra , proton-induced, measured fragment energies, deduced mass and energy distributions, mass-energy and mass-angle correlations.

Introduction

The charged-particle-induced fission of ^{226}Ra exhibits unique and interesting features. In particular, the fragment mass distribution for proton-induced fission of ^{226}Ra was found by Jensen and Fairhall¹ to contain three distinct peaks. Since the discovery of this "anomalous" mass distribution, radiochemical measurements for ^{226}Ra fission have been extended to include mass distribution studies of deuteron- and helium-ion-induced fission,² angular distribution measurements,³ and yield measurements for a few nuclei over a wider range of incident proton energies.⁴ More recently, a number of kinetic experiments have been carried out for deuteron-⁵ and helium-ion-induced^{5,6} fission of ^{226}Ra ; total fragment angular distribution measurements for proton-, deuteron-, and helium-ion-induced fission of ^{226}Ra have also been reported.⁷

It has seemed especially appropriate to us to study also in detail the kinetics of proton-induced fission of ^{226}Ra ; in this case the excitation energy of the compound nucleus (^{227}Ac) is sufficiently low so that the probability for second-chance (p, nf) fission is much reduced with respect to that for first-chance (p, f) fission. Thus the kinetic energies, mass distributions, etc., should

be characteristic of first-chance fission principally, and, in addition, a search for any appreciable correlation between the mass distribution and angle of emission of the fragments might be meaningful.

In the present work, detailed fragment-energy-correlation measurements were carried out for fragments emitted at a center-of-mass angle $\theta = 90^\circ$ with respect to the incident proton beam, for proton energies $E_p = 11.0, 12.0,$ and 13.5 Mev. In our search for a mass-angle correlation, similar measurements were carried out for $E_p = 13.5$ Mev at angles $\theta = 30, 40, 60,$ and 90° .

Experimental Method

A schematic diagram of the experimental arrangement is shown in Fig. 1, together with a block diagram of the electronic equipment. The target consisted of a 1-cm-diam vacuum-evaporated deposit of radium bromide about $20 \mu\text{g}/\text{cm}^2$ thick on a 2.5-cm-diam carbon backing film about $20 \mu\text{g}/\text{cm}^2$ thick. The proton beam was focused and collimated to a diameter of less than ~ 5 mm.

Rounded collimators were used in front of the silicon detectors, as shown in Fig. 1, to minimize low-energy tailing effects in the fragment pulse-height and energy spectra. The surface-barrier detectors were operated in the saturation region of the curve of pulse height vs applied bias. The absolute energy calibration of the detectors was accomplished with reference to ^{252}Cf spontaneous fission fragment spectra by the method previously developed and described in the other papers.^{8,9}

¹R. C. Jensen and A. W. Fairhall, *Phys. Rev.* **109**, 942 (1958).

²R. C. Jensen and A. W. Fairhall, *Phys. Rev.* **118**, 771 (1960).

³C. T. Coffin and I. Halpern, *Phys. Rev.* **112**, 536 (1958).

⁴R. L. Wolke, *Phys. Rev.* **120**, 543 (1960).

⁵H. C. Britt, H. E. Wegner, and J. C. Gursky, *Phys. Rev.* **129**, 2239 (1963).

⁶J. P. Unik and J. R. Huizenga, *Phys. Rev.* **134**, B90 (1964).

⁷J. E. Gindler, G. L. Bate, and J. R. Huizenga, *Phys. Rev.* **136**, B1333 (1964).

⁸H. W. Schmitt, W. E. Kiker, and C. W. Williams, *Phys. Rev.* **137**, B837 (1965).

⁹H. W. Schmitt *et al.*, paper SM 60/40 to be presented at IAEA Symposium on Fission, Salzburg, Austria, March 1965.

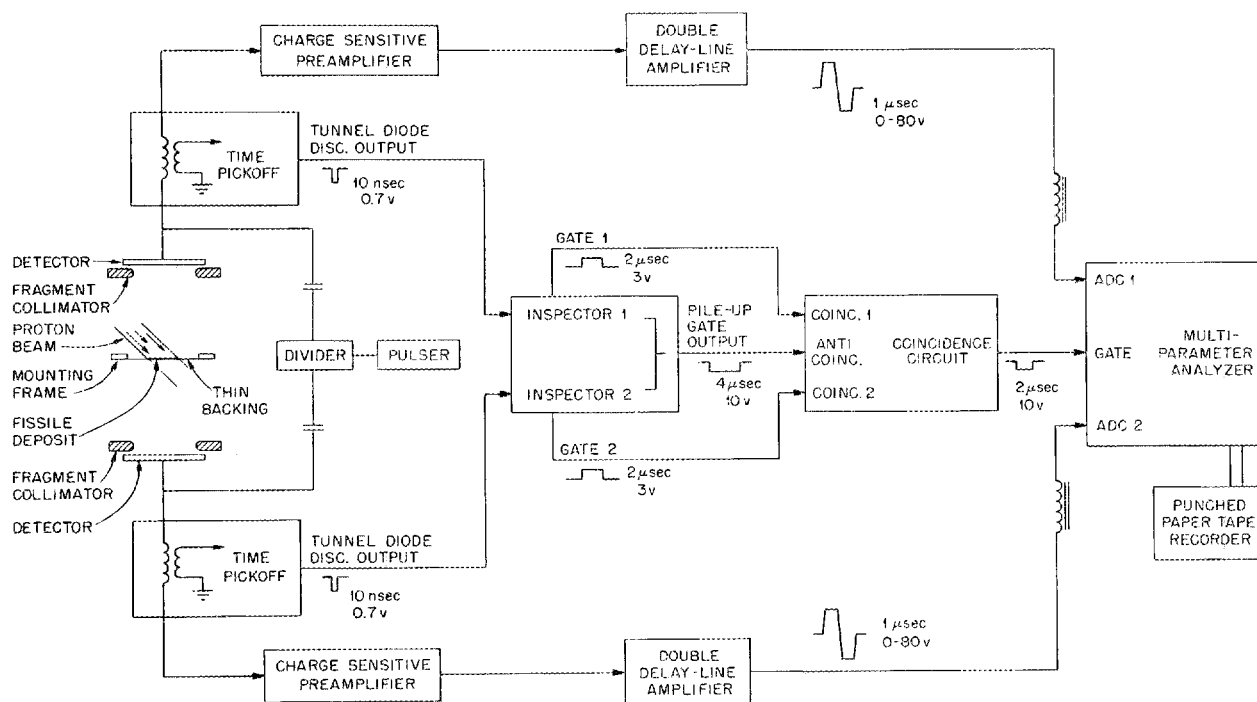


Fig. 1. Schematic Diagram of Source and Detector Arrangement and Block Diagram of Electronic Equipment for Fission-Fragment Energy Correlation Experiments.

The linear circuitry indicated in Fig. 1 is self-explanatory. All units were connected into the system throughout the runs; periodic checks of stability and linearity of the system were made with the pulser. The function of the inspector circuit was to reject pileup pulses, that is, pulses resulting from the near superposition of a fission fragment pulse with an accidental scattered-proton or natural alpha-particle pulse. Pairs of pulses in either detector whose time separations were in the range from 20 nsec to 2 μ sec were detected by the inspector circuit, and the anticoincidence signals generated in such cases served to reject these events. When no pileup occurred, the two coincident fission fragment pulse heights (channel numbers) were recorded event by event on punched paper tape; the data were sorted, summed, and otherwise processed by means of a digital computer.

Experimental Results

The two-parameter data array is given by $N(x_1, x_2)$, where N is the number of counts appearing in the

combination of channel numbers x_1 and x_2 corresponding to detectors 1 and 2 respectively. This array was transformed to an array given by $N(\mu_1, E_K)$, where E_K is the measured total kinetic energy and μ_1 is a "mass" of the fragment detected in detector 1. For fragments emitted at center-of-mass angle $\theta = 90^\circ$ with respect to the beam, the quantity μ_1 is calculated from the data with the assumption of linear momentum conservation applied to the measured fragment energies E_1 and E_2 ; the relationships among the various quantities are then

$$\mu_1 E_1 = \mu_2 E_2, \quad (1)$$

$$\mu_1 + \mu_2 = A, \quad (2)$$

$$E_1 + E_2 = E_K, \quad (3)$$

where A is the mass of the fissioning nucleus (in the present case 227 amu). The average total kinetic energy $\langle E_K \rangle$ as a function of μ_1 and the "mass" distribution $N(\mu_1)$ were obtained directly from the array $N(\mu_1, E_K)$. For fragment angles

other than 90° the data were processed in the same manner; then additional transformations of the final functions were carried out to correct for the center-of-mass motion.

We have chosen to use the symbols μ_1 and μ_2 to distinguish these "masses" from the actual pre-neutron-emission masses m_1^* and m_2^* (the asterisk denotes highly excited or neutron-rich nuclei) and post-neutron-emission masses m_1 and m_2 . In practice the μ_i do not differ greatly ($\lesssim 2$ amu) from the m_i^* , inasmuch as both fragments emit neutrons, and the error is to some extent canceled by the use of the measured, post-neutron-emission energies in Eq. (1). We have not included neutron emission corrections in the results reported here. Such corrections would change slightly the shape of the mass distributions; the total pre-neutron-emission kinetic energies E_K^* would be larger than the values of E_K reported here by an amount (up to a few percent) which takes into account the mass changes of the fragments in neutron emission.

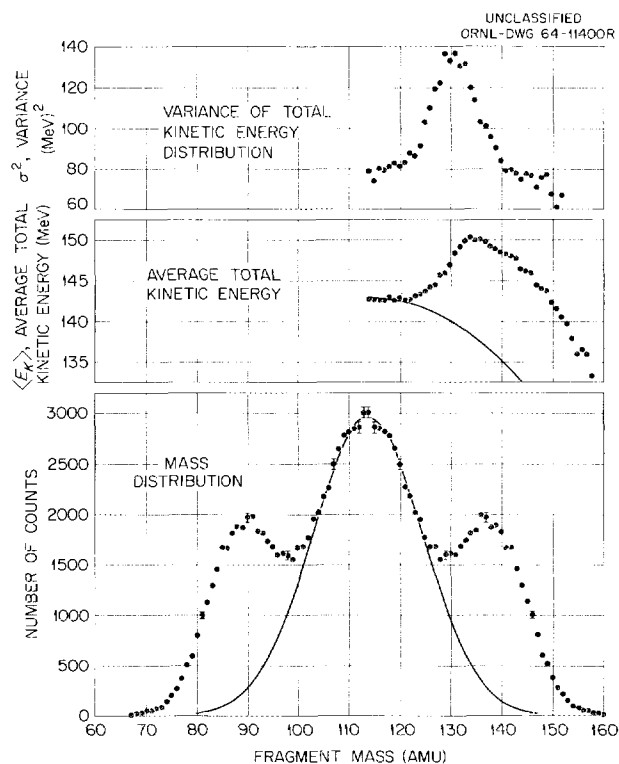


Fig. 2. Summary of Results for Proton-Induced Fission of ^{226}Ra ; $E_p \approx 13.5$ Mev, $\theta = 90^\circ$. No corrections for neutron emission have been included. The solid curves are calculated — see text for discussion.

A summary of the results for proton energy $E_p = 13.5$ Mev, for fragments emitted at a mean center-of-mass angle $\theta = 90^\circ$ with respect to the beam, is shown in Fig. 2. A similar summary of results for $E_p = 11.0$ Mev, $\theta = 90^\circ$, is given in Fig. 3. In the lowest part of each figure the mass distribution $N(\mu)$ is shown; the average total fragment kinetic energy $\langle E_K \rangle$ as a function of μ is shown in the center portion of each figure, and the variance σ^2 of the total kinetic energy distribution for a given μ is shown as a function of μ in the uppermost position of each figure. The mass distributions are triple-peaked, as expected from previous studies^{1,2,5,6} of proton-, deuteron-, and alpha-induced fission of ^{226}Ra . The average total kinetic energy is seen to reach a maximum in the region where the heavy-fragment mass is ~ 134 amu, slightly above the masses where the $Z = 50$ and $N = 82$ shells close. Maximum values of $\langle E_K \rangle$ in the region of $Z = 50$ or $N = 82$ nuclei have been observed for many cases of both intermediate and low excitation fission. The variance

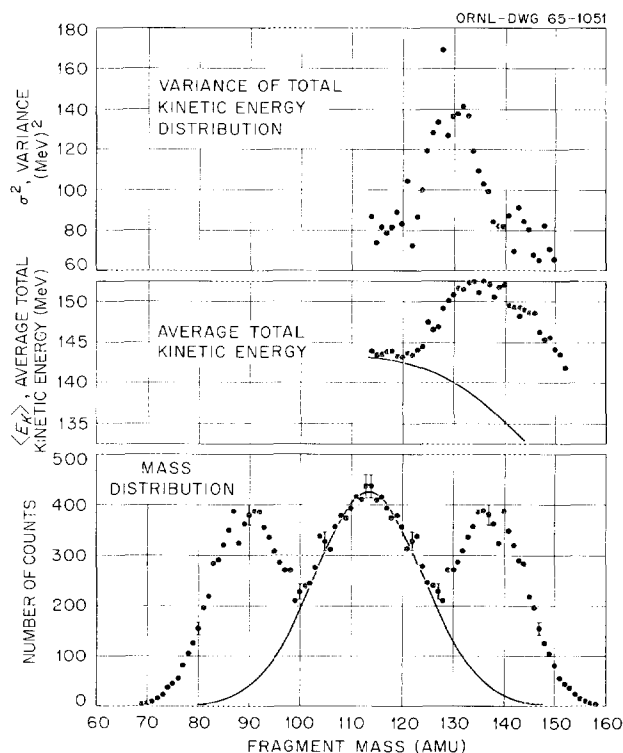


Fig. 3. Summary of Results for Proton-Induced Fission of ^{226}Ra ; $E_p = 11.0$ Mev. No corrections for neutron emission have been included. The solid curves are calculated — see text for discussion.

of the kinetic energy distribution as a function of mass appears to be nearly the same in the region of symmetric fission and very asymmetric fission, but peaks quite strongly in the region of $\mu \sim 130$ amu. Various features of these and related curves will be discussed further in a later section of this paper.

In Fig. 4 we have plotted the mass distributions for the three different proton energies: 11.0, 12.0, and 13.5 Mev. All of these distributions were obtained at $\theta = 90^\circ$. For ease of comparison we have drawn only the smooth curves through the points and normalized the distributions at the asymmetric peak. The ratio ρ of fragment abundance at the symmetric peak to that at the asymmetric peak is seen to increase from 1.11 for 11.0-Mev protons to 1.27 for 12.0-Mev protons, and to 1.54 for 13.5-Mev protons. The total increase in fragment yield at the symmetric peak relative to that at the asymmetric peak (i.e., the increase in ρ) is thus about 40% for the proton energy increase from 11.0 to 13.5 Mev.

In our search for a possible correlation between fragment mass and angular distribution, mass distributions were obtained at center-of-mass angles $\theta = 30, 40, 60,$ and 90° for $E_p = 13.5$ Mev. The ratio ρ was determined for each of these angles and is plotted in Fig. 5 as a function of θ . An increase of $\sim 5\%$ in ρ is observed from $\theta = 30^\circ$ to $\theta = 90^\circ$; the statistical uncertainties are quite large, as shown, and the uncertainty in the coefficient of $P_2(\cos \theta)$ is ± 0.03 .

Analysis and Discussion

We shall divide our discussion of the results into two parts. First, we shall consider the mass distributions obtained as a function of incident proton energy together with the total fragment kinetic energy as a function of mass, particularly as these functions relate to the two-mode hypothesis. Second, we shall consider the observed mass-angle correlation.

Kinetic Energy and Mass Distributions. — The suggestion that fission could be discussed meaningfully in terms of two modes, symmetric and asymmetric, was made by Turkevich and Niday¹⁰

¹⁰A. Turkevich and J. B. Niday, *Phys. Rev.* **84**, 52 (1951).

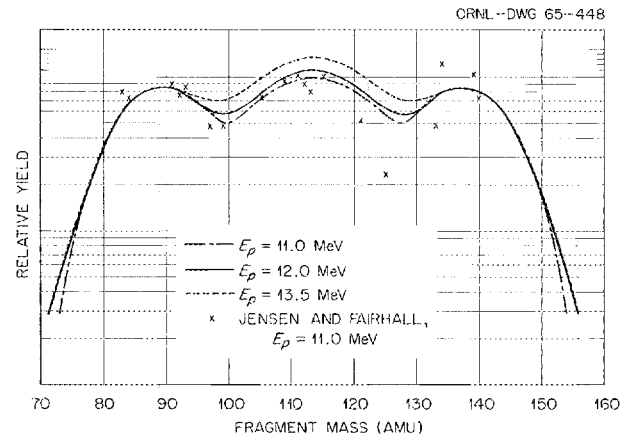


Fig. 4. Comparison of Fragment Mass Distributions Observed in Proton-Induced Fission of ^{226}Ra for $E_p = 11.0, 12.0,$ and 13.5 Mev. Smooth curves were drawn through the data points and are shown normalized at the asymmetric peak.

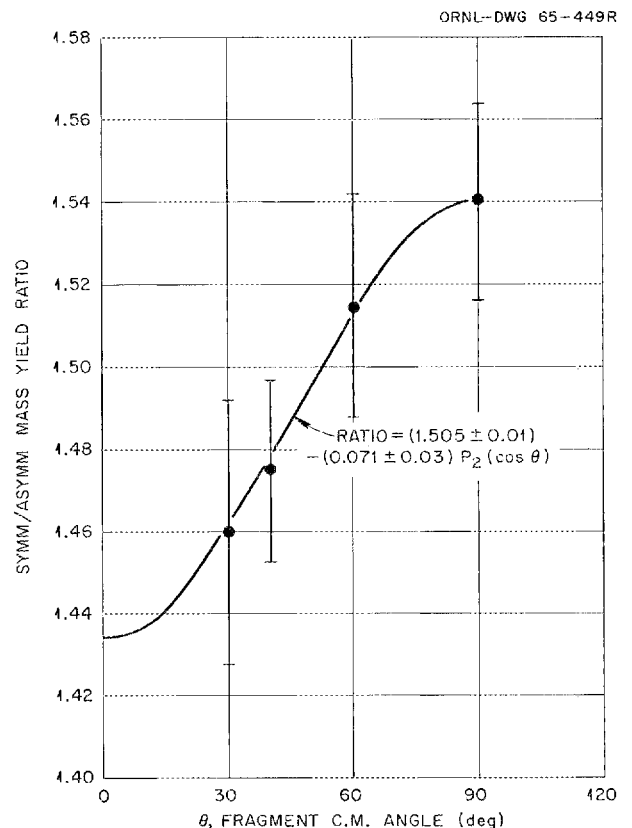


Fig. 5. Mass-Angle Correlations. $E_p = 13.5$ Mev. Symmetric/asymmetric peak mass-yield ratios are plotted as a function of fragment c.m. angle.

in 1951. A number of authors,¹¹ notably Jensen and Fairhall^{1,2} with respect to radium, have employed the two-mode hypothesis and have further suggested its validity in discussions of the differences in fragment mass distributions observed as functions of the Z and A of the fissioning nucleus and as functions of the energy of the bombarding particle. More recently, a number of authors^{5,6,12,13} have discussed the results of various kinetic experiments in terms of two modes of fission. These include results for deuteron-induced⁵ and helium-ion-induced^{5,6} fission of ^{226}Ra . Principal evidence in favor of the two-mode hypothesis consists of (1) the analysis of the shapes of the fragment mass distributions in terms of symmetric and asymmetric components whose relative yields are functions of the fissioning nucleus and incident particle energy, and (2) the analysis of the average total kinetic energy as a function of fragment mass in terms of an effective separation \bar{D} of charge centers which appears to have different, but approximately constant, values for the two modes.

In the present experiment, the two-mode hypothesis suggests itself almost immediately in the results of Fig. 4. The principal difference in the mass distributions is seen in the increased yield of the entire symmetric peak relative to the asymmetric peak as the incident proton energy is increased. Because of this result, and particularly in view of the recent success of nonviscous-liquid-drop model calculations¹⁴ as applied in the case of ^{209}Bi (ref. 6) and other nuclei whose mass yields are symmetric and single peaked, it is tempting to analyze the data of the present experiment in terms of two modes of fission with the symmetric mode described by the nonviscous-liquid-drop model. The region of masses around radium, $A \sim 226$, represents roughly the upper limit of validity of Nix's calculations;¹⁴ hence some minor departures may be expected. Nonetheless, we have carried out a preliminary analysis from this basic assumption, as follows.

On the assumption that the contribution of the asymmetric mode is negligible near symmetry, we obtained least-squares fits of the mass distributions covering 18 mass units centered about symmetry to the Gaussian function:¹⁴

$$N = N_0 \exp - \{ [0.5 - (\mu/A)]^2 / C_m \}. \quad (4)$$

For proton energies $E_p = 11.0$ and 13.5 Mev, the values of the constant C_m (Nix's notation) were found to be 0.00453 and 0.00456 respectively. These values agree within their uncertainties and correspond to an equivalent standard deviation in mass of ~ 10.8 amu. Plots of the calculated distributions are given as solid curves in Figs. 2 and 3, along with the measured distributions.

The total translational kinetic energy at symmetry is given by Nix in terms of the surface energy $E_s^{(0)}$ at the saddle point and as a function of the fissionability parameter x , where $x = (Z^2/A) / (Z^2/A)_{\text{crit}}$, with $(Z^2/A)_{\text{crit}} = 50.13$. The surface energy is given as

$$E_s^{(0)} = a_s A^{2/3}, \quad (5)$$

where a_s is a constant and is specified¹⁴ as 17.80 Mev. The calculated total kinetic energy for symmetric fragments in the present case would then be $E^{(0)} \simeq 158$ Mev, or ~ 15 Mev larger than the measured value and ~ 12 Mev larger than the approximate neutron-corrected value. This discrepancy can be accounted for by errors in the nuclear constants (e.g., $\sim 10\%$ error in a_s). Since such constants of the mass formula are not precisely known for nuclei in the region of fission fragments, perhaps it is justified to consider a_s as a somewhat free parameter adjusted (within 10%) so that for the present discussion $E^{(0)} = \langle E_K \rangle_{\text{sym}} = 143$ Mev, as measured. (A simple calculation based on Nix's equations then leads to an effective temperature t at the saddle point of ~ 0.95 Mev.) We have used Nix's formulation with the adjusted values of a_s to calculate the average total fragment kinetic energy characteristic of liquid-drop fission as a function of fragment mass. The results are shown as solid curves in the center portions of Figs. 2 and 3, along with the measured values of $\langle E_K \rangle$ for $E_p = 13.5$ and 11.0 Mev respectively. We shall discuss these curves again below.

¹¹I. Halpern, *Ann. Rev. Nucl. Sci.* **9**, 245 (1959).

¹²H. C. Britt and S. L. Whetstone, *Phys. Rev.* **133**, B603 (1964).

¹³S. L. Whetstone, *Phys. Rev.* **133**, B613 (1964).

¹⁴J. R. Nix, UCRL-11338 (1964), unpublished.

Note now, however, that the measured $\langle E_K \rangle$ is approximately the same at symmetry for the two proton energies (Figs. 2 and 3, center portions), while in the region of the asymmetric mass yield peak, $\langle E_K \rangle$ is somewhat lower for the higher proton energy. This observation may be accounted for as follows: If the total kinetic energy which is characteristic of liquid-drop fission is lower than that characteristic of the asymmetric mode, then as the contribution in yield at the asymmetric peak from the symmetric mode increases, the average measured kinetic energy $\langle E_K \rangle$ for those masses must decrease. We may express this by means of an equation of the form

$$\langle E_K \rangle = f_{LD} E_{KLD} + (1 - f_{LK}) E_{KA}, \quad (6)$$

where E_{KLD} and E_{KA} are the average total kinetic energies at mass μ characteristic of the "liquid-drop" mode and "asymmetric" mode respectively. Thus, for example, in the mass region $\mu \sim 138$ amu, the liquid-drop fission energy E_{KLD} is, from Fig. 3, ≈ 136.4 Mev, the measured energy is $\langle E_K \rangle \approx 149.3$ Mev for $E_p = 13.5$ Mev, and $f_{LD} \approx 0.12$; the calculated energy E_{KA} characteristic of the asymmetric mode is then 151 Mev, a value which is quite consistent with low-excitation fission systematics.

A complete analysis would give quantitative results on these points for all masses; however, neutron-emission and mass-resolution effects must be taken into account for detailed accuracy, and we have not included these in the preliminary calculations reported here. Note that a straightforward calculation for the variance σ^2 which is based on the two-mode hypothesis can be carried out, since the yields, energy distributions, and variances of the two modes can be estimated or deduced. These calculations have been postponed until the neutron-emission and mass-resolution corrections have been made. The peaks in the variance curves of Figs. 2 and 3 appear to be consistent with this hypothesis, however.

It is suggested, then, on the basis of analyses to date, that the two-mode hypothesis is valid for ^{226}Ra (p , fission), and further that one of the two modes is describable in terms of the nonviscous liquid-drop model¹⁴ and is therefore indeed a symmetric mode. The so-called "asymmetric mode" may possibly have no fixed, general description or configuration, but may exhibit properties de-

termined by the nuclear structure parameters of the fragments themselves, as occurs for the low-excitation fission of heavier elements.¹⁵

Mass-Angle Correlation. — The present form of the theory of angular distribution of fission fragments was advanced by Bohr.¹⁶ For cases where the compound nucleus is oriented by virtue of the incoming angular momentum, the theory has been amplified and applied by many authors, including Halpern and Strutinski,¹⁷ Griffin,¹⁸ and Huizenga and co-workers.^{7,19} In the theory the angular distribution is determined by the K distribution of the compound nucleus before scission, where K is the projection of the total angular momentum I on the nuclear symmetry axis. For moderately high excitation energies, for which statistical considerations may be applied, the K distribution is characterized by a parameter K_0^2 defined by

$$K_0^2 = t \mathcal{J}_{\text{eff}} / \hbar^2, \quad (7)$$

where t is the effective nuclear temperature, and \mathcal{J}_{eff} is the effective moment of inertia given by $\mathcal{J}_\perp \mathcal{J}_\parallel / (\mathcal{J}_\perp + \mathcal{J}_\parallel)$, in which \mathcal{J}_\perp and \mathcal{J}_\parallel are the perpendicular and parallel components of the moment of inertia. For small values of K_0^2 , the theory predicts anisotropic fragment distributions which peak toward 0 and 180°; for larger values of K_0^2 , the theory predicts more nearly isotropic distributions.

The mass-angle effect observed (see Fig. 5) is not sufficiently large to indicate a difference in angular distributions for masses in the symmetric and asymmetric peaks for first-chance fission. The 5% effect which is observed may be interpreted on the basis of a small probability for second-chance fission; these arguments have been outlined by Halpern and Strutinski.¹⁷ In essence, the excitation energy of the compound

¹⁵R. Vandenbosch, *Nucl. Phys.* **46**, 129 (1963).

¹⁶A. Bohr, *Proc. 1st Intern. Conf. Peaceful Uses At. Energy*, Geneva **2**, 151 (1955).

¹⁷I. Halpern and V. M. Strutinski, *Proc. 2nd Intern. Conf. Peaceful Uses At. Energy*, Geneva **15**, 408 (1958).

¹⁸J. Griffin, *Phys. Rev.* **116**, 107 (1959); **127**, 1248 (1962).

¹⁹J. R. Huizenga and R. Vandenbosch, in *Nuclear Reactions 2* (P. M. Endt and P. B. Smith, eds.), chap. II, North Holland, Amsterdam, 1962.

nucleus in second-chance fission will be lower than that in the case of first-chance fission; hence K_0^2 for second-chance fission will be smaller, and the angular distribution will be more anisotropic for those events. It has been shown above and in Fig. 4 that asymmetric fission is relatively more abundant for lower excitations; therefore, if both first- and second-chance fission occur, the asymmetric fragments should exhibit a somewhat more

anisotropic angular distribution, as indeed occurs (Fig. 5).

Acknowledgments

The authors gratefully acknowledge the preparation of the radium target by E. H. Kobisk. The assistance of C. W. Nestor and Mary F. Patterson in processing the data is gratefully acknowledged.

AVERAGE NUMBER AND ENERGY OF GAMMA RAYS EMITTED AS A FUNCTION OF FRAGMENT MASS IN ^{235}U THERMAL-NEUTRON-INDUCED FISSION¹

H. Maier-Leibnitz²

H. W. Schmitt

P. Armbruster³

NUCLEAR FISSION. ^{235}U , measured correlated prompt γ and fragment energies, deduced $\langle E_\gamma \rangle$ as function of fragment mass.

The average number and energy of gamma rays emitted as a function of fragment mass in ^{235}U thermal-neutron-induced fission have been measured. A three-parameter correlation experiment was performed in which two silicon surface-barrier detectors were used to measure the fragment energies, and a 12.5-cm-diam, 10-cm-thick NaI(Tl) scintillation crystal was used to measure the gamma-ray energies. Extreme care was taken in the experimental arrangement to avoid counting direct-fission neutrons, scattered gamma rays and neutrons, and other false events. Data were recorded event-by-event in a system similar to that used in previous energy correlation experiments at Oak Ridge, and were analyzed according to a "weighting method" developed by Maier-Leibnitz.

The total number and energy of the gamma rays for both fragments, as a function of mass ratio, were obtained directly. The number and energy

of gamma rays for individual fragment masses were determined by noting the variation in laboratory angular distribution of the gamma rays in relation to the velocity of the gamma-emitting fragment. In particular, the 0 to 180° ratio of the number of gamma rays from a moving source emitting isotropically in its center-of-mass system is proportional to $1 + 2v/c$; similarly, the 0 to 180° ratio of average gamma energy is proportional to $1 + 3v/c$. Thus, by comparing appropriate ratios in the analysis for light and heavy fragments moving toward or away from the gamma-ray detector, one obtains these quantities as a function of individual fragment mass.

Results of preliminary analyses show interesting similarities in the behavior of the fragments to the results for neutrons. Both the total number and total energy of gamma rays are essentially constant over most of the range of mass ratios; however, a broad minimum is observed in the region where $M_H \sim 130$, that is, where $z_H \sim 50$ and/or $N_H \sim 82$. An increase is observed in both total number and energy as the mass ratio approaches unity. The average number and energy of gamma rays emitted from individual fragments are observed to increase in both fragment groups, as has been observed for $\nu(M)$ by Apalin *et al.*

¹Abstract of paper to be published in the *Proceedings of the IAEA Symposium on the Physics and Chemistry of Fission*, Salzburg, Austria, March 1965.

²Visitor to Oak Ridge National Laboratory, from Physikalisches Institut, Technische Hochschule, München, Germany, October 1963 to May 1964.

³Visitor to Oak Ridge National Laboratory, from Kernforschungsanlage, Jülich, Germany, April to July 1964.

PRECISION MEASUREMENTS OF CORRELATED ENERGIES AND VELOCITIES OF ^{252}Cf FISSION FRAGMENTS¹

H. W. Schmitt

W. E. Kiker²C. W. Williams³

NUCLEAR FISSION. ^{252}Cf , measured correlated fragment energies and velocities, deduced mass and energy distributions, mass-energy correlations, and $\nu(M)$; absolute energy calibration for semiconductor detectors.

Correlated energies and velocities of single fission fragments from the spontaneous fission of ^{252}Cf have been measured. Absolute energies and times of flight are obtained with estimated accuracies of $\pm 0.5\%$ from direct comparison measurements with 30- to 120-Mev ^{79}Br , ^{81}Br , and ^{127}I ions from the Tandem Van de Graaff accelerator. The post-neutron-emission kinetic parameters obtained from this experiment for ^{252}Cf fragments are compared with pre-neutron-emission quantities obtained from double-time-of-flight experiments of Whetstone and of Milton and Fraser. Of special

interest is the fine structure which appears in the post-neutron-emission mass distribution. This structure reflects the fine structure observed in the pre-neutron-emission mass distribution, which in turn is known to reflect certain energetically preferred even-even fragment configurations in ^{252}Cf spontaneous fission. Within the $\sim 2.5\%$ mass resolution of the present experiment, no additional fine structure appears as a result of neutron boil-off to specific fragment masses. The number of neutrons $\nu(M)$ as a function of fragment mass has been calculated from the pre- and post-neutron-emission mass distributions. A "universal" energy calibration procedure for solid-state detectors for fission fragments is given; this procedure is based on the present absolute fragment energy determinations and takes into account the mass dependence of the pulse-height vs energy relation.

¹Abstract of published paper: *Phys. Rev.* 137, B837 (1965).

²Oak Ridge Graduate Fellow, University of Tennessee; present address: University of California, Lawrence Radiation Laboratory, Livermore, Calif.

³Present address: Oak Ridge Technical Enterprises Corp., Oak Ridge, Tenn.

ABSOLUTE ENERGY CALIBRATION OF SOLID-STATE DETECTORS FOR FISSION FRAGMENTS AND HEAVY IONS¹

H. W. Schmitt

W. M. Gibson²J. H. Neiler³F. J. Walter⁴T. D. Thomas⁵

NUCLEAR FISSION. Absolute energy calibration and pulse-height response of semiconductor detectors for fission fragments and heavy ions.

Detailed measurements of the pulse-height response of silicon solid-state detectors to energetic heavy ions and fission fragments have been made.

These studies have now led to a reliable method of *absolute* energy calibration of solid-state detectors for fission fragments, as well as to a better understanding of the somewhat peculiar response characteristics of the detectors to fission fragments and heavy ions.

¹Abstract of paper to be published in the *Proceedings of the IAEA Symposium on the Physics and Chemistry of Fission*, Salzburg, Austria, March 1965.

²Bell Telephone Laboratories, Inc., Murray Hill, N.J.

³Present address: Oak Ridge Technical Enterprises Corp., Oak Ridge, Tenn.

⁴Present address: Radiation Instrument Development Laboratories, Oak Ridge, Tenn.

⁵Princeton University, Princeton, N.J.

The use of silicon solid-state detectors in fragment kinetic energy measurements in recent years has been widespread. At the same time, questions have been raised about the detailed interpretation of such measurements because of the increasing evidence for anomalous behavior in charge production, charge collection, and charge multiplication in the case of densely ionizing particles. The present report discusses the systematics and possible origins of these effects. Application of the absolute energy calibration method, which takes into account the mass and energy dependence of the response, is based simply on a ^{252}Cf or ^{235}U fragment pulse-height spectrum. Our studies were carried out with monoenergetic ^{71}Br , ^{81}Br , and ^{127}I ions of energies from 30 to 120 Mev, and with fission fragments from spontaneous fission of ^{252}Cf and neutron-induced fission of ^{235}U and ^{239}Pu . It is shown that for a given

fragment mass, over a wide energy range, the fragment energy vs pulse-height relationship is of the form $E = ax + b$, where E is the fragment energy and x is the measured pulse height. A dependence of pulse height on fragment mass has also been established which leads to an energy vs pulse-height relationship, for the range of fission fragment masses and energies, of the form $E = (a + a'm)x + b + b'M$, where M is the fragment mass. The effects of detector window and detector type, resistivity, and electric field have been studied. Guides to the selection of detectors and to their use with fission fragments are given. The effect of the more exact calibration procedure outlined above, relative to standard approximate calibration methods, is discussed quantitatively with the aid of appropriate comparisons of fission fragment mass and energy distributions derived from correlated fragment energy measurements.

CORRELATED ENERGY AND TIME-OF-FLIGHT MEASUREMENTS OF FISSION FRAGMENTS WITH SEMICONDUCTOR DETECTORS: SYSTEM DESIGN AND PERFORMANCE¹

C. W. Williams² W. E. Kiker³ H. W. Schmitt

NUCLEAR FISSION. Instrumentation for correlated energy and velocity measurements.

A system for the measurement of correlated energies and times of flight of fission fragments has been developed. This system, adaptable for use with other charged particles as well, includes a fast-response transformer coupling scheme in which the charge originating in a solid-state detector

passes through the transformer primary to a low-noise, charge-sensitive amplifier; the fast timing signal is obtained from the transformer secondary. The noise thereby added to the linear energy signal is negligible. The measured time resolution of the system for particles in a narrow band of energies was $\lesssim 0.4$ nsec, full width at half maximum. The design of the system is described, and the detailed results of performance tests, including tests with coincident ^{252}Cf spontaneous fission fragments and energy-time correlation measurements for bromine and iodine ions (artificial fission fragments), are given.

¹Abstract of published paper: *Rev. Sci. Instr.* **35**, 116 (1964).

²Present address: Oak Ridge Technical Enterprises Corp., Oak Ridge, Tenn.

³Present address: University of California, Lawrence Radiation Laboratory, Livermore, Calif.

NUCLEAR DATA PROJECT

K. Way	A. Artna	W. B. Ewbank	N. B. Gove	M. J. Martin
H. Ogata	A. K. Sen Gupta	E. C. Campbell ¹	G. H. Fuller ²	C. S. Han ³

Compilation of the data on level properties and decay properties of 104 nuclei in the mass region $A = 150$ to $A = 171$ has been completed and published with comments and diagrams of "best" level schemes in the *Nuclear Data Sheets*. In connection with this work, studies have been made of the systematics of rotational band parameters (by M. J. Martin) and gamma transition half-lives (by N. B. Gove and C. S. Han). C. S. Han also completed 601 plots of conversion coefficients which have saved the Group a great deal of time. These large-scale drawings, not very suitable for duplication, are available in the library of the Nuclear Data Group.

Consideration is given constantly to the specification of "strong" grounds for spin and parity assignments, since it is necessary, of course, for members of the Group to use similar points of view in making spin-parity assignments. A new list of propositions, basic to strong and weak arguments, has been prepared for Set 4, Vol. 6.

A new edition of *Recent References*, a bibliography of articles and reports not yet analyzed for the *Sheets*, is also being issued in Vol. 6. These references are arranged according to nucleus.

A four-year project of compiling values of nuclear moments according to the experimental method used for their determination has been completed by Mrs. Gladys H. Fuller in collaboration with V. W. Cohen of the Brookhaven National Laboratory. Spins, magnetic dipole and octupole moments, and electric quadrupole moments are covered. A summary table of "rounded-off" values gives one value of each measured moment, to the number of significant figures on which there is experimental agreement, and refers to the appropriate subsections where all experimental results are listed. The 148-page table will be published as an appendix to the *Nuclear Data Sheets* and also

offered for sale separately by the National Academy of Sciences -- National Research Council (NAS-NRC) Printing and Publishing Office, 2101 Constitution Avenue, Washington, D.C., 20418, at a price of about \$3.00. Mrs. Fuller also completed a convenient list of measured values of nuclear moments published during the period October 1956 to September 1963. The list was published with Set 1 of Vol. 6 of the *Nuclear Data Sheets*.

The Group continues to collect all data on nuclear masses. A computer program for making least-squares mass adjustments, developed by the Mainz-Amsterdam group, has, with the help of Werner Thiele of Mainz, been adapted to our needs for making adjustments in limited regions. The *Nuclear Data Sheets* now give the best values of neutron and proton separation energies and beta-decay energies as determined by the program, rather than values found by hand computation and approximate methods. A summary of measured nuclear reaction ground-state Q values published between October 1956 and December 1963, prepared by former research assistant H. T. Tu and by N. B. Gove, will be published with the *Nuclear Data Sheets*, Set 4, Vol. 6.

Group members have taken an active interest in general problems of scientific information. They were instrumental in the establishment of an International Union of Pure and Applied Physics Subcommittee on Nuclear Data. The Group is represented in the NAS-NRC Subcommittee on Techniques for the Distribution of Scientific Information, the NAS-NRC Subcommittee on Nuclear Structure, and the planning committee of the Gordon Conference series on Scientific Information Problems in Research. The key-word system proposed by the Group is being tried by the journal of *Nuclear Physics*.

The idea of a compilation journal, first proposed in 1961, has been discussed with a number of publishers during 1964. Specific plans for the establishment of such a journal are nearing completion.

¹Part time employee.

²At National Bureau of Standards, part time.

³At University of Maryland, part time.

COMPILATION OF CHARGED-PARTICLE NUCLEAR CROSS SECTIONS

F. K. McGowan H. J. Kim W. T. Milner

The past year has been devoted primarily to maintaining an up-to-date literature search, compiling cross-section data in tabular form, and preparing two volumes of the series *Nuclear Cross Sections for Charged-Particle-Induced Reactions*. ORNL-CPX-1, which includes data for Mn, Fe, and Co, was completed in June 1964 and was included in the material presented by the U.S. delegation at the third Geneva conference. The

second volume, ORNL-CPX-2, which includes data for Ni and Cu, was completed in August 1964 and will be distributed in January 1965.

Approximately 3500 sets of data have been key punched and processed by computer programs. Of these, about 2500 sets are stored on magnetic tape. In the future all tabular data which are entered in the system will be stored on magnetic tape.

WAVE FUNCTIONS FOR MUON CAPTURE IN HYDROGEN μ -MOLECULAR IONS

R. L. Becker M. R. Patterson¹

The determination of the coupling constants for muon capture, $p + \mu^- \rightarrow n + \nu_\mu$, in liquid hydrogen is subject to an uncertainty in the probability γ of finding the muon at a proton in the $p\mu p$ molecule. The calculation of γ by Weinberg² has an estimated uncertainty of 10%, since it is based on the adiabatic wave function of Cohen *et al.*,³ which includes only first-order corrections to the Born-Oppenheimer approximation (BOA). Moreover, the BO wave functions had been computed variationally by using the Guillemin-Zener trial function. In October 1963 we began a calculation of more accurate wave functions, the first step of which, the computation of exact BO muonic wave functions, was reported in ORNL-3582.⁴

The expansion parameter for the corrections to the BOA is $\epsilon = 4m_\mu/(2M + m_\mu)$ for homonuclear

molecules, where M is the mass of the nucleus (p , d , or t). For $p\mu p$, $\epsilon \approx 2/9$. We have calculated the first-order correction to the BO static potential from the exact BO wave functions, ψ_{nlm} . For the ground state, both the static potential, $W_+(R)$, and the first-order correction,

$$\begin{aligned} \epsilon g_{++}(R) = \epsilon \cdot \frac{\pi}{4} \int \vec{\nabla}_n \psi_{100}(\xi, \eta; r_n) \\ \cdot \vec{\nabla}_n \psi_{100}(\xi, \eta; r_n) r_n^3 (\xi^2 - \eta^2) d\xi d\eta, \end{aligned}$$

differ somewhat, though not appreciably, from the results of Cohen *et al.*³ Energy eigenvalues and wave functions have been obtained for the low-lying states of nuclear motion in the adiabatic potential $W_+(R) + \epsilon g_{++}(R) + 2/R$; as expected, the energies differ only slightly from those of ref. 3. Similar but apparently less accurate results of Belyaev *et al.*,⁵ for which the adiabatic potential was approximated by a Morse potential, are given

¹Central Data Processing, ORGDP.

²S. Weinberg, *Phys. Rev. Letters* **4**, 575 (1960).

³S. Cohen, D. L. Judd, and R. R. Riddell, Jr., *Phys. Rev.* **119**, 384, 397 (1960).

⁴*Phys. Div. Ann. Progr. Rept. Jan. 31, 1964*, ORNL-3582, p. 130.

⁵V. B. Belyaev *et al.*, *Zh. Eksperim. i Teor. Fiz.* **37**, 1652 (1959); *Soviet Phys. JETP (English Transl.)* **37**, 1171 (1960).

for comparison in Table 1. In this table, L is the angular momentum of molecular rotation. For $p\mu p$, the $L = 0$ and $L = 1$ states are rigorously para and ortho states, respectively, in the adiabatic spin-independent approximation used. We regard the comparison with ref. 3 to show that the Guillemin-Zener approximation to the adiabatic state is indeed a good one. The question of the importance of higher-order corrections remains, however. The higher-order corrections involve the functions³

$$\vec{f}_{ij}(R) = \frac{1}{8} \int \psi_i(\xi, \eta, \phi_\mu; r_n) \vec{\nabla}_n \psi_j(\xi, \eta, \phi_\mu; r_n) r_n^3 (\xi^2 - \eta^2) d\xi d\eta d\phi_\mu.$$

Codes are being written to calculate the \vec{f}_{ij} and to solve the coupled equations for the nuclear motion. While this coding effort was in progress, two variational calculations were reported.^{6,7} In each of these a significant increase in binding

⁶W. R. Wessel and P. Phillipson, *Phys. Rev. Letters* **13**, 23 (1964).

⁷A. Halpern, *Phys. Rev. Letters* **13**, 660 (1964).

energy and a decrease in the overlap probability γ were found (see Table 2). The improvement in binding energy indicates that the admixture of higher BO states is considerable. It is not clear to the writers whether the variational parameters have been chosen in such a way as to guarantee an accurate value of γ . This question would be answered by the present calculation if the convergence turns out to be rapid enough to attain an equally good binding energy. A value of γ known to be accurate to within 1% would be of great help to weak interaction theory, especially in pinning down the effective pseudoscalar coupling constant.

Table 1. Binding Energies (ev) in the Adiabatic Approximation

System	L	Present Work	Ref. 3	Ref. 5
$p\mu p$	0	241.04	241	252
	1	94.41	93	109
$d\mu d$	0	320.99	322	330
	1	222.26	223	226

Table 2. Muon-Proton Overlap, γ , and Mean Internuclear Separation, $\langle R \rangle^a$

System	L	Adiabatic				Variational			
		Present Work		Ref. 2		Ref. 6		Ref. 7	
		2γ	$\langle R \rangle$	2γ	$\langle R \rangle$	2γ	$\langle R \rangle$	2γ	$\langle R \rangle$
$p\mu p$	0	1.3044	3.142	1.308	1.1466	3.13			
	1	1.1718	3.948	1.166	1.000	3.83	1.010	3.89 ± 0.02	
$d\mu d$	0	1.2552							
	1	1.1614	3.098						

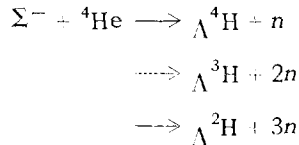
^aIn units of the muon reduced Bohr radius appropriate to $p\mu p$ or $d\mu d$, that is, $a_{p\mu p} = a_\mu^{(\infty)}(1 + m_\mu/2m_p)^{-1}$ and $a_{d\mu d} = a_\mu^{(\infty)}(1 + m_\mu/2m_d)^{-1}$.

SEARCH FOR HYPERFRAGMENTS IN THE $\Sigma^- + \text{He}$ REACTION

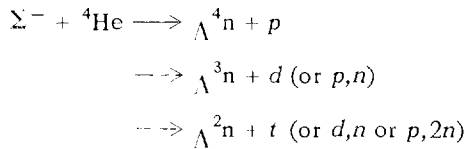
H. O. Cohn

W. M. Bugg¹

We have scanned film from a slow K^- exposure in the Northwestern University Helium Bubble Chamber in search of hyperfragments formed by slow Σ^- interactions. The only hypothetically allowed reactions that leave a hyperfragment in the final states are:



and



Energetically, no pions may be emitted. It should be pointed out that neutron hyperfragment formation in this reaction is the more difficult process, since it requires $\Lambda Q = 2$.

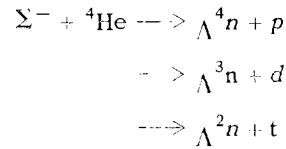
Apart from hyperfragment formation, only a lambda and one charged nucleon are allowed in the final state for Σ^- absorption. Thus, hyperfragments that decay via the charged mesic mode are readily identifiable.

Over 400 candidates for Σ^- interactions were examined. Only events that could definitely be classed as genuine $\Sigma^- + \text{He}$ interactions were considered. This reduced the sample to 370 events. A considerable fraction of these events have a π^+ at the first vertex but no discernable π^- , thus guaranteeing that a Σ^- was indeed involved in the reaction.

Five events were found that can be identified as hydrogen hyperfragments. This number needs to be corrected for scanning efficiency, for missed events that looked like decays (short hyperfragment and no stub), and, most importantly, for the ratio of charged mesic to neutral mesic and nonmesic decay modes. Applying these corrections brings the total number of hydrogen hyperfragments to

seven. Hence, we conclude that 2% of all $\Sigma^- + \text{He}$ interactions result in hydrogen hyperfragments.

The only hope of seeing neutron hyperfragments is in the two-body final state interactions:



The respective momenta are: 284 Mev/c (proton), 356 Mev/c (deuteron), 381 Mev/c (triton), with ranges of 12 cm, 4.5 cm, and 2 cm respectively. Since the Σ^- interacts at rest, the Λn and the stub must be collinear. Such an event can look like an ordinary Σ^- interaction, but with the stub and the direction to the Λ vertex collinear.

The momentum spectrum of the stubs from $\Sigma^- + \text{He}$ interaction is shown in Fig. 1. Three scales are shown, assuming the stub to be a triton, deuteron, or proton. The shaded area corresponds to events for which the angle between the stub and the lambda had cosine between -0.9 and -1.0 .

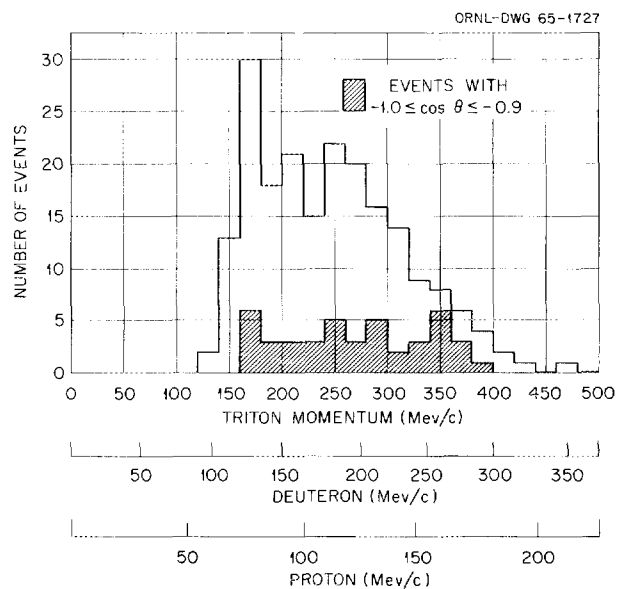


Fig. 1. Momentum Distribution of the Charged Particle (Stub) Emitted in $\Sigma^- + \text{He}$ Interaction. The shaded area corresponds to events for which the lambda and stub are collinear.

¹Consultant from the University of Tennessee.

Three events had tracks that left the chamber. On the basis of stub lengths, no candidates were found for $\Lambda^4 n$, except for the three leaving tracks. Two of these had associated noncollinear Λ 's and thus must be eliminated as candidates. The third did not have a Λ . Thus, no evidence for $\Lambda^4 n$ is seen.

Only one event with stub length in the required range for an $\Lambda^3 n$ was seen. This event had no Λ associated with it. Again, we must conclude that no evidence for $\Lambda^3 n$ is seen.

Next, we examine candidates for $\Lambda^2 n$. Ten candidates with $360 \leq p \leq 400$ Mev/c were found; 4 had no Λ , 2 had noncollinear Λ 's, and 4 had $\cos \theta$ between -0.9 and -1.0 . All of these were accurately measured. Two events had $\cos \theta$ consistent with -1.0 , the other two had $\cos \theta$ several standard deviations away from -1.0 . More important, all the Λ momenta were above 250 Mev/c, whereas the expected momentum is only 206 Mev/c. We thus conclude that no evidence for neutron hyperfragments is found.

EXCHANGE MECHANISM FOR ω PRODUCTION IN π^+n INTERACTIONS

H. O. Cohn

W. M. Bugg¹G. T. Condo¹

Recently, considerable attention has been focused on decay correlations and exchange mechanisms in the production of ρ mesons in π -nucleon interactions. The one-meson exchange model with absorptive corrections, as developed by several authors,² has exhibited considerable success in describing the salient features of ρ and N^* production from π -nucleon encounters as well as of K^* and N^* production in K -nucleon collisions. The purpose of this note is to present the corresponding data for ω production in the reaction $\pi^+ + n \rightarrow p + \omega$. The production of ω mesons in π^+p collisions has been reported by the ABC Collaboration,³ by Shen *et al.*,⁴ and by Alff *et al.*⁵ However, the reactions are not directly comparable, since in the latter case the ω is produced either in conjunction with an N^* or an uncorrelated π^+, p pair.

We have analyzed ~ 2800 events of the type $\pi^+ + d \rightarrow (p) + p + \pi^+ + \pi^- + \pi^0$ from 3.25 Bev/c π mesons incident on the BNL 20-in. deuterium bubble chamber. These events arise from two topologies: 4-prong events and 3-prong events where the spectator proton does not leave a visible recoil in the chamber. The latter events were kinematically fitted by setting the spectator momentum equal to zero. All events were required to have at least one proton identifiable by ionization, which delimits our discussion to momentum transfers $\leq 50 m_\pi^2$. No corrections have been incorporated in the momentum transfer distributions for those events where the spectator proton was not visible.

Figures 1a and b show the Chew-Low plots for the 3π events as well as for 2800 2π events from the reaction $\pi^+ + d \rightarrow (p) + p + \pi^+ + \pi^-$. The narrow ω band at $m_{3\pi}^2 = 0.6$ Bev is clearly resolved and shows that ω production is present at much higher momentum transfer (Λ^2) than is ρ production, which has practically vanished at $\Lambda^2 \leq 15m_\pi^2$. These plots also indicate the presence of the η and f^0 mesons in our experiment as well as a 3π resonance in the mass region of the A_2 (1310). As in the recent π^+d experiment of the Saclay-Orsay-Bari-Bologna Collaboration,⁶ we have been unable to demonstrate that this is a ρ - π resonance

¹Consultant from the University of Tennessee.

²F. Salzman and G. Salzman, *Phys. Rev.* **120**, 599 (1960); E. Ferrari and F. Selleri, *Nuovo Cimento*, Suppl. **24**, 453 (1962); L. Stodolsky and J. J. Sakurai, *Phys. Rev. Letters* **11**, 90 (1963); J. D. Jackson and H. Pikhun, *Nuovo Cimento* **33**, 906 (1964); K. Gottfried and J. D. Jackson, *Phys. Letters* **8**, 144 (1964); *Nuovo Cimento* **33**, 309 (1964); J. D. Jackson, to be published in the *Reviews of Modern Physics*. The last is a comprehensive introduction to the subject.

³Aachen-Berlin-CERN Collaboration, *Phys. Letters* **12**, 356 (1964).

⁴B. Shen *et al.*, *Bull. Am. Phys. Soc.* **9**, 722 (1964).

⁵C. Alff *et al.*, *Phys. Rev. Letters* **9**, 322 (1962).

⁶Saclay-Orsay-Bari-Bologna Collaboration, *Phys. Letters* **11**, 347 (1964).

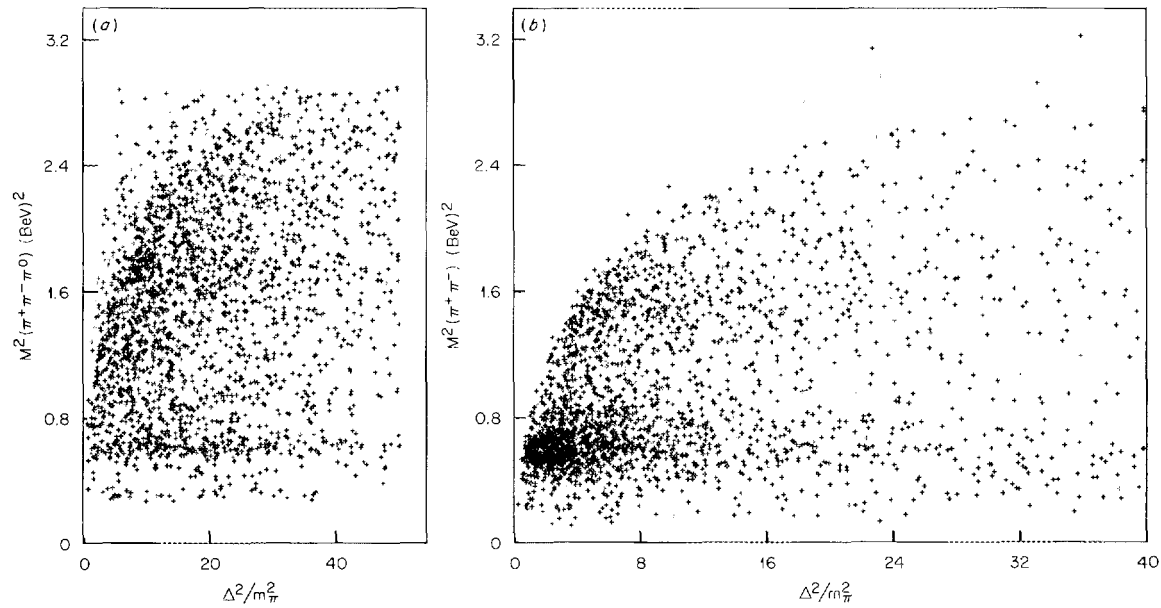


Fig. 1. Chew-Low Plots (a) for 3π System and (b) for 2π System.

as might be expected from its close equality with the $A_2(1310)$ mass.

An important test of the validity of any model for resonance production is the variation of the production cross section with momentum transfer. It is the narrowness of this distribution in ρ production that requires modification of the one-pion exchange model either via the application of form factors or through the introduction of absorptive effects. In Fig. 2a we present a histogram of ω production vs Δ^2 . No background subtraction was deemed necessary due to the narrow width of the ω and the similarity of the distribution for adjacent mass regions. The theoretical curves are due to Jackson,⁷ assuming ρ exchange as the dominant mechanism. The parameters γ_1 and C_1 are related to the elastic-scattering cross section for the initial state, while γ_2 and C_2 refer to the final state. A detailed discussion of these parameters may be found in the review article by Jackson.² The parameter

$$y = \frac{2G_T}{G_T + G_V},$$

where G_T and G_V are the tensor and vector coupling constants for the $n\rho n$ vertex. The value $y = 1.575$ corresponds to the assumption that ρ dominates the electromagnetic form factor of the nucleon, so that $G_T/G_V = \mu'_p - \mu'_n = 3.71$.

Figures 2b and c show the decay angular distributions for the decay of the ω . The angle Θ is the angle between the incident π^+ and the normal to the decay plane measured in the rest system of the ω , and Φ is the azimuthal angle specified by choosing the normal to the production plane as the y axis.

For a $J = 1$ resonance, the decay angular distributions are of the form

$$\frac{d\sigma}{d \cos \Theta} = \text{const} \times [(1 - \rho_{00}) + (3\rho_{00} - 1) \cos^2 \Theta],$$

$$\frac{d\sigma}{d\Phi} = \text{const} \times [1 - 2\rho_{1,-1} \cos(2\Phi)],$$

where the $\rho_{MM'}$ are the elements of the spin density matrix of the resonance. For the ω region with no background subtraction, a least-squares fit

⁷J. D. Jackson, private communication.

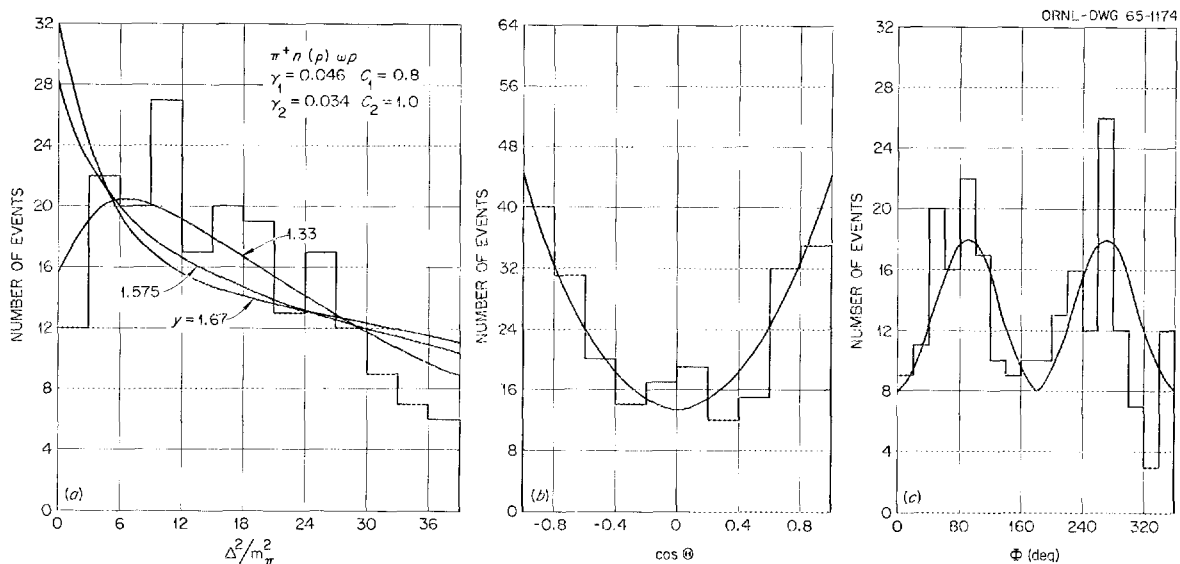


Fig. 2. Production and Decay of the ω . (a) ω production as a function of momentum transfer (the theoretical curves are due to Jackson⁷); (b) and (c) decay angular distributions for the ω decay.

yields⁸ $\rho_{00} = 0.62_{-0.04}^{+0.15}$ and $\rho_{1,-1} = 0.19 \pm 0.05$. The assumption of pure vector meson exchange without absorptive corrections predicts $\rho_{00} = 0$, while $\rho_{1,-1}$ is expected to be large. It is therefore seen that such a model yields only poor agreement with experiment. The inclusion of absorptive effects (see Table 1) improves the agreement considerably. It is recalled that for ρ production the one-pion exchange model without absorptive corrections predicts decay correlations which agree rather well with experiment⁹ ($\rho_{00} = 0.7$ vs $\rho_{00} = 1.0$ for one-pion exchange, while the model fails to predict the variations of cross section with momentum transfer. Inclusion of absorptive effects decreases ρ_{00} and alters the production cross section, so that agreement with experiment is quite good.¹⁰ In the ω case, the absorptive corrections predict decay correlations which are much closer to those experimentally observed, while

Table 1. Prediction for the Spin-Density Matrix Elements with Absorptive Corrections

The averages are taken over momentum transfer (see ref. 7)

y	G_T/G_V	$\bar{\rho}_{00}$	$\bar{\rho}_{1,-1}$
1.33	2	0.24	0.35
1.575	3.7	0.45	0.20
1.67	5	0.55	0.14

retaining a reasonable variation of production cross section with momentum transfer. We therefore conclude that, whereas the one- ρ exchange model with absorption does not fit the data as well as might be hoped, it represents a considerable improvement over strict one- ρ exchange.

Acknowledgements

We are grateful to J. Steinberger for making the bubble-chamber film available to us and thank him and N. Gelfand and G. Lutjeans for permission to include data from a previous collaboration in this analysis. We also acknowledge the thoughtfulness of J. D. Jackson in providing us with theoretical curves and for his interest and suggestions.

⁸The large upper limit is intended to reflect uncertainty in the true value of ρ_{00} due to the difficulty in effecting a proper background subtraction. The value of $\rho_{1,-1}$ was not altered by the background subtraction.

⁹Aachen-Berlin-Birmingham-Bonn-Hamburg-London (J. C.)-Munich Collaboration, *Nuovo Cimento* **34**, 495 (1964); I. Derado, V. P. Kenney, and W. D. Shephard, *Phys. Rev. Letters* **13**, 505 (1964).

¹⁰K. Gottfried and J. D. Jackson, *Nuovo Cimento* **34**, 735 (1964).

NEUTRAL DECAY AND ISOTOPIC SPIN OF THE f^0 ¹

N. Gelfand² G. Lutjens² M. Nussbaum² J. Steinberger²
 H. O. Cohn W. M. Bugg³ G. T. Condo³

We have analyzed the reactions (1) $\pi^+ + d \rightarrow p + p + \text{neutrals}$ and (2) $\pi^+ + d \rightarrow p + p + \pi^+ + \pi^-$ in an effort to determine the isotopic spin of the f^0 .

The effective two-pion mass in reaction (1) shows prominent peaks corresponding to the ρ and f^0 . The missing mass distribution for reaction (2) shows peaks at the masses of the η , ω , and f^0 . It is argued that this peak for the f^0 is primarily due to the two- π^0 decay of the f^0 . From the observed branching ratio, $(f^0 \rightarrow \text{neutrals})/(f^0 \rightarrow \text{charged})$, it is concluded that the f^0 isospin is zero.

¹Abstract of published paper: *Phys. Rev. Letters* 12, 567 (1964).

²Columbia University.

³Consultant from the University of Tennessee.

ANALYSIS OF Σ^- ABSORPTION IN HELIUM¹

K. H. Bhatt² H. O. Cohn W. M. Bugg³

The momentum spectra of the lambda and the triton observed in the reaction Σ^- (at rest) + ${}^4\text{He} \rightarrow \Lambda + n + {}^3\text{H}$ have been calculated, assuming a phenomenological interaction Hamiltonian

for the basic process $\Sigma^- + p \rightarrow \Lambda + n$. Final-state interactions were neglected. Reasonable agreement is obtained for the Λ spectrum and also for the neutron spectrum. Marked deviation is obtained between the calculated and the experimental triton spectrum, indicating strongly the possibility of a Λ - n resonance at about 43 Mev in a Λ - n system.

¹Abstract of paper submitted to *Nuovo Cimento*.

²Electronuclear Division.

³Consultant from the University of Tennessee.

REACTION $\Sigma^- + {}^4\text{He} \rightarrow \Lambda^0 + n + {}^3\text{H}$ ¹

H. O. Cohn K. H. Bhatt² W. M. Bugg³

The absorption of Σ^- at rest in helium was studied. Most of the events were found to have a

three-body final state: Λ , n , ${}^3\text{H}$. The momentum spectra for the Λ and the neutron were found to agree well with the prediction of the impulse model. The triton spectrum, however, disagreed drastically. It is suggested that the anomaly in the triton spectrum is due to a resonance in the Λ - n system at a mass value $2098 \pm 6 \text{ Mev}/c^2$.

¹Abstract of published paper: *Phys. Rev. Letters* 13, 668 (1964).

²Electronuclear Division.

³Consultant from the University of Tennessee.

PUBLICATIONS

Publications which have appeared in print (since the preparation of last year's publication listing in the Annual Report) by Physics Division staff members have included book and journal articles; additionally, reports published have included Ph.D. theses, topical reports, the annual progress report itself, and Information Center reports.

Book and Journal Articles

- Austern, N., R. M. Drisko, E. C. Halbert, and G. R. Satchler, "Theory of Finite-Range Distorted-Waves Calculations," *Phys. Rev.* **133**, B3-16 (1964).
- Bair, J. K., C. M. Jones, and H. B. Willard, "Neutrons from the Proton Bombardment of ${}^6\text{Li}$, ${}^7\text{Li}$, ${}^9\text{Be}$, ${}^{11}\text{B}$, and ${}^{18}\text{O}$," *Nucl. Phys.* **53**, 209-18 (1964).
- Bassel, R. H., R. M. Drisko, G. R. Satchler, L. L. Lee, Jr., J. P. Schiffer, and B. Zeidman, "Elastic Scattering of Deuterons by ${}^{40}\text{Ca}$," *Phys. Rev.* **136**, B960-70 (1964).
- Bassel, R. H., G. R. Satchler, and R. M. Drisko, "Elastic and Inelastic Scattering of Carbon from Carbon," pp. 45-49 in *Proc. Conf. Reactions Complex Nuclei, 3rd, Pacific Grove, Calif., Apr. 1963* (ed. by A. Ghiorso, R. M. Diamond, and H. E. Conzett), University of California Press, 1963.
- Becker, R. L. (book review), *Perturbation Theory and the Nuclear Many Body Problem*, by K. Kumar (North Holland Publishing Co., Amsterdam; Interscience, New York), *Nucl. Sci. Eng.* **19**, 137-38 (1964).
- Bjerregaard, J. H., H. R. Blieden, O. Hansen, G. Sidenius, and G. R. Satchler, "Low-Lying Levels in ${}^{42}\text{Ca}$ Excited by the ${}^{43}\text{Ca}$ (d,t) Reaction," *Phys. Rev.* **136**, B1348-54 (1964).
- Cable, J. W., W. C. Koehler, and E. O. Wollan, "Magnetic Order in Rare Earth Intermetallic Compounds," *Phys. Rev.* **136**, A240-42 (1964).
- Cable, J. W., R. M. Moon, W. C. Koehler, and E. O. Wollan, "On the Antiferromagnetism of Praseodymium," *Phys. Rev. Letters* **12**, 553-55 (1964).
- Cable, J. W., E. O. Wollan, and W. C. Koehler, "The Crystal Structure of Nickel Hydride," *J. Phys. (Paris)* **25**, 460 (1964).
- Cable, J. W., E. O. Wollan, W. C. Koehler, and H. R. Child, "Alignment of Rare Earth Moments in Dilute Pd-Fe Alloys," *J. Phys. Chem. Solids* **25**, 1453-57 (1964).
- Charles, G. W., "Comments on 'The Isotope Effect in the Spectrum of Thorium' (by Vernyi and Egorov)," Letter to Editor, *J. Opt. Soc. Am.* **54**, 267-68 (1964).
- Cohn, H. O., K. H. Bhatt, and W. M. Bugg, "The Reaction $\Sigma^- + {}^4\text{He} \rightarrow \Lambda^0 + n + {}^3\text{H}$," *Phys. Rev. Letters* **13**, 668-70 (1964).
- Condo, G. T., "On the Absorption of Negative Pions by Liquid Helium," *Phys. Letters* **9**, 65-66 (1964).
- Davies, K. T. R., and G. R. Satchler, "Spin-Spin Interactions and Scattering from Polarized Nuclei," *Nucl. Phys.* **53**, 1-21 (1964).
- Drisko, R. M., and G. R. Satchler, "Finite-Range Effects in the Distorted-Wave Theory of Stripping Reactions," *Phys. Letters* **9**, 342-45 (1964).
- Drisko, R. M., G. R. Satchler, and R. H. Bassel, "Pick-Up of Heavy Clusters," pp. 85-89 in *Proc. Conf. Reactions Complex Nuclei, 3rd, Pacific Grove, Calif., Apr. 1963* (ed. by A. Ghiorso, R. M. Diamond, and H. E. Conzett), University of California Press, 1963.
- Felcher, G. P., J. W. Cable, and M. K. Wilkinson, "The Magnetic Moment Distribution in Cu_2MnAl ," *J. Phys. Chem. Solids* **24**, 1663-65 (1963).

- Ford, J. L. C., Jr., J. K. Bair, R. L. Robinson, and H. B. Willard, "A Search for Interference Effects Between Nuclear Resonance and Coulomb Excitation in the $^{23}\text{Na}(p,p')$ Reaction," *Nucl. Phys.* **55**, 43-48 (1964).
- Fowler, J. L.,¹ "The Interaction of Neutrons with ^{208}Pb ," Program of the *Topical Conference on Compound Nuclear States*, ORNL-CF-63-10-89, pp. 8-11 (1963).
- Fowler, T. K., "Bounds on Plasma Instability Growth Rates," *Phys. Fluids* **7**, 249-56 (1964).
- Fowler, T. K., and M. Rankin, "Ambipolar Scattering Losses from Magnetic Mirrors," *J. Nucl. Energy: Pt. C* **6**, 513-14 (1964).
- Gelfand, N., G. Lutjens, M. Nussbaum, J. Steinberger, H. O. Cohn, W. M. Bugg, and G. T. Condo, "Neutral Decay and Isotopic Spin of the f^0 ," *Phys. Rev. Letters* **12**, 567-68 (1964).
- Ginocchio, J. N., and J. B. French, "Energies of $f_{7/2}$ -Shell Nuclei," *Phys. Letters* **7**, 137-39 (1963).
- Halbert, M. L., F. E. Durham, C. D. Moak, and A. Zucker, "Fluctuations in the $^{12}\text{C}(^{16}\text{O},\alpha)^{24}\text{Mg}$ Reaction," pp. 213-18 in *Proc. Conf. Reactions Complex Nuclei, 3rd, Pacific Grove, Calif., Apr. 1963* (ed. by A. Ghiorso, R. M. Diamond, and H. E. Conzett), University of California Press, 1963.
- Harvey, J. A., G. G. Slaughter, J. R. Bird, and G. T. Chapman, "Gamma-Ray Spectra from Resonance Neutron Capture in the Tin Isotopes," Paper III-4, pp. 230-35 in *Proc. Intern. Conf. on Physics with Reactor Neutrons (Argonne National Laboratory, October 1963)*, ANL-6797 (1963).
- Haybron, R. M., H. McManus, A. Werner, R. M. Drisko, and G. R. Satchler, "Polarization in High-Energy Inelastic Scattering," *Phys. Rev. Letters* **12**, 249-51 (1964).
- Johnson, C. H., and C. C. Trail, "Neutron Spectra from $^7\text{Li}(d,n)^8\text{Be}$ and $^{19}\text{F}(d,n)^{20}\text{Ne}$ for 1.98-MeV Deuterons," *Phys. Rev.* **133**, B1183-90 (1964).
- Johnson, C. H., C. C. Trail, and A. Galonsky, "Thresholds for (p,n) Reactions on 26 Intermediate Weight Nuclei," *Phys. Rev.* **136**, B1719-29 (1964).
- Koehler, W. C., E. O. Wollan, H. R. Child, and J. W. Cable, "Some Magnetic Structure Properties of Rare Earth Alloys," pp. 199-208 in *Conference on Rare Earth Research II (Proc. 3rd Rare Earth Conf., Clearwater, Fla., Apr. 1963)* (ed. by K. S. Vorres), Gordon and Breach, 1964.
- Koehler, W. C., H. L. Yakel, E. O. Wollan, and J. W. Cable, "A Note on the Magnetic Structure of Rare Earth Manganese Oxides," *Phys. Letters* **9**, 93-95 (1964).
- Krause, M. O., M. L. Vestal, W. H. Johnston, and T. A. Carlson, "Readjustment of the Neon Atom Ionized in the K-Shell by X-Rays," *Phys. Rev.* **133**, A385-90 (1964).
- Kronsbein, J., and T. A. Welton, "Note on Parametrization of the Four-Dimensional Real Symplectic Group," *J. London Math. Soc.* **39**, 291-95 (1964).
- Lee, L. L., J. P. Schiffer, B. Zeidman, G. R. Satchler, R. M. Drisko, and R. H. Bassel, " $^{40}\text{Ca}(d,p)^{41}\text{Ca}$, a Test of the Validity of the Distorted-Wave Born Approximation," *Phys. Rev.* **136**, B971-93 (1964).
- McGowan, F. K., P. H. Stelson, and W. G. Smith, "Cross Sections for the $^{58}\text{Ni}(\alpha,\gamma)$ and $^{59}\text{Co}(\alpha,n)$ Reactions," *Phys. Rev.* **133**, B907-10 (1964).
- Macklin, R. L., "The MnSO_4 Bath and Graphite Pile Flux Measuring Techniques," in *Proceedings EANDC Symposium on Absolute Determination of Neutron Flux in the Energy Range 1-100 keV (Oxford, England, September 1963)*, EANDC-33 (1963).
- Macklin, R. L., "Resonance Self-Shielding in Neutron Capture Cross Section Measurements," *Nucl. Instr. Methods* **26**, 213-15 (1964).

¹For the Introductory Note by J. L. Fowler and the Invited Papers from the Topical Conference on Compound Nuclear States see *Rev. Mod. Phys.* **36**, 1065-1102 (1964).

- Macklin, R. L., P. J. Pasma, and J. H. Gibbons, "Resonance Neutron Capture and Transmission in Sulfur, Iron, and Lead," *Phys. Rev.* **136**, B695-702 (1964).
- Miller, P. D., J. L. Duggan, and M. M. Duncan, "Absence of States in ^8Be at 7.56, 13.91, and 18.00 MeV," *Nucl. Phys.* **54**, 155-60 (1964).
- Moak, C. D., "Experiments with Heavy Ions," *Proc. Third Intern. Accelerator Conf., Boston, Mass., Nov. 1963* [*Nucl. Instr. Methods* **28**, 155-59 (1964)].
- Moak, C. D., W. M. Good, R. F. King, J. W. Johnson, H. E. Banta, J. Judish, and W. H. duPreez, "Nano-second Pulsing for Van de Graaff Accelerators," *Rev. Sci. Instr.* **35**, 672-79 (1964).
- Moon, R. M., J. W. Cable, and W. C. Koehler, "The Magnetic Structure of Neodymium," *J. Appl. Phys., Suppl.* **35**, 1041-42 (1964).
- Owen, L. W., and G. R. Satchler, "Multipole Moments of a Rounded Charge-Distribution," *Nucl. Phys.* **51**, 155-60 (1964).
- Paya, D., J. W. T. Dabbs, J. A. Harvey, and H. Horstmann, "Acceleration of Free Neutrons Under Gravity," paper I-5, pp. 30-34 in *Proc. Intern. Conf. on Physics with Reactor Neutrons (Argonne National Laboratory, October 1963)*, ANL-6797 (1963).
- Penny, S. K., and G. R. Satchler, "Inelastic Effects in Stripping and Other Direct Reactions," *Nucl. Phys.* **53**, 145-58 (1964).
- Pleasanton, Frances, and C. H. Johnson, "System for Continuous Generation and Fast Transfer of Radioactive Gases," *Rev. Sci. Instr.* **35**, 97-102 (1964).
- Powers, D., J. K. Bair, J. L. C. Ford, Jr., and H. B. Willard, "The Elastic Scattering of Alpha Particles by ^{18}O ," *Phys. Rev.* **134**, B1237-42 (1964).
- Roberts, L. D., and J. O. Thomson, "A Study of the Magnetic Properties of Gold in Alloys with Iron, Cobalt, and Nickel at 4.2°K by the Recoilless Radiation Method," pp. 267-68 in *Proc. Intern. Conf. Low Temp. Phys., 8th, London, 1962* (1963).
- Robinson, R. L., F. K. McGowan, and P. H. Stelson, "Coulomb Excitation of ^{63}Cu and ^{65}Cu ," *Phys. Rev.* **134**, B567-74 (1964).
- Sakai, M., H. Ikegami, Y. Nakagima, K. Yagi, E. Ejiri, and G. R. Satchler, "Excitation of Low Excited States in ^{114}Cd by (p, p') Reaction," *Phys. Letters* **8**, 197-200 (1964).
- Sakai, M., and T. Tamura, "Inelastic Scattering of Protons by ^{114}Cd and Possible Quadrupole-Octupole Two-Phonon States," *Phys. Letters* **10**, 323-25 (1964).
- Satchler, G. R., "The Distorted-Waves Theory of Direct Nuclear Reactions with Spin-Orbit Effects," *Nucl. Phys.* **55**, 1-33 (1964).
- Satchler, G. R., "Distorted-Wave Calculations and Spectroscopic Factors," pp. 23-50 in *Proc. Topical Conf. Nucl. Spectroscopy with Direct Reactions (Chicago, Ill., March 1964)*, ANL-6878 (1964).
- Satchler, G. R., R. M. Drisko, and R. H. Bassel, "Optical Model Analysis of Quasi-Elastic (p, n) Reactions," *Phys. Rev.* **136**, B637-47 (1964).
- Satchler, G. R., and R. M. Haybron, "Optical Model Analysis of 182 MeV Proton Scattering," *Phys. Letters* **11**, 313-15 (1964).
- Satchler, G. R., J. L. Yntema, and H. W. Broek, "Shell-Model Selection Rules and Excitation of 4^+ States in the $\text{Ti}(\alpha, \alpha')$ Reaction," *Phys. Letters* **12**, 55-56 (1964).
- Schmitt, H. W., "Remarks on Absolute Heavy Element Neutron Capture Cross Sections Determined by the Sphere-Transmission Method," pp. 41-43 in *Proc. EANDC Symp. on Absolute Determination of Neutron Flux in the Energy Range 1-100 keV (Oxford, England, September 1963)*, EANDC-33 (1963).
- Schmitt, H. W., and N. Feather, "Interpretation of the Fragment Mass Distribution for ^{235}U Thermal-Neutron-Induced Fission with Long-Range Alpha Emission," *Phys. Rev.* **134**, B565-67 (1964).

- Sheldon, Eric, "Legendre Hyperpolynomials in Angular Correlation" (Appendix to "Angular Correlation in Inelastic Nucleon Scattering"), *Rev. Mod. Phys.* **35**, 849-53 (1963).
- Stelson, P. H., and F. K. McGowan, "Cross Sections for (α, n) Reactions for Medium-Weight Nuclei," *Phys. Rev.* **133**, B911-19 (1964).
- Stelson, P. H., and R. L. Robinson, "Excitation of Collective States by Inelastic Scattering of 14-MeV Neutrons," p. 852 in *Direct Interactions and Nuclear Reaction Mechanisms, Nuclear Physics Vol. I* (Proc. Intern. Symp. on Direct Interactions and Nuclear Reaction Mechanisms, Padova, Italy, September 1962) (ed. by E. Clementel and C. Villi), Gordon and Breach, New York, 1963.
- Tamura, T., "Coupled-Channel Analysis of the Scattering of Protons by ^{165}Ho and ^{156}Gd ," *Phys. Letters* **9**, 334-36 (1964).
- Tamura, T., "Adiabatic and Non-Adiabatic Coupled Channel Calculations of the Scattering of Protons by Deformed Nuclei," *Phys. Letters* **12**, 121-23 (1964).
- Tamura, T., and T. Terasawa, "Optical Model plus Resonance Analysis of the Elastic Scattering of Protons by ^{12}C ," *Phys. Letters* **8**, 41-43 (1964).
- Tamura, T., and T. Udagawa, "Higher Random Phase Approximation Applied to the Description of the Spherical Vibrational Nuclei," *Nucl. Phys.* **53**, 33-53 (1964).
- Terasawa, T., and G. R. Satchler, "The Shape of the Symmetry-Term in the Nuclear Optical Potential," *Phys. Letters* **7**, 265-67 (1963).
- Wagner, R., P. D. Miller, T. Tamura, and H. Marshak, "The Interaction of 350 keV Polarized Neutrons with Oriented ^{165}Ho Nuclei," *Phys. Letters* **10**, 316-18 (1964).
- Walter, F. J., H. W. Schmitt, and J. H. Neiler, "Correlated Fragment Energy Measurements for Low Energy Neutron Induced Fission," paper V-5, pp. 441-48 in *Proc. Intern. Conf. on Physics with Reactor Neutrons (Argonne National Laboratory, October 1963)*, ANL-6797 (1963).
- Walter, F. J., H. W. Schmitt, and J. H. Neiler, "Fragment Mass Distributions for Thermal Neutron Induced Fission of ^{239}Pu and ^{241}Pu ," *Phys. Rev.* **133**, B1500-2 (1964).
- Way, K. (book reviews)
Isobaric Nuclei with the Mass Number A = 73 by Grigor'ev; *Isobaric Nuclei with the Mass Number A = 74* by Dzheleпов; *Isobaric Nuclei with the Mass Number A = 110* by Dzheleпов and Khukovskii; *Isobaric Nuclei with the Mass Number A = 140* by Dzheleпов, Prikhodtseva, and Kohl'nov. Russian translations, ed. by R. W. Clarke, Pergamon, Oxford - Macmillan, New York, 1963. *Phys. Today* **17**(11), 72 (1964).
- Willard, H. B., J. K. Bair, and C. M. Jones, "*N-D* Scattering: A Search for Effects Due to the Dineutron," *Phys. Letters* **9**, 339-41 (1964).
- Williams, C. W., and J. A. Biggerstaff, "Sub-Nanosecond Timing with Semiconductor Detectors," *Nucl. Instr. Methods* **25**, 370 (1964).
- Williams, C. W., W. E. Kiker, and H. W. Schmitt, "Correlated Energy and Time-of-Flight Measurements of Fission Fragments with Semiconductor Detectors: System Design and Performance," *Rev. Sci. Instr.* **35**, 1116-23 (1964).
- Williams, C. W., H. W. Schmitt, F. J. Walter, and J. H. Neiler, "Instrumentation for Fission-Fragment Energy Correlation Experiments with Pile-Up Reduction Capabilities," paper IV-4, pp. 438-40 in *Proc. Intern. Conf. on Physics with Reactor Neutrons (Argonne National Laboratory, October 1963)*, ANL-6797 (1963).
- Williams, C. W., H. W. Schmitt, F. J. Walter, and J. H. Neiler, "Instrumentation for Fission Fragment Energy Correlation Experiments," *Nucl. Instr. Methods* **29**, 205-12 (1964).
- Yagi, K., H. Ejiri, M. Furukawa, Y. Ishizaki, M. Koike, K. Matsuda, Y. Nakajima, I. Nonaka, Y. Saji, E. Tanaka, and G. R. Satchler, "Excitation of Low-Lying Levels in ^{40}Ca by (p, p') Scattering at $E_p = 55$ MeV," *Phys. Letters* **10**, 186-91 (1964).

Yntema, J. L., and G. R. Satchler, "(d,³He) Reaction on ⁴⁰Ca and the Titanium Isotopes," *Phys. Rev.* **134**, B976-84 (1964).

Yntema, J. L., and G. R. Satchler, "Nucleon Capture Reactions near A = 40," p. 177 in *Proc. Topical Conf. on Nuclear Spectroscopy with Direct Reactions (Argonne National Laboratory, March 1964)*, ANL-6848 (1964).

Theses

Forester, D. W., *Mössbauer Studies of the Hyperfine Structure Spectra of ⁵⁷Fe in FeRh Alloys, α -Fe₂O₃, and FeNH₄(SO₄)₂ · 12H₂O*, Ph.D. Thesis, University of Tennessee, ORNL-3705.

Harlow, M. V., *The Yield of Elastically Scattered 17 to 21 MeV Neutrons from the Reaction ¹²C(n,n)¹²C*, Ph.D. Thesis, University of Texas, ORNL-3615.

Kiker, W. E., *Correlated Energy and Time-of-Flight Measurements of Fission Fragments*, Ph.D. Thesis, University of Tennessee, ORNL-3692.

Muir, R. B., *A Study of Hyperon Production by 430 MeV/c K⁻ Mesons in Helium*, Ph.D. Thesis, University of Tennessee, ORNL-3717.

Physics Division Annual Progress Report

Fowler, J. L., H. B. Willard, and E. O. Wollan, *ORNL Physics Division Annual Progress Report for the Period Ending January 31, 1964*, 156 pp., ORNL-3582.

Topical Reports

Johnson, M. B., and L. W. Owen, *Slater Integrals and Form Factors for Inelastic Scattering Using Realistic Single-Particle Wave Functions: The Code ATHENA*, ORNL-TM-964.

Perey, F. G., and A. M. Saruis, *Effects of Non-Locality in Off-Diagonal Potentials*, ORNL-TM-967.

Reeves, Mark, III, *Q Values of 3-Body Nuclear Reactions*, ORNL-TM-938.

Stelson, P. H., *Some Recent Nuclear Cross Section Measurements at the Oak Ridge National Laboratory, June 2, 1964-October 1, 1964*, ORNL-TM-954.

Willard, H. B., *Nuclear Cross Section Program at the Oak Ridge National Laboratory, August 1, 1963-January 2, 1964*, ORNL-TM-761.

Willard, H. B., *Nuclear Cross Section Program at the Oak Ridge National Laboratory, January 2, 1964-June 1, 1964*, ORNL-TM-874.

Information Center Reports

McGowan, F. K., W. T. Milner, and H. J. Kim,² *Nuclear Cross Sections for Charged-Particle Induced Reactions Mn, Fe, Co*, ORNL-CPX-1.

Way, K., A. Artna, E. C. Campbell, W. B. Ewbank, N. B. Gove, M. J. Martin, H. Ogata, and A. K. Sen Gupta,³ *Nuclear Data Sheets: Vol. 5, Set 6, A = 150, 152, 154, 156, 158, 160; Appendix 1, Table F. Vol. 6, Set 1, A = 162, 163, 164, 167, 169; Nuclear Moments; Appendix 4. Vol. 6, Sets 2-3, Recent References.*

Way, K., A. Artna, E. C. Campbell, W. B. Ewbank, N. B. Gove, M. J. Martin, H. Ogata, and A. K. Sen Gupta,³ *Nuclear Theory Index, Cumulation for 1963, Booklet 4.*

Way, K.,³ *World-Wide News of Compilations in Nuclear Physics*, vol. 1, No. 2, June 1964.

²Charged Particle Cross Section Data Center.

³Nuclear Data Group.

PAPERS PRESENTED AT SCIENTIFIC AND TECHNICAL MEETINGS

Australian and New Zealand Association for the Advancement of Science, Australian National University, Canberra, Australia, January 20-24, 1964

J. L. Fowler, "Nuclear Physics at the Oak Ridge National Laboratory,"

American Physical Society Meeting, New York, New York, January 22-25, 1964

S. Bernstein and E. C. Campbell, "Polarization of Totally Reflected Mössbauer Radiation."

T. A. Carlson and M. O. Krause, "Atomic Readjustment to Inner Shell Vacancies in Neon and Argon."

H. O. Cohn and W. M. Bugg, " Σ^- Interaction with Helium."

J. C. Hiebert and J. A. McIntyre, "The $^{14}\text{N}(^{14}\text{N}, ^{13}\text{N})^{15}\text{N}$ Reaction at E (c.m.) = 7.2, 8.0, and 8.8 MeV."

M. O. Krause and T. A. Carlson, "Ionization of Krypton by X-Rays."

F. K. McGowan, R. L. Robinson, P. H. Stelson, J. L. C. Ford, and W. T. Milner, "Coulomb Excitation of Vibrational Triplet States and Octupole States in the Even Cadmium Nuclei."

H. Maier-Leibnitz, "Proposed Method for Obtaining Beams of Homogeneous Energy from Low-Energy Accelerators."

H. Marshak, R. K. H. Wagner, and P. D. Miller, "Search for a Spin-Spin Effect in the Interaction of Polarized Neutrons with a Polarized ^{165}Ho Target. II."

P. D. Miller, J. L. Duggan, and M. M. Duncan, "Absence of States in ^8Be at 7.56, 13.91, and 18.00 MeV."

D. S. Onley and T. Tamura, "Shell Model Description of Transition Charge Distribution for Excitation of Vibrational States in Nuclei."

H. W. Schmitt, F. J. Walter, and J. R. Oleson, "Fission Fragment Energy Correlation Measurements: Fission at Low Excitation Energies."

G. G. Seaman, J. S. Greenberg, D. A. Bromley, and F. K. McGowan, "Collective Excitations in the Even-Even Samarium Isotopes."

R. K. H. Wagner, P. D. Miller, and H. Marshak, "Search for a Spin-Spin Effect in the Interaction of Polarized Neutrons with a Polarized ^{165}Ho Target. I."

H. B. Willard, J. K. Bair, and C. M. Jones, " n - D Scattering and the Di-Neutron."

Electron Microscope Meeting, Argonne National Laboratory, Argonne, Illinois, February 13-14, 1964

T. A. Welton, "The ORNL Program in Electron Microscopy."

American Chemical Society (Kentucky Lake Section), Paducah, Kentucky, February 13-14, 1964

P. M. Griffin, "An Introduction to the Optical Maser, with Demonstrations."

National Symposium on Nuclear Spectroscopy, Tbilisi, U.S.S.R., February 14-22, 1964

P. H. Stelson, "Excitation of Collective States by Coulomb Excitation and by (n, n') ."

Biophysical Society (8th Annual Meeting), Chicago, Illinois, February 26-28, 1964

T. A. Welton, "Molecular Structure Determination by High-Resolution Electron Microscopy."

Scintillation and Semiconductor Counter Symposium (9th Annual Meeting), Washington, D.C., February 26-28, 1964

F. J. Walter, "Multiplication in the Fission Fragment Pulse Height Response of Silicon Surface Barriers."

Conference on Nuclear Spectroscopy with Direct Reactions (Topical Conference of the American Physical Society and Argonne National Laboratory), Chicago, Illinois, March 9–11, 1964

G. R. Satchler, "Distorted-Wave Calculations and Spectroscopic Factors."

T. Tamura, "Analysis of the Scattering of Protons by ^{165}Ho in Terms of the Coupled Channel Calculation."

J. L. Yntema and G. R. Satchler, "Nucleon Capture Reactions near $A = 40$."

American Physical Society Meeting, Philadelphia, Pennsylvania, March 23–26, 1964

J. W. Cable, W. C. Koehler, and E. O. Wollan, "Magnetic Order in Rare Earth Intermetallic Compounds."

H. R. Child, W. C. Koehler, E. O. Wollan, and J. W. Cable, "Magnetic Properties of Intra-Rare-Earth Alloys."

W. C. Koehler, H. R. Child, E. O. Wollan, and J. W. Cable, "Magnetic Structures of Rare-Earth/Lanthanum Alloys."

Instrument Society of America (Carolina Piedmont Section), Charlotte, North Carolina, April 17–18, 1964

P. M. Griffin, "An Introduction to the Optical Maser, with Demonstrations."

Fourth Rare Earth Conference, Phoenix, Arizona, April 22–25, 1964

W. C. Koehler, H. L. Yakel, E. O. Wollan, and J. W. Cable, "The Magnetic Structures of Rare Earth Manganites RMnO_3 ."

American Physical Society Meeting, Washington, D.C., April 27–30, 1964

R. H. Bassel, G. R. Satchler, and R. M. Drisko, "Analysis of Mutual and Double Excitation Processes in the Scattering of Heavy Ions."

S. Bernstein, "Total Reflection of Gamma Rays from ^{57}Fe in the Region of Nuclear Anomalous Dispersion (Mössbauer Effect)."

J. A. Biggerstaff, J. H. Gibbons, W. M. Good, R. L. Macklin, and P. J. Pasma, "keV-Range Neutron Resonances in ^{32}S , ^{56}Fe , ^{206}Pb , ^{207}Pb , and ^{208}Pb ."

C. F. Coleman, F. E. Obenshain, L. D. Roberts, and J. O. Thomson, "A Mössbauer Study of the Effective Field at the ^{57}Fe Nucleus in Hydrated Ferric Ammonium Alum."

J. W. T. Dabbs, F. J. Walter, and G. W. Parker, "Resonance Fission of Oriented ^{235}U Nuclei."

N. Gelfand, M. Nussbaum, J. Steinberger, H. O. Cohn, W. M. Bugg, and G. T. Condo, "The Isotopic Spin of the f^0 and Its Possible Identity with the Buddha."

C. H. Johnson and J. L. Fowler, "Phase Shift Analysis of Neutron Scattering from ^{16}O ."

C. M. Jones, J. K. Bair, C. H. Johnson, and H. B. Willard, "Alpha-Alpha Correlations in the Reaction $^7\text{Li} + d \rightarrow 2\alpha + n$."

J. B. McGrory and W. T. Pinkston, "Calculation of Beta-Decay Transition Rates for the Decay of ^{208}Tl ."

L. D. Roberts, F. E. Obenshain, R. L. Becker, and J. O. Thomson, "The Residual Resistance Due to Gold in an Alloy Containing Two Atomic Percent of Gold in Nickel."

R. L. Robinson, P. H. Stelson, H. J. Kim, and J. Rapaport, "Excitation of Collective States by Inelastic Scattering of 14-MeV Neutrons."

P. H. Stelson, "Excitation of Collective Motions of Nuclei by Inelastically Scattered 14-MeV Neutrons."

P. H. Stelson, F. K. McGowan, R. L. Robinson, and J. L. C. Ford, Jr., "Coulomb Excitation of States in ^{92}Mo and ^{119}Sn ."

C. W. Williams, W. E. Kiker, and H. W. Schmitt, "Correlated Energy and Time-of-Flight Measurements of Fission Fragments with Semiconductor Detectors: System Design and Performance."

American Physical Society Meeting, Denver, Colorado, June 25-27, 1964

J. L. Duggan, P. D. Miller, M. M. Duncan, and V. H. Webb, "The $^{14}\text{C}(^3\text{He},\alpha)^{13}\text{C}$ and $^{14}\text{C}(^3\text{He},p)^{16}\text{N}$ Reactions."

International Symposium on Diffusion of Plasma Across a Magnetic Field, Munich, Germany, June 29-July 3, 1964

T. K. Fowler, "Bounds on Diffusion by Microinstabilities."

Congrès International de Physique Nucléaire, Paris, France, July 2-8, 1964

J. K. Bienlein and F. Pleasonton, "Internal Bremsstrahlung Accompanying the β -Decay of ^{42}K ."

P. F. Fettweis and E. C. Campbell, "Conversion Electrons of (p,n) Excited States in ^{114}In and ^{116}In ."

C. M. Jones, J. K. Bair, C. H. Johnson, and H. B. Willard, "Sequential Emission in the Reaction $^7\text{Li}(d,n)^2^4\text{He}$."

K. Way, "Proposal of Key-Word System."

K. Way, "Exposition of Organization of the American Group."

Fisk University Infrared Institute (15th Annual Meeting), Nashville, Tennessee, August 10-14, 1964

P. A. Staats, "Experimental Infrared Spectroscopy."

Ninth International Conference on Low Temperature Physics, Columbus, Ohio, August 31-September 4, 1964

J. W. T. Dabbs, "Method for Obtaining Second Derivatives in Electron Tunneling."

F. E. Obenshain, L. D. Roberts, C. F. Coleman, D. W. Forester, and J. O. Thomson, "A Study of the Hyperfine Interactions in Ferric Ammonium Alum as a Function of H/T in the Liquid Helium Temperature Region."

L. D. Roberts, F. E. Obenshain, R. L. Becker, and J. O. Thomson, "A Correlation of the Mössbauer Isomer Shift and the Residual Electrical Resistivity for ^{197}Au Alloys: Experiments and Theory."

Gordon Research Conference on Nuclear Reaction Mechanisms, New London, New Hampshire, August 31-September 4, 1964

J. L. Fowler, "Elastic Neutron Scattering from Closed Shell Nuclei and Intermediate States."

G. R. Satchler, "Direct Reaction Calculations."

P. H. Stelson, "Review of Neutron Reactions Involving Direct Interactions."

International Conference on Magnetism, Nottingham, England, September 7-11, 1964

W. C. Koehler, J. W. Cable, H. R. Child, R. M. Moon, and E. O. Wollan, "Neutron-Magnetic Scattering Studies at the Oak Ridge National Laboratory."

Society for Applied Spectroscopy (3rd National Meeting), Cleveland, Ohio, September 28-October 2, 1964

H. W. Morgan, P. A. Staats, and R. G. Steinhardt, "A Low Temperature Liquid Infrared Absorption Cell."

Electron Microscopy Society of America, Detroit, Michigan, October 13, 1964

T. A. Welton, "Molecular Structure Determination by Electron Microscopy."

Conference on Correlations of Particles Emitted in Nuclear Reactions (Topical Conference of the American Physical Society and Oak Ridge National Laboratory), Gatlinburg, Tennessee, October 15-17, 1964

C. M. Jones, J. K. Bair, C. H. Johnson, and H. B. Willard, "Sequential Emission in the Reaction ${}^7\text{Li}(d,n){}^2{}^4\text{He}$."

Metallurgical Society of the American Institute of Mining and Metallurgical Engineers, Philadelphia, Pennsylvania, October 19-22, 1964

W. C. Koehler, "Neutron Diffraction and Magnetic Structure."

American Physical Society Meeting, Chicago, Illinois, October 23-24, 1964

G. G. Slaughter and J. A. Harvey, "Gamma Ray Spectrum from the Capture of Thermal Neutrons in Bismuth."

Division of Plasma Physics of the American Physical Society (6th Annual Meeting), New York, New York, November 4-7, 1964

T. K. Fowler, "Effect of Plasma Potential on Minimum- B Stability."

Southeastern Section Meeting of the American Physical Society, Chattanooga, Tennessee, November 5-7, 1964

G. W. Charles, "Hyperfine Structure of ${}^{209}\text{Po}$."

H. O. Cohn and W. M. Bugg, "Search for Hyperfragments in the $\Sigma^- + \text{He}$ Reaction."

J. L. Fowler and C. H. Johnson, "Differential Scattering of Neutrons from ${}^{16}\text{O}$."

P. M. Griffin, H. W. Morgan, O. B. Rudolph, P. A. Staats, K. L. Vander Sluis, and G. K. Werner, "Description of an Easily Built, Inexpensive, Helium-Neon Demonstration Laser."

R. L. Kernell, C. H. Johnson, and S. T. Thornton, "Cross Sections for the (p,n) Reaction for Five Isotopes of Sn and the ${}^{120}\text{Sn}(p,n){}^{120}\text{Sb}$ Threshold."

W. E. Kinney, J. K. Dickens, J. A. Biggerstaff, and F. G. Perey, "Study of Neutron Inelastic Scattering for $3 \text{ MeV} < E_n < 5 \text{ MeV}$."

J. B. McGroary and K. H. Bhatt, "The Residual n - p Interaction in Isotopes of Nb and Mo."

H. W. Morgan, "Infrared Studies on the Solid State."

W. B. Newbolt, W. K. Robinson, J. O. Thomson, F. E. Obenshain, and L. D. Roberts, "The Lifetime of the 77.3 keV First Excited State of ${}^{197}\text{Au}$ by the Mössbauer Method."

F. E. Obenshain, L. D. Roberts, C. F. Coleman, and J. O. Thomson, "Hyperfine Structure Coupling in Ferric Ammonium Sulfate as a Function of Magnetic Field and Temperature."

W. K. Robinson, W. B. Newbolt, J. O. Thomson, F. E. Obenshain, and L. D. Roberts, "The ${}^{197}\text{Au}$ Mössbauer Isomer Shift as a Function of Composition for Au-Ni Alloys."

R. L. Robinson and P. H. Stelson, "Gamma-Ray Spectroscopy with a Lithium-Drifted Germanium Detector."

G. G. Slaughter and J. A. Harvey, "Neutron Capture Gamma Ray Measurements with a Lithium-Drifted Germanium Detector."

J. O. Thomson, W. B. Newbolt, W. K. Robinson, F. E. Obenshain, and L. D. Roberts, "The Magnetic Field at the ${}^{197}\text{Au}$ Nucleus in Au-Ni Alloys."

S. T. Thornton, C. H. Johnson, and J. L. Fowler, "Errors of Phase Shifts Resulting from Elastic Differential Scattering Analysis."

H. B. Willard, "Cooperative Efforts Between Universities and the National Laboratories in the Training of Physicists."

Conference on Magnetism and Magnetic Materials (10th Annual Meeting), Minneapolis, Minnesota, November 16-19, 1964

J. W. Cable, W. C. Koehler, and H. R. Child, "Magnetic Structure Versus Electron Number for Some Rare Earth Intermetallic Compounds."

W. C. Koehler, "The Magnetic Properties of Rare Earth Metals and Alloys."

R. M. Moon, W. C. Koehler, and J. J. Farrell, "Magnetic Structures of Rare Earth-Cobalt (RCO_2) Intermetallic Compounds."

Symposium on Chemical Effects Associated with Nuclear Reactions and Radioactive Transformations, Vienna, Austria, December 7-11, 1964

T. A. Carlson and R. M. White, "Explosion of Multi-Charged Molecular Ions: Chemical Consequences of Inner Shell Vacancies."

FOREIGN TRAVEL

Talks presented by Physics Division staff members at conferences outside the United States during the past year are included in the two preceding sections either as proceedings articles in the "Publications" section or in the section entitled "Papers Presented at Scientific and Technical Meetings"; a few talks are also listed under a later section headed "University Seminars." In addition to these talks, and connected visits while abroad to atomic energy installations and universities for discussions on scientific subjects of mutual interest, the following Division members engaged in foreign travel during 1964.

J. K. Bair (High Voltage Group) began a one-year assignment at the Atomic Energy Research Establishment in Harwell, England, where he is engaged in research concerning nuclear structure physics. This assignment is a continuation of the profitable liaison in physics between AERE and ORNL, which originated in 1959, and is the fifth such exchange-type assignment of a Physics Division staff member to the Harwell Laboratory.

T. A. Carlson¹ (Charge Spectrometry Group) was assigned for five weeks during January and February to the Pakistan Atomic Energy Center at Lahore, Pakistan. He was engaged in setting up a program for calculations of charge spectra measurements which are now being carried out on the ORNL 1604 computer. This visit was a continuation of collaboration between F. B. Malik² of Pakistan and T. A. Carlson on the problem of relativistic electron wave functions.

T. K. Fowler (Plasma Physics Group) was a member of a United States team of scientists who visited controlled fusion research facilities in the U.S.S.R. Visits and contacts during the two-week period spent there in February were arranged by the U.S. Atomic Energy Commission.

¹ORNL Chemistry Division.

²1964 summer employee with the ORNL Physics Division; presently at Yale University on leave from the Pakistan Atomic Energy Center.

T. K. Fowler additionally spent the three-month period of June through September at the Culham Laboratory in Abingdon, England, where he was engaged in the pursuit of theoretical plasma physics research at the invitation of Dr. J. B. Taylor, Head of the Theoretical Division at Culham. This research provided valuable scientific liaison between ORNL and the Culham Laboratory in the field of plasma physics.

J. H. Gibbons³ (High Voltage Group) spent two weeks as Special Representative of the Oak Ridge Institute of Nuclear Studies University Relations Division at the United States Atomic Energy Commission's "Atoms in Action" exhibit which opened April 15 in Madrid, Spain. He supervised final arrangements and preparations for the ORINS Lecture Demonstration Program and participated in the first week of program presentation. The program was basically one of presenting modern lecture demonstration techniques for the teaching of science at the secondary school level. He also presented seminars in Madrid on current research in neutron capture work at ORNL.

Frances Pleasonton (Charge Spectrometry Group) consulted with J. K. Bienlein⁴ at CERN, Geneva, Switzerland, for three weeks during September and October for the completion of joint internal bremsstrahlung research.

K. Way (Nuclear Data Group) was cochairman (with Professor L. Rosenfeld of Nordita, Copenhagen, Denmark) of a Session on Scientific Information held at the Congrès International de Physique Nucléaire in Paris, France, in July. W. B. Ewbank (Nuclear Data Group) also attended the Paris conference as an observer and reporter; in the same capacity he attended the 7th "Brookhaven" Conference on Molecular Beams, which was held in Uppsala, Sweden, during June.

³On leave to the Oak Ridge Institute of Nuclear Studies for this assignment.

⁴Former consultant with the ORNL Physics Division.

ANNOUNCEMENTS

Listed in other sections of this report are those Ph.D. candidates engaged in thesis research, co-op students, consultants under subcontract, and summer investigators (including research participants, visitors, and student trainees) who have been associated with the Physics Division during 1964. Additionally, nine investigators from six foreign countries began or completed temporary assignments which varied from six months to two years in duration. Presently with the Laboratory from abroad are G. Mazzone¹ of the Comitato Nazionale per l'Energia Nucleare in Rome, Italy (Neutron Diffraction Group) and D. M. Seyboth of the University of Erlangen in Erlangen, Germany (Mössbauer Experimental Program). Assignments were completed by the following individuals who have returned to their home organizations abroad: P. J. Armbruster of the Kernforschungsanlage Jülich in Jülich, Germany (Physics of Fission Group); C. F. Coleman of the Atomic Energy Research Establishment in Harwell, England (High Voltage

¹Now with the ORNL Solid State Division.

Group); Y. Hamaguchi of the Japan Atomic Energy Research Institute in Tokai, Japan (Neutron Diffraction Group); H. Maier-Leibnitz, Director of the Laboratorium für Technische Physik der Technischen Hochschule in Munich, Germany (ORNL Director's Division and collaborator with the Physics of Fission Group); D. Paya² of the Commissariat à l'Energie Atomique in Paris, France (Low Energy Neutron Time-of-Flight Spectrometry Group); Anna Maria Saruis of the Centro di Calcolo, Comitato Nazionale per l'Energia Nucleare, in Bologna, Italy (Theoretical Physics Group); and R. K. H. Wagner of the University of Basel in Basel, Switzerland (High Voltage Group).

Loanees assigned temporarily to the Division during this period have included R. M. Haybron, professor of physics from Michigan State University (Theoretical Physics Group); and three students in physics from the University of Tennessee -- M. Brown,³ a graduate student (High Voltage Group -- Tandem Accelerator); J. T. Humphreys, an undergraduate student (High Energy Physics Group); and S. T. Thornton,⁴ a graduate student (High Voltage Group).

An academic-year leave of absence (1964-65) was granted to S. Bernstein (Mössbauer Experimental Program), during which time he will be engaged as professor of physics at the University of Illinois.

In the fall of 1964, J. H. Gibbons (High Voltage Group) began a part-time assignment of one year with the ORNL Civil Defense Study Program, which is headed by E. P. Wigner.

There were seven intralaboratory transfers among research personnel during the year. G. W. Charles (Spectroscopy Research Group) transferred to the Thermonuclear Division. The Neutron Diffraction Group, a highly active and productive research team within the Physics Division for the past twenty years, transferred to the Solid State Division late in 1964. E. O. Wollan, group leader since the inception of the neutron diffraction program at ORNL and Associate Division Director since 1948, is now Special Scientific Advisor to the Director's Division. Members of the group who are now a part of the Solid State Division include W. C. Koehler (newly appointed group leader), J. W. Cable, H. R. Child, G. Mazzone,⁵ and R. M. Moon, Jr.

Technician D. G. Peach (Physics of Fission Group) terminated employment with the Laboratory during this report period.

²Exchange visitor. G. de Saussure of the Neutron Physics Division was the ORNL exchange visitor to the Paris laboratory.

³Assignment completed.

⁴1964 summer employee with the ORNL Physics Division.

⁵Temporary assignment.

ADVISORY COMMITTEE

Advisory committees are attached to the majority of the research divisions of the Oak Ridge National Laboratory for the purpose of offering advice on the cogency and effectiveness of the many scientific programs under way.

At the June 22–26, 1964, Annual Information Meeting,¹ 15 Physics Division investigators presented talks before Laboratory staff members, Advisory Committee members, and guests from the AEC and other installations, which covered 21 areas of research during the year. Advisory Committee members at that time included:

Dr. A. M. Clogston	Bell Telephone Laboratories Murray Hill, New Jersey
Prof. B. L. Cohen	University of Pittsburgh Pittsburgh, Pennsylvania
Prof. Martin Deutsch	Massachusetts Institute of Technology Cambridge, Massachusetts
Prof. D. L. Judd	Lawrence Radiation Laboratory University of California Berkeley, California
Prof. L. J. Rainwater	Columbia University New York, New York
Prof. J. A. Wheeler	Princeton University Princeton, New Jersey

¹The Electronuclear Division and the Physics Division hold their Annual Information Meetings jointly and are served by the same Advisory Committee.

AMERICAN PHYSICAL SOCIETY

Southeastern Section Meeting

The Thirty-first Meeting of the Southeastern Section of the American Physical Society was co-sponsored by the University of Chattanooga and the Oak Ridge National Laboratory and took place on the campus in Chattanooga November 5–7, 1964. The elected Chairman of the Society for 1963–64 was L. D. Roberts of the Physics Division; on the 12-member Program Committee from the Division were H. B. Willard and J. O. Thomson.¹ In addition to the active part taken by the above-mentioned individuals in planning and conducting the meeting, there were 2 invited papers and 14 contributed papers presented by others of the Division.

¹Faculty member of the University of Tennessee and consultant to the ORNL Physics Division.

NUCLEAR CROSS SECTIONS ADVISORY GROUP

Oak Ridge Meeting

A meeting of the Nuclear Cross Sections Advisory Group to the Division of Research of the U.S. Atomic Energy Commission was held at the Oak Ridge National Laboratory October 13 and 14, 1964. Physics Division staff members H. B. Willard (Associate Director) and P. H. Stelson (Director of the High Voltage Laboratory), retiring member and newly appointed NCSAG member, respectively, arranged and conducted the meeting, which was attended by 20 NCSAG members and guests.

MISCELLANEOUS ACTIVITIES OF DIVISIONAL PERSONNEL

Physics Division staff members are frequently requested or appointed to assume certain professional duties which, although related to, are incident to their primary responsibilities at ORNL. Such duties may be in connection with scientific journals, societies, committees, institutes, etc., and have included during the past year the following:

- | | |
|----------------------------|--|
| J. L. Fowler | Member of the National Research Council to represent the American Physical Society in the Division of Physical Sciences
Member of Brookhaven National Laboratory Physics Visiting Committee
Member of Carnegie Institute of Technology Physics Visiting Committee
Member of AEC Accelerator Review Panel (1964) |
| T. K. Fowler | Chairman of Sherwood Theory Meeting (Gatlinburg, Tennessee, May 1964)
Member of the Board of Editors of <i>Physics of Fluids</i> |
| N. B. Gove | Secretary of the National Academy of Sciences—National Research Council Subcommittee on Nuclear Structure
Secretary of the National Academy of Sciences—National Research Council Subcommittee on Techniques for the Distribution of Scientific Information
Reviewer for <i>Computing Reviews</i>
Member of the Program Committee for the Gordon Research Conference on Critical Tables |
| J. A. Harvey | Reviewer for <i>Computing Reviews</i>
Reviewer for <i>Nuclear Science and Engineering</i>
Assistant in the preparation of Supplement 2, Second Edition of BNL-325, "Neutron Cross Section Compilation" (Vol. 1 published in 1964) |
| W. C. Koehler ¹ | Committeeman (Solid State Physics), National Research Council Advisory Committee on Basic Research to the U.S. Army Research Office, Durham
Member of Advisory Committee for the "Conference on Magnetism and Magnetic Materials"
Member of the ORNL High Flux Isotope Reactor Review Committee |

¹Now with the ORNL Solid State Division.

- R. L. Macklin
Member of the Oak Ridge Gaseous Diffusion Plant Nuclear Safety Committee
Member of the Membership Committee for the Research Society of America (Oak Ridge Branch)
Member of the ORNL Reactor Operations Review Committee
- P. D. Miller
Reviewer for *Computing Reviews*
Representative from the Physics Division for the ORNL Computer Advisory Committee
- C. D. Moak
Reviewer for *Reviews of Scientific Instruments*
Member of the Program Committee for the American Physical Society Topical Conference on Particle Accelerators (Washington, D.C., March 1965)
- H. W. Morgan
Faculty Member of Fisk Infrared Spectroscopy Institute
Member of Subcommittee on Infrared Band Intensities of the International Union of Pure and Applied Chemistry
- Frances Pleasonton
Compiler and coeditor of brochure entitled "The Oak Ridge National Laboratory and Its Scientific Activities" (published in 1964)
- L. D. Roberts
Chairman of the Southeastern Section of the American Physical Society (1963-64)
Chairman of the Fritz London Award Committee
Member of Organizing Committee for "Ninth International Conference on Low Temperature Physics"
- G. R. Satchler
Member of the ORNL Graduate Fellow Selection Panel
Reviewer for *Physical Review*
Member of Organizing Committee for "Gordon Research Conference on Nuclear Reaction Mechanisms"
- P. A. Staats
Faculty Member of Fisk Infrared Spectroscopy Institute
- P. H. Stelson
Member of the National Academy of Sciences-National Research Council Subcommittee on Nuclear Structure
Member of the Atomic Energy Commission Nuclear Cross Section Advisory Group
- K. L. Vander Sluis
Member of the National Academy of Sciences-National Research Council Committee on Line Spectra of the Elements
- Katharine Way
Chairman of the National Academy of Sciences-National Research Council Subcommittee on the Techniques for Distribution of Scientific Information
Member of the Subcommittee on Nuclear Data of the International Union of Pure and Applied Physics (Commission on Low-Energy Nuclear Physics)
- T. A. Welton
Reviewer for *Journal of Applied Physics*

H. B. Willard

Member of the Atomic Energy Commission Nuclear Cross Section Advisory Group (until September 1964)

Member of the ORNL Graduate Fellow Selection Panel (former Panel Chairman)

ACTIVITIES RELATED TO EDUCATIONAL INSTITUTIONS

Research Participants

The Research Participation Program of the Oak Ridge Institute of Nuclear Studies¹ enables selected university faculty members to participate in research, primarily during the summer months, at several major installations of the U.S. Atomic Energy Commission. The Oak Ridge National Laboratory provides most of these appointments; some projects are conducted at the University of Tennessee Agricultural Research Laboratory and at the Oak Ridge Institute of Nuclear Studies. In addition, appointments are now possible at the Puerto Rico Nuclear Center and at the Savannah River Laboratory. Of mutual benefit to the participant and to the laboratory where he carries out his work, this arrangement between the Oak Ridge Institute of Nuclear Studies and laboratories in Oak Ridge has, since its inception in 1947, also been extremely important to the progress of nuclear energy research and development, not only in the South, but in the entire nation. To date, 767 faculty members from 222 colleges and universities in 45 states, Puerto Rico, and the District of Columbia have engaged in research under this program.

In the summer of 1964, 57 Research Participants, representing 48 colleges and universities in 28 states, received appointments. The following 6 investigators were engaged in research with the Physics Division of the Oak Ridge National Laboratory: G. T. Condo² (Assistant Professor, University of Tennessee), High Energy Physics Group; R. T. Folk (Associate Professor, Lehigh University), Theoretical Physics Group; W. E. Hunt (Assistant Professor and Chairman, Physics Department, David Lipscomb College), Charge Spectrometry Group; W. B. Newbolt (Instructor, Washington and Lee University), Low Temperature Physics Group and the Mössbauer Program; W. K. Robinson (Associate Professor, St. Lawrence University), Mössbauer Program; and W. W. Walker (Assistant Professor, University of Alabama), High Voltage Group and Physics of Fission Group.

Summer Visitors

Summer visitors with the Division in 1964 included: W. M. Bugg² (Associate Professor, University of Tennessee), High Energy Physics Group; F. B. Malik³ (Senior Scientific Officer, Pakistan Atomic

¹Under contract with the U.S. Atomic Energy Commission.

²Consultant to the ORNL Physics Division.

³Visiting Fellow at Yale University from fall 1964 to spring 1967.

Energy Commission), Theoretical Physics Group; M. Reeves III (graduate student and teaching assistant, University of Tennessee), High Voltage Group; and S. T. Thornton⁴ (graduate student under AEC Nuclear Science and Engineering Fellowship, University of Tennessee), High Voltage Group.

Physics Division staff members were pleased also to have had close association and collaboration with investigators assigned to other ORNL Divisions during the summer months. These included W. C. Marshall (Atomic Energy Research Establishment, Harwell, England), M. A. Melvin (Professor, Florida State University) J. A. Wheeler⁵ (Professor, Princeton University), and R. M. White (Assistant Professor, Baker University).

Summer Student Trainee Program

The Summer Student Trainee Program is administered by the Oak Ridge Institute of Nuclear Studies in cooperation with the Oak Ridge National Laboratory under the sponsorship of the U.S. Atomic Energy Commission. The program offers temporary summer appointments, on a competitive basis, to a limited number of students who have completed their junior year of college and who are majoring in the sciences. Primarily for students (citizens of the United States) from small colleges in the southern region, this arrangement affords students the opportunity of working in a full-time research laboratory during the summer months and serves to encourage them to carry on graduate work after they have attained the bachelor degree in science.

In 1964, the sixth year of the Student Trainee Program, students with the Physics Division under the auspices of this program were selected from 41 applicants whose majors were either physics or mathematics. These included: Edith A. Adams (Oklahoma City University), Theoretical Physics Group; A. C. Bolling (Pfeiffer College), Spectroscopy Research Group; Sarah M. Farlow (Asbury College), Theoretical Physics Group; D. W. Holland (Union University), High Energy Physics Group; J. C. Propes (Eastern New Mexico University), High Voltage Group; and Wendy N. Torrance (Occidental College), Neutron Diffraction Group.

Cooperative Education Program for Undergraduate Students

Promising students in science and engineering, who have completed at least two quarters of undergraduate study, are selected to participate in the Cooperative Education Program of the Oak Ridge National Laboratory. Students alternate between equal periods of time spent in school attendance and in work at the Laboratory.

Now in its 13th year at ORNL, the Co-op Program continues to prove a highly successful means both for promoting the professional development of students and for providing valuable technical assistance in the varied research programs at the Laboratory.

⁴Now assigned to the ORNL Physics Division as a loanee.

⁵Member of the Advisory Committee for the Physics Division and the Electronuclear Division of ORNL.

Eleven Co-op students were with the Physics Division during the past year; five were assigned to the High Energy Physics Group, three to the Theoretical Physics Group, two to the High Voltage Group, and one to the Physics of Fission Group. These students included: E. R. Golston, Jr., of the Georgia Institute of Technology in Atlanta, Georgia; D. T. Olson⁶ of the University of Louisville, Kentucky; M. B. Johnson and M. Lynne McFadden of the Virginia Polytechnic Institute in Blacksburg, Virginia; D. J. Burkholz⁶ and S. L. Kramer of the Drexel Institute of Technology in Philadelphia, Pennsylvania; and R. G. Beidel, D. N. Mashburn, R. J. Metzger, J. R. Penland, and A. Rebecca Tyson of the University of Tennessee in Knoxville.

Cooperative Program in Graduate Education Between ORNL and the University of Tennessee Supported by the Ford Foundation

The Ford Foundation grant to the University of Tennessee now supports 24 ORNL staff members as part-time faculty members in the Departments of Chemistry, Mathematics, Physics, Biological Sciences, Nuclear Engineering, Engineering Mechanics, Chemical Engineering, and Metallurgical Engineering. These joint appointments, under AEC approval, allow the participants to be released from their Laboratory duties in order to spend 20% of their time at the University teaching courses, supervising theses, consulting with students and other professors, and participating in seminars, staff meetings, and examinations. Physics Division staff members who have continued in this arrangement as Professors of Physics include L. D. Roberts, T. A. Welton, and H. B. Willard.

Oak Ridge Graduate Fellowship Program

There were 23 new applications for predoctoral fellowships during the 1964 calendar year, of which 17 were recommended for fellowships by the ORNL Graduate Fellow Selection Panel. At present, Panel members from the Physics Division are G. R. Satchler and H. B. Willard.

The current distribution of approved Oak Ridge Graduate Fellows includes 14 physicists (A. D. MacKellar and M. L. West II of the Physics Division), 4 chemists, 5 biologists, 3 mathematicians, 3 nuclear engineers, 1 electrical engineer, and 1 chemical engineer.

AEC Postdoctoral Program

At the present time there are eight AEC Postdoctoral Fellows at the Laboratory, including F. P. Gibson⁷ in the Physics Division. This program has not grown a great deal in the past year, because of budgetary restrictions.

⁶Terminated Co-op assignment during this period.

⁷Ph.D in physics from Massachusetts Institute of Technology, 1963.

Ph.D. Thesis Research

During the past year, 20 Physics Division staff members served in an advisory or supervisory capacity for thesis research conducted by 18 Ph.D. candidates; 6 of these candidates received their doctorates and 1 completed the required thesis research in 1964. Following is a listing of the individuals concerned:

Ph.D. Candidate	Staff Member(s)	Field of Research
Raymond Carpenter University of Tennessee	H. W. Morgan and P. A. Staats	High Resolution Infrared Spectroscopy of Tritiated Molecules
H. R. Child ⁸ University of Tennessee	E. O. Wollan ⁹ and W. C. Koehler ⁸	Magnetic Properties of Rare Earth Alloys
D. W. Forester ^{10,11} University of Tennessee	L. D. Roberts and F. E. Obenshain	Mössbauer Studies of the Hyperfine Structure Spectra of ^{57}Fe in FeRh Alloys, $\alpha\text{-Fe}_2\text{O}_3$, and $\text{FeNH}_4(\text{SO}_4)_2 \cdot$ $12\text{H}_2\text{O}$ (see ORNL-3705)
M. V. Harlow ^{10,11} University of Texas	R. L. Robinson and J. L. Fowler	The Yield of Elastically Scattered 17 to 21 MeV Neutrons from the Reaction $^{12}\text{C}(n,n)^{12}\text{C}$ (see ORNL-3615)
R. W. Hockenbury Rensselaer Polytechnic Institute	R. C. Block	Neutron Capture Measurements
R. L. Kernell ¹² University of Tennessee (on leave from College of William and Mary)	C. H. Johnson	Neutron Capture Cross Sections in the Kilovolt Range
W. E. Kiker ^{10,11} University of Tennessee	H. W. Schmitt	Correlated Energy and Time-of- Flight Measurements of Fission Fragments (see ORNL-3692)
T. King Rensselaer Polytechnic Institute	R. C. Block	Neutron Capture Measurements
A. D. MacKellar ¹⁰ Texas A and M University	R. L. Becker and T. A. Welton	Brueckner Theory for Finite Nuclei
J. H. Marable University of Tennessee	T. A. Welton	Nuclear Three-Body Problem
W. T. Milner University of Tennessee	F. K. McGowan	Coulomb Excitation with Heavy Ions

⁸Now with the ORNL Solid State Division.

⁹Now with the ORNL Directors Division.

¹⁰Oak Ridge Graduate Fellow.

¹¹Doctorate received in 1964.

¹²National Science Foundation Faculty Predoctoral Fellow.

R. B. Muir ^{10,11} University of Tennessee	H. O. Cohn	A Study of Hyperon Production by 430 MeV/c K^- Mesons in Helium (see ORNL-3717)
C. W. Nestor, Jr. Vanderbilt University	G. R. Satchler	Theory of Nuclear Structure
T. C. Oakberg ¹¹ University of Cincinnati	P. M. Griffin	Experimental Determination of Atomic Transition Probabilities Using a D-C Arc Plasma Jet
S. K. Penny University of Tennessee	G. R. Satchler	Theory of Nuclear Reactions
Gordon Soper ^{10,11} University of Tennessee	T. K. Fowler	Studies of the Ion Cyclotron Resonance Instability (see ORNL-3696)
F. J. Walter ¹³ University of Tennessee	J. W. T. Dabbs and H. W. Schmitt	The Kinetics of Thermal- and Resonance-Neutron-Induced Fission
M. L. West II ¹⁰ University of Texas	H. B. Willard and C. H. Johnson	(n,p) Differential Scattering Cross Section

Oak Ridge Resident Graduate Program of the University of Tennessee

During the past year three members of the Physics Division staff have been affiliated with the Oak Ridge Resident Graduate Program of the University of Tennessee – E. C. Campbell as Acting Director, and R. L. Becker, E. C. Campbell, and W. C. Koehler⁸ as lecturers in physics.

There are at present 316 students enrolled in the Oak Ridge Resident Graduate Program, of which 27 are candidates for the Ph.D. degree in physics and 29 are candidates for the Master's degree in physics. Since the Graduate Program of the University began operation in 1947, about one-half of the 66 Ph.D.'s granted in physics have been conferred on students enrolled in the Oak Ridge Resident Graduate Program.

Consultants Under Subcontract

Staff members of universities, both in the United States and in Europe, who have served as consultants to the Division during the past year are listed below. Numerous other consultants have presented seminar talks and have worked in collaboration with the various Physics groups during this period.

M. Baranger Carnegie Institute of Technology	Theoretical Physics Group
L. C. Biedenharn, Jr. Duke University	Theoretical Physics Group

¹³Thesis research completed in 1964; now with Radiation Instrument Development Laboratory, Oak Ridge.

W. M. Bugg University of Tennessee	High Energy Physics Group
G. T. Condo University of Tennessee	High Energy Physics Group
R. D. Edge University of South Carolina	High Voltage Group
J. B. French University of Rochester	Theoretical Physics Group
J. H. Goldstein Emory University	Spectroscopy Research Group
W. G. Holladay Vanderbilt University	Theoretical Physics Group
J. M. Jauch ¹⁴ University of Geneva, Geneva, Switzerland	Theoretical Physics Group
T. Lauritsen ¹⁴ California Institute of Technology	High Voltage Group
R. W. Lide University of Tennessee	Physics of Fission Group
J. B. Marion University of Maryland	Low Energy Neutron Time-of-Flight Spectroscopy Group
S. A. Moszkowski University of California at Los Angeles	Theoretical Physics Group
H. W. Newson Duke University	High Voltage Group
A. H. Nielsen University of Tennessee	Spectroscopy Research Group
W. T. Pinkston Vanderbilt University	Theoretical Physics Group
W. Thiele ¹⁴ Max-Planck Institut für Chemie Mainz, Germany	Nuclear Data Group
J. O. Thomson University of Tennessee	Low Temperature Group and Mössbauer Program
H. H. F. Wegener ¹⁴ University of Erlangen Erlangen, Germany	Mössbauer Program
K. Wildermuth Florida State University	Physics of Fission Group
J. H. Wise Washington and Lee University	Spectroscopy Research Group

¹⁴Subcontract closed during 1964.

Three graduate students were also under subcontract with the Division as part-time consultants during the year:

J. Ginocchio ¹⁴ University of Rochester	Theoretical Physics Group
C. S. Han ¹⁴ University of Maryland	Nuclear Data Group
R. Nutt ¹⁵ University of Tennessee	High Voltage Group

Traveling Lecture Program

The Traveling Lecture Program is conducted in cooperation with the Oak Ridge Institute of Nuclear Studies as a part of the U.S. Atomic Energy Commission's program of encouraging the dissemination of scientific and technical information to universities, particularly those in the South. Laboratory personnel present in their lectures unclassified information to university undergraduate and graduate students and to faculty members. The lectures serve to stimulate interest in research in the university departments and also assist the teaching staff in expanding the scope of instruction offered under the regular curricula. Through such personal contacts, ORNL staff members are also able to observe departmental activities at the universities. During the current academic year (1964-65), 13 members of the Physics Division have to date accepted invitations to present 24 lectures under this program; a complete listing of these will appear in the next annual report.

Listed below are 14 members of the Division who participated in the Traveling Lecture Program during the academic year 1963-64, presenting a total of 53 lectures at 45 different colleges and universities:

J. W. T. Dabbs	Louisiana State University in New Orleans, March 18, 1964 Texas A and M University, March 20, 1964 "Resonance Neutron-Induced Fission of Oriented Uranium Nuclei"
K. T. R. Davies	Christian Brothers College, April 9, 1964 "Classical Mechanics with Special Emphasis on the Hamiltonian Operator" University of Maryland, April 23, 1964 "Symmetry Properties of the S-Matrix with Application to Resonance Reactions"
J. L. Fowler	University of Miami, February 27, 1964 "Elastic Neutron Scattering and Nuclear Structure"

¹⁵On leave from the ORNL Instrumentation and Controls Division.

K. L. Vander Sluis	University of Miami, February 17, 1964
	Tuskegee Institute, February 19, 1964
	University of Alabama, February 20, 1964
	Louisiana State University, February 25, 1964
	Sam Houston State College, February 27, 1964
	University of Arkansas, February 28, 1964
	Hamline University, April 6, 1964
	Luther College, April 8, 1964
	St. Olaf College, April 7, 1964
	University of Notre Dame, April 10, 1964
	“An Introduction to the Optical Maser, with Demonstrations”
G. K. Werner	University of Oklahoma, October 29, 1963
	University of Dallas, October 25, 1963
	Phillips University, October 28, 1963
	University of Nebraska, October 31, 1963
	“Introduction to the Optical Laser, with Demonstrations of the Gas Laser”

Visiting Scientists Program in Physics – Colleges

The Visiting Scientists Program in Physics -- Colleges, now in its eighth year, is sponsored jointly by the American Association of Physics Teachers and the American Institute of Physics under grants from the National Science Foundation. The Program has the following objectives: (1) to stimulate interest in physics among undergraduates in colleges and universities through visits by leaders in physics research, (2) to provide opportunities for physics staff members of the visited institutions to discuss their research and teaching problems with the visiting physicists, and (3) to acquaint other members of the academic community and the public with recent developments in physics. Emphasis is placed on visits to the smaller colleges and universities. Two Physics Division staff members lectured under this program during the past year:

R. C. Block	West Virginia University, March 19, 1964
	“Physics Research at a National Laboratory”
L. D. Roberts	St. Lawrence University
	“Nuclear Alignment”
	“The Mössbauer Effect”

University Seminars

In addition to lectures presented under the Traveling Lecture Program and the Visiting Scientists Program in Physics, and to talks given at scientific meetings and conferences, Divisional staff members receive numerous requests from universities and colleges for seminar talks. Seventeen such invitations were accepted from 15 different educational institutions during this report period:

- J. L. Fowler University of Auckland, New Zealand, January 30, 1964
 "Elastic Neutron Scattering and Phase Shift Analysis"
- T. K. Fowler Princeton University, December 2, 1964
 "Bounds on Anomalous Diffusion"
- P. M. Griffin Antioch College, March 13, 1964
 "Introduction to the Optical Maser, with Demonstrations"
- J. A. Harvey Rensselaer Polytechnic Institute, October 28, 1964
 University of Saskatchewan, Canada, July 14, 1964
 "Neutron Spectroscopy, Capture Gamma Ray Spectra from Neutron Capture,
 and Resonant Gamma Ray Absorption"
- W. C. Koehler¹⁶ University of Pittsburgh, July 15, 1964
 "Magnetic Structures of Rare Earth Metals and Alloys"
- H. Maier-Leibnitz¹⁷ Rensselaer Polytechnic Institute, February 20, 1964
 "Some Work on Fission Using Thermal Neutrons"
- H. W. Morgan Loyola University, March 14, 1964
 Louisiana State University, March 14, 1964
 Davidson College, May 7, 1964
 "An Introduction to the Optical Maser, with Demonstrations"
- R. L. Robinson Vanderbilt University, May 15, 1964
 "Coulomb Excitation of Medium Weight Even-Odd Nuclei"
- G. R. Satchler University of Michigan, October 29 and November 2, 1964
 "Optical Model of the Nucleus"
 "Recent Studies of Direct Nuclear Reactions"
- Michigan State University, November 4, 1964
 "Optical Model of the Nucleus"
- P. H. Stelson University of Rochester, November 19, 1964
 "Excitation of Collective Motions by Coulomb Excitation and Direct Inter-
 actions"
- T. Tamura Institute for Nuclear Research, Dubna, U.S.S.R., December 17-23, 1964
 Institute for Theoretical Physics, Copenhagen, Denmark, December 26, 1964
 "Analyses of the Scattering of Nuclear Particles by Collective Nuclei in
 Terms of the Coupled-Channel Calculation"

ORINS-ORNL Summer Institute

A Summer Institute in Modern Physics for physics teachers from small colleges was held in Oak Ridge June 15 through August 7, 1964. This was the fourth such Institute conducted by the Oak Ridge Institute of Nuclear Studies in cooperation with the Oak Ridge National Laboratory and sponsored by the U.S. Atomic Energy Commission. As in past years, the Institute was designed primarily to give participants an opportunity to review modern physics, acquire an understanding of current developments, become familiar with new equipment, and gain greater insight into the development of college courses in the fields of their interests.

¹⁶Now with ORNL Solid State Division.

¹⁷Temporary assignment to the ORNL Directors Division.

Attendance at the Summer Institute was restricted to 20 college physics teachers from as many colleges. The scheduled program was geared to adhere to normal academic work loads; the major portion of the formally scheduled time was used for classroom lectures, laboratory assignments, and visits to Oak Ridge laboratories. Additional unscheduled time was provided for group discussions, library work, individual study, and attendance at lectures and discussions given by distinguished visiting scientists.

Included among the lecturers during the eight-week Institute were four Physics Division staff members. Fifteen lectures were presented by J. L. Fowler on "Nuclear Physics"; R. L. Becker presented two lectures on "Theory of Beta Decay" and three lectures on "Particles of Physics"; and P. M. Griffin and W. C. Koehler¹⁶ lectured, respectively, on "Lasers" and "Neutron Diffraction."

Demonstrations and tours conducted by members of the Division were as follows:

L. D. Roberts	Mössbauer Experiment at ORNL
H. B. Willard	Tour of the High Voltage Laboratory
J. A. Harvey	Neutron Chopper and the Oak Ridge Research Reactor

ORINS Conference on "Science and Contemporary Social Problems"

The Oak Ridge Institute of Nuclear Studies sponsored a Conference on "Science and Contemporary Social Problems," which was held in Oak Ridge, June 15 through July 15, 1964. The Oak Ridge National Laboratory cooperated with ORINS in this venture with regular participation by five Laboratory staff members and informal discussions between other staff members and conference participants. J. H. Gibbons, of the Physics Division's High Voltage Group, spoke on two topics - "Accelerators: Their Development and Purpose" and "Low Energy Research at ORNL: Kinds of Problems Dealt With; Kinds of Questions Asked; Ways of Finding Answers."

The Conference was attended by 25 participants, most of whom hold academic positions, and was based on three themes: (1) characteristics of the scientific activity, especially as exemplified by ORNL; (2) the social aspects of science and scientists, and their consequence for modern society; and (3) selected social and intellectual problems in contemporary society, sharpened by the impact of science and technology.

ORNL PHYSICS SEMINARS

Divisional seminars are normally held at the Laboratory each Friday at 3:15 PM; for topics of especial timeliness or interest additional talks are frequently scheduled. R. L. Becker assumed the duties of seminar chairman in July 1964, replacing H. O. Cohn, who served as seminar chairman the preceding two years. Lectures presented during calendar year 1964 are listed below:

January 10	Everett Fuller, National Bureau of Standards "Nuclear Photoeffect in Deformed Nuclei"
January 13	P. F. M. Fettweis, Centre d'Etude de l'Energie Nucléaire, Mol, Belgium "Conversion Electrons from Nuclear States of Indium Excited by (p,n) Reactions"

- January 17 Eugene Guth, ORNL
"Excitation of Nuclei by X-Rays and Electrons"
- January 31 Roy Middleton, University of Pennsylvania
"Some Experiments with the Aldermaston Multiangle Spectrograph"
- February 3 F. P. Gibson, ORINS-ORNL
"Effect of Finite-Range n - p Potential in Coulomb Stripping Reactions"
- February 14 H. Maier-Leibnitz, Director, Laboratorium für Technische Physik der Technischen Hochschule, München, Germany
"Detailed Investigation of the Fission Process Using Slow Neutrons"
- February 28 Michel Baranger, Carnegie Institute of Technology
"Nuclear Deformations in the Pairing plus Quadrupole Model"
- March 6 Anton Peterlin, Camille Dreyfuss Laboratory, Research Triangle Institute
"NMR and Electron Microscope Investigations of Drawn Polymers"
- March 13 Katharine Way, ORNL
"Nuclear Systematics and Scientific Information"
- March 20 L. R. B. Elton, Battersea College of Technology, London, England
"Rotational States in Light Nuclei"
- April 3 Yuval Ne'eman, California Institute of Technology
"The Eight-Fold Way and the Omega Minus"
- April 7 Y. Yoshizawa, Osaka University, Japan, and Indiana University
"Coulomb Excitation of Some Deformed Nuclei"
- April 10 J. W. T. Dabbs, ORNL
"Gravitational Acceleration of Free Neutrons"
- April 16 Juergen Heberle, Argonne National Laboratory
"The Magnetic Moment of the 26.8 keV State of Iodine-129 Measured with the Aid of Superconducting Magnets"
- April 24 A. H. Snell and T. K. Fowler, ORNL
"Thermonuclear Research in the U.S.S.R."
- May 1 P. Swan, Rice University
"Method for Deducing Potentials from Phase Shifts"
- May 6 Y. A. Rocher, University of Paris, France
"Resonance Effects in Rare Earth Metals"
- May 8 Hans Frauenfelder, University of Illinois
"Mössbauer Effect"
- May 15 C. F. Coleman, Atomic Energy Research Establishment, Harwell, England
"Experiments Using the Rutherford Laboratory 51-MeV Proton Linac"
- May 20 L. C. Biedenharn, Duke University
"Operator Structures in the Unitary Groups"
- May 22 P. Armbruster, Kernforschungsanlage, Jülich, Germany
"Measurement of the Mean Primary Charge for ^{235}U Fission Fragments"
- June 4 J. W. Beams, University of Virginia
"Some Uses of Constant Speed Rotation"
- June 12 R. C. Block, ORNL
"Research with the 30-MeV Electron Linac at Harwell"
- June 19 D. D. Clayton, Rice University
"Current Events and Developments in Cosmology"

- June 30 Y. Hamaguchi, Japan Atomic Energy Research Institute
"Neutron Diffraction Study of Cr-Dilute Alloys"
- July 2 J. A. Wheeler, Princeton University
"Gravitational Contraction and Baryon Conservation"
- July 7 J. L. Beeby,¹ University of Illinois
"A Comparison of Propagator Methods and Band Structure Calculations"
- July 9 Martin Blume,¹ Brookhaven National Laboratory
"Relaxation Problems in the Mössbauer Effect"
- July 10 K. H. Bhatt, ORNL
"Nuclear Spectroscopy of the Isotopes of Nb, Mo, and Tc"
- July 17 Joseph Ford, Georgia Institute of Technology
"The Ubiquitous Non-Linear Oscillator"
- July 23 M. A. Melvin,¹ Florida State University
"Introduction to General Relativity: I. The Magnetic Universe"
- July 24 Sven Wahlborn, Los Alamos Scientific Laboratory
"Parity Impurities in Nuclear States"
- July 30 M. A. Melvin,¹ Florida State University
"Introduction to General Relativity: II. Electromagnetism in General Spacetimes"
- July 31 Marvin Abraham, ORNL
"Electron Spin Resonance on Rare Earth Ions in ThO₂"
- August 6 A. Isihari,¹ Brooklyn Polytechnic Institute
"Pair Correlation Function of a Many-Body System"
- August 14 Shiro Yoshida, Osaka University, Japan
"Nuclear Spectroscopy of Deformed Nuclei"
- August 21 H. Ikegami, Tokyo Institute of Technology, Japan
"Capture Gamma Ray Spectroscopy and the Capture Mechanism"
- August 25 R. D. Edge, Yale University
"Electrodisintegration in the Region Up to 100 MeV"
- August 25 S. Moszkowski,¹ University of California at Los Angeles
"Nuclear Many Body Theory"
- August 27 M. A. Melvin,¹ Florida State University
"Introduction to General Relativity: III. Time, Length, Light Velocity and Red Shift in Curved Spacetimes"
- September 3 M. A. Melvin,¹ Florida State University
"Introduction to General Relativity: IV. Energy and Stability of a Universe"
- September 11 R. B. Muir, ORNL
"The Interactions of 430 MeV/c K^- -Mesons in Helium"
- September 18 A. Chetham-Strode, ORNL
"The Transuranic Program at ORNL"
- September 25 J. M. Rowell, Bell Telephone Laboratories
"Tunneling in Superconductors"
- October 2 F. K. McGowan, ORNL
"Coulomb Excitation of Vibrational States"

¹Presented as part of a Special Theoretical Seminar Series coordinated by R. L. Becker.

- October 9 P. R. Bell, ORNL
"Discussion of Pictures from Ranger-7 Moon Shot"
- October 23 W. M. Good, ORNL
"Neutron Physics in the Kilovolt Region"
- October 30 R. J. Fox and Russell Robinson, ORNL
"Fabrication and Use of Lithium-Drifted Germanium Gamma-Ray Detectors"
- November 3 Marcos Moshinsky, University of Mexico
"Group Theory and Nuclear Structure"
- November 13 F. A. Wedgwood, Massachusetts Institute of Technology
"A Theory of Spiral Spin Structures"
- November 20 Sheldon Datz, ORNL
"Molecular Beam Scattering"
- December 4 Peter Fong, Utica College of Syracuse University
"Statistical Theory of Nuclear Fission"
- December 11 R. D. Birkhoff, ORNL
"Experiments and Theory on the Electron Slowing Down Flux"
- December 11 D. W. Colvin, Neutron Compilation Centre, Saclay, France
"The ENEA Neutron Compilation Center at Saclay"
- December 14 J. B. French, University of Rochester
"Multipole Sum Rules in Nucleon Transfer Reactions"
- December 18 C. M. Jones, ORNL
"Nuclear Reactions Leading to Three Particles"

INTERNAL DISTRIBUTION

- | | |
|-------------------------------------|-------------------------------|
| 1. Biology Library | 148. G. G. Kelley |
| 2-4. Central Research Library | 149. M. T. Kelley |
| 5. Laboratory Shift Supervisor | 150. H. J. Kim |
| 6. Reactor Division Library | 151. W. C. Koehler |
| 7-8. ORNL - Y-12 Technical Library | 152. R. W. Lamphere |
| Document Reference Section | 153. C. E. Larson |
| 9-84. Laboratory Records Department | 154. N. H. Lazar |
| 85. Laboratory Records, ORNL R.C. | 155. R. S. Livingston |
| 86. J. K. Bair | 156. R. N. Lyon |
| 87. C. F. Barnett | 157. H. G. MacPherson |
| 88. P. R. Bell | 158. F. C. Maienschein |
| 89. J. A. Biggerstaff | 159. F. K. McGowan |
| 90. D. S. Billington | 160. C. J. McHargue |
| 91. E. P. Blizard | 161. J. R. McNally, Jr. |
| 92. R. C. Block | 162. A. Meyer |
| 93. C. J. Borkowski | 163. A. J. Miller |
| 94. G. E. Boyd | 164. P. D. Miller |
| 95. M. A. Bredig | 165. C. D. Moak |
| 96. R. B. Briggs | 166. R. M. Moon, Jr. |
| 97. J. W. Cable | 167. H. W. Morgan |
| 98. E. C. Campbell | 168. K. Z. Morgan |
| 99. T. A. Carlsen | 169. R. B. Murray |
| 100. H. R. Child | 170. M. L. Nelson |
| 101. F. L. Culler | 171-172. F. E. Obenshain, Jr. |
| 102. J. W. T. Dabbs | 173-174. R. B. Parker |
| 103. K. T. R. Davies | 175. R. W. Peelle |
| 104. G. deSaussure | 176. J. J. Pinajian |
| 105. D. E. Ferguson | 177. F. Pleasonton |
| 106. J. L. C. Ford, Jr. | 178. C. A. Preskitt |
| 107-131. J. L. Fowler | 179. L. D. Roberts |
| 132. J. L. Gabbard | 180. R. L. Robinson |
| 133. C. G. Gardner | 181. G. R. Satchler |
| 134. J. H. Gibbons | 182. H. W. Schmitt |
| 135. W. M. Good | 183. H. E. Seagren |
| 136. C. D. Goodman | 184. E. D. Shipley |
| 137. P. M. Griffin | 185. M. J. Skinner |
| 138. Eugene Guth | 186. G. G. Slaughter |
| 139. C. S. Harrill | 187. A. H. Snell |
| 140. C. C. Harris | 188. P. H. Stelson |
| 141. J. A. Harvey | 189. R. W. Stoughton |
| 142. A. Hollaender | 190. C. D. Susano |
| 143. A. S. Householder | 191. E. H. Taylor |
| 144. C. H. Johnson | 192. K. L. Vander Sluis |
| 145. R. W. Johnson | 193. K. Way |
| 146. C. M. Jones | 194. A. M. Weinberg |
| 147. W. H. Jordan | 195-196. H. B. Willard |

- | | |
|-------------------------------|-----------------------------------|
| 197. G. C. Williams | 202. M. Deutsch (consultant) |
| 198. E. O. Wollan | 203. D. L. Judd (consultant) |
| 199. W. Zobel | 204. L. J. Rainwater (consultant) |
| 200. A. Zucker | 205. J. A. Wheeler (consultant) |
| 201. B. L. Cohen (consultant) | 206. E. P. Wigner (consultant) |

EXTERNAL DISTRIBUTION

207. Roland J. Schuttler, Service SEPP, CEN/FAR (Fort de Chatillon), Fontenay-aux-Roses (Seine), France
208. K. K. Seth, Department of Physics, Northwestern University, Evanston, Illinois
209. C. F. Coleman, Atomic Energy Research Establishment, Nuclear Physics Division, Harwell, Berkshire, England
210. Anna Maria Sarius, Centro di Calcolo Comitato Nazionale Energie Nucleare, Bologna, Italy
211. R. W. McNamee, Union Carbide Corporation, New York
212. Research and Development Division, AEC, ORO
213. V. B. Bhanot, Physics Department, Panjab University, Chandigarh-3, India
214. Jacobo Rapaport, University of Chile, Box 2777, Institute of Science, Santiago, Chile
215. T. Springer, Kernforschungsanlage Julich, Julich 517, Postfach 365, West Germany
216. Ingmar Bergstrom, Nobel Institute of Physics, Stockholm 50, Sweden
- 217-327. Given external distribution
- 328-932. Given distribution as shown in TID-4500 (39th ed.) under Physics category (75 copies - CFSTI)